INFORMATION TO USERS

This manuscript has been reproduced from the microfilm master. UMI films the text directly from the original or copy submitted. Thus, some thesis and dissertation copies are in typewriter face, while others may be from any type of computer printer.

The quality of this reproduction is dependent upon the quality of the copy submitted. Broken or indistinct print, colored or poor quality illustrations and photographs, print bleedthrough, substandard margins, and improper alignment can adversely affect reproduction.

In the unlikely event that the author did not send UMI a complete manuscript and there are missing pages, these will be noted. Also, if unauthorized copyright material had to be removed, a note will indicate the deletion.

Oversize materials (e.g., maps, drawings, charts) are reproduced by sectioning the original, beginning at the upper left-hand corner and continuing from left to right in equal sections with small overlaps.

Photographs included in the original manuscript have been reproduced xerographically in this copy. Higher quality 6" x 9" black and white photographic prints are available for any photographs or illustrations appearing in this copy for an additional charge. Contact UMI directly to order.

Bell & Howell Information and Learning
300 North Zeeb Road, Ann Arbor, MI 48106-1346 USA
800-521-0600

UMI®

DISSERTATION

HYDRAULIC DESIGN OF STEPPED SPILLWAYS

Submitted by

Jason Paul Ward

Department of Civil Engineering

In partial fulfillment of the requirements

for the Degree of Doctor of Philosophy

Colorado State University

Fort Collins, Colorado

Spring 2002

COLORADO STATE UNIVERSITY

March 28, 2001

WE HEREBY RECOMMEND THAT THE DISSERTATION PREPARED UNDER OUR SUPERVISION BY JASON PAUL WARD ENTITLED HYDRAULIC DESIGN OF STEPPED SPILLWAYS BE ACCEPTED AS FULFILLING IN PART REQUIREMENTS FOR THE DEGREE OF DOCTOR OF PHILOSOPHY.

Committee on Graduate Work

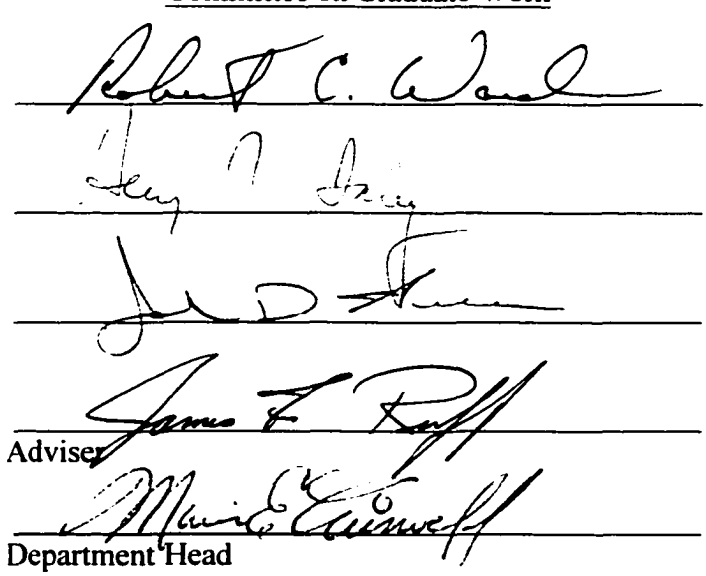

Adviser

Department Head

ABSTRACT OF DISSERTATION

HYDRAULIC DESIGN OF STEPPED SPILLWAYS

Overflow conditions occur on spillways during regular periods of release or during emergency flood events. During extreme events, overtopping of the entire crest of the dam may occur and the downstream face is exposed to erosive flow conditions compromising the integrity of the dam or leading to catastrophic failure. In recent years, there has been an increased interest in the use of stepped overlays on dams and spillways to dissipate the erosive energy from overtopping flows.

Roller Compacted Concrete (RCC) is becoming an increasingly popular method of constructing and protecting dam embankments. RCC naturally lends itself to a stepped configuration by the construction technique of roller compacting successive horizontal concrete lifts. To date, there have been numerous RCC stepped spillways constructed worldwide, yet there is the lack of a general design that quantifies the hydraulics characteristics of the overtopping flow for a given step height, dam height, and slope.

The present study is the continuation of a research program conducted at Colorado State University in cooperation with the United States Bureau of Reclamation (Bureau) concerning overtopping spillway flows. Tests were conducted at near prototype conditions on an existing outdoor flume located at Colorado State University's Engineering Research Center. Horizontal steps fabricated from lumber and plywood were placed in the flume providing a simulated stepped spillway with step heights of h =

1.0 ft and h = 2.0 ft. Additional testing of the smooth surface chute with the steps removed was conducted for comparison purposes.

Specialized instrumentation, provided by Colorado State University and the Bureau, was used to collect air concentration and velocity data within the stepped spillway flow. The data were analyzed to quantify flow depth, energy dissipation, and an estimate of flow resistance in the form of the Darcy friction factor f. Results of the analysis were then used to propose a design procedure for estimating the hydraulic characteristics of stepped spillway flow using typical required information.

Jason Paul Ward
Department of Civil Engineering
Colorado State University
Fort Collins, CO 80523
Spring 2002

ACKNOWLEDGMENTS

Completion of this dissertation and chapter in my life was achieved not by my efforts alone, but through the assistance and encouragement from the many individuals who have supported me in this endeavor. My time at Colorado State University was touched by all of those recognized here and I can only attempt to repay them by saying "Thank You".

First and foremost I am indebted to Dr. James Ruff for his unwavering commitment to me as my mentor and advisor. Your guidance and patience has seen me through from my time as a "lost" undergraduate to completion of my doctoral dissertation. You are an inspiration to me both professionally and personally, and I want sincerely thank you for your support and contribution to this time in my life.

The vision and financing of this research would not have been possible with out the support of U.S. Bureau of Reclamation engineer Ms. Kathleen Frizell. Sincere appreciation is given to Kathy and Reclamation for continuing their joint effort research with Colorado State University. A special thanks goes to Kathy and "Cal" for their help in the field during for those long, hot days on the spillway.

Sincere appreciation is extended to my graduate committee members Dr. Henry Falvey, Dr. John Nelson, and Dr. Robert Ward for their critical and valued review of this dissertation. I have greatly benefited from your observations, challenges, and discussions.

These acknowledgments would not be complete without recognizing my friends and colleagues at the Engineering Research Center (ERC). Special thanks go to Brian McKenna, Tom Gill, and John Brookman for your dedication to this project. Thanks are also due to the ERC shop personnel Horacio "Junior" Garza, Robert Brennan, Bart Rust, and Jay Bryner for their continuous support in constructing the model this research was based on.

It is with deepest gratitude that I recognize and acknowledge my parents. Thank you for giving me life and believing in me with your unconditional love. In the same token, I want to thank my Estes Park family who are too numerous to list. You know who you are!

In the course of my doctoral program, I met my beautiful wife Bethany who is a continual inspiration to me. Thank you for supporting me with your love, understanding and patience.

Financial support for this project was provided by the Colorado Agricultural Experiment Station (project number COLO 0708) and the U.S. Bureau of Reclamation (agreement number 99FC810156) in a joint research program with Colorado State University.

DEDICATION

To My Parents

To My Wife, Bethany

TABLE OF CONTENTS

LIST OF TABLES

LIST OF FIGURES

LIST OF SYMBOLS

English Symbols

Symbol	Definition
A	Cross-sectional flow area; area under electronic waveform
b	Spillway width; regression coefficient
c_p	Probe air concentration
c	Calibrated air concentration
$\overline{C}$	Depth-integrated average air concentration
d_w	Clear water depth
E_l	Energy head at any location along spillway
E_o	Total available energy
f	Darcy-Weisbach friction factor
F_r	Froude number
g	Acceleration due to gravity
h	Height of step
h_f	Head loss due to friction
H	Spillway height measured from crest down
k	Roughness height; height of step perpendicular to slope, $k = h\cos\theta$
l	Length of step
L	Channel section length ; stilling basin length
m	Regression exponent

N	Step number with reference to first step at spillway crest
P	Wetted perimeter
p_a	Atmospheric pressure at operating conditions
p_d	Kinetic pressure head
p_s	Static pressure head
p_{sa}	Standard atmospheric pressure
q	Unit discharge
q_w	Clear water unit discharge
q_m	Measured unit discharge
Q	Total volumetric discharge
Q_a	Actual discharge at operating conditions (acfm);
Q_s	Discharge at standard operating conditions (scfm);
R_h	Hydraulic radius
s	Station
S_f	Friction slope
S_o	Spillway or channel slope
t	Time
T	Waveform sample duration
T_a	Temperature at operating conditions
u	Velocity
$\overline{U}$	Depth-integrated average velocity
U_{avg}	Average velocity
V	Voltage

w	Channel width
y	Depth measured perpendicular to spillway floor from pseudo-bottom formed by a plane passing through the tips of the steps
y_{90}	Depth where local air concentration equals 90%
y_c	Critical depth

Greek Symbols

Symbol	Definition
β	Momentum correction factor
Δp	Differential pressure head
Δx	Section between stations
ε	Bulking coefficient, $\varepsilon = y_{90}/d_w$
γ	Unit wieght
λ	Pitot tube pressure coefficient
θ	Spillway or channel slope
ρ_m	Mixture fluid density
ρ_w	Density of water
τ_b	Bed shear stress
τ_w	Wall shear stress

CONVERSION TABLE

Mass

1 slug	=	14.594 kg

Length

1 ft	=	0.3048 m
1 in	=	25.4 mm

Temperature

°C	=	$\frac{5}{9}(°F - 32°)$

Force

1 lb	=	4.448 N

Pressure

1 psi	=	6.895 kPa
1 psf	=	47.88 Pa
1 atm	=	101 kPa
1 atm	=	2116.8 psf

Volume

1 gal	=	0.134 ft^3
1 ft^3	=	7.4805 gallons
1 gal	=	3.785 L
1 ft^3	=	28.317 L

Volumetric flow rate

1 ft^3/s (cfs)	=	448.831 gallons per minute (gpm)
1 gpm	=	0.002228 cfs
1 cfs	=	0.0283 m^3/s (cms)
1 cfs/ft	=	0.0929 cms/m

Gravity

g	=	32.174 ft/sec2
g	=	9.807 m/s

CHAPTER 1

INTRODUCTION

1.1 Background

Use of a stepped slope to slow the movement of water overflowing a dam or weir dates to antiquity. Earliest documented overflow weirs using stepped downstream faces date to 700 BC Iraqi water supply dams built under the Assyrian king Sennacherib for the capital city of Nineveh (Schnitter, 1994). Most of these dams were low diversion weirs of rubble masonry with upstream vertical faces, broad overflow crests, and stepped downstream faces. China's Tianping weir, built in 219 BC, was a structure where notable use of a stepped slope was incorporated. The rubble filled downstream side was covered with tightly packed vertical slabs creating a gently sloping stepped face. This orientation dissipated much more of the energy of the overflowing water than ordinary horizontal slabs at the same time being more stable (Schnitter, 1994). In the 7th and 8th centuries, several early Moslem dams and overflow weirs using steps were built in central Arabia near the cities of Mecca and Medina. During the 10th century, early Spanish settlers built stepped overflow weirs for irrigation near the city of Valencia, Spain.

Dams and weirs similar to those mentioned have been built worldwide throughout the centuries and are fairly well documented (Chanson, 1994; Schnitter, 1994; and Schuyler, 1912). More recent, in the past century, there has been an increased interest in

the use of stepped spillways to dissipate energy from dam spillway flows. The fairly new construction technique using Roller Compacted Concrete (RCC) ideally suites a stepped configuration. Construction of new dams and the rehabilitation or replacement of aging dams are applications where RCC is rapidly becoming a popular choice. For spillway and embankment overtopping protection, RCC naturally lends itself to a stepped configuration by the construction technique of roller compacting concrete in successive horizontal lifts. To date, there have been numerous RCC and conventional concrete stepped spillways constructed worldwide (Frizell, 1992), however, there is the lack of a general design criteria that quantifies hydraulic characteristics of the overtopping flow for a given step height, dam height and slope.

The main advantages of selecting RCC over conventional concrete as a construction material are reduced construction time and reduced material quantities. Both of these advantages can result in significant cost savings, especially for the construction, rehabilitation or upgrading of overflow spillways. Approximate costs of RCC constructed dams have been shown to range from 25 to 50% less than conventionally placed concrete (ASCE, 1994). Figure 1.1 shows a cost comparison of RCC and conventional concrete used in dam construction.

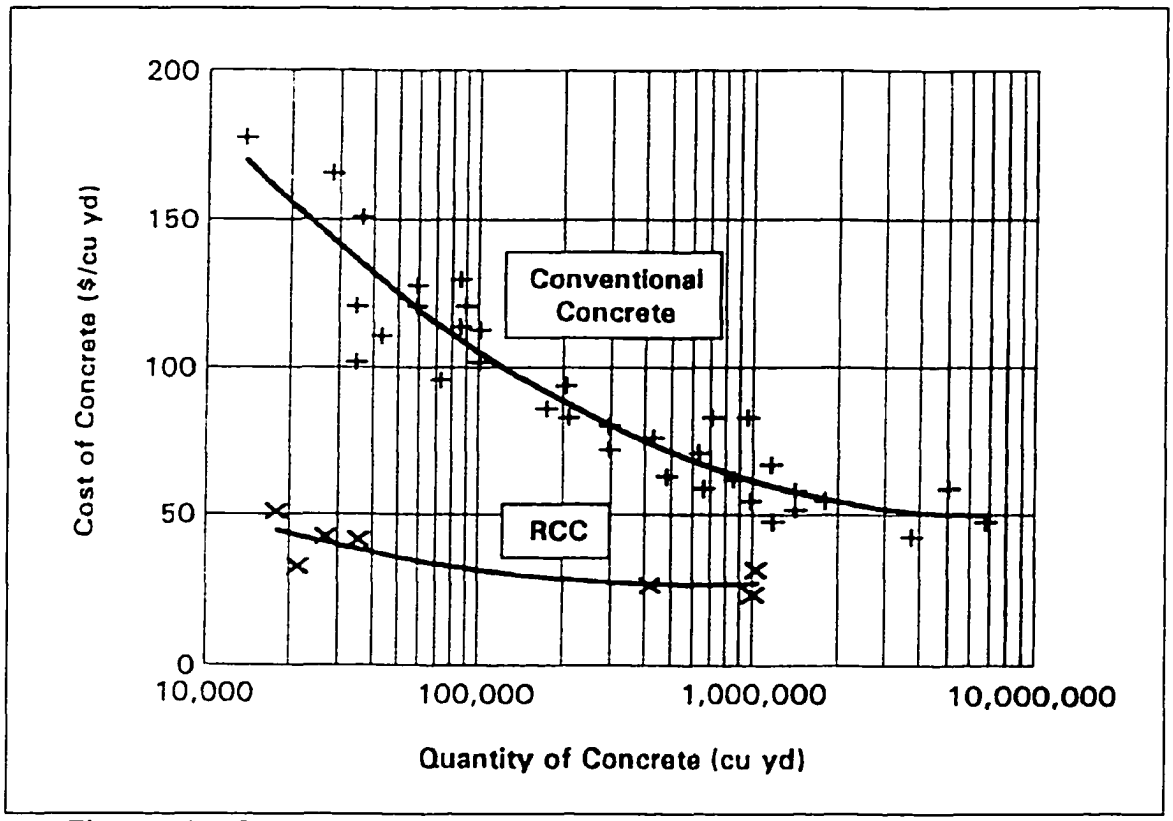

Figure 1.1 – Cost comparison of RCC and conventional concrete (ASCE, 1994).

Stepped spillways have been shown to significantly reduce velocities at the toe of the spillway (Diez-Cascon et. al. 1991; Frizell, 1992; Rice et. al.1996; Robinson et. al. 1998; Johnson et. al. 1997). Toe velocities are used to size the required downstream stilling basin and lowering these velocities allows for design of a smaller basin representing a significant savings in construction time and costs. In addition, design of the stilling basin requires an accurate estimation of the hydraulic performance of the stepped spillway including knowledge of important flow characteristics such as velocity, flow depth, and air entrainment.

The present study is the continuation of a research program conducted at Colorado State University in cooperation with the United States Bureau of Reclamation (Bureau) concerning overtopping spillway flows. Tests were conducted at near prototype

flow conditions on an existing outdoor flume located at Colorado State University's Engineering Research Center. Horizontal steps fabricated from lumber and plywood were placed in the flume providing a simulated stepped spillway with step heights of h = 1.0 ft and h = 2.0 ft.

1.2 Purpose of the Present Study

The purpose of the present study was to collect near-prototype scale data on the hydraulic characteristics of stepped spillway flow including air concentration, bulked flow depth, clear water depth, and flow velocity. The collected data were analyzed to quantify energy dissipation and estimate flow resistance in the form of the Darcy friction factor. Results of the analysis were then used to propose a design procedure for estimating the hydraulic characteristics of stepped spillway flow using typical required information. An additional objective was to gain knowledge on the application and limitations of the specialized instruments used in the study.

The findings of this study will contribute to the existing body of experimental data from previous investigations on stepped spillway flow. The proposed design procedure was developed around the physical constraints of the present study. However, it is anticipated that the results will be of tremendous value in future investigations lending to a greater understanding of stepped spillway flow over a broad range of conditions.

1.3 Limitations of the Present Study

The present study was conducted within a fixed budget and schedule over an approximately three-year period consisting of design, construction, and testing of the physical model, data collection and analysis, and preparation of this dissertation. Throughout the research project, certain assumptions and theories generally accepted in both hydraulic engineering and the recent history of stepped spillway research were adopted. The instrumentation used in this study to collect air concentration and velocity were considered experimental and resulted in a significant portion of the research. Data collection and analysis progressed in a logical manner limited to the available resources including time, funding, instrumentation, and technical references.

Throughout this study, numerous difficulties that included instrument damage and destruction occurred during both calibration and data collection. In later stages of the project, many of these difficulties were resolved while some were found to be inherent and unavoidable characteristics of the instruments themselves. As with any data collection, the quality of the results and conclusions are directly related to interpretation of the instrument output. All of the data and results produced in this study were evaluated and analyzed for reasonableness and compared to theoretical results and published stepped spillway data from similar studies. In addition, statistical analysis was implemented where necessary to eliminate data outside of set parameters. In general, much of the data generated in this study fell within a reasonable range of theoretical values and the majority of published data.

The outcome of this research is a design procedure for determining the hydraulic characteristics of stepped spillway flow. The conclusions of this study are based on

instrumentation that may not be as precise as instrumentation used to collect data in smaller scale models and the data demonstrate considerable scatter. Due to the importance of this research with regard to the safety and structural integrity of dams and spillways, the individual designer of a stepped spillway should scrutinize results produced by the design procedure. As with all design procedures based on empirical data, sound engineering judgment should be the ultimate basis of the accuracy of a design.

CHAPTER 2

REVIEW OF LITERATURE

Stepped overflow weirs and spillways have been used for hundreds of years. Design of these structures naturally paralleled dam-building which, in ancient times, lacked the presence of a rational approach (Smith, 1972). With advancement of technology and the ever-increasing need for safety, the knowledge and design of dams broadened into the current design methods of today. However, advancement in design of appurtenant structures, such as stepped spillways, appears to have lagged dam design, and only in recent years has it become an important topic of research.

The difficulty in studying hydraulically rough surfaces like stepped spillways is the presence of highly turbulent, air entrained flow. Classic hydraulics theory and instrumentation can only approximate characteristics such as air entrainment, depth, and velocity of the two-phase flow. In recent years, significant amounts of time and money have been devoted to laboratory model studies in order to study these characteristics.

Following is a review of selected articles on research of stepped spillway flow. Selection of the articles was based on research conducted with physical scale models or of literature that has significantly contributed to the knowledge of stepped spillway flow. The articles are categorized into sections depending upon the main theme presented. Section 2.1 defines flow regimes generally accepted in stepped spillway flow research, Section 2.2 contains hydraulic studies, and Section 2.3 reviews studies on self-aerated

flow. The articles are presented chronologically for each section, and each review is "independent" from the others in that *variable symbols refer to that review only and do not reflect variable notation in the remainder of this dissertation.* All dimensions are prototype scale and in English units unless otherwise specified. Table 2.1 at the end of this chapter includes a comprehensive list of physical model tests known to date.

2.1 Flow Regimes Defined

Research literature generally recognizes two types of flow behavior on a stepped slope: *nappe flow regime* and *skimming flow regime.* Research on the hydraulics of stepped spillway flow usually concentrates on one regime or the other with the type of regime dictated by a combination of step geometry and flow discharge. Nappe flow normally occurs for low discharges and small flow depths while skimming flow occurs for high discharges and large flow depths.

Nappe flow regime is distinguished by a series of plunges from one step to another with the formation of a nappe at each drop. This type of flow can be approximated by a series of single-step drop structures (Chamani and Rajaratnam 1994; Chanson 1993). The flow leaves the step as a free-falling jet and impinges on the tread of the next step. Energy dissipation occurs by jet breakup, jet mixing on the step, and the formation of a partially or fully developed hydraulic jump on the step (Chanson 1994; Rajaratnam 1990). In the case of a fully developed hydraulic jump (Figure 2.1a), referred to as *isolated nappe flow* (Essery and Horner 1978; Peyras et. al. 1992), the flow passes through critical depth at the brink of the step forming a supercritical free-falling jet and returns to subcritical flow downstream of the jump. Flow with a partially developed

hydraulic jump, referred to as *nappe interference* (Essery and Horner 1978) or *partial nappe flow* (Peyras 1992 et. al.), overshoots the next step and does not fully impinge on the step tread. For nappe flow to occur, the step horizontal tread needs to be greater than the water depth (Stephenson 1991; Lejeune et. al. 1994). In dam design, this would normally result in a relatively flat slope.

In *skimming flow regime* (Figure 2.1b), water flows down the stepped face as a coherent stream, skimming over the steps and cushioned by the recirculating fluid trapped between them (Rajaratnam 1990). The skimming stream is supported by a psuedo-bottom formed by the external edges of the steps and horizontal-axis recirculating vortices. Energy dissipation occurs by momentum transfer, or the transmission of turbulent shear stress, between the skimming stream and the vortices (Chanson 1994).

Skimming flow is characterized by complete submergence of the steps with the development of fully aerated uniform flow in the downstream region (Figure 2.2). Along the upstream steps, a non-aerated flow region exists within which a turbulent boundary layer develops. Air entrainment in the flow begins where the boundary layer intersects the free surface, referred to as the point of inception. Downstream from the point of inception, the flow continues aerate and varies gradually in depth. The flow eventually becomes fully aerated, uniform flow in which the water depth, velocity, and air concentration are constant (Bindo et. al. 1993).

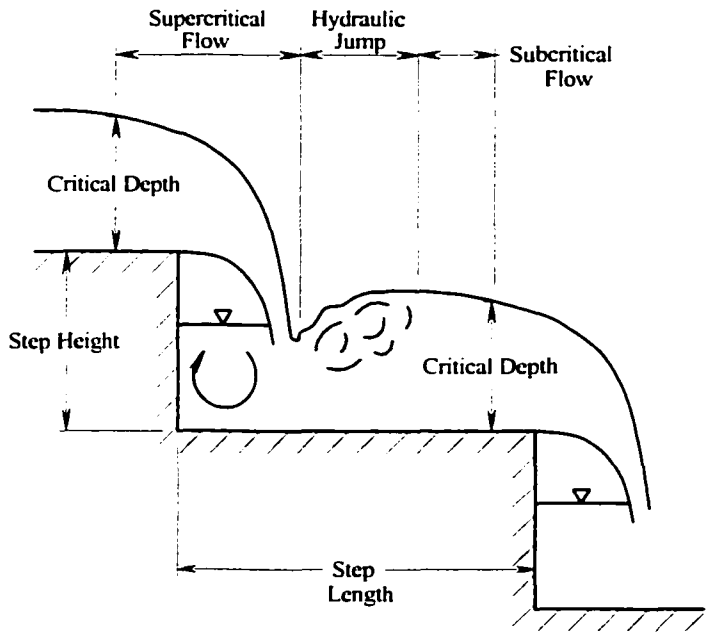

a) Nappe flow regime with fully-developed hydraulic jump.

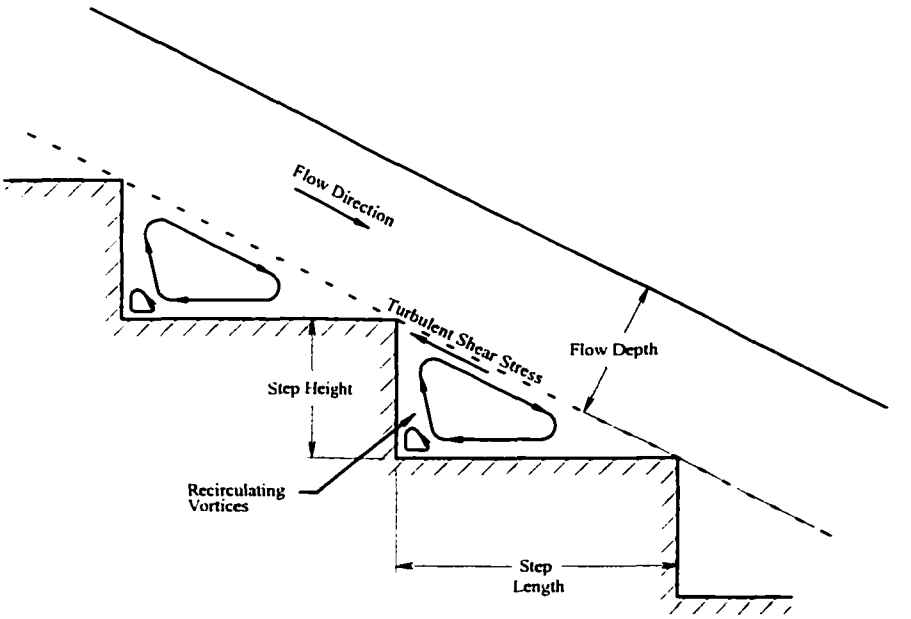

a) Skimming flow regime.

Figure 2.1 – Nappe and Skimming Flow Regimes.

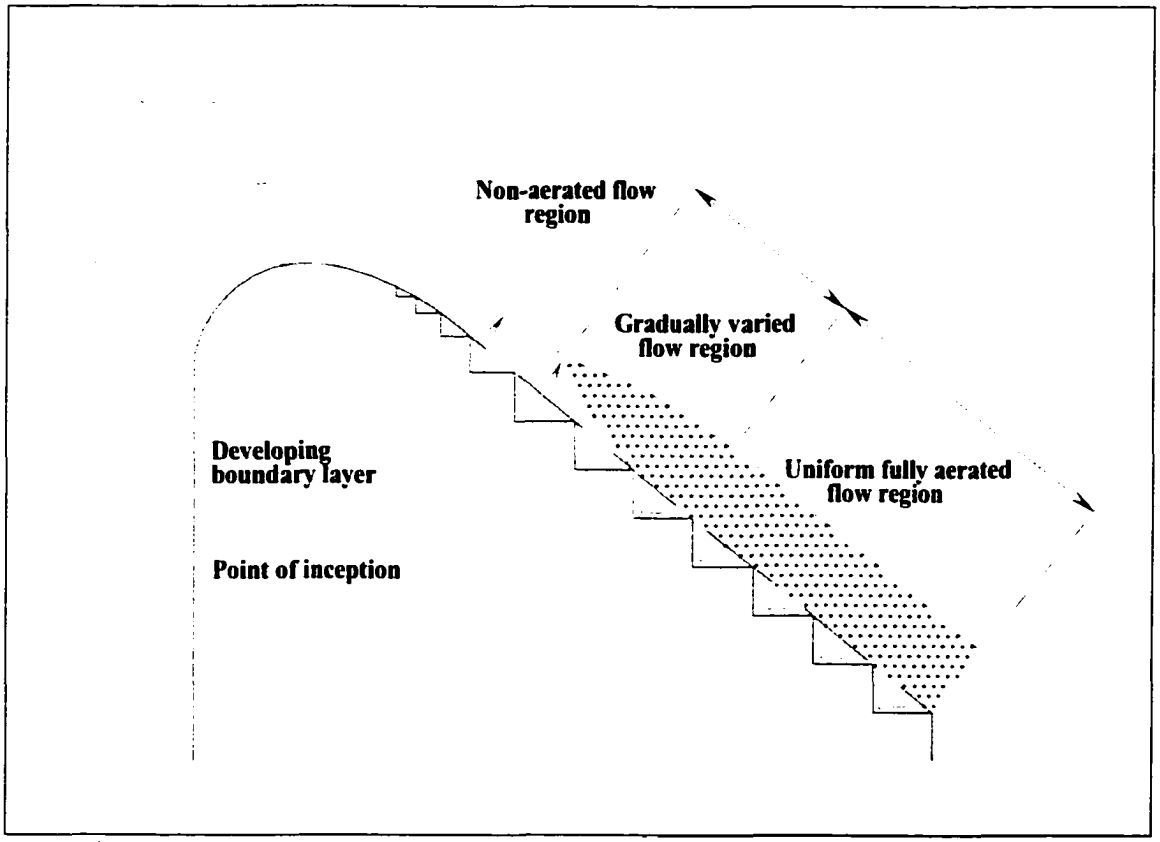

Figure 2.2 – Flow regions of skimming flow regime (after Bindo et. al., 1993).

Much of the research on stepped spillway skimming flow has concentrated on determining the profile of the turbulent boundary layer, the location of the point of inception, and the concentration of air in the flow. All of these factors influence the design of stepped spillways. Specifically, the knowledge of the concentration and distribution of aeration become important in determining the water depth, velocity and hence the amount of energy dissipation along the slope. Obtaining physical measurements of the air-water flow are difficult due to the "bulking" of the flow from air entrainment.

2.2 Hydraulic Studies

2.2.1 Essery and Horner (1978)

Essery and Horner (1978), of the Construction Industry Research Information Association of the U.K., appear to be the earliest researchers to thoroughly investigate the hydraulics of stepped spillways. The research was conducted by means of model studies covering a wide range of step configurations and slopes. Numerous tests were carried out varying the parameters of step height-to-length ratio (slope) H/L, step length L, inclination of the step tread θ, and the number of steps N. Model parameters spanned a wide range with overall slopes from 0.421 to 1.0, step length from 0.22 ft to 0.82 ft, step inclination from 0° to 20°, and the number of steps from 10 to 30.

For each test, velocity measurements were taken using Pitot tubes placed in the flow at a horizontal section downstream of the last step. Distance from the last step varied accordingly such that the flow was free of air entrainment. The most important characteristics of the flow at the horizontal section were described by specific energy E_s, and specific force F_s, given by:

$$E_s = y + \frac{v^2}{2g} \tag{2-1}$$

$$F_s = \frac{v^2 y}{g} + \frac{y^2}{2} \tag{2-2}$$

where: y = mean depth;

v = mean velocity;

g = acceleration due to gravity.

Attempts were made to classify flows into type and category. Flow type consisted of visual observations between isolated nappe, interference nappe, and skimming flow. Flow categories consisted of classification between subcritical, mixed, and supercritical flow regimes. To assist in quantifying the results, the dimensionless parameters of energy number E_N, force number F_N, and flow number Q_N, were defined by dimensional analysis:

$$E_N = \frac{E_s}{L} \tag{2-3}$$

$$F_N = \frac{\sqrt{F_s}}{L} \tag{2-4}$$

$$Q_N = \frac{y_c}{L} \tag{2-5}$$

where: y_c = the critical depth of flow given by $\left(\frac{q^2}{g}\right)^{1/3}$;

q = discharge per unit width.

Numerous plots were developed combining the model parameters, dimensionless correlations, and visual observations. Most notably, the plots incorporate the breakpoints for flow type and category as a function of discharge and spillway configuration. The authors go on to apply the results to the design of stilling basins at the base of a stepped spillway.

2.2.2 Sorensen (1985)

Sorensen (1985) conducted a model study to evaluate the proposed design of a stepped spillway for the new Monksville Dam in New Jersey. The profile of the spillway was a modification of the Waterways Experiment Station (WES) ogee crest profile. From the crest to the point of tangency, the spillway face followed the WES profile. Below the point of tangency, the spillway had a constant slope of 0.78H:1V. Steps were fit into the spillway in such a manner that the envelope of their tips followed the WES profile and the downstream slope. The prototype concrete dam and spillway were designed for 2.00 ft vertical by 1.56 ft horizontal steps below the point of tangency. Above the point of tangency, step sizes decreased in transition to the standard nonstepped ogee profile.

Three scale models of the Monksville Dam spillway were tested. Model A consisted of a 1:10 scale model of the upper 22.75 ft of the spillway tested to evaluate the flow transition over the spillway crest and the first several steps. The model extended down to seven steps below the point of tangency. Model B was a 1:25 scale model of the entire, standard, nonstepped WES profile spillway. This model was tested to provide comparison data. Model C was a 1:25 scale model of the entire stepped spillway profile. All model tests were conducted in a 1.0 ft wide flume with a maximum discharge of just under 3.0 cfs. Measurements of flow depth were made at several locations along the spillway for each model test over a range of discharges. When air entrainment was present, the flow depths were estimated taking into account the bulk of the flow.

Spillway discharges ranged from a minimum of 0.056 cfs/ft to a maximum of 2.53 cfs/ft with corresponding upstream head measurements of 0.063 ft and 0.710 ft,

respectively. Average flow velocities were calculated from continuity. It was noted that some of the velocities were checked with a stagnation tube and measurements were reported to yield results within 10-15% of the values calculated from continuity. In addition, scaled velocities from model B were 15-20% higher than the prototype data. Proposed reasoning was that air entrainment was not present in the flow during the testing of model B and in the prototype, air entrainment would be expected. This scaling effect was described to be the primary cause for the velocity differences.

It was found that the kinetic energy of the flow at the stepped spillway toe varied from about 6 - 12% of the energy at the standard spillway toe for the range of model discharges. For the prototype design, toe velocities were scaled up using Froude scaling ratios and velocities for model B were compared with prototype velocities found on similar spillways using "experience" data from Bradley and Peterka (1957). It was estimated that the stepped spillway for the Monksville dam may provide up to 84% kinetic energy dissipation at design discharges.

Sorensen also recorded the step number, from the top, at which air entrainment commenced for each run. It was noted that typically, the depth decreased as the flow descended from the crest to the point at which air entrainment commenced. Beyond that point, the depth continually increased due to bulking of the flow by air entrainment.

2.2.3 Houston (1987)

The U.S. Bureau of Reclamation conducted hydraulic model studies for design of the spillway for the Upper Stillwater dam in Utah. The dam incorporates Roller Compacted Concrete (RCC) construction techniques used for the dam into construction of the stepped spillway. The principle objective of the study was to design and analyze

the configuration of the stepped spillway to provide information on sizing the stilling basin. Providing increased energy dissipation using steps resulted in reduction in size and cost of the stilling basin. Several sectional models of the spillway were tested ranging in scale from 1:5 to 1:10.

The final spillway design follows the theoretical nappe shape for an ogee crest. Several small steps began at the crest and gradually protruded into the profile downstream. The profile intersected a point of tangency where the slope became constant at 0.32H:1V. Following the shape of the dam, the slope changed to 0.6H:1V approximately one-third of the full distance down the face. The beginning steps varied in size and were determined based on model results. Step size was selected to prevent the jet produced from a protruding step from springing free of the spillway. The final design maintained a uniform flow against the spillway face. The stilling basin was designed using the model of the final spillway design. Based on stilling basin velocities at the design discharge, it was estimated that 72% energy dissipation was provided by the spillway.

2.2.4 Rajaratnam (1990)

Rajaratnam (1990) presented a method for predicting shear stress and frictional energy loss for a skimming flow regime. It was proposed that the average Reynolds shear stress between the skimming stream and the recirculating fluid underneath can be estimated by finding the coefficient of fluid friction for a given set of flow conditions. For a stepped spillway of constant slope, $S_o = \sin\alpha$, and fully developed flow with a constant mean velocity V_o, and normal depth y_o, the shear stress may given by:

$$\tau = y_o \gamma \sin\alpha \tag{2-6}$$

where: γ = weight per unit volume of water;

τ = average Reynolds shear stress between the skimming flow and the recirculating fluid.

It was also assumed that the turbulent shear stress could be approximated by:

$$\tau = c_f \frac{\rho V_o^2}{2} \tag{2-7}$$

where: c_f = coefficient of fluid friction;

ρ = mass density of water.

Equations (2-6) and (2-7) are combined and solved for the fluid friction coefficient to obtain:

$$c_f = \frac{2 y_o^3 g \sin\alpha}{q^2} \tag{2-8}$$

where: g = acceleration due to gravity;

q = discharge per unit width of the spillway.

Rajaratnam evaluated values of c_f for skimming flow using experimental data from Sorensen (1985) on a 1:25 scale model of Monksville dam. Using the experimental data from Sorensen's model test, C1-C8, Rajaratnam found c_f to vary from 0.11 to 0.20 with an average value of 0.18. He states that this is an estimate due to the aeration occurring in the flow and that flow depths measured by Sorensen are approximate.

An estimate of the energy loss for skimming flow on a stepped spillway was found by comparing energy loss caused by the steps E, to that caused by a smooth spillway E', given by:

$$\Delta E = E' - E \tag{2-9}$$

Relative energy loss was defined as $\Delta E/E'$ and is given by the expression:

$$\frac{\Delta E}{E'} = \frac{(1-A)+\frac{F_o'^2}{2}\frac{(A^2-1)}{A^2}}{1+\frac{F_o'^2}{2}} \tag{2-10}$$

where: $A = (c_f/c_f')^{1/3}$;

c_f' = coefficient of skin friction for a smooth spillway;

F_o' = Froude number at the toe of a smooth spillway.

Taking, $c_f \cong 0.18$, $c_f' \cong 0.0065$, $A \cong 3$, and for a relatively large value of F_o', $\Delta E/E'$ is approximately equal to $(A^2 - 1)/A^2$, which further reduces to a value of 8/9 or 89%. It was concluded from this that a considerable energy loss could be produced by the steps.

Rajaratnam also performed an analysis with data from Essery and Horner (1978). He found that the type of flow regime existing on a stepped spillway depends on the ratio y_c/h, where y_c is critical depth and h is the vertical height of the step. For a ratio of y_c/h greater than 0.8, skimming flow occurs and for a ratio less than 0.8, nappe flow exists.

2.2.5 Stephenson (1991)

Stephenson (1991) examined the data of White (1943), Rand (1955), and Stephenson (1988) for a single straight drop in an attempt to extrapolate the results to stepped spillways. He developed curves, that for uniform flow, showed that "....the energy dissipation increases up to a certain limit as the step sizes are increased, beyond which there is limited advantage in increasing the step height" (Figure 2.3 and 2.4). It was also noted that "....energy dissipation can be increased until the stage when the water depth is approximately one third of the critical depth."

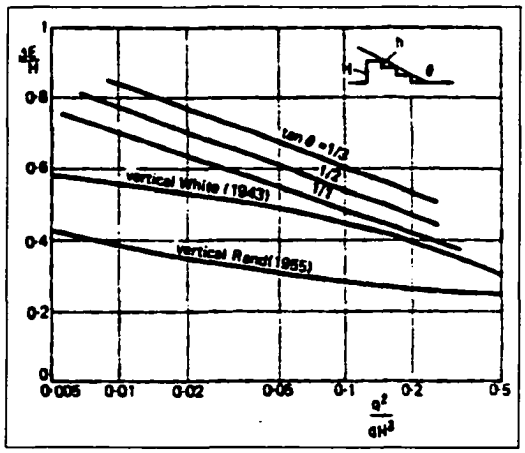

Figure 2.3 – Energy loss ratio for three steps of varying angle, Stephenson (1991).

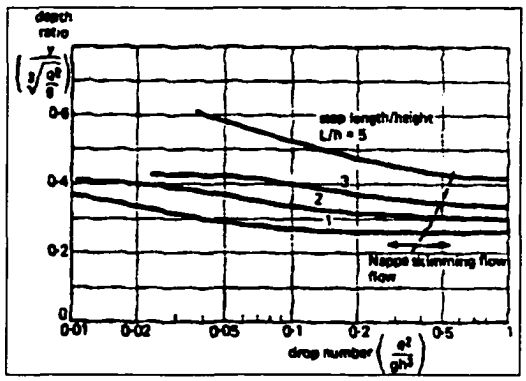

Figure 2.4 – Depth ratio for uniform flow over steps, Stephenson (1991).

Stephenson proposed that energy dissipation down a stepped spillway face, for uniform flow, could be calculated using the Darcy equation:

$$S_f = \frac{f}{4y}\frac{v^2}{2g} \tag{2-11}$$

where: S_f = slope of the energy-grade line;

f = Darcy-Weisbach friction factor;

y = flow depth;

v = average velocity;

g = acceleration due to gravity.

An energy loss ratio was then derived as:

$$\frac{\Delta E}{H} = 1 - \left(\frac{4S_f}{f} + 1\right)\left(\frac{f}{8S_f}\right)^{1/2}\left(\frac{y_c}{H}\right) \tag{2-12}$$

where: ΔE = energy loss down the face entire face of the dam;

H = dam height;

y_c = critical flow depth.

The Darcy-Weisbach friction factor was obtained from the turbulent rough boundary layer equation:

$$f = 1/\left(1.14 + 2\log\left(\frac{y_c}{k}\right)\left(\frac{8f}{S_f}\right)^{1/3}\right)^2 \tag{2-13}$$

where: k = roughness height.

Conclusions were drawn from a plot of $\Delta E/H$ versus H/y_c (Figure 2.5) using data from Rand (1955) and from a model study of Kennedy's Vale dam by Stephenson (1988). A theoretical line was plotted using equations (2-12) and (2-13) for different values of H. Stephenson concluded that the energy loss ratio increases as the ratio of H to y_c increase to a point where the ".....incremental energy loss is equal to the increase in dam height." It was noted that because of these results it might be more appropriate to examine the residual specific energy rather than the energy loss ratio. The experimental data points indicated a higher energy loss ratio than did the theoretical line for the same H/y_c values. Stephenson commented that this is because scale model tests over predict the energy loss due to a lower Reynolds number and the presence of air entrainment.

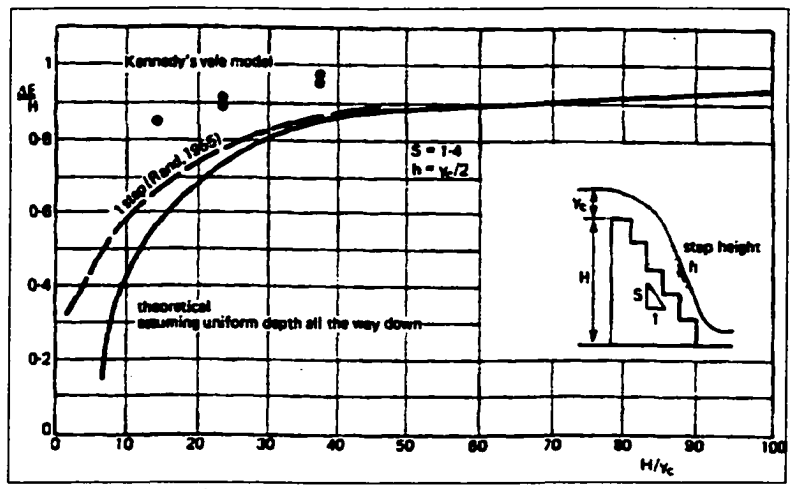

Figure 2.5 – Energy loss ratio down a stepped slope, Stephenson (1991).

2.2.6 Christodoulou (1993)

Christodoulou (1993), conducted model studies on a stepped spillway with a crest conforming to the standard WES profile. The crest profile was followed by a series of steps on a constant slope of 0.7H:1V. Seven transition steps of variable length-to-height ratios preceded eight steps on the constant slope. Model dimensions of the lower steps were 0.057 ft horizontal length by 0.082 ft vertical height. It was pointed out that this is considered a moderately sized stepped spillway.

The vertical water depth at steps 10 and 13 were measured using a point gage. Water depth was recorded at three equally spaced points across the width of the step. The arithmetic mean of the three values was considered as the vertical depth. Using the measured water depth, the head loss Δh, was calculated at each step as:

$$\Delta h = H_o - H \tag{2-14}$$

where: H_o = head upstream of spillway;

H = head on step under consideration.

Experimental data was applied to an equation for the coefficient of skin friction, c_f, defined by Rajaratnam (1990) as:

$$c_f = \frac{2y_o^3 g \sin\alpha}{q^2} \tag{2-15}$$

where: y_o = uniform flow depth;

α = slope;

q = unit discharge.

An average c_f value 0.089 and 0.076 was found at step 13 and 10, respectively, which was lower than expected.

A plot of relative head loss H/H_o versus the ratio of critical depth to step height, y_c/h (Figure 2.6a), was presented with the experimental data and data from Sorensen (1985). The experimental data, obtained for fewer numbers of steps than Sorensen, indicated significantly less energy loss. Another plot was developed collapsing all of the data into a single experimental curve expressing H/H_o to y_c/Nh (Figure 2.6b). It was found that the number of steps N, appreciably contributes to the energy dissipation, especially for low values of y_c/Nh.

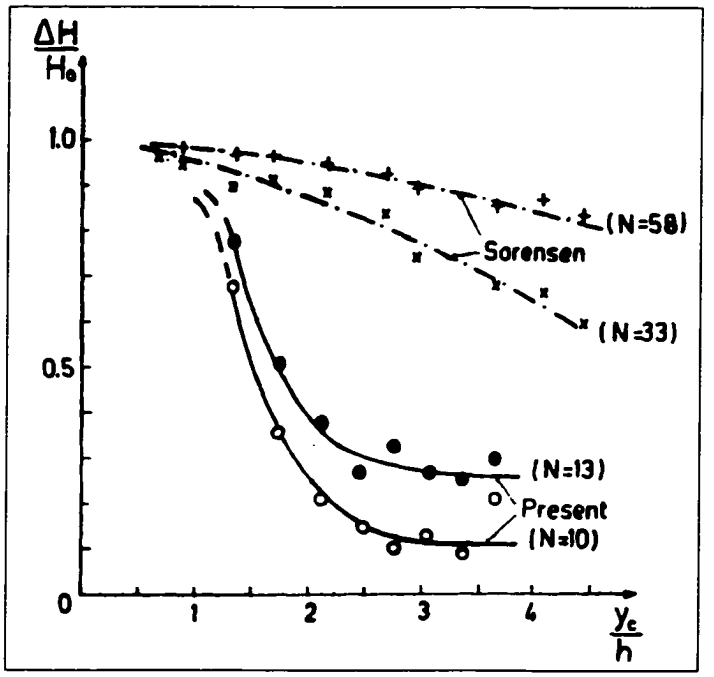

Figure 2.6a – Variation of relative head loss $\Delta H/H_o$ with y_c/h, Christodoulou (1993).

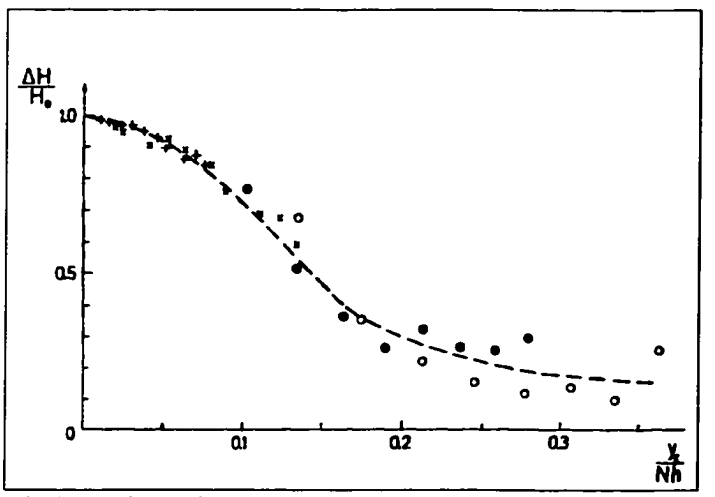

Figure 2.6b – Variation of relative head loss $\Delta H/H_o$ with y_c/Nh, Christodoulou (1993).

2.2.7 Tozzi (1994)

Tozzi (1994) performed model studies on a 1:15 scale, 1V:0.75H slope, stepped spillway chute. Five step heights were tested in the model: 0.016, 0.033, 0.066, 0.098, and 0.197 ft. A method was proposed for determining the non-aerated flow depth, h, along the chute. This depth could then be used to find the residual energy at the spillway

toe. It was proposed to find the depth through computation of the gradually varied flow profile using the Standard Step Method.

Determining the flow depth analytically requires determination of the Darcy-Weisbach friction factor *f*. In order to apply the friction factor concept to steps, the roughness height *k* was defined as the step height from the spillway chute to the step tip, perpendicular to the flow. The friction factor was first investigated using air flow in a closed conduit. For $h/k < 1.80$, f became constant at 0.163, for $h/k > 1.80$, the following relationship was found:

$$\frac{1}{\sqrt{f}} = 2.16 + 1.24 \log\left(\frac{h}{k}\right) \tag{2-16}$$

Similar relationships were found for slopes 1V:2H and 1V:6.69H.

Analytically determined depths were compared with experimentally determined depths and were found to differ by around 7% regardless of step height. The friction factor relationship appeared to adequately represent water flow. For water, the depth of flow was defined as the normal depth from the step tip to the point of maximum velocity (using a Pitot-static tube) above which the velocity was essentially constant.

The analytically computed non-aerated flow depth was found for the toe of the spillway for different flowrates and step heights (roughness). The residual energy was then calculated by:

$$E_t = h + \frac{q^2}{2gh^2} \tag{2-17}$$

Results from the stepped test found the residual energy to be 25-50% of the total head for unit discharges varying between 53.8 and 129.2 cfs/ft. For comparison, the model tests

were run with a hydraulically smooth chute. Results showed that the stepped spillway was able to dissipate three to four times more energy than the smooth chute.

Further investigations were carried out to define the development of the turbulent boundary layer. The thickness of the layer was considered the flow depth at the point of inception of aeration, as computed by the Standard Step Method. The data was shown to fit well to an equation developed by Campbell (1963):

$$\frac{h}{L_A} = 0.080\left(\frac{L_A}{k}\right) - 0.233 \tag{2-18}$$

where: L_A = the total length of the spillway.

The steps at which inception of air entrainment took place, found by the analytical method, were compared to the model data from Sorensen (1985) and were found to check very closely.

2.2.8 Matos and Quintela (1995)

Matos and Quintela (1995) presented a reanalysis of data from Tozzi (1992, 1994), Lejeune et. al. (1994), Houston and Richardson (1988) and Diez-Cascon et. al. (1992). The first point of interest was a plot of friction factor f, versus k_s/D_h for the reported experimental data, where $k_s = h\cos\alpha$, h is the step height, α the spillway slope, and D_h the hydraulic diameter. A similar plot was presented by Chanson (1995) where the friction factor was computed as:

$$f = \frac{2gJD_h d^2}{q_w^2} \tag{2-19}$$

where: $J = \sin\alpha$;

q_w = water discharge per unit width.

The f values for the reported data were recalculated by Matos and Quintela using Chanson's formula and four different methods of estimating flow depth. The selection of method appeared to be determined by the type of data obtained by the researcher. Where appropriate, the flow depth was recalculated either by estimating a characteristic flow depth as defined by Tozzi (1994), by an equivalent water depth as defined by the authors, by computing the conjugate flow depth upstream of the hydraulic jump at the toe, or by velocity data obtained at the toe by Pitot tube measurements. The resulting plot showed a large amount of scatter and a lack of correlation between f versus k_s/D_h.

A plot was then constructed of C_{mean} versus H_d/d_c, where C_{mean} is the equilibrium mean air concentration, H_d is the dam crest height above the spillway toe, and d_c is the critical depth (Figure 2.7). The values of C_{mean} were directly given for the experiments of Lejeune et al (1994) and were calculated by $C_{mean} = 1 - d/y_f$ for the remaining data sets, where y_f is the normal depth of flow. The results of this plot suggested that not all of the researchers reported data for fully aerated uniform flow. This was thought to explain the scatter and lack of correlation between f versus k_s/D_h. Another result noted from this plot was that for high values of H_d/d_c, C_{mean} approaches an equilibrium value for unstepped slopes, suggesting that k_s/D_h might not have significant influence over C_{mean}.

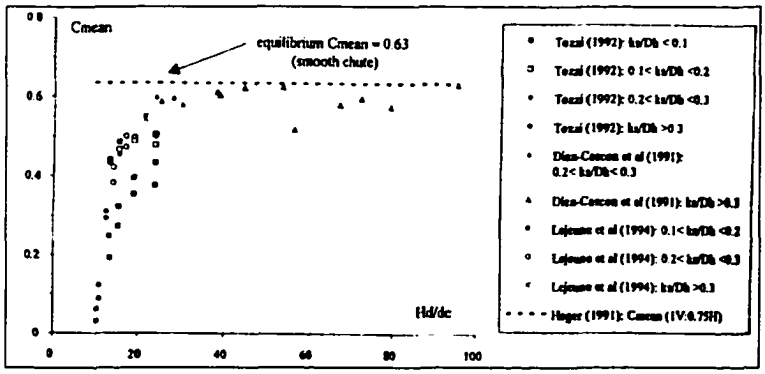

Figure 2.7 – Mean air conc. at the toe of stepped spillways, Matos and Quintela (1995).

The authors go on to compare the energy dissipation and optimal step height suggested by the referenced researchers. It was noted that various predicted values of f have a great influence on estimating energy dissipation. Similarly, suggested values of the optimum step height vary in the literature. However, it was noted that the current accepted step height is one that satisfies the criteria of $h \cong 0.3\ d_c$.

Conclusions were made that evaluating residual energy at the toe of a stepped spillway can be considerably underestimated if air entrainment is not taken into account, which can lead to unsafe designs. Suggestions for further research were made concerning collection and analysis of experimental data, specifically, air concentrations and velocities along the stepped chute.

2.2.9a Rice and Kadavy (1996)

The U.S. Department of Agriculture Soil Conservation Service, Temple, Texas, performed a model study of the proposed spillway for the Salado Creek Site 10, San Antonio, Texas. The 1:20 scale model was intended to represent a 50 ft width section of the 240 ft wide spillway. The proposed step dimensions were 2.0 ft high and 5.0 ft long, resulting in a spillway slope of 2.5H:1V. An anticipated maximum prototype discharge of 156 $ft^3/s/ft$ was tested to simulate the probable maximum flood event. Water-surface elevations were measured with both a manually operated point gauge and with piezometers located at several locations along the slope. Pitot-static tubes were used to measure velocities. It was noted that air entrainment did not exist in the flow at the design discharge. Therefore, the use of a Pitot-static tube was acceptable. Tests were first conducted on a smooth surface spillway to compare results with the stepped surface.

Energy dissipation by momentum transfer with the steps was determined by the total energy loss between the spillway crest and a given step:

$$\Delta h = H_o - H \tag{2-20}$$

where: H_o = head upstream of spillway;

H = head on the step under consideration.

Energy loss from crest to toe of the spillway, for the design discharge, varied from 48% with the stepped surface to 20% for the smooth surface. For a lower discharge of 62.5 $ft^3/s/ft$, the energy loss was even greater, varying from 71% for the stepped surface to 25% for the smooth surface. It was determined that the energy loss permitted a stilling basin approximately 70% as long as that required for a conventional smooth spillway.

Results from the Salado Creek model were compared to the results presented by Christodoulou (1993). The comparison showed the Salado Creek results followed very closely. This was not expected because of the steeper slope (0.7H:1V) used by Christodoulou. The comparison results were plotted in the form $\Delta h/H_o$ versus y_c/h and $\Delta h/H_o$ versus y_c/Nh. It was suggested that the similarity in results was due the longer slope length of a flatter slope. ".....For a given spillway height, step height, and discharge, a steep spillway slope will have a larger friction coefficient and thus a larger energy loss per unit of slope length compared with a flatter spillway slope. However, the flatter slope will have a longer slope length so the total energy loss for the flatter slope may approximate the energy loss for the steeper slope."

2.2.9b Rice and Kadavy (1997)

The U.S. Department of Agriculture Hydraulic Engineering Research Unit, Stillwater, Oklahoma was contracted to conduct a physical model study of the proposed

emergency spillway and stilling basin for Cedar Run Site 6, Fauquier County, Virginia. The spillway chute had a slope of 0.7H:1.0V and the model scale was 1:24. Three spillway configurations were tested: (1) ogee (WES) crest with a smooth chute; (2) ogee crest to point of tangency (P.T.) with 3 ft high by 2.10 ft long steps below P.T. (standard step); (3) ogee crest with variable height by 2.13 ft long steps to P.T. and 3 ft high by 2 ft long steps below P.T. (modified step). The standard and modified step configurations were tested with a U.S. Bureau of Reclamation Type III stilling basin and with a flip bucket and plunge pool for comparison. A stilling basin was not used with the smooth chute and was tested only to permit comparison of the energy dissipation between stepped and conventional concrete spillway surfaces.

Based on the design specifications, prototype discharges of 30,000, 50,000, 68,506, and 103,000 cfs were selected for detailed observations and analysis. Velocities were measured using a Pitot-static tube, differential pressure transducer and a digital voltmeter. Velocity measurements were taken along the centerline at depths normal to the plane of the chute to identify velocity profiles. The profiles were then numerically integrated to give a mean velocity. Due to air entrainment observed at 30,000 cfs, Pitot-static tube measurements were not taken at this or discharges lower than this and air entrainment was not observed at higher discharges. Tests were run at lower discharges only for the purpose of observing and recording the location at which air entrainment began. It was also observed that the flow transitioned from nappe to skimming flow regime at a flow less than 5000 cfs.

The mean velocity data were used to determine energy loss for the smooth, standard step, and modified step surfaces. Energy dissipation H_L, in percent, is given by:

(2-21)

$$H_L = \left[\frac{(H_e - H_i)}{H_e}\right] \times 100$$

where: H_e = total energy head;

H_i = energy head at i^{th} location.

Results indicated that the steps were very effective in dissipating energy compared to the smooth chute surface. At Q = 69,000 cfs , energy dissipation with the steps was approximately 4.5 times greater than the energy dissipation with the smooth chute. It was noted that there was no significant difference between the two step surfaces. Energy loss for the stepped surfaces were 28.4% and 37.6% for the lowest and highest discharges, respectively. At the design discharge, Q = 69,000 cfs, the Type III stilling basin length was predicted to be reduced by 20 to 25% without negatively affecting the energy dissipation in the basin.

An article later written by Johnson et. al. (1997), indicated that the stepped chute with a flip bucket was chosen for the design. Johnson et. al. concluded that "... conducting the hydraulic model study for the Cedar Run 6 project proved to be a cost-effective endeavor. Had it not been performed, the designers may have been compelled to recommend a much longer Type II stilling basin. Not only did the model justify the design of the Type III basin, it enabled designers to further reduce the length of the Type III basin, as well as evaluate the performance of other alternatives, including the flip bucket. The total cost for performing the hydraulic study was about $30,000 which, when compared to estimated savings in construction cost of over $700,000 for the flip bucket versus the Type II basin, was money well spent."

2.2.10 Chamani and Rajaratnam (1999)

Chamani and Rajaratnam (1999) performed laboratory experiments on a relatively large stepped spillway model of width 1.0 ft and overall height 8.20 ft. Two series of test were carried out, one with slope 0.6 and the other with slope 0.8, defined as l/h, where, l is the horizontal length and h is the height of a step. For the 0.6 slope, tests were performed on steps with h equal to 0.41, 0.21, and 0.10 ft, and for the 0.8 slope, steps with h equal to 0.41 and 0.10 ft were used.

Experiments were conducted in the skimming flow regime to determine several hydraulic characteristics of the flow such as air concentration and velocity profiles, skin friction resistance, and energy dissipation. Air concentration, C, was measured using a probe developed by Lamb and Killen (1950). Stagnation pressure in the air-water flow was determined using a Prandtl tube connected to a water manometer with a flushing system used to remove air bubbles from the system. A relationship was then developed to determine velocity from pressure and air concentration. In addition, a high-speed video camera system was used for visual observations of the flow.

An analysis of the air concentration and velocity profiles showed that the flow could be divided into lower and upper regions. The depth at which the air concentration is 90% was defined as $y_{0.9}$. Another depth used to describe the aerated flow was the transition depth y_T, where the rate of increase of C with depth y is a maximum and defined the upper level of the lower region. The results were found to agree with equations developed by Straub and Anderson (1958) to describe the air concentration distribution in the upper and lower regions. An equation for the mean air concentration, $\overline{C}$,presented in the same form as ASCE (1961), was fit to the experimental data:

$$\overline{C} = 0.93 \log \frac{(\sin\theta)^{0.1}}{q^{0.3}} + 1.05 \tag{2-22}$$

where: θ = inclination of spillway slope to horizontal;

q = unit discharge

A general relation for the skin friction coefficient was found using the additional data and known relationships from other researchers. A mean curve drawn through the data resulted in the following equation for the skin friction coefficient:

$$\frac{1}{\sqrt{c_f}} = 3.85 \log\left(\frac{Y}{k}\right) + 3.53 \tag{2-23}$$

where: c_f = skin friction coefficient;

Y = depth of flow;

k = roughness height given as $k = \frac{hl}{\sqrt{h^2 + l^2}}$

Energy dissipation was determined using the total upstream head and determining mean velocity and depth at a downstream location. It was observed that overall relative energy loss varied 48-63% for the range of discharges, 0.78 to 2.21 cfs/ft.

2.3 Self-Aerated Flow Studies

2.3.1 Ehrenberger (1926)

The work of Ehrenberger (1926) is frequently cited as the first research conducted on self-aerated open channel flow. Laboratory experiments were undertaken to increase the knowledge of velocity and air distribution in the flow on a steep chute. The research was prompted by the construction of a steep chute used to divert excess high-head flows at the Rutz Works hydropower facility in Austria. Laboratory studies were conducted in

a 0.82 ft wide, 11.5 ft high, variable slope, rectangular chute. Experiments were carried out for five different slopes of 15.5, 20.6, 32.0, 49.5 and 76.2 with four different discharges of 0.353, 0.706, 1.09, and 1.57 cfs for each slope.

Several different measurement methods were attempted to determine velocity and air distribution in the flow. High speed photography and a method of splitting the flow to measure cross-sectional area and water volume were two of the methods, both of which had difficulties. The final method used Pitot tubes to measure velocity in the lower unaerated portion of the flow and the photographic method in the upper aerated portion. Using these methods, an average normal velocity curve (".....the average velocity over the whole width of the chute at various depths normal to the bottom") was obtained. Next, the amount of aeration, p_w, in a single horizontal layer of flow was assumed to be found by the following equation:

$$p_w = \frac{2gh}{v^2} \tag{2-24}$$

where: h = water velocity head measured with the Pitot tube;

g = acceleration due to gravity;

v = average normal velocity.

Therefore, the average aeration in an entire cross section was computed as the average of the values found in each horizontal layer.

From visual observations of the flow, Ehrenberger theorized that air entrained flow was made of up four separate layers. His observations were that ".....At the top, droplets of water interspersed through the air are first noticed. Below this layer, there is a layer consisting of a mixture of air and water, which in turn covers a layer of water

containing individual air bubbles, and finally there is a layer of unaerated water adjacent to the bottom.".

Results of the experiments yielded a set of data and curves of velocity and aeration in the flow for different values of slope and discharge. Given the technological abilities and limited knowledge of spillway flows at that time, the results were ground breaking. However, research conducted since that time has shown the experimental methods to be questionable. Notably, the most significant results of Ehrenberger's work are the visual observations made in the experiments.

2.3.2 Straub and Anderson (1958)

Straub and Anderson are also classified as being among the earliest researchers to extensively investigate air-entrained flow. Model studies were performed with a variable slope, 50 ft long, 1.5 ft wide, and 1 ft deep flume at the St. Anthony Falls Hydraulics Laboratory. The test flume is considered a smooth spillway with regards to a stepped versus smooth configuration. However, an artificial roughness was applied to the floor of the flume to intensify the air-entrainment process. Multiple tests were performed in attempt to determine distribution of air throughout the flow depth for various slopes and discharges.

Measurement of air concentration and velocity were obtained using instruments developed in earlier laboratory test. Air concentration measurements were made using an electrical probe developed by Lamb and Killen (1954). The probe consisted of measuring the difference between the conductivity of an air-water mixture and the conductivity of ambient water alone. An analytical correlation between conductivity and air concentration was derived for the probe. A salt-water injection instrument was used

to measure velocities in the air-water mixture by injecting a salt solution tracer into the flow and measuring the time for the ionized tracer to pass two fixed electrodes.

Observations from the test concluded that there are two regions of self-aerated flow separated by a transition zone. The upper region of the flow consists of ".....heterogeneous clumps, globules, and droplets of water ejected from the flowing liquid stream into the atmosphere at more or less arbitrary velocities". The lower region was described as ".....consisting of air bubbles distributed through the flow by turbulent transport fluctuations." Between the two regions is a transition zone whose depth is located at the mean of the fluctuating transition surface.

Using theory from probability distributions, separate equations were developed to determine the air-concentration in the upper and lower regions. It was assumed that the distance water particles leaving the surface traveled above the surface could be represented by one half of a Gaussian distribution. Incorporating this theory with the concept of air concentration, or the number of water particles per unit area, yielded the following equation for air concentration in the upper region above the transition depth, d_T:

$$\frac{1-C}{1-C_T} = \frac{2}{h\sqrt{\pi}} \int_{y'}^{\infty} e^{-\left(\frac{y'}{h}\right)^2} dy' \qquad (2\text{-}25)$$

where: C = air concentration at any distance y' above the transition depth;

C_T = air concentration at the transition depth;

h = measure of the mean distance the particles are projected above d_T.

Air concentration in the lower region was determined to follow a parabolic distribution. The following equation was developed for the lower region:

$$C = C_1\left(\frac{y}{d_T - y}\right)^z \tag{2-26}$$

where: C_1 = air concentration at $y = d_T / 2$;

z = a constant determined by the flow parameters.

The experimental data was plotted against the theoretical equations and was shown to match extremely well.

Further analysis of the results yielded several important conclusions about self-aerated flow. The flow depth of aerated flow was shown to increase rapidly with mean air concentration. This concludes that the depth of aerated flow is greater than that for nonaerated flow due to the bulking effect of the entrained air. Furthermore, it was shown that the velocity in aerated flow is greater than that of a corresponding nonaerated flow.

The results from the experimental tests of Straub and Anderson have proven to lay the groundwork for future research in self-aerated flows. The data set from these experiments has come to be known as the "classic data set" for self-aerated flow.

2.3.3 Falvey (1979)

Falvey (1979) used dimensional analysis to determine an expression for the mean air concentration C_{mean} in fully aerated spillway flow. His conclusion was that mean air concentration is primarily a function of the Froude number F and the turbulent-interfacial tension force ratio W. The latter term was not well defined nor was there mention of how it is measured.

Falvey used laboratory and field data from several other researchers, including Straub and Anderson (1960), to correlate the functional expression. The resulting mean concentration correlation is given approximately by:

$$C_{mean} = 0.05F - \frac{(\sin\alpha)^{1/2}W}{63F} \tag{2-27}$$

where: $= \alpha$ slope angle.

It was noted that this equation is deemed valid for values of C_{mean} between 0.00 and 0.60.

2.3.4 Cain and Wood (1981)

Cain and Wood (1981) produced a two-part paper on instrumentation (part one) developed to measure air concentration and velocities (part two) within self-aerated flows on the spillway of Aviemore Dam in New Zealand. Two probes were developed, one for air concentration and one for velocity measurement.

An initial probe, shown in Figure 2.8, was constructed based on a principle developed by Keller (1972) that predicted velocities from measurements of air concentration and stagnation pressure. Air concentration was measured between the two electrodes by an electrical resistance method first adapted for self-aerated flows by Lamb and Killen (1950). Stagnation pressure was measured by a pressure transducer connected to the stagnation point and a fluid filled pressure inlet tube. Cain and Wood verified use of the conductivity portion of the probe to determine air concentrations, however, due to difficulties in determining stagnation pressure, a separate probe was developed to determine velocities.

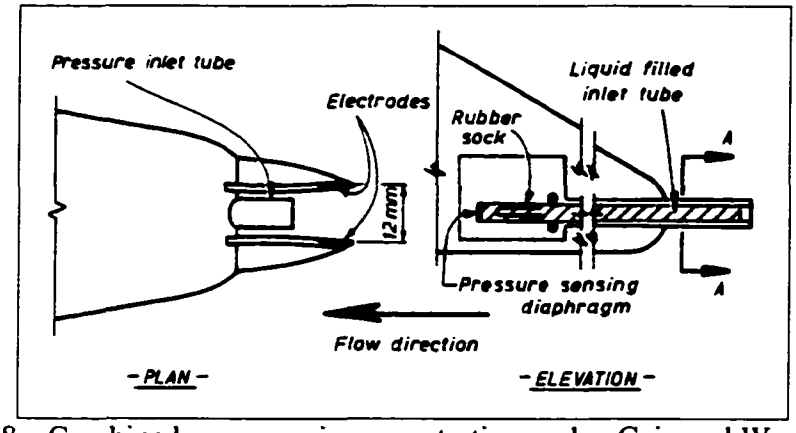

Figure 2.8 – Combined pressure air concentration probe, Cain and Wood (1981).

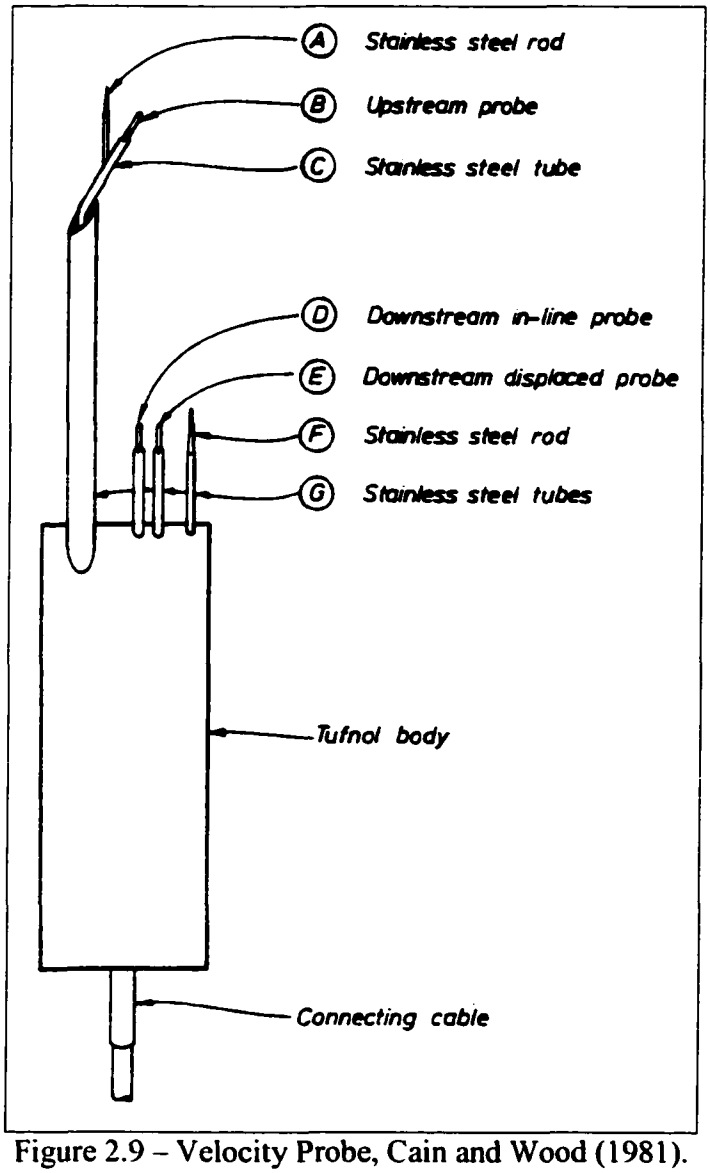

Figure 2.9 – Velocity Probe, Cain and Wood (1981).

The second probe for measuring velocities incorporated two resistivity probes aligned in the flow direction and utilized a cross-correlation technique to calculate velocity (Figure 2.9). Water velocity was essentially calculated from the time of travel of an air-water interface between the probe tips. ".....Ideally the two signals would be identical but separated by a time delay. In practice, they will differ because the upstream probe will disturb the flow. In this case, the probable time delay can be found by cross-correlating the two signals."

The second of the two papers presents the results of measurements taken in the developing region of self-aerated flow on the spillway of Aviemore Dam. From observations of the spillway flow, three regions were defined: 1) A non-aerated flow region from the spillway gate to the point of inception of air entrainment; 2) The final uniform flow region in which the air concentration and velocity profile do not change with distance down the spillway; and 3) The gradually varied flow region connecting regions 1 and 2.

Air concentration profiles were measured at five stations along the spillway and smooth curves were drawn through the data for use in further calculations. Velocity measurements were also taken at the same locations using the cross-correlation method outlined in the first paper. As a check of the accuracy of the data, the water discharge was calculated at each station by integrating over the depth, the product of velocity and (1-c) up to the limit of $c = 0.95$, where, c is air concentration. The choice of $c = 0.95$ was dictated by the maximum air concentration measured at the most downstream station. A comparison of discharge at all stations yielded errors of only 4 to 5%.

Conclusions were drawn from examining the distribution of velocity and air concentration at nondimensional distances down the spillway. It was determined that the distributions of c, $u / u_c = 90$, and $y / y_c = 90$ were functions of x / y_I , where: c = air concentration; x = the distance measured downstream from the point of inception; y_I = depth normal to the spillway at the point of inception; y = depth normal to the spillway; $y_c = 90$ = a characteristic depth where the air concentration is 90%; u = velocity; and u_c=90 = velocity at the characteristic depth. The results were presented and reported for the Aviemore Dam for a 45° slope.

2.3.5 Chanson (1993)

In recent years, several publications pertaining to self-aerated spillway flow have come from Hubert Chanson of the University of Queensland. Chanson is one of few researchers specifically addressing air entrainment in stepped spillway flows. However, in contrast to other researchers, Chanson does not use original data and the majority of his research comes from the re-analysis of data from other researchers. Nonetheless, it is of value to review a portion of his work.

The majority of Chanson's results are a refinement of previous research in the literature and he appears in agreement with most researchers on the mechanics of flow, energy dissipation and regimes on stepped spillways. Of particular interest are the results and conclusions on the effects of air entrainment in the uniform flow region along the spillway. Chanson stated that ".....the rate of energy dissipation on smooth spillways is affected much more by air entrainment than on stepped spillways. On stepped spillways, air entrainment seems to have little effect on the energy dissipation." However, an analysis of the residual energy showed that ".....residual energy is strongly

underestimated if the effect of air entrainment is neglected." It was suggested that "....aeration of the flow decreases the friction factor and increases kinetic energy of the flow. As a result, residual energy increases with air concentration."

Chanson's conclusions were mainly derived from a combination of friction factor and energy dissipation equations developed by previous researchers. However, he does present the notion of a separate set of equations for the case of air entrained flow. Specifically, these equations differ by an aerated flow versus a non-aerated flow friction factor. This separate friction factor is a function of average air concentration, Reynolds number, the non-aerated flow friction factor, and relative roughness (step geometry). It would appear that the lack of available data to determine these parameters would make the friction factor(s) difficult to calculate. Chanson makes several assumptions in his analysis to arrive at his conclusions. In his defense, Chanson presents several interesting theories and recognizes the requirements for further measurements of air concentration and velocity in aerated flows on stepped spillways.

2.4 Recommendations From Literature

Review of stepped spillway literature recognizes the need for future research in the field of stepped spillway design. In determining those needs, it is of value to review specific suggestions made by several authors:

Sorensen (1985) suggested that there is a need ".....to provide additional information necessary to optimize the step geometry for a given spillway discharge, face slope, and crest elevation." This design information will ".....optimize response to construction and energy dissipation requirements."

Houston (1987) emphasized the need to ".....determine the practical maximum unit discharge for stepped spillways based upon generalized design data that relates flow depths to energy dissipation."

Chanson (1994) identified flow characteristics of the skimming flow regime and air entrainment as two areas where future research is necessary. Additional information on the mechanisms of flow recirculation in the cavities produced by skimming flow will provide further insight pertaining into energy dissipation along the spillway. In addition, measurement of air entrainment presently remains an area that lacks experimental data and accurate instrumentation.

Rajaratnam (1990) made no direct suggestions for future research, however, his prediction as to the onset of skimming flow as a function of y_c/h is frequently tested. Additional experimental data of this phenomenon may provide conclusions on the transition of flow regimes from nappe to skimming flow.

Diez-Cascon et. al. (1991) expressed the need for additional research concerning air entrainment in stepped spillway flow.

Bindo et. al. (1993) and Zhou (1997) both indicated the need for further research into air entrainment. Both authors also noted the need for prototypical observations and data.

Matos et. al. (1995) commented upon the need for accurate measurement of water velocities and air concentration. Suggestions for further areas of research included flow recirculation mechanics and the gradually varied flow region between the point of inception and the uniform flow region.

Suggestions from the literature clearly indicate the need for continued research in the field of stepped spillways. Of greatest importance is accurately quantifying energy dissipation provided by the steps. Energy dissipation is dependent on many factors such as step geometry, embankment slope, flow regime, and the number of steps. Determining the kinetic energy of the flow requires accurate measurement the velocity distribution in the flow. As stated by most, if not all, researchers, this is difficult because of "bulking" of the flow due to air entrainment. Conventional means of measuring velocities with a Pitot-static tube underestimate velocities and, therefore, underestimate residual energy at the spillway toe.

Data presented in the reviewed literature were obtained from scale models ranging from 1:5 to 1:60 (Table 2.1). Presently, two references, Ruff and Frizell (1994) and Hewlett et. al. (1997), appear to be the only ones to evaluate and document prototypical scale stepped spillways. In both cases, pre-formed overlapping concrete blocks were used with step heights generally less than 1.64 ft. To date, there is no knowledge of existing data for step heights greater than 1.64 ft, where most applications are for step heights of up to 2.0 ft. Gathering prototype scale data would have a two-fold effect by verifying scale model results and adding to the existing body of experimental data. Both of these effects are seen as beneficial in any research field and can be especially beneficial in the area of stepped spillway design. Suggestions from the literature for continued stepped spillway flow research therefore include:

i) measurement of air concentration, depth of flow, and velocity;

ii) energy dissipation;

iv) prototype scale data.

Table 2.1 - Summary of model tests.

Reference	Slope (deg)	Slope, H:V H:1.0	Model Scale	Prototype Step Height (ft)	Model Step Height (ft)	Number of Steps	Prototype Unit Discharge (cfs/ft)	Model Unit Discharge (cfs/ft)
Essery and Horner (1978)	11.31	5.00			0.16	12		
	21.80	2.50			0.03	20		
	22.83	2.38			0.09	30		
	22.83	2.38			0.17	20		
	22.83	2.38			0.33	10		
	22.83	2.38			1.48	8		
	27.74	1.90			0.12	30		
	27.74	1.90			0.42	10		
	32.25	1.58			0.50	10		
	36.35	1.36			0.16	30		
	36.35	1.36			0.58	10		
	40.10	1.19			0.19	30		
	40.10	1.19			0.67	10		
	45.00	1.00			0.03	20		
Sorensen (1985)	52.05	0.78	1/10	2.00	0.20	11	17.0 to 793.3	0.05 to 2.51
			1/25	2.00	0.08	59		
Houston (1987)	31	1.66	1/15	0.61	0.13	85		
Bayat (1991)	51.3	0.80	1/25	1.97	0.08		202.0 to 2354.0	0.065 to 0.75
				2.46	0.10			
				1.64	0.07			
Diez-Cascon et al. (1991)	53.1	0.75	1/10	0.30	0.10	100+	7.32 to 36.27	0.24 to 0.30
	53.1	0.75		0.60	0.20	50+		
Bietz and Lawless (1992)	51.3	0.80	1/60	3.94	0.07	10	180 to 27,911	0.006 to 1.00
	48	0.90						
Frizell (1992)	26.6	2.00			0.17	80+		6.21, various
Peyras et al. (1992)	18.4	3.01	1/5	1.00	0.66	3	7.5 to 30.1	0.43 to 2.70
	26.6	2.00		1.00	0.66	4		
	45.0	1.00		1.00	0.66	5		
Bindo et. al. (1993)	51.3	0.80	1/20	0.80	0.13	31	193 to 2734	0.11 to 1.53
			1/40	0.40	0.07	43	762.5 to 4357.0	0.075 to 0.431
Christodoulou (1993)	55.0	0.70			0.08	15		0.22 to 1.00
Lejuene and Lejuene (1994	51.3	0.80	1/21	0.80	0.12	32	0 to 172.2	0 to 0.085
			1/42		0.06	64		0 to 0.015
Tozzi (1994)	53.13	0.75	1/15	0.08	0.02		53.8 to 129.2	0.06 to 0.15
				0.15	0.03			
				0.20	0.07			
				0.30	0.10			
				0.60	0.20			
Rice et al. (1996)	21.8	2.50	1/20	0.61	0.10	27	62.5 to 156.0	0.032 to 0.086
Rice and Kadavy (1997)	55	0.70	1/24	0.914	0.12	15	416.6 to 1431.2	0.15 to 0.50
Zhou et al. (1997)	53.13	0.75				45		0.125 to 2.03
Tozzi et al (1998)	52.22	0.775	1/15	0.80	0.17	50	10.8 m head	
Robinson et. al. (1998)	53.13	0.75	1/40	0.90	0.07	20?	<20 to 400	0.002 to 0.040
				1.80	0.15	40?		
Yildiz et. al. (1998)	30	1.73			0.08			0.43 to 2.60
	30	1.73			0.25			
	51.3	0.80			0.08			
	51.3	0.80			0.25			
	60	0.58			0.08			
	60	0.58			0.25			
Chamani and		0.6			0.41	>15		0.81 to 2.21
Rajaratnam (1999)		0.6			0.21			
		0.6			0.10			
		0.8			0.41			
		0.8			0.10			
Present Study	26.6	2.0			2.00	25		5 to 30
	26.6	2.0			1.00	50		

CHAPTER 3

TEST FACILITY AND EXPERIMENTAL PROGRAM

3.1 Test Facility

Tests were carried out at the outdoor testing facility located at the Colorado State University Engineering Research Center approximately four miles west of the main Colorado State University campus. The Dam Overtopping Facility is an existing chute structure built in 1991 under a cooperative research agreement between the Bureau of Reclamation and Colorado State University. The test facility is comprised of a water supply pipeline, baffled head box, entrance/transition, chute, stilling basin, and outlet works. The concrete chute is approximately 112 ft long, 10 ft wide and 5 ft deep on a 2:1 (horizontal : vertical) slope and has a total height of 50 ft.

For the present study, the width of the chute was reduced to 4 ft using a dividing wall (Figure 3.1). In addition, flashboards were placed on the walls of the test portion of the chute, extending the depth to 7 ft, providing additional freeboard. Plexiglass windows, 4 ft by 4 ft were installed at five locations in the dividing wall to provide observation of flow in the chute.

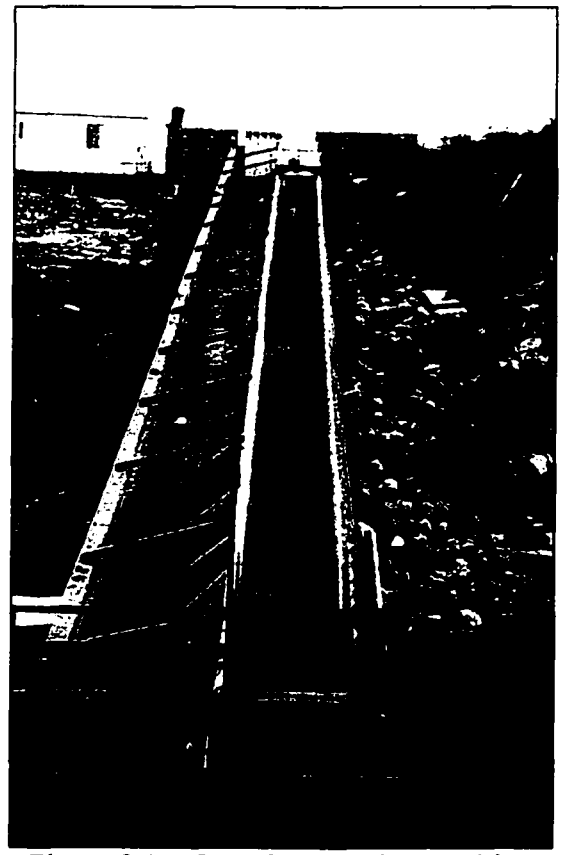

Figure 3.1 – Dam Overtopping Facility.

Water is supplied through a 3 ft diameter pipeline, approximately 1/2 mile long, from nearby Horsetooth Reservoir. At maximum reservoir elevation, the facility is capable of direct discharges up to approximately 120 cfs. For the 4 ft wide chute in the present study, a maximum unit discharge of 30 cfs/ft, corresponding to 4.6 ft of overtopping head, was attained. A series of valves along the pipeline are used to control discharge. Flow is monitored with a sonic flow meter in the supply pipeline to the facility headbox.

3.2 Experimental Program

The experimental program focused on evaluating hydraulic characteristics of flow over simulated roller compacted concrete (RCC) steps at near-prototype conditions. Two

series of tests with different step geometries were conducted. The first series consisted of twenty-five horizontal steps with height h = 2.0 ft and length l = 4.0 ft, thereby maintaining the 2:1 (horizontal : vertical) slope (Figure 3.2). Installation of an infill provided fifty steps with height h = 1.0 ft and length l = 2.0 ft, constituting the second test series (Figure 3.3). A third series was carried out on the smooth surface of the chute with the steps removed for reference and comparison purposes.

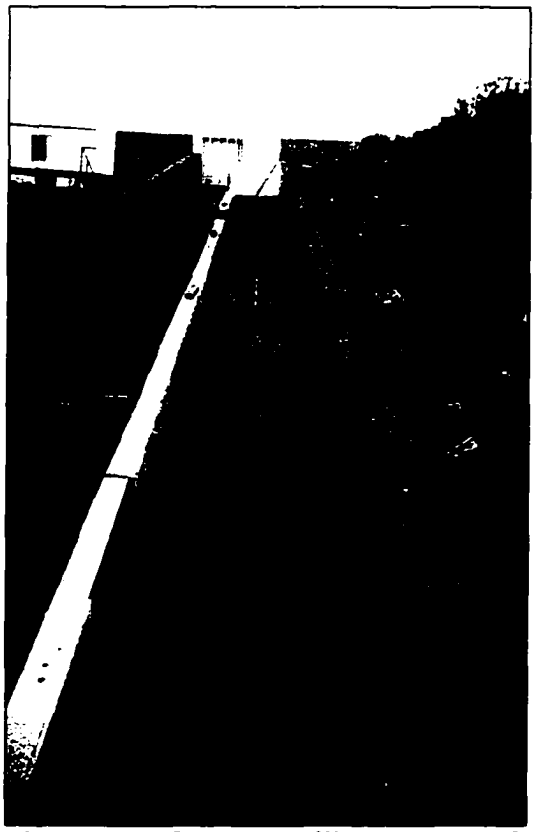

Figure 3.2 – Stepped Spillway, h = 2.0 ft.

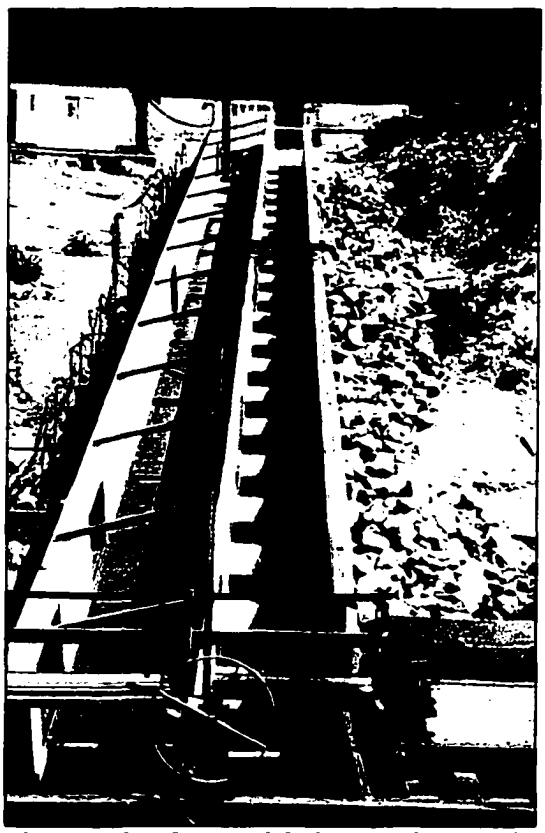

Figure 3.3 – Stepped Spillway, h = 1.0 ft (note: 1.0 ft infills are shown *not* painted.)

The steps were fabricated from pressure treated lumber and plywood. Selection of step size was based mainly on the size of available materials (i.e. 4.0 ft nominal width). However, a significant number of RCC and conventional stepped spillways have step heights on the order of 1.0 to 2.0 ft (Chanson, 1994). The h = 2.0 ft steps were constructed during the summer of 1999 and tested in the fall of 1999 and spring of 2000.

Construction and collection of data for the h = 1.0 ft steps and smooth surface were carried out during summer 2000. Due to weather restrictions of the outdoor testing facility, testing discontinued through the winter months.

A test series consisted of collecting data at selected locations over a range of flow rates. Data collected included: flow rate; overtopping head; impact pressures on the steps; air concentration profiles; and velocity profiles. In addition, visual documentation was obtained on videotapes in VHS format and 35-mm prints. Specialized instruments were developed and calibrated for collecting air concentration, velocity, and impact pressures. Detailed explanation of instrumentation and data acquisition is given in Chapter 4.

3.2.1 - Discharge

For h = 2.0 ft, data were collected at discharges of 20, 40, 60, 80, and 100 cfs. Initial observations revealed that this range of discharges provided data in both the nappe and skimming flow regimes. For h = 1.0 ft, the range of discharges were determined from the h = 2.0 ft test series according to the ratio y_c/h, where y_c is critical depth. Holding this ratio constant and solving for a new critical depth based on the new step height gave a range of discharges for the h = 1.0 ft test series (Table 3.1).

Table 3.1 – Determination of test series discharges.

Stepped Spillway $h = 2.0$ ft				Stepped Spillway $h = 1.0$ ft			
Total Discharge (cfs)	Unit Discharge (cfs/ft)	Critical Depth (ft)	y_c/h	*y_c/h	Critical Depth (ft)	Unit Discharge (cfs/ft)	Total Discharge (cfs)
20.0	5.0	0.92	0.46	0.46	0.46	1.8	7.1
40.0	10.0	1.46	0.73	0.73	0.73	3.5	14.1
60.0	15.0	1.91	0.96	0.96	0.96	5.3	21.2
80.0	20.0	2.32	1.16	1.16	1.16	7.1	28.3
100.0	25.0	2.69	1.34	1.34	1.34	8.8	35.4
116.0	29.0	2.97	1.48	1.48	1.48	10.3	41.0

*held constant.

In order to gather a reasonable amount of data and collect data in such a way that it may be compared during analysis, discharges of 7.1, 21.2, and 41.0 cfs from Table 3.1 and three higher discharges of 60, 80 and 100 cfs were selected for the h = 1.0 ft tests. This provided data that may be compared numerous ways during analysis between the two different step sizes. Table 3.2 shows the final selection of discharges for each test series.

Table 3.2 – Final discharges tested for each test series.

Stepped Spillway $h = 2.0$ ft		Stepped Spillway $h = 1.0$ ft		Smooth Spillway	
Total Discharge (cfs)	Unit Discharge (cfs/ft)	Total Discharge (cfs)	Unit Discharge (cfs/ft)	Total Discharge (cfs)	Unit Discharge (cfs/ft)
20.0	5.0	7.1	1.8	20.0	5.0
40.0	10.0	21.2	5.3	40.0	10.0
60.0	15.0	41.0	10.3	60.0	15.0
80.0	20.0	60.0	15.0	80.0	20.0
100.0	25.0	80.0	20.0		
[1]maximum		100.0	25.0		
		[1]maximum			

3.2.2 – Stationing

For each test series, air concentration and velocity profiles were measured at five locations along the spillway. Stationing was defined as the distance, s, measured parallel to the spillway floor from a designated reference datum to the point of data collection. It is accepted practice within stepped spillway research to assume that the tips of the steps form a psuedo-bottom from which references can be made (Figure 3.4). Therefore, for the stepped spillway tests with h = 2.0 ft and h = 1.0 ft, the reference datum is located at the tip of the first step, perpendicular to the spillway floor. For the smooth spillway tests, the reference datum is located at the crest of the concrete chute. Data collection stationing and corresponding step numbers for each test series are given in Table 3.3 and shown in Figure 3.4.

Table 3.3 – Data collection stationing for each test series.

Stepped Spillway h = 2.0 ft		Stepped Spillway h = 1.0 ft		Smooth Spillway	
Station, s (ft)	Corresponding Step Number	Station, s (ft)	Corresponding Step Number	Station, s (ft)	Corresponding Step Number
13.4	4	13.4	7	15.9	-
31.3	8	31.3	15	33.8	-
49.2	12	49.2	23	51.7	-
67.1	16	67.1	31	69.6	-
85.0	20	85.0	39	87.4	-

[1] Maximum discharge was considered the discharge obtained with a fully open control valve and was dependent on the water surface elevation available in Horsetooth Reservoir.

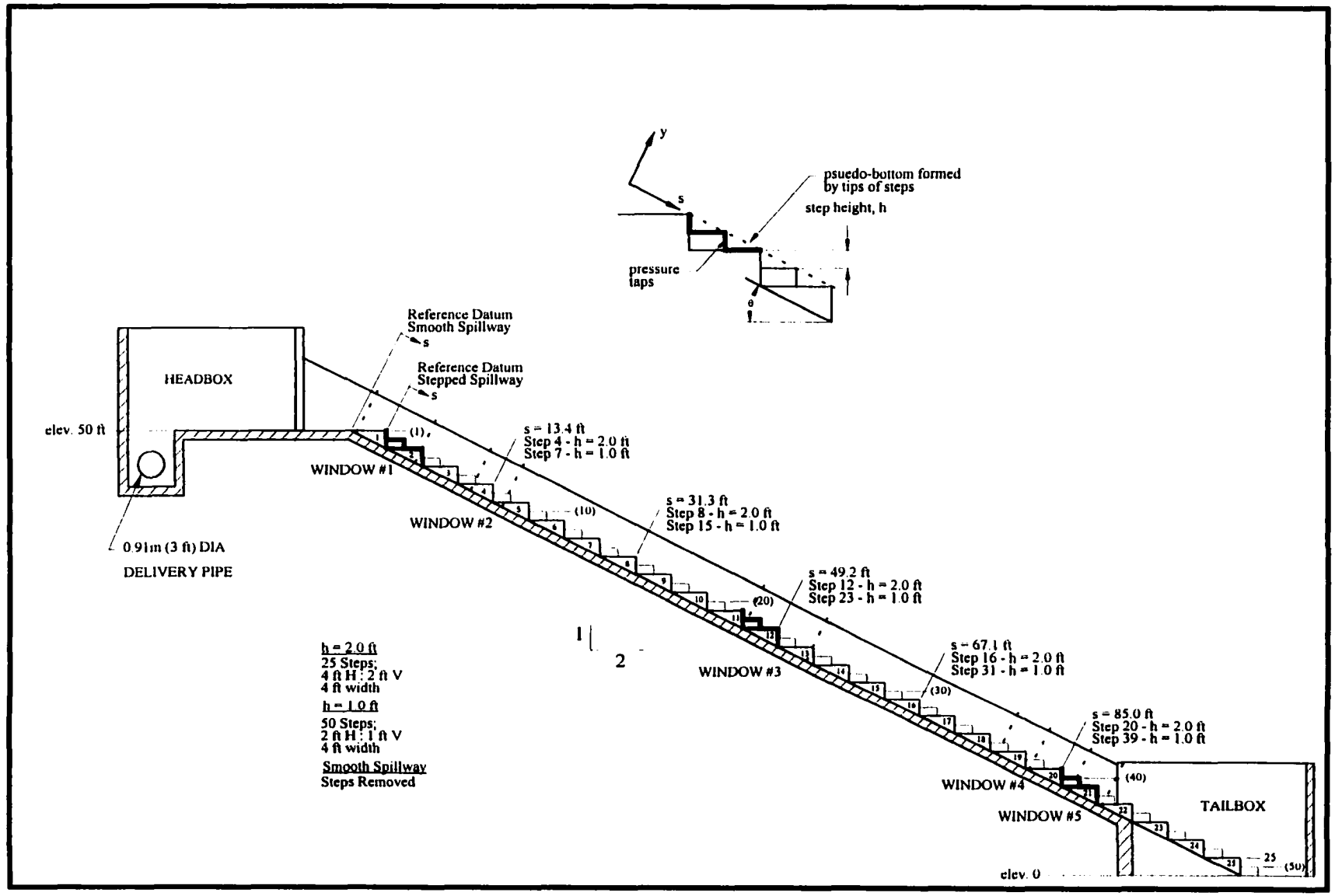

Figure 3.4 – Spillway Stationing.

Air concentration and velocity instrumentation were mounted on a point gage and carriage system for collecting data at the various stations (Figure 3.5). The manually operated carriage system allowed for two degrees of freedom with movement along the length of the spillway parallel to the floor, and lateral movement within the width of the spillway. The remote operated, motorized point gage allowed for vertical movement of the instrumentation perpendicular to the floor of the spillway to obtain data profiles within the flow.

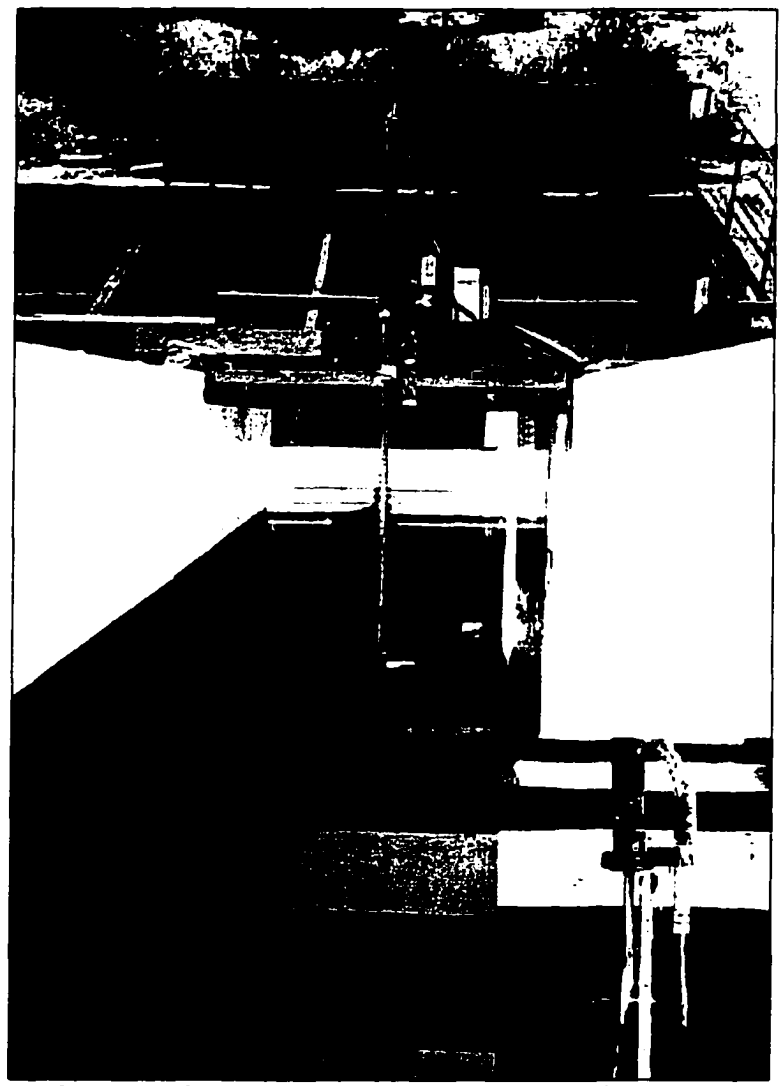

Figure 3.5 – Carriage and point gage system with instrumentation.

3.2.3 – Data Collection

More than 2,400 individual data points were collected over the course of the three test series. With exception of the pressure data, these data points were taken with the air concentration and velocity instrumentation mounted on the point gage shown in Figure 3.5 and described in Chapter 4. For each test series, air concentration and velocity profiles were taken for all discharges given in Table 3.2 at each of the five stations given in Table 3.3 for a total of approximately 85 profiles, not including retaken or preliminary data. All profiles were taken along the centerline of the flume (2 ft lateral distance from the wall) normal to the spillway floor. Each profile consisted of anywhere from three to thirty data points depending upon the depth of flow and reading interval chosen. The lowest readings were usually taken at approximately 0.05 ft from the tip of the step. The uppermost readings were generally taken where both instruments measured data that was near the dry-air readings and visually appeared almost out of the flow. In general, readings were taken at intervals of 0.1 ft for low flow depths and several points at the beginning and end of deeper flow depths. Intervals of 0.2 ft were normally chosen in the middle portion of deeper flow depths. Detailed discussion of characteristic flow depths and data profiles is given in Chapter 5.

Other data included visual observations of the flow, measurement of flowrate, and overtopping head. In general, these data sets were taken concurrently with the air concentration and velocity profiles. However, test sessions were occasionally conducted to specifically record and observe flow characteristics and other flow phenomena for each test series.

3.2.4 - Overtopping Head

The pipeline that delivers water to the overtopping spillway terminates in a baffled pipe section contained in a 4.0 ft deep sump within the spillway headbox. Water entering the facility fills the sump, overtops into the headbox, and is channeled through curved transition walls into the four-foot wide chute before cascading over the first step. The length of the curved transition area is approximately 4 ft long leading into a 6 ft straight section. Upon initial startup of the first test series with h = 2.0 ft, at low discharges, the flow was observed to spring free of the step surface near the crest. An immediate solution to this problem was installation of a 1.8 ft weir spanning the width of the chute. Location of the weir is approximately at the downstream end of the curved transition walls. The weir remained in place for the duration of all testing.

Staff gages in the headbox were used to measure water depth from the headbox floor to the water surface. Therefore, overtopping head was determined by subtracting the weir height from the staff gage readings. A rating curve for the headbox and 4 ft wide chute with the weir installed is shown in Figure 3.6.

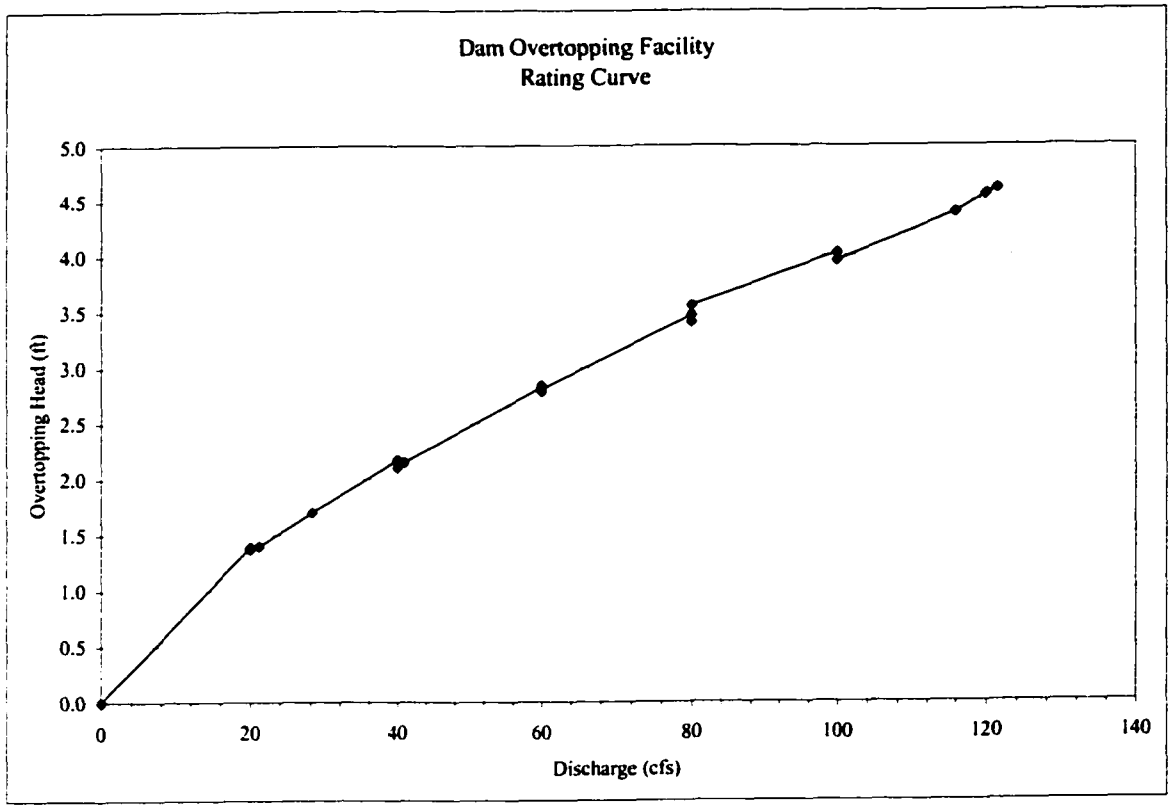

Figure 3.6 – Dam Overtopping Facility Rating Curve.

CHAPTER 4

AIR CONCENTRATION, VELOCITY, AND PRESSURE INSTRUMENTATION

4.1 Air Concentration Measurement

An air concentration probe based upon previous work by Cain and Wood (1981) was used to determine the percentage of air contained in the flow. The principle used for measuring air concentration is based on the difference in electrical resistivity between air and water. The probe acts as a bubble detector by passing a current through two conductors spaced a small distance apart and measuring the change in conductivity that occurs when a bubble impinges on the probe tip. The interruption of the current when a bubble passes is a step change from a relatively high conductivity with the probe in water, to nearly zero conductivity when a bubble breaks the conducting path. Integrating this signal over time gives the probability of encountering air in the air/water mixture. The probe and associated electronics used in the present study and discussed here were developed and constructed by the U.S. Bureau of Reclamation (Reclamation) based on this principle (Frizell et. al., 1994).

Before continuing into a full description of the air concentration probe, it is necessary to define the term *air concentration.* Many theories of self-aerated flow suggest that the flow depth is divided into at least two regions (Ehrenberger (1926), Straub and Anderson (1958), and Killen (1968)). The lower region consists of water

containing individual air bubbles distributed throughout the flow and exchanged with the upper region. The upper region contains an ill-defined wavy water surface in which air is trapped or surrounded by waves and other breaks in the surface. Based on this theory, Wilhelms (1994) makes the distinction between *entrained air* and *entrapped air* (Figure 4.1). Entrained air is contained and transported in the lower region of flow in the form of air bubbles. Entrapped air in the upper region is transported in the trapped region of the irregular, wavy surface. Entrained air and entrapped air together make up the total air transported with the flow. As mentioned above, the air probe used in this study is based on a break in the conducting path of the submerged probe tip. Therefore, the probe cannot distinguish between individual entrained air bubbles and entrapped air contained in breaks of the flow surface. However, the objective of this study is to determine a characteristic total flow depth for designing training walls and computing other parameters. The bulked flow depth is based on the content of air throughout the entire flow depth and the distinction between entrained and entrapped air is not necessary. Wilhelms (1994) states that ".....for bulking interests, total conveyed air is of prime importance, and the differentiation of entrained and entrapped air is of no consequence." In light of this, the term air concentration is used in this thesis to describe the total transported air within the flow, both entrained and entrapped.

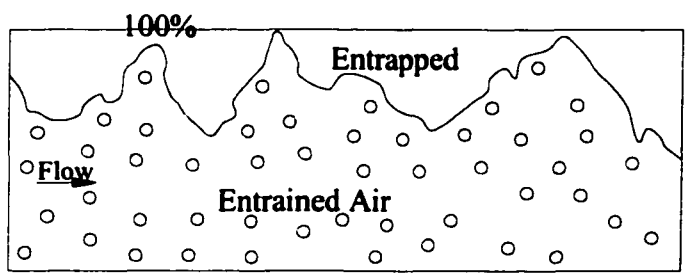

Figure 4.1 – Entrained versus entrapped air (after Wilhelms (1994)).

4.1.1 Air Probe

An earlier air probe developed by Reclamation has been used in similar flow conditions with successful results (Frizell et. al., 1994; Gaston, 1995; Ruff and Frizell, 1994). The earlier probe consisted of two concentric conductors, a 0.008 in (0.2 mm) platinum wire within a 0.03 in (0.8 mm) diameter stainless steel sleeve, encased in a protective support. The probe proved to work well, however, problems arose with electroplating of the conductors, degradation of the probe's brass encasement, water entering and shorting the conductors, and streamlining of the supportive mechanism.

The air probe used in the present study is a redesign of the earlier probe and consists of two platinum wires as conductors, separated by approximately 0.08 in (2.0 mm). The wires are encased in a nonconducting acrylic tip and fit into a 0.25 in (6.35 mm) stainless steel supporting tube (Figure 4.2).

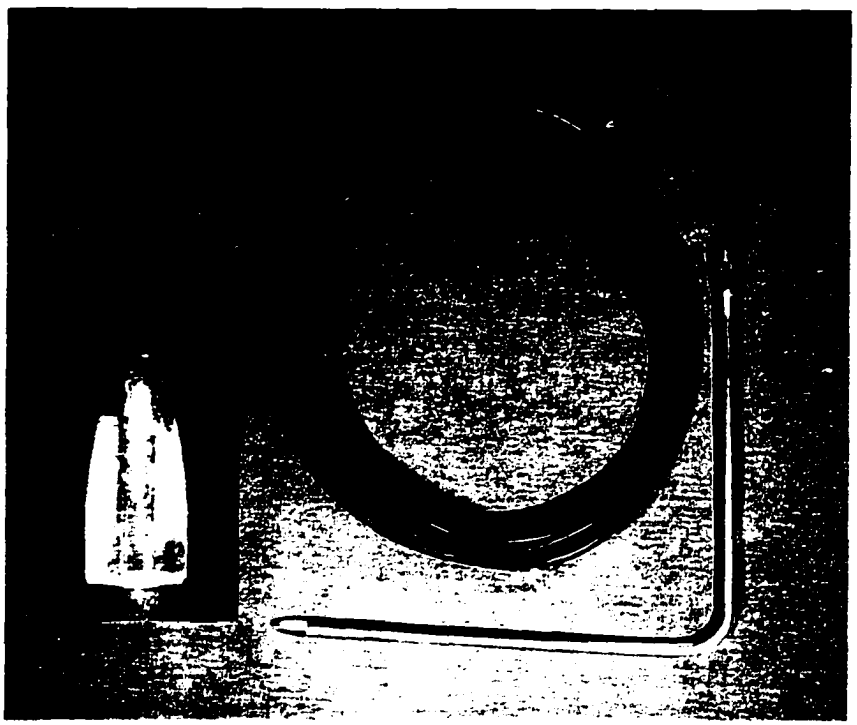

Figure 4.2 – Air concentration probe.

4.1.2 Air Probe Electronics

Electronics for producing and processing current through the air probe were also developed by Reclamation (Frizell et. al., 1994; Jacobs, 1997). The electronics package consists of the following general components: an anti-plating signal supplied to the probe to prevent electroplating and gassing on the probe tip; adjustable gain for the conductivity of the water being tested; amplification and averaging of the signal from the probe; and isolation of the output signal for further processing.

With the air probe in water and no air present, a constant high voltage (approximately 5.0 volts) is conducted across the probe tip. When an air void is detected by the probe tip, i.e. a bubble, the voltage drops to approximately zero volts. Inverters in the electronics package invert the output voltages resulting in a low voltage for clear water (zero volts) and a high voltage (5 volts) when air is detected. Consequently, a stream of pulses with constant height and variable width is generated which depends on the amount of air detected in the water. The ratio of air to water is approximately given by the ratio of time that a high voltage pulse is detected to the time that a low time voltage pulse is detected during the measurement period (Jacobs, 1997).

Two forms of output are provided from the electronics package. An analog voltage signal, representing a 10-second moving average of the high-low pulse stream, produces readout of air concentration on a LCD display. A digital voltage signal is also provided through an optical isolator that can be used for further processing. The LCD display was not used due to high fluctuations of the reading and the difficulty of estimating an average air concentration. Consequently, the digital signal was fed to data

acquisition hardware and a personal computer. The air probe and electronics package are shown in Figure 4.3.

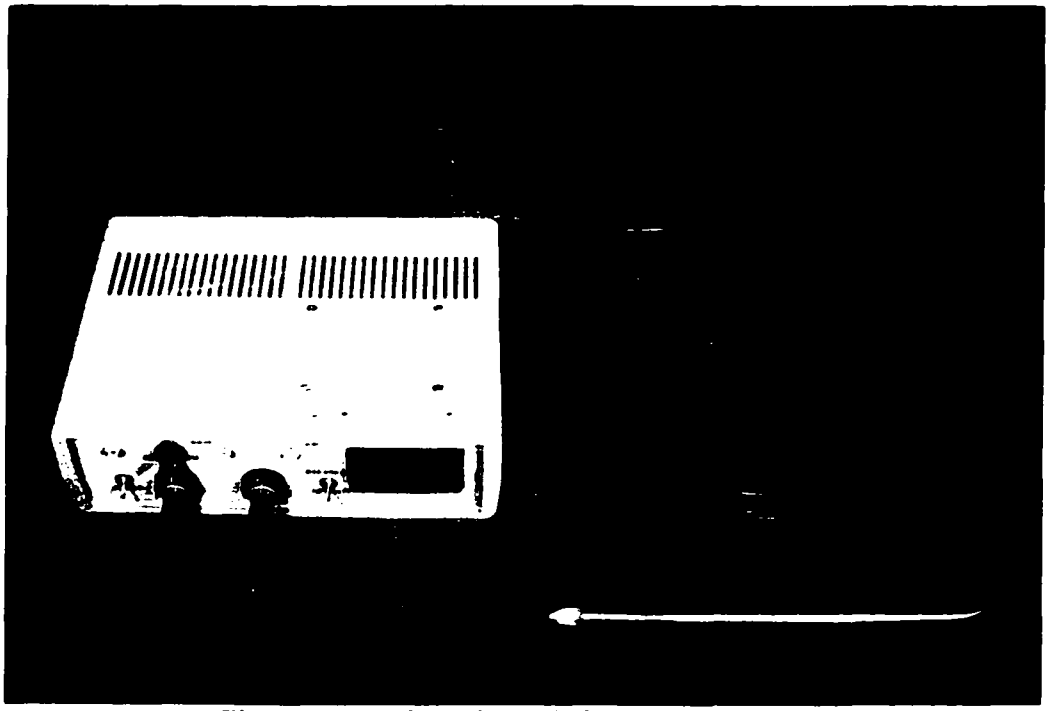

Figure 4.3 – Air probe and electronics package.

4.1.3 Data Acquisition and Air Concentration

The digital signal provided by the air probe electronics package was fed to a Dataq Instruments Inc., model DI-220, portable data acquisition system attached to a IBM compatible personal computer. The DI-220 system receives the isolated digital signal from the electronics package, processes it as an analog waveform, and outputs the waveform to the personal computer. The computer software provided with the acquisition system, WINDAQ/200, allows for realtime display and recording of the waveform. In addition, the system provides the capability of sampling the signal at variable frequencies and durations. For the air probe, a frequency of 15,000 Hz for a

duration of 5 seconds was selected based on laboratory testing and sensitivity analyses of sampling frequency. Further discussion is given in *Section 4.4 Sampling Frequency.*

The output stream of voltage pulses generated by the air probe were either 5.0 volts for 100% air or 0.0 volts for 0% air, resulting in an approximately square waveform. Therefore, average air concentration may be determined by computing the percentage of time the probe encounters air, or simply dividing the area under the waveform by the maximum voltage multiplied by the sample duration:

$$c_p = \frac{1}{V_{max} T} \int_0^T V(t)dt = \frac{A}{V_{max} T} \tag{4-1}$$

where: $V(t)$ = voltage waveform;

A = area under the air probe waveform (volt-seconds);

V_{max} = maximum voltage (volts);

T = duration of sample (seconds)

A statistics function within the WINDAQ/200 software provides the required information for equation (4-1). A portion of a typical air probe signal is shown in Figure 4.4. Note that the voltage ranges from approximately 0.24 volts for 0% air to 3.93 volts for 100% air. It was verified that the signal range is affected by the electronics of the optical isolator and causes the range to be other than 0 to 5 volts. Nonetheless, equation (4-1) still holds.

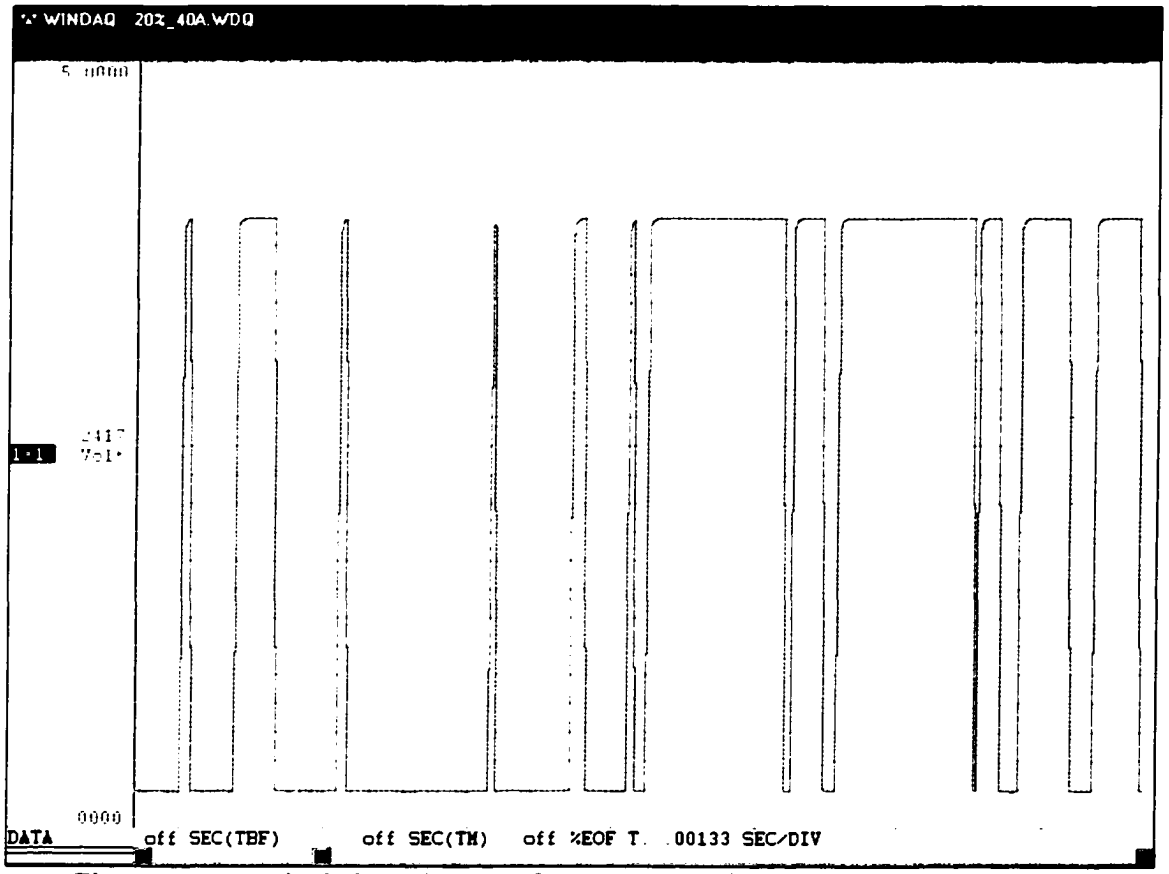

Figure 4.4 – Typical air probe waveform at a sampling frequency of 15,000 Hz.

4.2 Velocity Measurement

Flow conditions in the present study may be described as high-velocity, turbulent, two-phase flow. Therefore, a probe to measure velocity was required that would withstand high impact forces and be able to accommodate a nonhomogeneous fluid of varying density. Based upon previous work by Reclamation, a back flushing Pitot-static tube, designed for mounting on the fuselage of an airplane, was selected (Frizell et. al., 1994; Gaston, 1995; Ruff and Frizell, 1994; Matos and Frizell, 2000). The probe is sturdy and provides a means of continuous back flushing to ensure a single density fluid within the Pitot tube. A picture of the Pitot tube is shown in Figure 4.5.

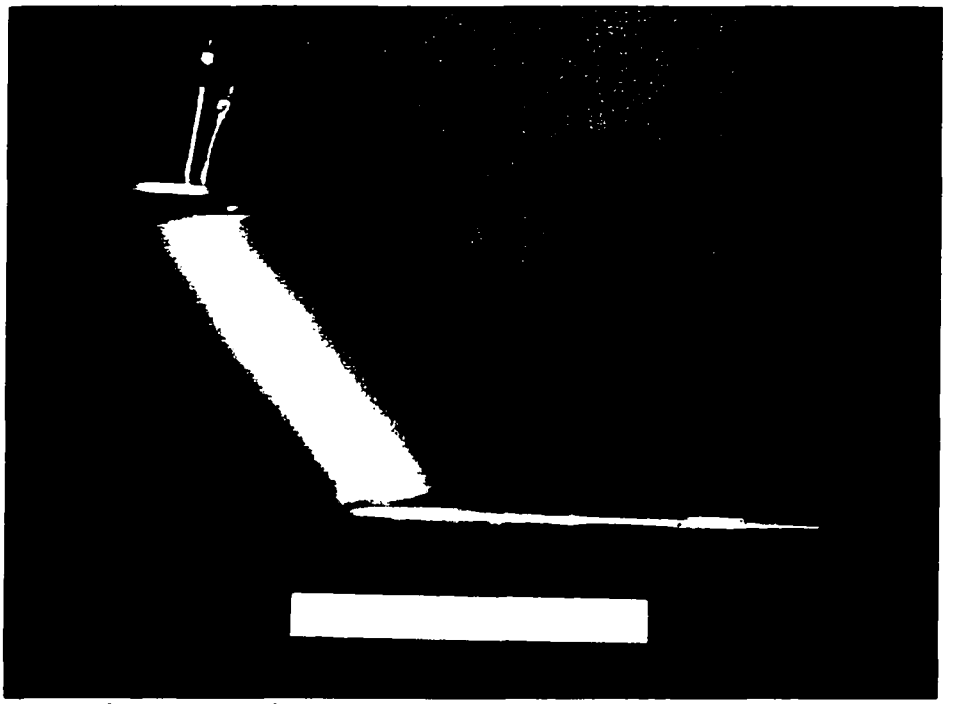

Figure 4.5 – Pitot tube (the scale shown is 15 cm in length).

Back flushing flow is provided to the Pitot tube from a constant head source. Selection of back flushing pressure and flow rate depends upon the pressures expected in the flow. Velocity from the Pitot tube is determined by the difference in pressures at the kinetic and static ports. Therefore, a balance between ensuring that air does not enter the Pitot tube and the sensitivity of the pressure difference must be found. Based on experience from previous experiments and laboratory testing, back flushing pressures of between 2.5 and 8.0 psi were selected for the present study conditions, approximately 10 – 20 gal/hr. The Pitot tube used in this study was patented in 1969 and manufactured by Rosemount, Inc. The Pitot tube was originally intended for mounting on the fuselage of an aircraft for measuring the velocity of air, not water with a back flushing flow. As a matter of curiosity, a surplus Pitot tube was cut in half to determine the internal flow path of the static and kinetic ports. Figure 4.6 shows the complex flow paths within the Pitot tube. The dynamic port is essentially a tube centered within the concentric outer shell

with an exit at the tip of the instrument. The static ports penetrate the outer shell into the annulus surrounding the center tube.

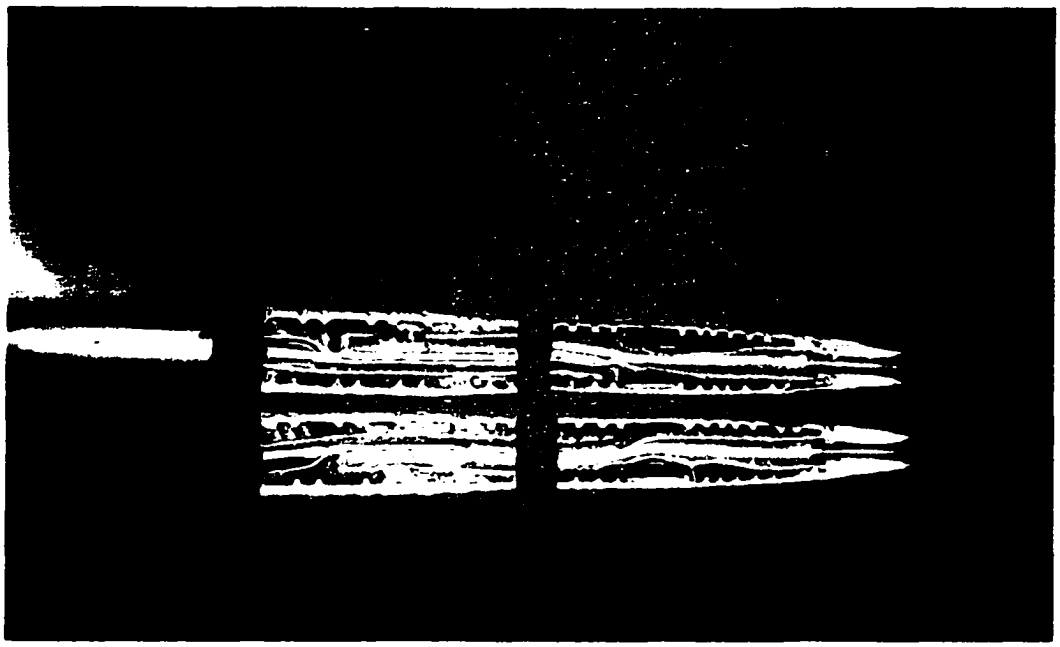

Figure 4.6 –Flow path through Pitot tube.

The differential pressure between the static and kinetic ports is recorded using a calibrated differential pressure cell. Voltage output from the pressure cell is fed into a Sensotec Inc., model GM Conditioner-Indicator where voltage span and zero adjustments can be made using potentiometers provided on the unit. Back flushing pressure and flow through the pressure cell are both adjusted in air without flowing water such that the Sensotec unit displays zero voltage, corresponding to zero differential pressure and zero velocity. The signal from the Sensotec unit is sent to the Dataq data acquisition system and recorded on the personal computer with the WINDAQ/200 software. Through laboratory testing and sensitivity analyses, a sampling frequency of 120 Hz for a duration of 20-seconds was selected for recording the Pitot tube waveform. Using the pressure cell calibration, an average voltage obtained from the Pitot tube waveform can be converted to pressure head. Figure 4.7 shows the Pitot tube and pressure cell setup.

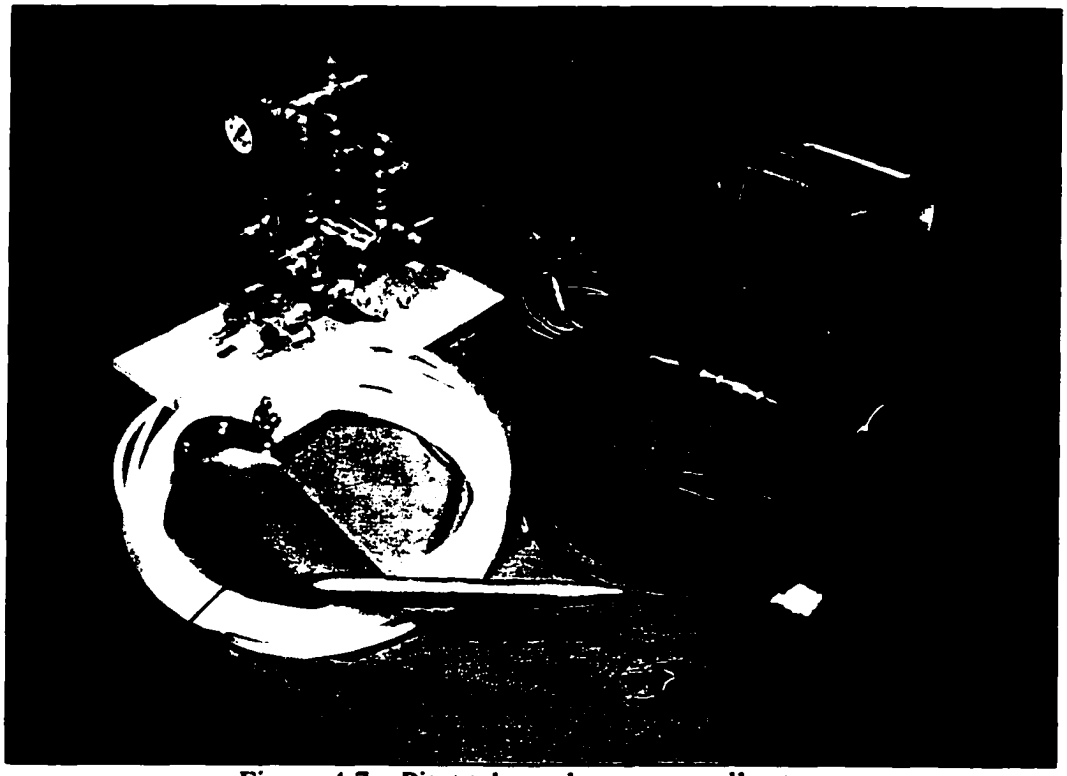

Figure 4.7 – Pitot tube and pressure cell setup.

Velocity from the measured pressure head of the Pitot tube may be determined by:

$$u = \sqrt{\frac{2(p_d - p_s)}{\rho_m}} \tag{4-2}$$

where: u = velocity (ft/s);

p_d = kinetic pressure (lb/ft^2);

p_s = static pressure (lb/ft^2);

ρ_m = air/water mixture density (slugs/ft^3)

Equation (4-2) shows that the Pitot tube velocity measurement is dependent on the fluid mixture density. In the present study, the density of the two-phase fluid varies through the flow depth with air concentration. Therefore, the Pitot tube must be

calibrated as a function of air concentration and the air concentration of the flow at the point of velocity measurement must also be determined (Frizell, et. al., 1994).

4.3 Instrument Calibration

The air probe and Pitot tube were calibrated for varying air/water mixtures and, for the Pitot tube, varying velocities. The calibration apparatus consists of a water delivery pipe system, compressed air delivery system and injection point, 2-inch diameter by 22-inch long mixing chamber with an exit nozzle, and an instrument mount (Figure 4.8). Water is supplied from the Hydraulics Laboratory Horsetooth pipeline, the same water source as the stepped spillway model, and the air source is supplied from the laboratory compressor. Both water and air flow rates were measured with variable area rotameters.

A calibration setting was determined by first selecting a value for the nozzle exit velocity and computing total volumetric discharge required to obtain that velocity. Setting the percentage of air in the total discharge was then achieved by adjusting air and water flow rates to the desired ratio of volumetric air to water. For example, a nozzle exit velocity of 40 ft/s requires a total discharge of 13.1 cubic feet per minute (cfm) through a 1-inch nozzle. A calibration setting of 20% air concentration would then require flow rates of 2.6 cfm air and 10.5 cfm water.

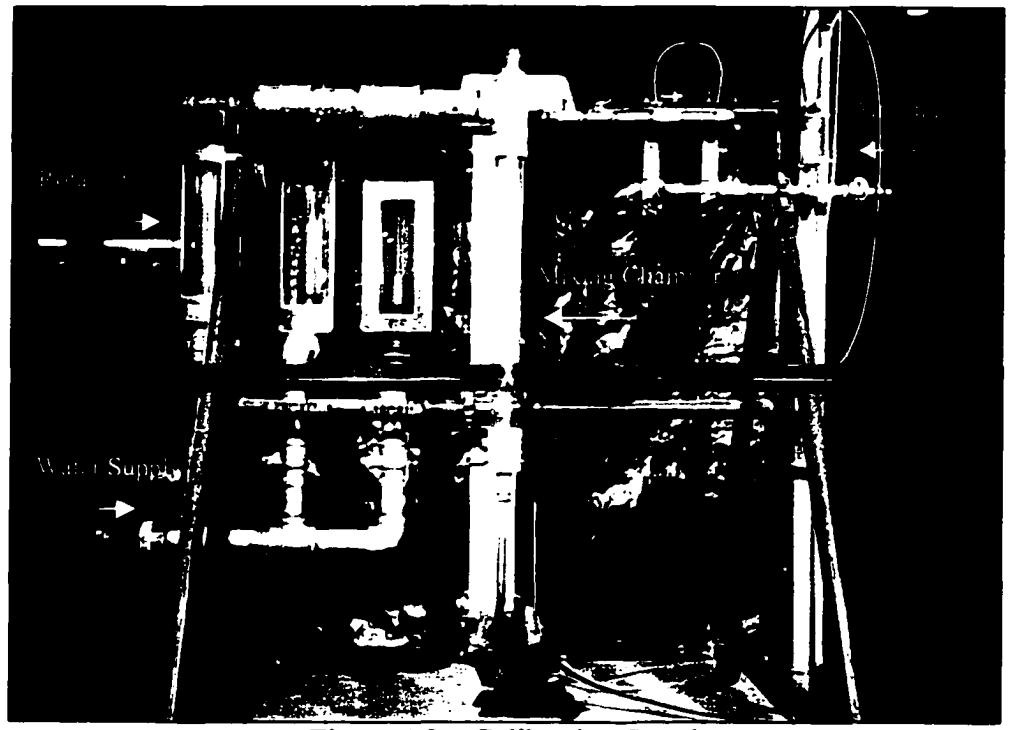

Figure 4.8 – Calibration Stand

The air and water flow rotameters are calibrated for direct reading of volumetric flow rate. However, the air rotameter is calibrated to read flow rate in standard cubic feet per minute (scfm) at standard operating conditions (atmospheric pressure at sea level and 70°F), and must be adjusted to reflect the actual operating conditions (in actual cubic feet per minute, acfm), approximately 12.5 psi atmospheric pressure and 68°F. The following equation was used to make this adjustment (Omega, 1995):1

$$Q_a = Q_s\left(\frac{p_{sa}}{p_a}\right)\left(\frac{T_a + 460}{530}\right) \tag{4-3}$$

where: Q_a = actual flow rate at operating conditions (acfm);

Q_s = flow rate reading (scfm);

p_{sa} = standard atmospheric pressure (14.7 psi);

p_a = atmospheric pressure at operating conditions (psi);

T_a = temperature at operating conditions (°F)

Calibrations were carried out on the air probe and Pitot tube for air concentrations ranging from 0% to approximately 80% with velocities ranging from 5 ft/s to approximately 85 ft/s. A mixing chamber was added to provide back pressure and obtain a relatively smooth, completely mixed, uniform jet of air/water mixture leaving the nozzle. Selection of the nozzle diameter was based on achieving adequate backpressure and obtaining the range of velocities expected in the stepped spillway model. The calibration apparatus was setup so that both the air probe and the Pitot tube could be independently mounted in the jet issuing from the nozzle and tested without changing the air/water discharge. The instrumentation mount provided lateral movement, enabling each probe to slide into position within the free jet for calibration. This ensured that both probes were calibrated for the same air/water mixture and velocity. Vertical placement of the probe tips relative to the nozzle was approximately flush or within one tip diameter of the end and centered within the free jet.

4.3.1 Air Probe Calibration

Air concentration can be determined using the air probe output and equation (4-1). Calibration of the air probe was carried out by setting a known air/water mixture on the calibration stand and measuring air concentration with the probe. It was found that air concentration is not always distributed uniformly across the jet exiting the nozzle. Measurements were sampled with the probe in the center of the jet and to the left and right of center. Fine lateral adjustment of the probe was not available on the calibration stand and location of the probe within the jet was visually estimated. Care was taken to repeat the measurement locations as accurately as possible. Under certain conditions, it was found that air concentration measurements varied significantly across the jet for a

fixed setting. The differences were significant enough that it was obvious when a value outside of the expected air concentration was encountered. In these instances, examination of the jet was made by checking the air concentrations to the left and right of the centerline values. These values tended to differ as much as 30% to over 50% from the expected value and were the result of irregularities in the exiting jet rather than from the air probe. If the air concentrations varied by more than 20%, a different air/water setting was established and uniformity across the jet was checked again. Values within plus or minus 20% of the expected value were considered representative of the calibration air concentration.

For certain air/water mixture settings, particularly combinations of high velocity and high air concentration, surging was noticed in the nozzle and jet. It was also found that nozzle diameter affected surging and overall performance of the calibration stand. When surging occurred, the exiting jet was slightly skewed to one side rather than exiting uniformly from the nozzle. In extreme cases of surging, nonuniformity across the diameter of the jet could be visually observed. The irregularities observed in the jet under these conditions are likely related to the differences in air concentration encountered by the air probe. A final calibration was performed with nozzle exit diameters of 1.0 inch and 0.63 inches with care taken to set combinations of air concentration and velocity where surging was not visibly observed.

Results of the final calibration are shown in Figure 4.9. Linear regression of the data results in a calibration line with a 1:1 ratio (i.e. a direct reading of the air probe). It was felt that this provides an accurate measurement of the actual air concentration encountered by the probe. A higher degree of confidence was placed in the probe and its

electronics than was placed on the nozzle and setting of the probe in the calibration stand. It was concluded that the wide distribution of air concentration measurements was due to poor flow conditions in the nozzle and lack of precision in positioning the probe in the calibration stand rather than the air probe and the electronics.

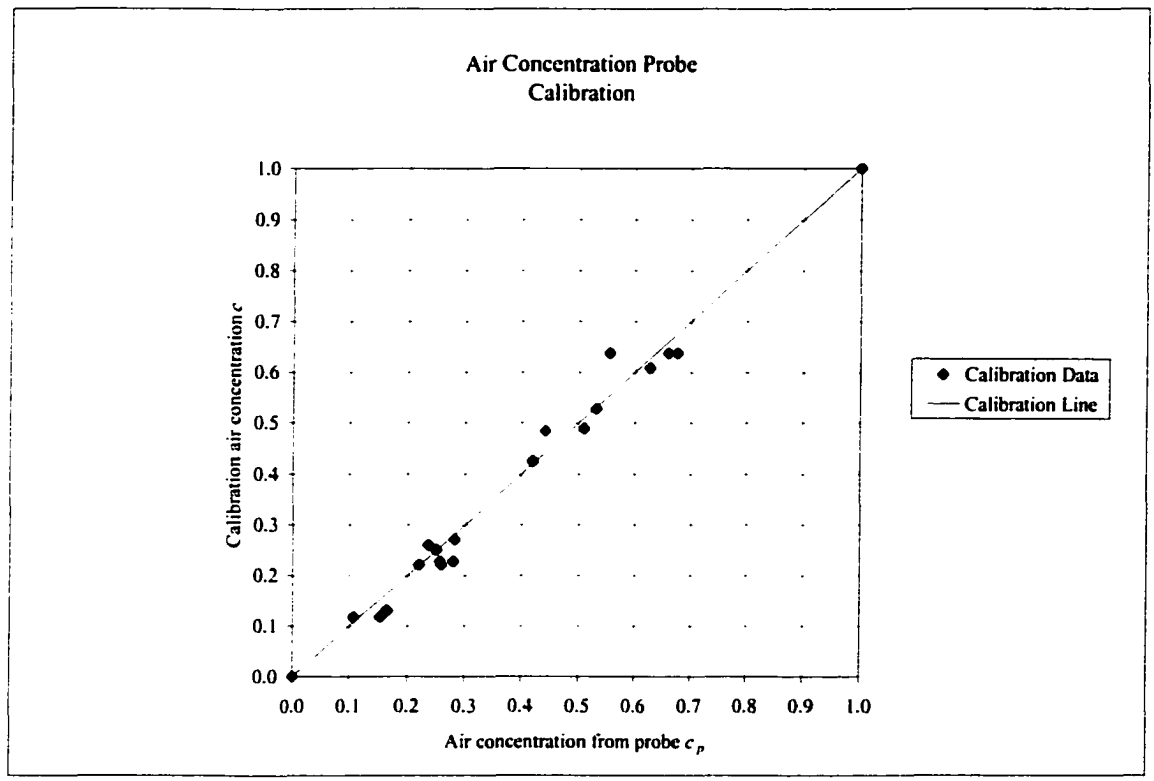

Figure 4.9 – Air probe calibration.

4.3.2 Pitot Tube Calibration

Equation (4-2) shows that velocity measured with a Pitot tube is a function of the fluid density and the measured difference in pressure head between the static and dynamic ports. As with the air concentration probe, a calibration was performed on the Pitot tube with various combinations of flow density and velocity. Calibration flows were set for an estimated range of air concentration from 0% to 80% with velocities ranging from 10 ft/s to 60 ft/s. Figure 4.10 shows a plot of Δp versus u for each corresponding air concentration, where Δp is the measured differential pressure head from the Pitot tube in pounds per square foot (lb/ft^2) and u is the calibration stand exit velocity determined from continuity.

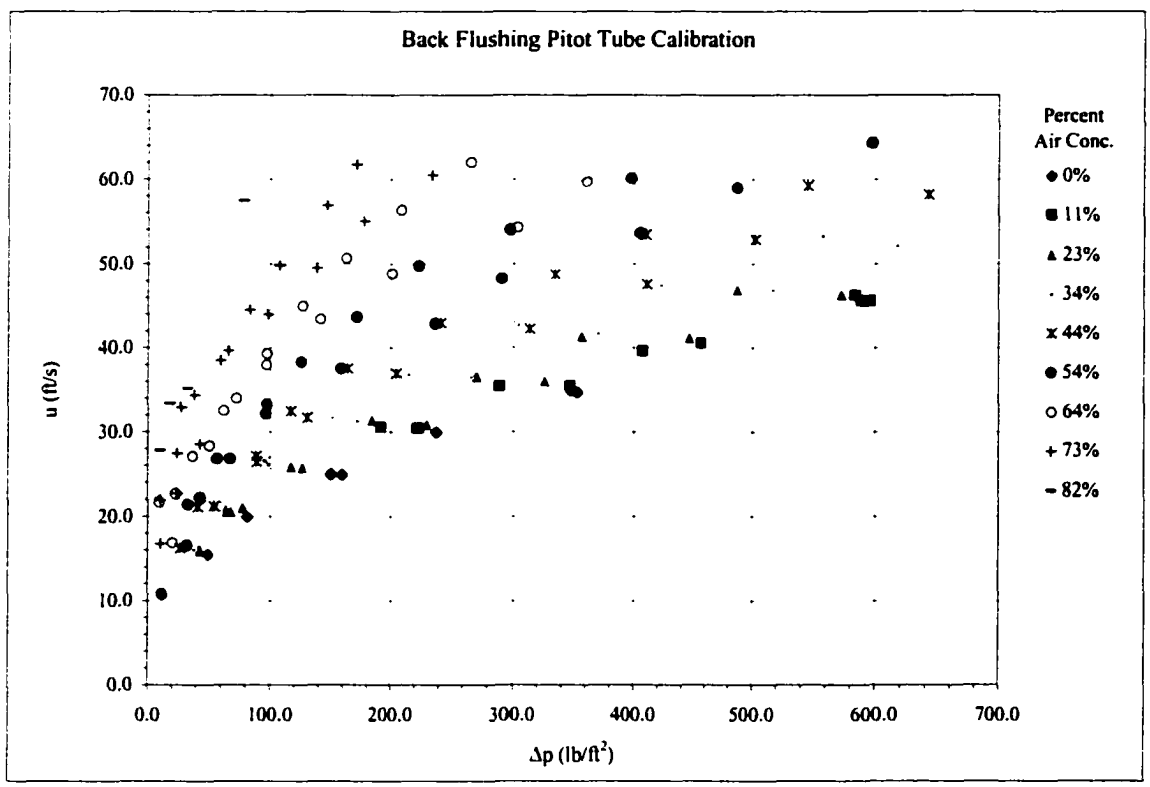

Figure 4.10 – Pitot tube calibration data.

Notice in Figure 4.10 that for each air concentration, u is increasing with Δp which can be written in the form of a power function, or $u = b\Delta p^m$, where b and m are the regression coefficient and exponent. Taking the natural log of both variables in Figure 4.9 results in a linear relationship of the data in the form (Figure 4.11):

$$\ln(u) = m\ln(\Delta p) + \ln(b) \tag{4-4}$$

Figures 4.10 and 4.11 show that the data represent a family of curves, each dependent on air concentration. Fundamentally, the exponent value of the relationship should be 0.5 as given by the radical in equation (4-2). Linear regression was carried out on each log-linear data set with slope m held constant at 0.5. The intercept of each linear equation (for each air concentration) was solved for the coefficient b in the power function relationship. Figure 4.11 and Table 4.1 show the family of curves and the results of each linear regression, where r^2 is the coefficient of determination for each regression.

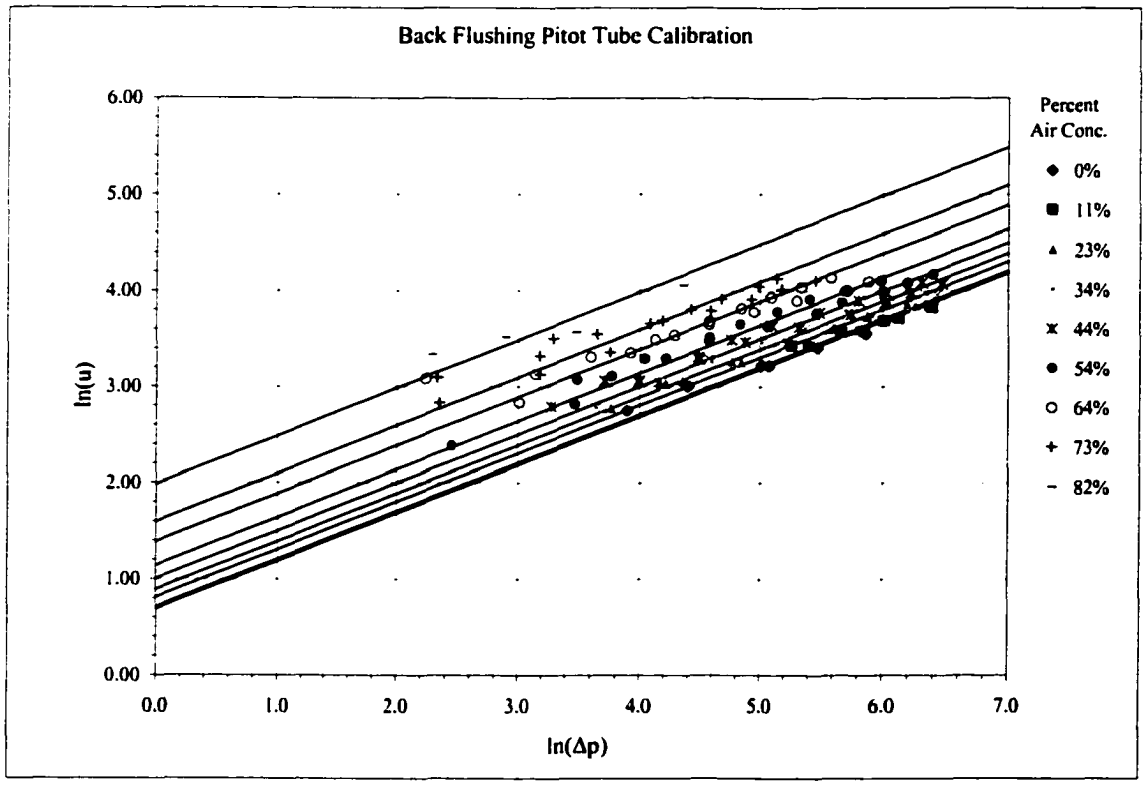

Figure 4.11 – Pitot tube calibration family of curves.

Table 4.1 – Power function coefficient and exponents.

Air Concentration	Exponent (slope) m	Intercept ln (b)	Coefficient b	Coefficient of Determination r^2
0%	0.5	0.70	2.02	0.94
11%	0.5	0.68	1.98	0.89
23%	0.5	0.80	2.23	0.93
34%	0.5	0.89	2.43	0.93
44%	0.5	1.00	2.71	0.92
54%	0.5	1.14	3.12	0.95
64%	0.5	1.39	4.00	0.78
73%	0.5	1.59	4.91	0.85
82%	0.5	1.98	7.27	0.70

Wood (1983) showed that for air/water flow, equation (4-2) can be rewritten in as:

$$u = \lambda\sqrt{\frac{2\Delta p}{\rho_w(1-c)}} \tag{4-5}$$

where: u = velocity (ft/s)

λ = Pitot tube pressure coefficient;

Δp = differential pressure head (lb/ft^2);

ρ_w = density of water (slugs/ft^3)

The coefficient λ takes into account how Δp is affected by changes in density of the air/water mixture and is, therefore, a function of air concentration. Equation (4-5) can be written as:

$$u = \lambda\sqrt{\frac{2\Delta p}{\rho_w(1-c)}} = \lambda\sqrt{\frac{2}{\rho_w(1-c)}}\sqrt{\Delta p} = b\sqrt{\Delta p} = b\Delta p^{0.5} \tag{4-6}$$

where:

$$b = \lambda\sqrt{\frac{2}{\rho_w(1-c)}} = \text{constant for a given value of c.} \tag{4-7}$$

If air concentration is held constant in equation (4-7), then the coefficient b is constant and a value of λ can solved for each air concentration. Figure 4.12 shows a plot of λ versus air concentration c. A three parameter power function in the form $\lambda = \lambda_o + ac^k$ where the independent variable is air concentration c, and values a and k are regression parameters. Following is the final calibration equation for the Pitot tube (Figure 4.12):

$$\lambda = 1.92 + 2.62c^{4.39} \tag{4-8}$$

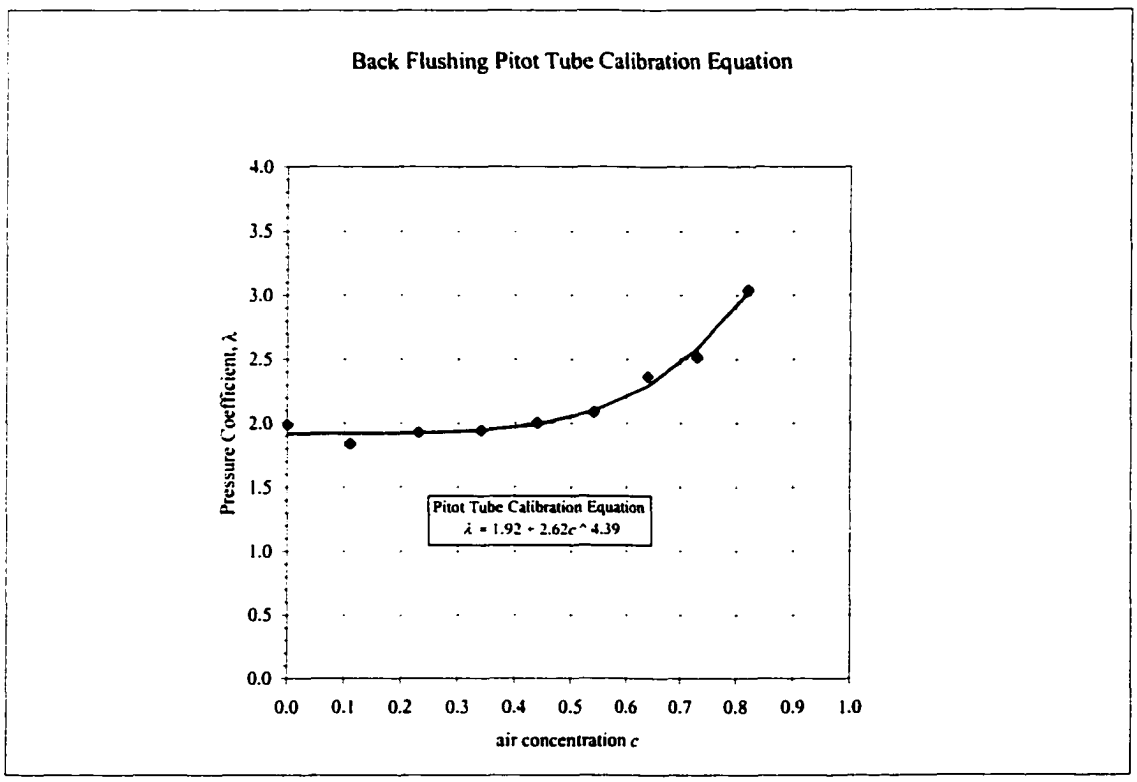

Figure 4.12 – Pitot tube calibration equation.

Notice in equation (4-8) that when $c = 0\%$, the value of λ_o equals 1.92. Normally, a Pitot tube pressure coefficient takes on a value around 1.00 for clear water (ASME, 1959). This surprising result was thoroughly investigated to determine if the data or the instrumentation were in error. Frizell et. al. (1994), performed a calibration on an

identical Pitot tube and found a calibration curve of similar shape, however, with a λ_o value near 1.00 (Figure 4.13). Consultation with Frizell and other Reclamation engineers, as well as experiments conducted in the laboratory failed to resolve the discrepancy. However, the high values of λ found in the present study were confirmed to be due to the arrangement of the pressure transducer. Figure 4.14 shows a schematic of the pressure transducer plumbing used in the present study. Notice that incoming back flushing flow is split at a tee upstream of the transducer, routed through the positive and negative sides of the pressure cell, and finally through lead lines to the static and dynamic ports of the Pitot tube. The setup procedure for data collection involved fully opening valves B and C, establishing back flushing flow and pressure at valve A, then adjusting flow through valve B until the differential pressure equaled zero. At this point, the Pitot tube and pressure transducer were considered balanced and ready for data collection. With this setup, the positive and negative sides of the pressure cell (i.e. the dynamic and static ports of the Pitot tube) are not isolated from one another and pressure can be transmitted between them. Therefore, the full differential pressure was not measured between the Pitot tube ports resulting in inflated values for the pressure coefficient. In addition, variations in pressure at the exit of either port (i.e. approach velocity head) directly affect back flushing flow rates through the Pitot tube. For example, it was clearly observed that manually blocking or retarding back flushing flow through the dynamic port (i.e. by placing a finger over the exit port) increased flow exiting the static port, and vice versa.

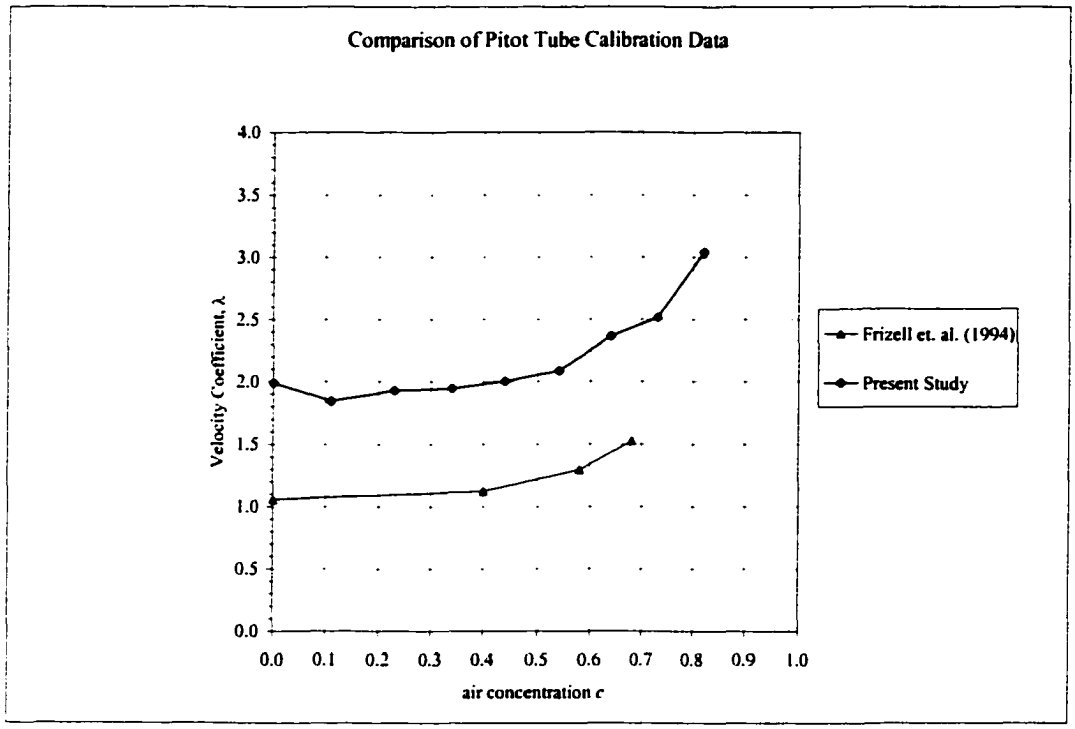

Figure 4.13 – Comparison of Pitot tube calibration data.

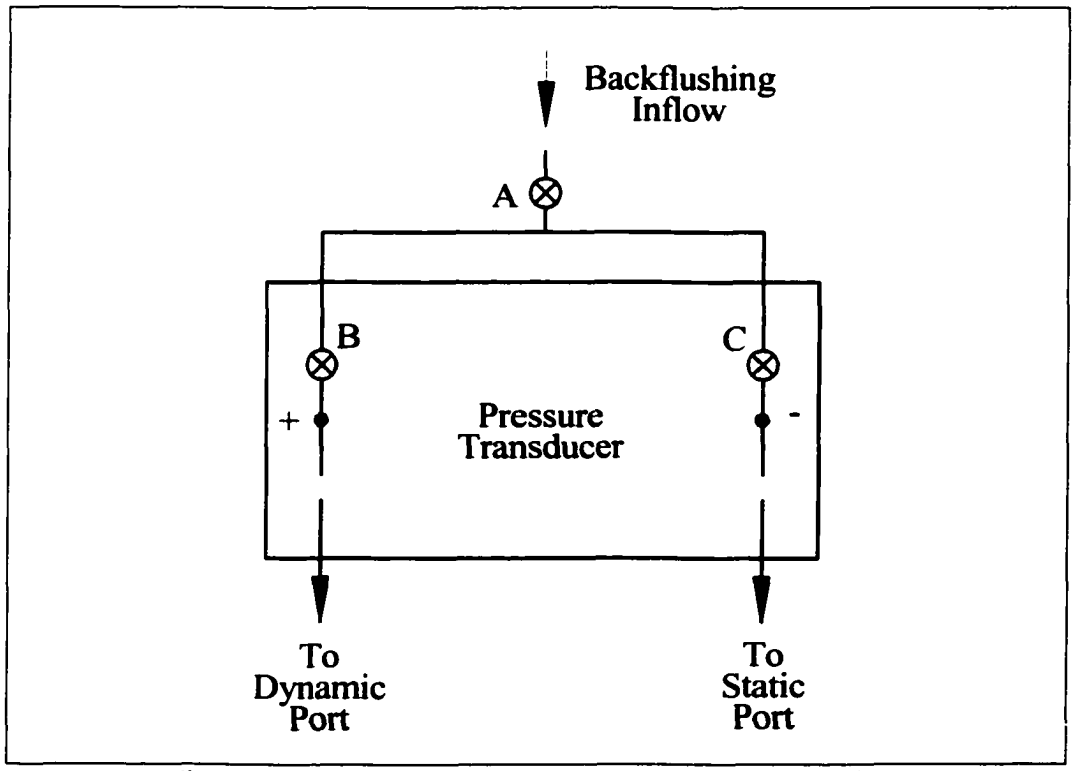

Figure 4.14 – Schematic of pressure transducer plumbing.

In order to further investigate the mechanics of the Pitot tube, a transient analysis computer program was developed to model the back flushing system. Modeling of the back flushing flow, pressure transducer, lead lines, and Pitot tube dynamic and static ports were all incorporated into the simulation. The computer model was used to simulate approaching clear water velocity head at the Pitot tube dynamic port and obtain resulting pressures and flow rates throughout the back flushing system. The transient analysis is time dependent and produces results in incremental time steps over a specified period.

The computer program is written in FORTRAN code and essentially models a three-reservoir problem using the method of characteristics to solve the unsteady fluid flow equations. Initial pressure heads and back flushing flow rates in the system at time $t = 0$ were modeled as constant values to simulate conditions of the Pitot tube and pressure transducer that represent zero approach velocity with a differential head across the transducer. Back flushing pressure was modeled by setting a constant head entering the system (reservoir 1) at a tee upstream of the pressure transducer. Initial heads at the dynamic port (reservoir 2) and the static port (reservoir 3) were determined from the head loss generated by the initial back flushing flow rates in the transducer plumbing, lead lines, and Pitot tube between the incoming flow line and the Pitot tube ports. Initial back flushing flow rates through the Pitot tube were measured in the laboratory for corresponding back flushing pressures used in the study and in the computer model. Physical characteristics of the lead lines, transducer plumbing, and Pitot tube were also measured in the laboratory and modeled in the computer simulation.

Approach velocity head was simulated at the beginning of the transient analysis as an incremental increase in pressure at the Pitot tube dynamic port (reservoir 2) over a short period of time until the desired velocity head was reached. Pressure head at the Pitot tube static port (reservoir 3) remained constant. The model was run for a sufficient amount of time (approximately 7.0 seconds) in order for resulting pressures and flow rates in the system to reach steady state. As expected, the computer model revealed that flow rates through the dynamic and static ports are variable and a function of the approaching velocity head. In fact, for large values of velocity similar to those encountered in this study, the dynamic port flow rate was negative, or reversed flow through the lead lines. Additionally, it was found that flow rate through the static port increased with increasing approach velocity at the dynamic port.

Table 4.2 shows results of the computer model for simulated approach velocity heads of 10, 20 and 30 feet (simulated velocities of 25.38, 35.89 and 43.95 ft/s) at back flushing pressures of 2.5, 5.0 and 8.0 psi. Pressures and flow rates given in Table 4.2 are steady state values at the end of the simulation unless otherwise indicated. Figures 4.15 and 4.16 show sample results of pressures heads and flow rates as a function of time at the transducer static and dynamic ports. The Pitot tube pressure coefficient λ was found by comparing velocity applied at the dynamic port to velocity computed from the resulting differential pressure head across transducer. It can be seen that values of λ found from the computer model are approximately equal to those found in the calibration at $\lambda \cong 2.0$.

Table 4.2 – Results of computer model Pitot tube simulation.

Back Flushing Pressure (lb/in^2)	Approach Velocity Head (ft)	Approach Velocity (ft/s)	Dynamic Port Back Flushing Flow Rate (gal/hr)		Static Port Back Flushing Flow Rate (gal/hr)		Pitot Tube Dynamic Port Pressure Head (ft)	Transducer Dynamic Port Pressure Head (ft)	Transducer Static Port Pressure Head (ft)	Pitot Tube Static Port Pressure Head (ft)	Pitot Tube Velocity (ft/s)	Pressure Coefficient
			Initial	Steady State	Initial	Steady State						
2.5	10.0	25.38	5.1	-5.33	10.4	16.10	13.90	13.11	10.86	3.63	12.02	2.11
2.5	20.0	35.89	6.8	-10.69	7.6	21.30	23.90	20.72	16.29	3.63	16.89	2.12
2.5	30.0	43.95	8.7	-14.68	5.8	25.15	33.90	27.90	21.28	3.63	20.64	2.13
5.0	10.0	25.38	5.1	-2.61	10.4	16.88	18.27	18.08	15.80	7.84	12.12	2.09
5.0	20.0	35.89	6.8	-8.29	7.6	22.46	28.27	26.35	21.89	7.84	16.96	2.12
5.0	30.0	43.95	8.7	-12.39	5.8	26.45	38.27	33.99	27.34	7.84	20.69	2.12
8.0	10.0	25.38	5.1	1.21	10.4	17.75	22.99	23.03	20.59	11.82	12.54	2.02
8.0	20.0	35.89	6.8	-4.98	7.6	23.83	32.99	32.29	27.67	11.82	17.26	2.08
8.0	30.0	43.95	8.7	-9.29	5.8	28.06	42.99	40.58	33.76	11.82	20.94	2.10

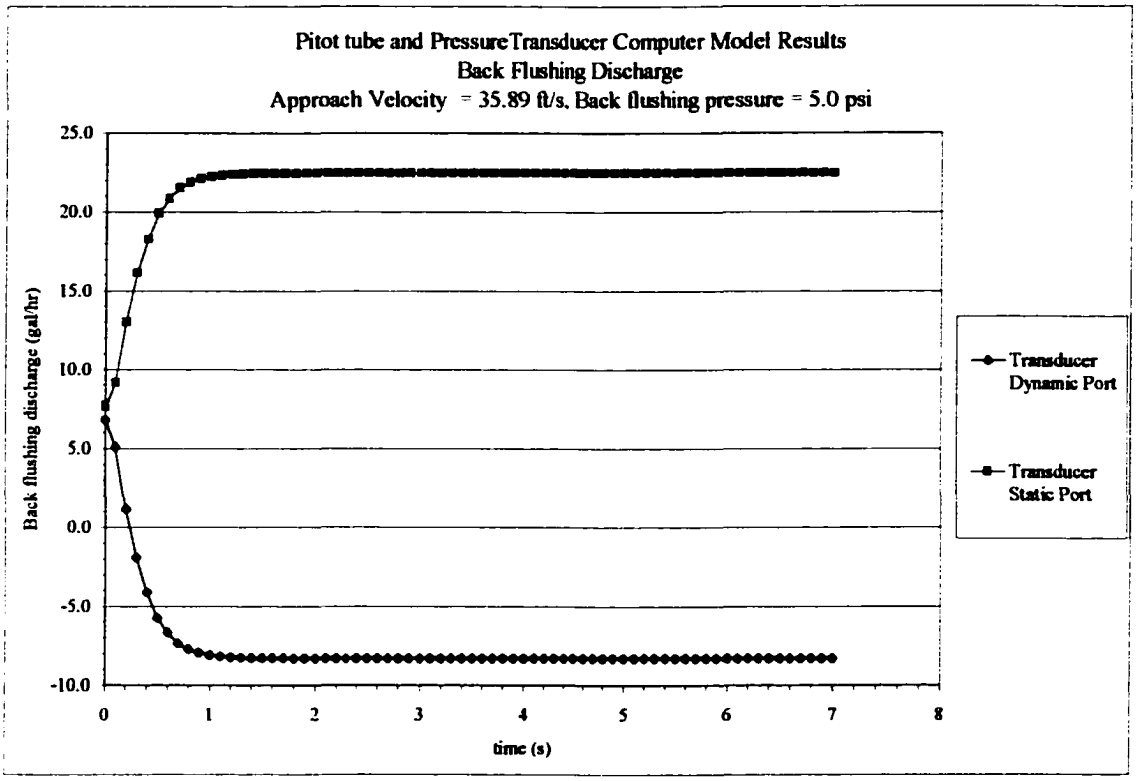

Figure 4.15 – Computer model sample results – back flushing discharge

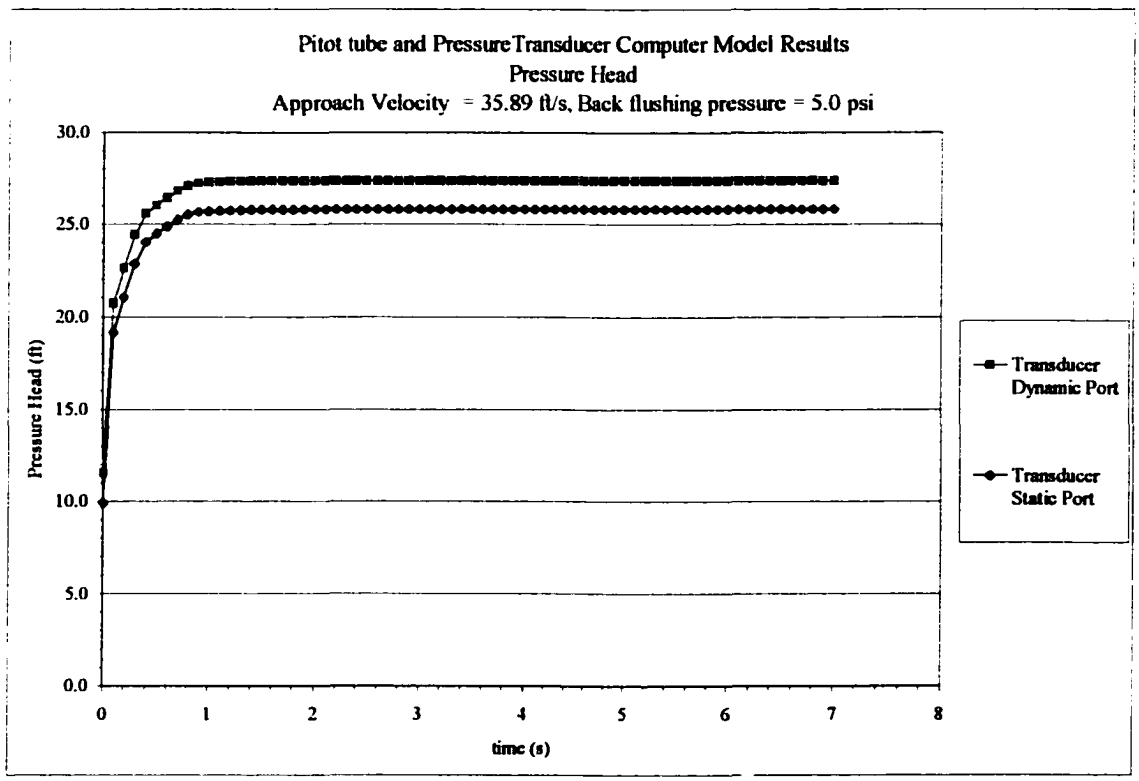

Figure 4.16 - Computer model sample results – transducer pressure head

4.4 Sampling Frequency

During calibration of the air probe, several issues developed regarding the sampling frequency and duration of record required for analyzing the probe waveforms. In past experiments using the same equipment, a sample frequency of 500 Hz recorded for at least 1.0 minute appeared sufficient. However, at this frequency, the shape of the waveform appears in analog form with peaks of variable height as opposed to the expected square waveform of constant height (0 to 5 volts) and variable width, as discussed in *Section 4.1.2.* Previously, it was not clear why this occurred and the issue was never investigated. Through laboratory experiments in the present study and discussion with Reclamation engineers, it was discovered that sampling frequency significantly affects the shape of the waveform. Increasing the sampling frequency showed that the waveform tends towards the expected waveform at higher frequencies. Figures 4.17 and 4.18 show typical air probe waveforms for the same percent air concentration and flow rate at sampling frequencies of 500 Hz and 15,000 Hz, respectively. Note that these figures are random samples taken at different periods in time.

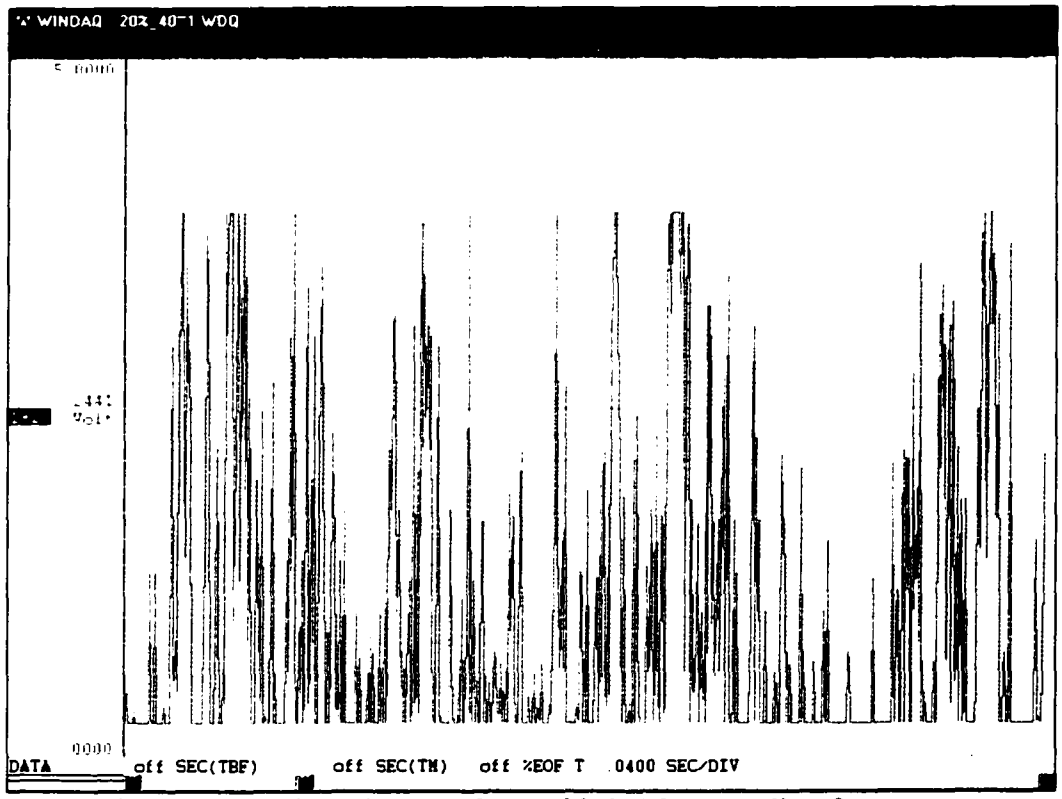

Figure 4.17 - Air probe waveform with 500 Hz sampling frequency.

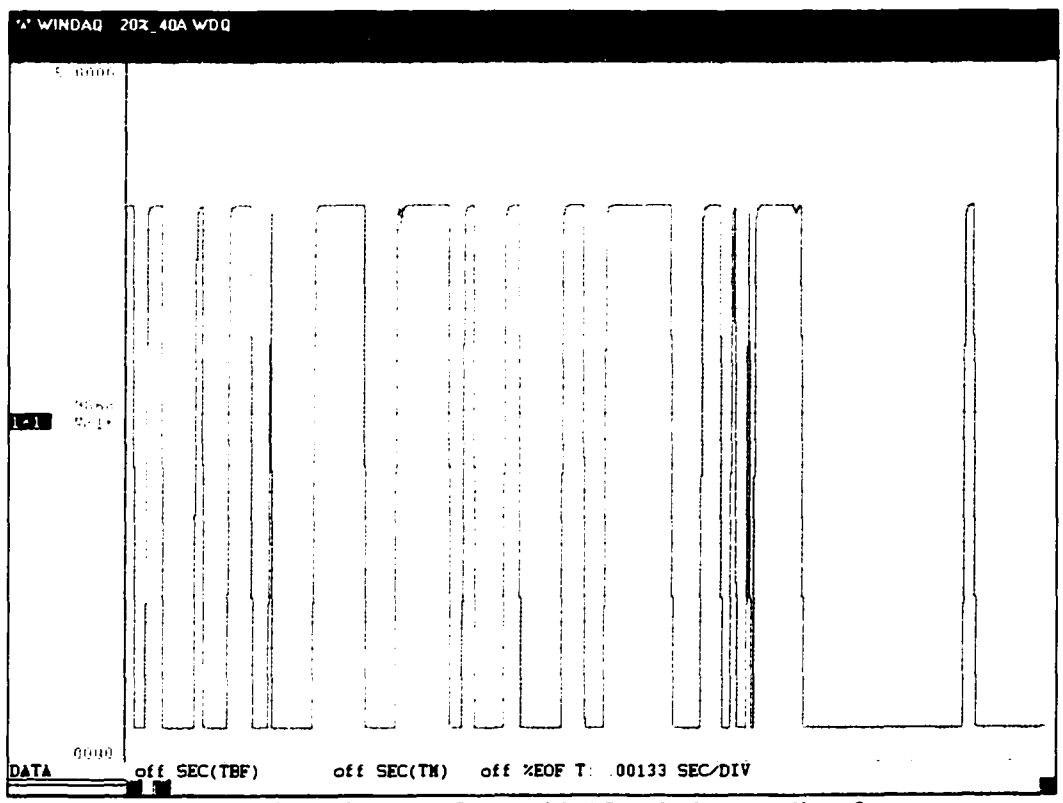

Figure 4.18 - Air probe waveform with 15,000 Hz sampling frequency.

In order to investigate and trace the air probe signal, an oscilloscope was used to compare and verify the signal at various points along the signal path. It was first verified that a square, digital signal was indeed the output of the air probe electronics package as expected. The oscilloscope exhibited a square wave even at sampling frequencies as low as 500 Hz. Next, the signal was compared and verified at the end of the cabling prior to entering the DI-220 data acquisition unit. Again, the oscilloscope showed a square wave at this location. It was determined that processing of the signal within the DI-220 unit changes the signal in such a manner that a high sampling frequency is required to reconstruct the signal. It is possible that this is due to the analog-to-digital converter contained within the DI-220 unit. Therefore, sampling the DI-220 output signal at relatively low sample frequencies caused poor reconstruction of the original signal. This phenomenon is frequently referred to as signal aliasing. To avoid aliasing, the sampling frequency for the air probe was set at the highest possible sampling rate reasonable for the capabilities of the Windaq/200 software and the IBM personal computer. A rate of 15,000 Hz was selected.

Another limitation of the DI-220 unit was the affect of sampling multiple channels. The DI-220 unit is capable of sampling up to 16 channels simultaneously. However, in the case of the air probe waveform, it was found that a better signal was received using a single channel. In similar studies, two channels were frequently used, one for the air probe and one for the Pitot tube, and sampled simultaneously. In the present study only one channel is used and the instruments sampled separately.

4.5 Pressure Profiles

Pressures were measured on both the vertical and tread faces of the steps at three specific locations down the slope (Figure 3.3, Chapter 3). For the h = 2.0 ft tests, three stations were instrumented with pressure taps on the tread and adjacent vertical faces at each station. The pressure taps were flush-mounted along the centerline of each step (2 ft lateral distance from the wall) with eight taps on the step tread and four taps on the vertical faces for a total of sixteen taps per station (Figure 4.19). The pressure taps were adapted for the h = 1.0 ft so that two full treads and adjacent vertical faces were instrumented at each station. This allowed for four pressure taps per tread and two pressure taps per vertical face for a total of fourteen taps per station. Pressures were monitored with the differential pressure cell and WINDAQ/200 software configuration used for the Pitot tube measurements. The positive side of the pressure cell was used to measure pressure and the negative side left open to the atmosphere. Pressure at each tap was determined by simply subtracting the elevation pressure head between the pressure tap and the pressure cell from the measured pressure head. Data were taken for the same range of discharges as velocity and air concentration data.

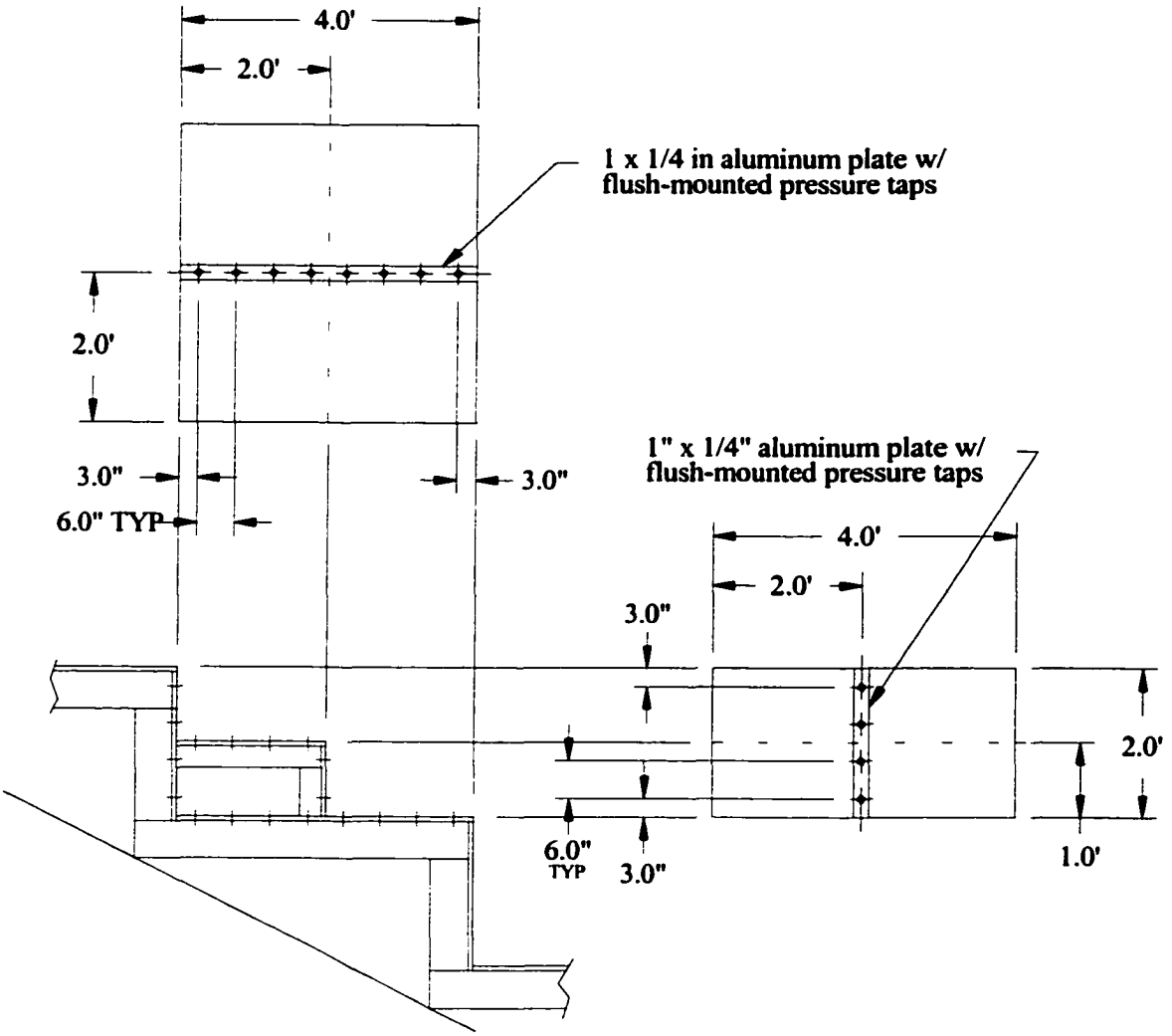

Figure 4.19 – Flush mounted pressure taps.

4.6 Data Acquisition Summary

In general, the following steps were used to determine local air concentration and velocity in the flow:

4.6.1 – Local Air Concentration Calculation

1. Determine air probe maximum voltage V_{max}, area under waveform A, and duration of sample T from WINDAQ/200 software statistics function.
2. Calculate probe local air concentration c_p from equation (4-1).

4.6.2 – Local Velocity Calculation

1. Determine pressure transducer mean voltage from WINDAQ/200 software statistics function.
2. Subtract 'zero' offset from mean voltage, if needed. The zero offset measurement was taken prior to beginning of data collection with balanced pressure transducer.
3. Multiply mean voltage times pressure transducer calibration coefficient (approximately 2.00) to obtain differential pressure in *psi*.
4. Multiply pressure times 2.31 to obtain differential pressure head in *ft of water*.
5. Determine Pitot tube velocity coefficient λ using local air concentration value c and equation (4-8).
6. Calculate local velocity in u ft/s from equation (4-5).

CHAPTER 5

TESTS OBSERVATIONS AND RESULTS

5.1 – Introduction

Data were taken at five locations along the spillway slope over a range of discharges incrementally increased for each test. Over 1,700 individual data points of local velocity and air concentration were collected along with several hours of flow observations recorded on videotapes and 35 mm prints. As with most scientific data, there is the inevitable need to reduce the raw data into a descriptive and logical format. As well, the presence of residuals or outliers often requires statistical methods to either quantify or discount these data. This chapter describes the data obtained from the model tests and the methods used to reduce the data into a format where results are presented. Flow observations and attempts to classify the flow are first described with analysis of the raw data, definitions of characteristic flow depths and analysis methods following.

Drawing conclusions from scientific data is often subject to how the data is analyzed and presented. For the present study, substantial amounts of data were collected in the form of voltage waveforms collected from the velocity and air concentration probes described in chapter 4. Calibration of these instruments allowed for reduction of the voltage waveforms into local values of velocity and air concentration. Subsequently, through theoretical and empirical relationships the data were used to quantify hydraulic

characteristics of the flow over the steps. Objectives of the study were used as a guide for progression of the analysis and include:

i) observe flow conditions over the steps and along the spillway at various flow rates.

ii) develop centerline profiles of local air concentration and velocity at several locations along the length of the spillway.

iii) determine average air concentration and velocity from the centerline profiles at several locations along the length of the spillway.

iv) define characteristic depths and verify the data using continuity.

v) examine bulking of the flow due to air entrainment and develop characteristic depths.

vi) quantify and examine flow resistance due to the steps and their effect on flow characteristics.

vii) determine energy dissipation along the length of the spillway.

Results of items *i* through *iii* are described in this chapter with analysis of items *iv* through *vii* addressed in Chapter 6.

5.2 – Flow Observations

Observations of the flow conditions were made for each test series over a range of discharges. Videotape recordings and still photographs were used to document the flow at the overtopping crest and along the spillway length. Flow conditions were observed and recorded through each of five plexiglass windows located along the sidewall of the spillway. Locations of these windows are shown in Chapter 3, Figure 3.3, and are located approximately between the following stations: Window #1 – crest of spillway to

station s = 4.4 ft; Window #2 – station s = 11.4 ft to 15.4 ft; Window #3 – Station s = 45.6 ft to 53.6 ft; Window #4 – Station s = 77.8 ft to 81.8 ft; Window #5 – Station s = 86.9 ft to 90.9 ft. Visual records were cataloged and continually referenced in describing the flow conditions. For the first test series with h = 2.0 ft, flow conditions are described in detail while for the second test series with h = 1.0 ft, specific differences and comparisons are given. Characteristics of the initial flow over the crest, variation of flow depth and air entrainment along the spillway, surface conditions, classification of flow regime, and other observations are described in these sections.

5.2.1 – Flow Observations, h = 2.0 ft

By visual comparison, it is convenient to classify the flow into the categories of nappe or skimming flow regime. Consensus in the literature is that for a given slope and step height, a distinct discharge (normally referenced to critical depth y_c) exists at which the flow transitions from nappe to skimming flow. Rajaratnam (1990) found that for ratios of y_c/h greater than 0.8, skimming flow occurs. For the present study, the discharge at which skimming flow is first observed can be estimated using the definition of skimming flow given in section 2.1, and from observations of flow profiles through the viewing windows. Skimming flow is characterized by complete submergence of the steps with water flowing down the slope as a coherent stream cushioned by recirculating vortices in the interior of the step. For the 2 ft steps, at 20 cfs (y_c/h = 0.46), nappe flow existed with ponded water in the interior of the step beneath a cascading free jet (Figure 5.1). At 40 cfs (y_c/h = 0.73), partial impact of the flow near the end of the step and incomplete filling of the step cavity suggest a partial nappe flow regime, or transition state (Figure 5.2). The condition of skimming flow was first observed at 60 cfs or greater

(y_c/h = 0.96, Figure 5.3; y_c/h = 1.35, Figure 5.4). The onset of skimming flow occurred between 40 and 60 cfs. However, detailed observations were not recorded in this range and a prediction of the exact discharge could not be given with confidence.

Figure 5.1 – Nappe Flow Regime, h = 2.0 ft, Q = 20 cfs (y_c/h = 0.46), Window #4.

Figure 5.2 – Transition Flow Regime, h = 2.0 ft, Q = 40 cfs (y_c/h = 0.73), Window #4.

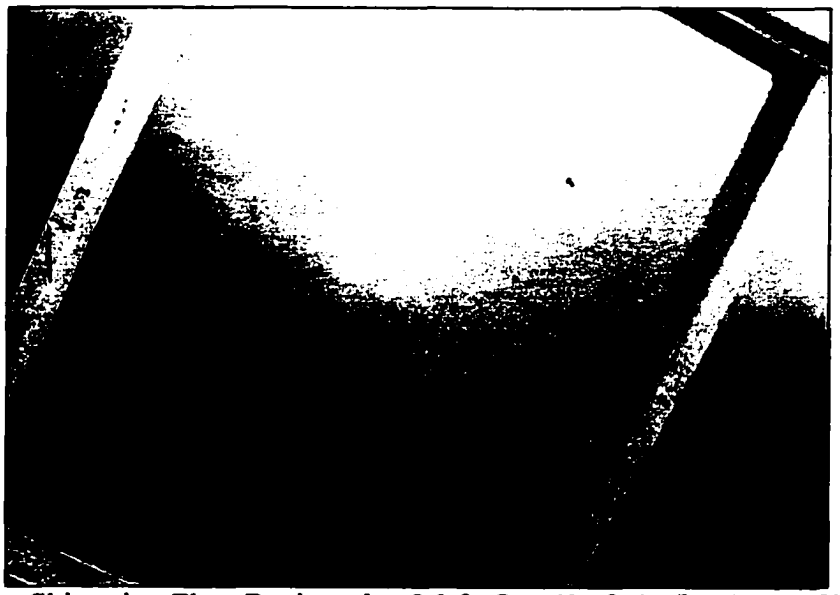

Figure 5.3 – Skimming Flow Regime, h = 2.0 ft, Q = 60 cfs (y_c/h = 0.96), Window #3.

Figure 5.4 – Skimming Flow Regime, h = 2.0 ft, Q = 100 cfs (y_c/h = 1.35), Window #3

Non-aerated flow existed prior to the crest of the first step with surface aeration initiating immediately thereafter. Aeration was observed to continue immediately after the first step for large flows, however, a fully aerated, flow profile was not observed until Window #3. It has been shown by other investigators that aeration in the flow begins when a turbulent boundary layer along the first few steps intersects the free surface,

referred to as the point of inception (Bindo et. al. 1993). Beyond the point of inception, air entrainment is observed to penetrate throughout the bulked depth of flow. These characteristics were observed in the present study and reflected in the amount of visible aeration noted in photographs near the crest at low and high discharges (Figures 5.5, 5.6, 5.7, and 5.8). At low discharges, fully aerated flow appeared to occur very near the crest. As discharge increased, a non-aerated region was observed to steadily progress downstream from the crest. An attempt was made to visually determine an inception point, however, the combination of a turbulent, ill-defined free surface and erratic surface aeration made this extremely difficult. In addition, the limitation of specifically located viewing windows prohibited observing an accurate location where a fully aerated flow profile began. Chamani (1997) observed similar conditions in a scale stepped spillway model and noted that any air entrainment prior to the inception point was due to surface longitudinal vortices or sidewall generated turbulence.

Another important flow characteristic was observed in the transverse cross sectional surface flow pattern viewed from above, or in plan view. A distinct "U" shape of surface aeration was often noted near the crest and along the entire length of the spillway indicating resistance along the walls and a nonuniform velocity distribution across the flume (Figures 5.5, 5.6, 5.7, and 5.8). Especially observed in skimming flow regime, waves formed along the sidewalls that appeared to slightly super elevate the water surface from which the waves would collapse or roll into the main flow. From visual observations, the highest velocity region appeared to be located in the center of the cross section.

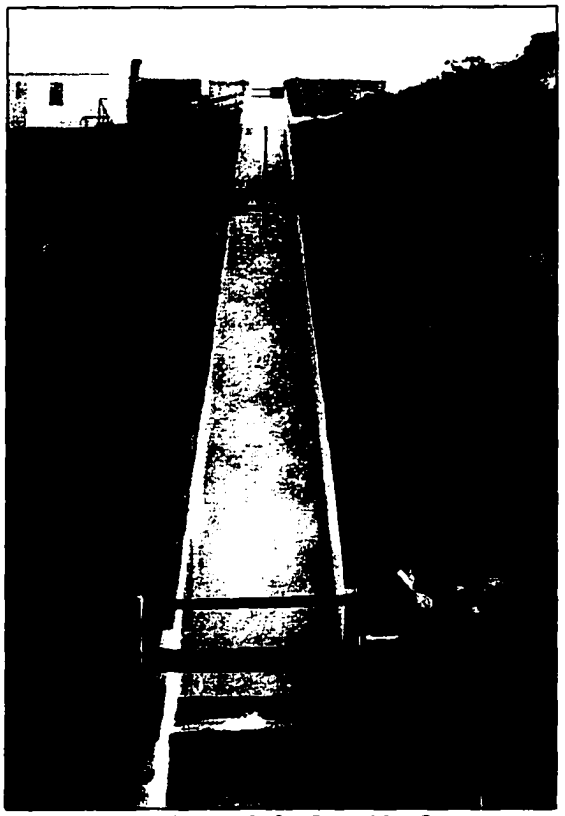

Figure 5.5 – h = 2.0 ft, Q = 40 cfs.

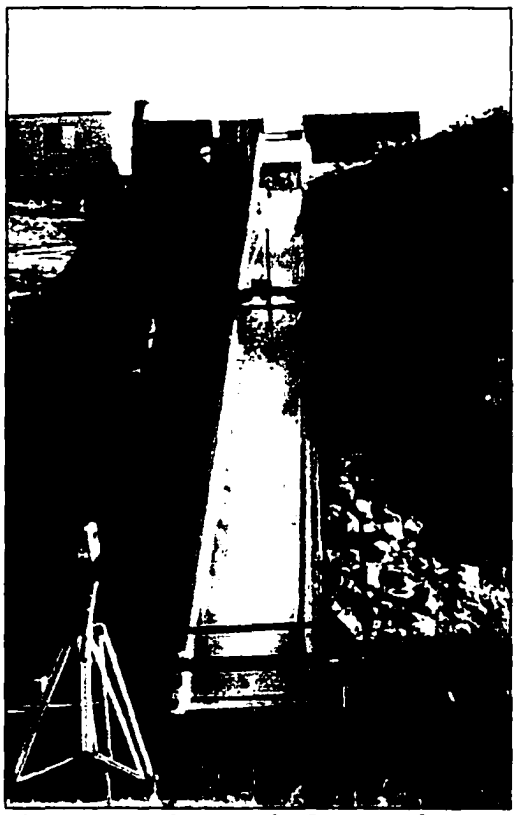

Figure 5.6 – h = 2.0 ft, Q = 80 cfs.

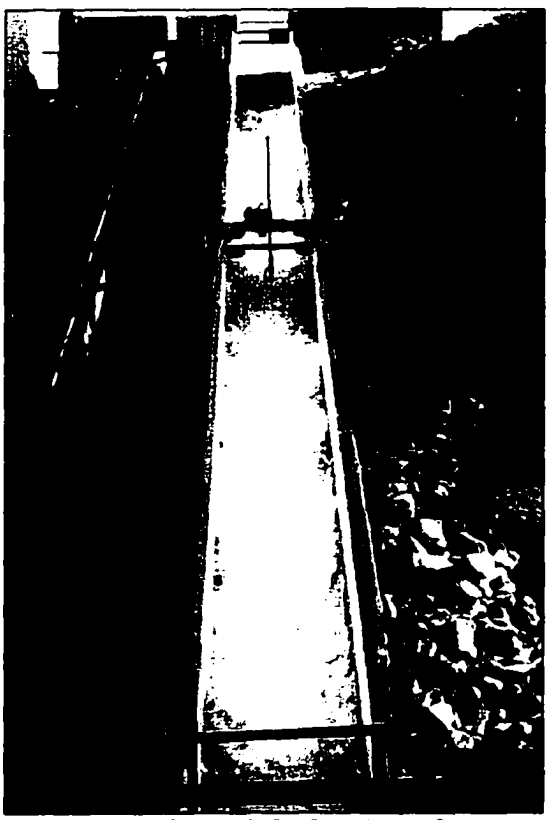

Figure 5.7 – h = 2.0 ft, Q = 100 cfs.

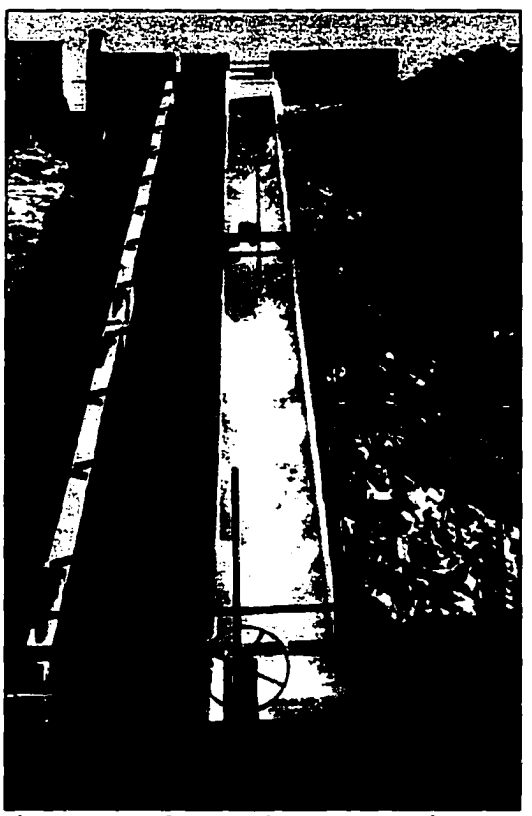

Figure 5.8 – h = 2.0 ft, Q = 120 cfs.

At high discharges (i.e. skimming flow), observations through windows #3, #4 and #5 in the lower reaches of the spillway indicated the flow to be fully developed with the overall bulked flow depth and the amount of aeration remaining fairly constant from section to section. However, the general flow conditions were extremely turbulent along the entire spillway with erratic flow patterns and significant splash occurring at all flow rates. The main volume of flow appeared to be contained in a fairly constant bulked flow depth along the entire length of the spillway. Above this depth, the flow exhibited an extremely turbulent, highly irregular free surface from which water droplets were projected up to three to four times the mean observed bulked flow depth (Figure 5.9). The majority of these droplets maintained the direction of flow and returned to the main stream. However, several droplets were projected along paths other than in the direction of flow and were ejected from the flume.

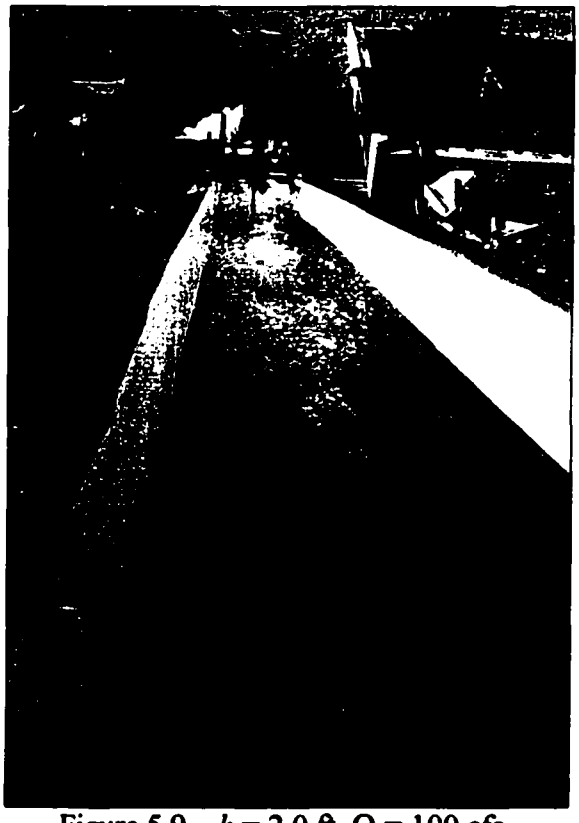

Figure 5.9 – h = 2.0 ft, Q = 100 cfs.

5.2.2 – Flow Observations, h = 1.0 ft

Many of the same characteristics noted for the h = 2.0 ft steps were observed for the h = 1.0 ft steps. However, certain noticeable differences were observed that necessitate discussion. Observations were documented at the same locations as the h = 2.0 ft tests, but at discharges designated for h = 1.0 ft (Table 3.2).

Based upon the previous discussion of flow classification, flow at 7.1 cfs (y_c/h = 0.46) exhibited behavior in the nappe flow regime (Figure 5.10) with skimming flow observed at the next highest discharge of 21.2 cfs (y_c/h = 0.96, Figure 5.11). Again, the onset of skimming flow occurred between these flow rates but an exact discharge cannot be stated with confidence. It is interesting to note that flow conditions at 21.2 cfs met the requirements of skimming flow regime with the exception of a partially filled void existing below the crest of the first step. This condition, not observed with the 2 ft steps, was repeatedly observed throughout testing of the 1 ft steps.

Figure 5.10 – Nappe Flow Regime, h = 1.0 ft, Q = 7.1 cfs (y_c/h = 0.46), Window # 4.

Figure 5.11 – Skimming Flow Regime, h = 1.0 ft, Q = 21.2 cfs (y_c/h = 0.96), Window #4.

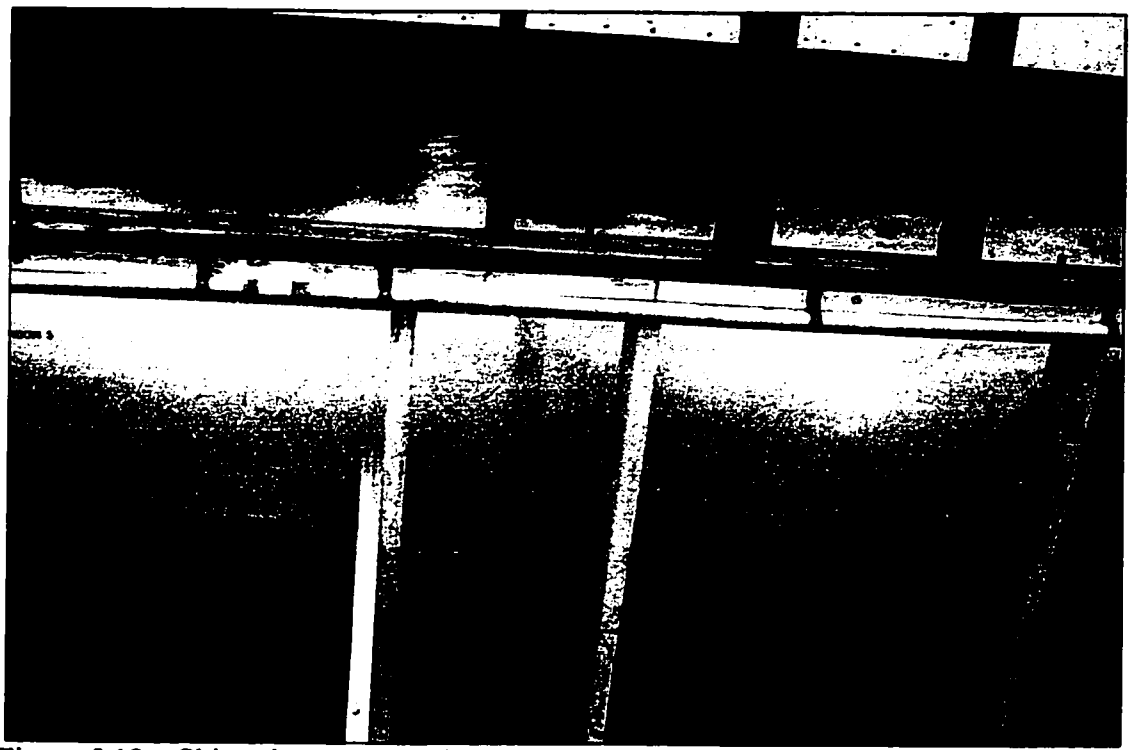

Figure 5.12 – Skimming Flow Regime, h = 1.0 ft, Q = 100 cfs (y_c/h = 2.69), Window #3.

As with the h = 2 ft steps, a non-aerated region existed near the crest with surface aeration commencing immediately downstream. Significant longitudinal roll waves again indicated that initial surface aeration was attributed mainly to wall effects. In addition, downstream progression of a non-aerated region as flow rate increased was again observed (Figures 5.13, 5.14, 5.15, and 5.16). However, surface turbulence and limited sidewall viewing made prediction of an inception point impractical.

General flow conditions along the spillway could again be considered very turbulent with an irregular free surface consisting of water droplets projected above the main stream of flow. However, the most notable difference between the 2.0 ft steps and the 1.0 ft steps was the visual difference in the amount of turbulence generated by the steps, particularly in the skimming flow regime. For the same flow rates, relative bulking of the flow along the 1.0 ft steps appeared to be less than for the 2.0 ft steps. Projection of water droplets above the main stream of flow were much lower than for the 2.0 ft steps and ranged on the order of less than one times the bulked flow depth (Figure 5.17). As well, flow velocities appeared lower for the same flow rates and review of video recordings comparing the two test series reinforced this observation. Again, as with the 2.0 ft steps, the transverse profile of the aerated water surface exhibited a distinct "U" shape indicating boundary-induced drag along the sidewalls (Figures 5.13, 5.14, 5.15 and 5.16). The highest velocity region was visually observed to be located in the center of the cross section.

Figure 5.13 – h = 1.0 ft, Q = 7.1 cfs.

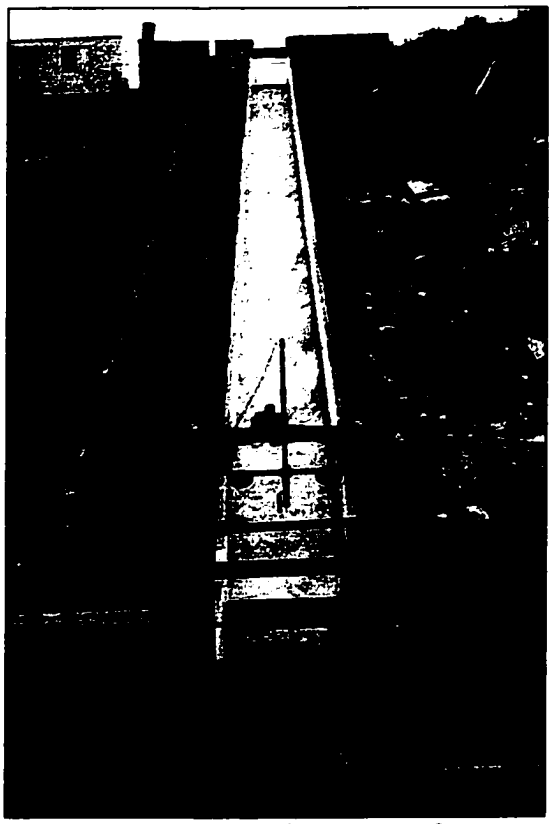

Figure 5.14 – h = 1.0 ft, Q = 40 cfs.

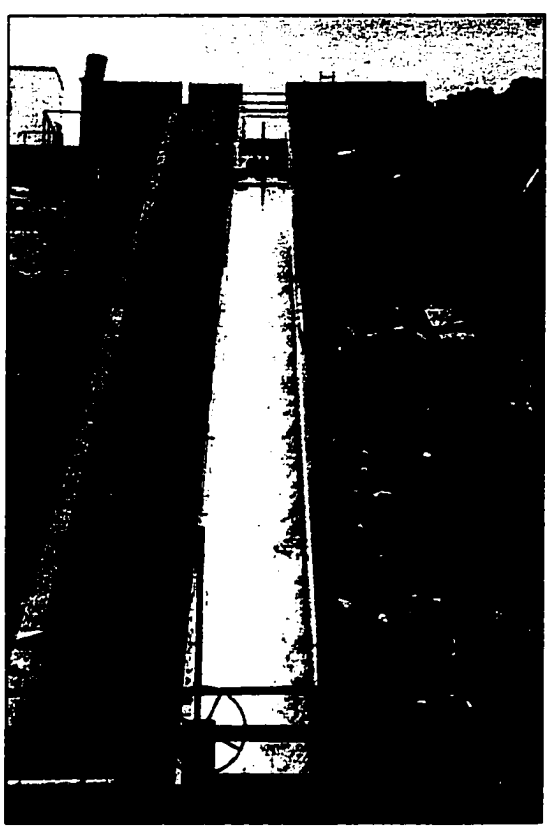

Figure 5.15 – h = 1.0 ft, Q = 60 cfs.

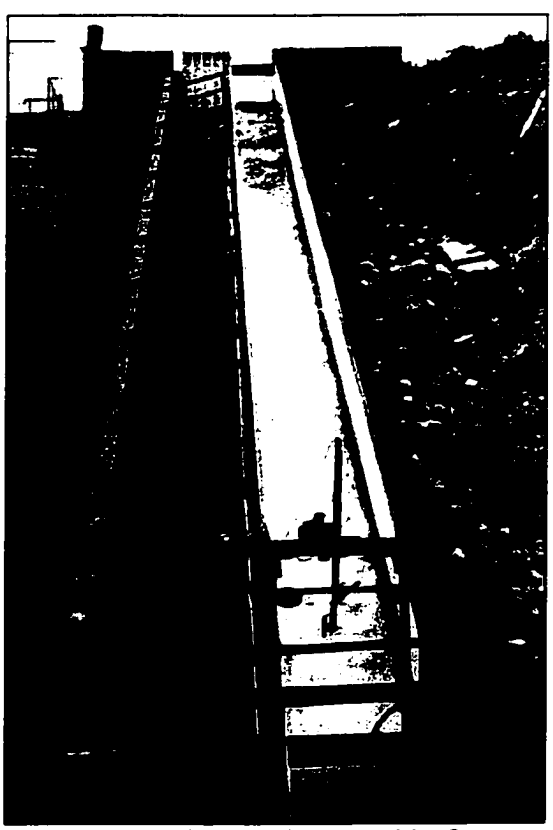

Figure 5.16 – h = 1.0 ft. Q = 100 cfs.

Figure 5.17 – h = 1.0 ft, Q = 100 cfs.

5.2.3 – Summary

It is interesting to note the general differences between observations given here and those made by other investigators on smaller scale models. Observations have been recorded and well documented by nearly all investigators of flow over stepped spillway models. Descriptions of flow conditions on small-scale models tend to be clear and unambiguous. Definite flow characteristics are distinguishable and repeatable to the point of obtaining data from these observations. Conditions on the prototype-scale model in the present study were not as forgiving. The presence of an extremely turbulent free

surface and the variability of flow characteristics throughout testing provided opportunity for only broad, general conclusions to be drawn from the observations. Regardless, these observations are of value in many ways including supporting data analysis, determining design needs, and evaluating scale effects.

5.3 – Air Concentration

The percentage of air entrained in the flow at a given point was measured using the calibrated electronic resistivity probe described in section 4.1.1. Air concentration, c, in the stepped spillway flow was determined using the air probe output and equation (4-1).

5.3.1 – Air Concentration Profiles

Air concentration profiles consisted of local air concentration values obtained at chosen intervals over a distance, y, normal to the spillway floor. Details of the profile intervals and stationing are described in section 3.2.3. Figure 5.18 shows a typical set of air concentration profiles for h = 2.0 ft at a given station over a range of discharges. Trends exhibited in these curves are typical of those found on stepped spillway models using similar instrumentation (Straub and Anderson, 1958 (smooth spillway); Gaston, 1995; Ruff and Frizell, 1994; Boes and Hager, 1998; Matos and Frizell, 2000; Chamani and Rajaratnam, 1999). For this study, flow conditions in the skimming flow regime ($\geq$ 60 cfs) showed air concentration increasing gradually from the bed and more rapidly in the middle region of the profile. Near the surface, the change in air concentration with depth begins to decrease prior to reaching the surface. Flow conditions in the nappe or transition regime (20 and 40 cfs) exhibit a less defined lower and middle region. In

addition, as discharge increases, apparent depth increases with the shape of the curve remaining fairly constant. A distinct difference can be noted in the shape and slope of the curves at 20 and 40 cfs compared to those at higher discharges, reflecting differences between nappe and skimming flow regimes.

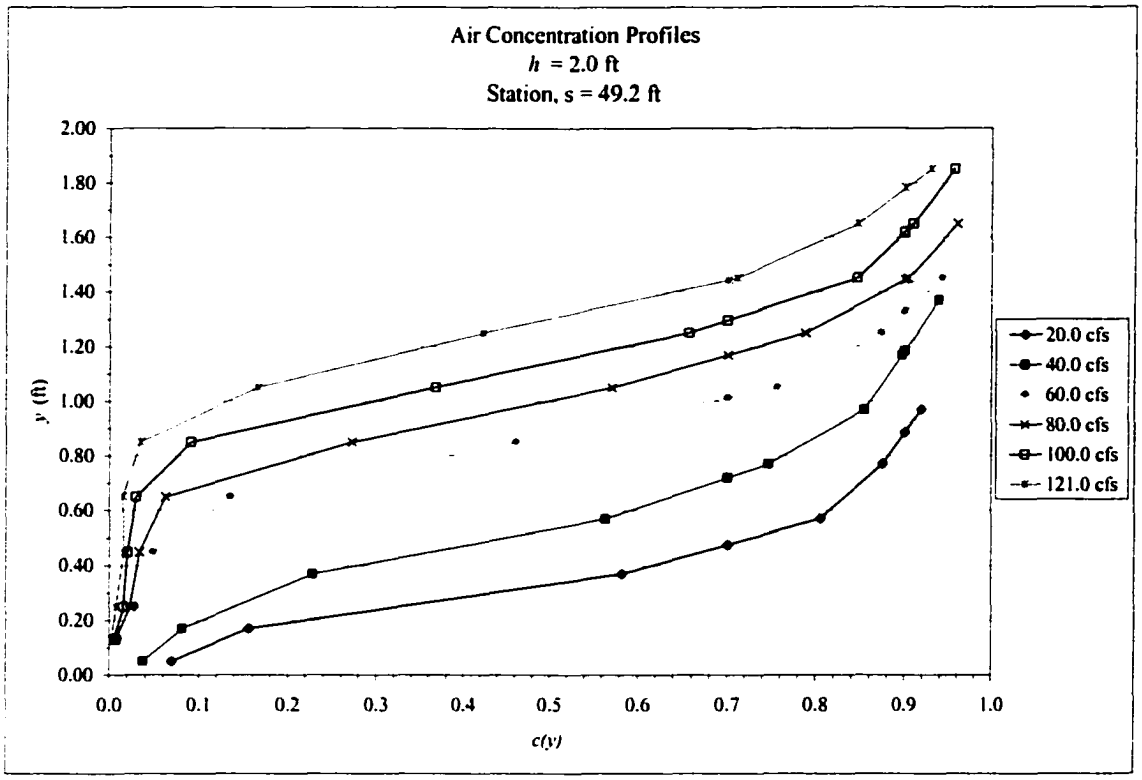

Figure 5.18 – Typical air concentration profiles (h = 2.0 ft, Station s = 49.2 ft).

Figure 5.19 shows air concentration profiles for h = 1.0 ft at station s = 49.2 for various discharges. With exception of a few points at 21.2 cfs, the profiles exhibit the same sort of trends as the curves in the h = 2.0 ft tests. Note, however, that the profiles have overall flatter slopes than those in Figure 5.18, indicating higher average air concentrations for the 1.0 ft steps.

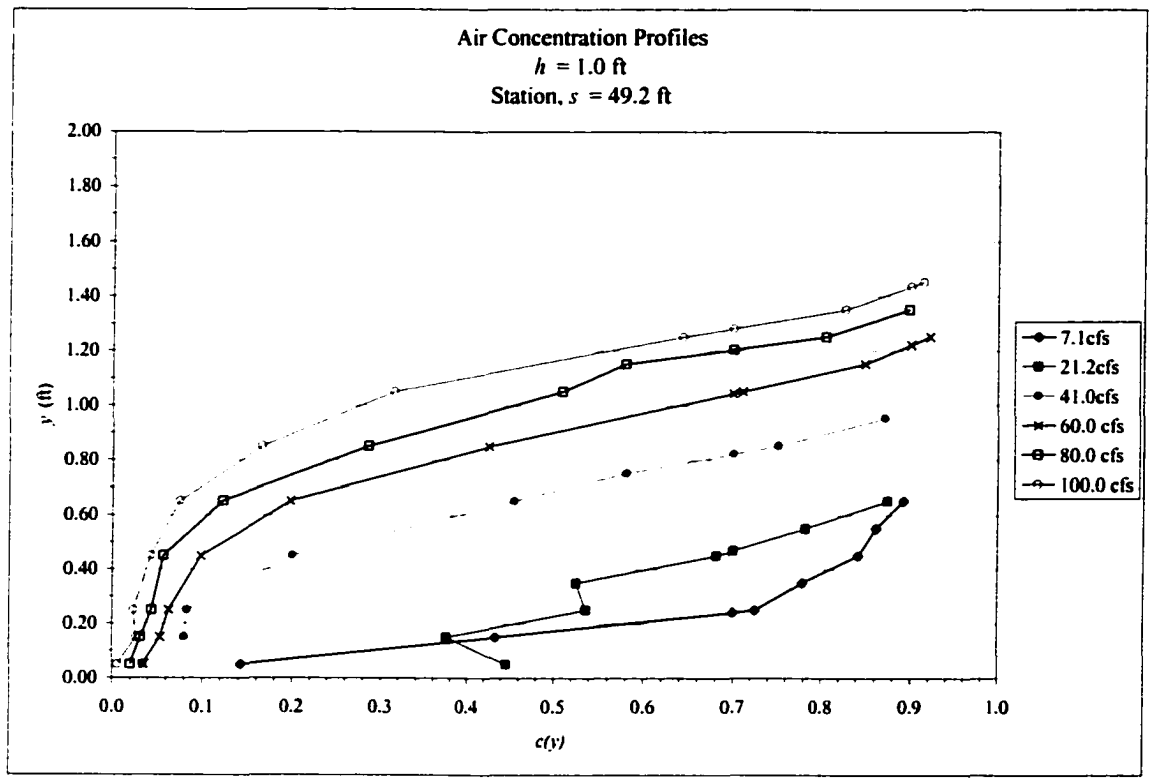

Figure 5.19 - Typical air concentration profiles (h = 1.0 ft, Station s = 49.2 ft).

For comparison, typical air concentration profiles for the smooth spillway are shown in Figure 5.20. Notice that, in general, air concentration is lower throughout the entire profile depth until the near the surface of the main flow. As expected, this indicates that average air concentration and bulking of the flow is much higher in stepped spillway flow than in smooth spillway flow.

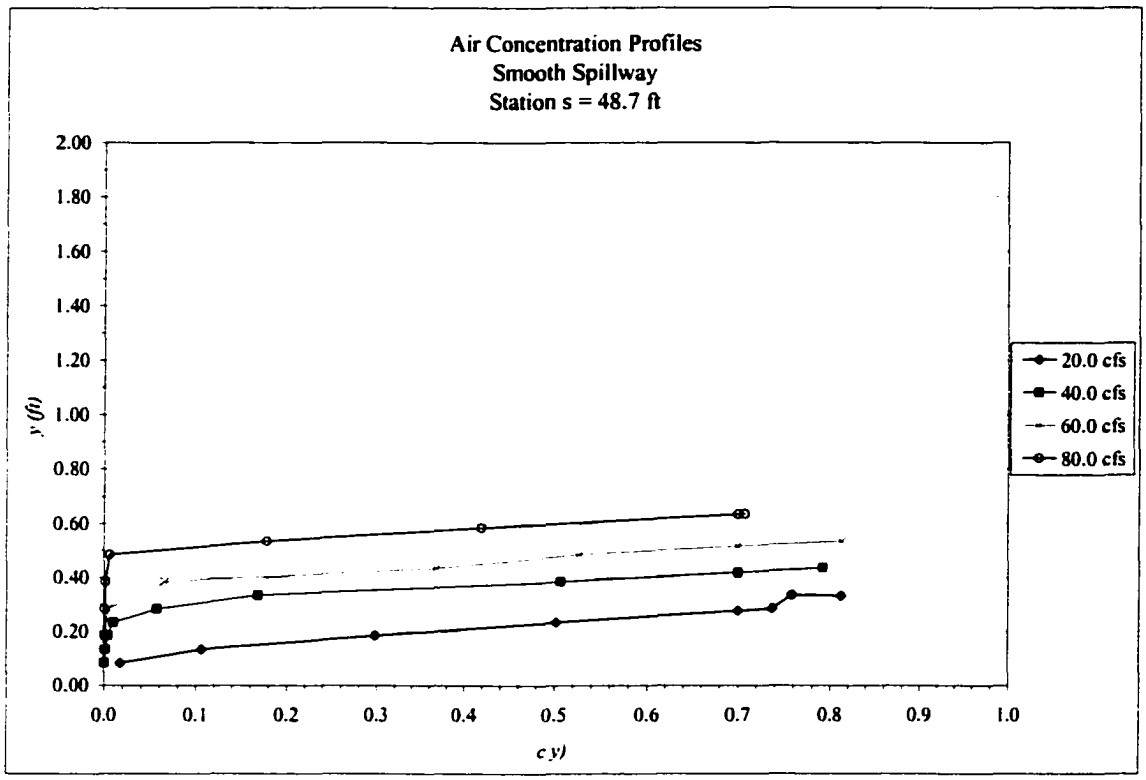

Figure 5.20 - Typical air concentration profiles (smooth spillway, Station s = 48.7 ft).

Figure 5.21 shows a typical set of air concentration profiles for h = 2.0 ft at each station for a single discharge. It is clearly shown that there is minimal variation in the profiles along the length of the spillway indicating that the average air concentration remains approximately constant for a given discharge. As expected, however, a slight difference is noticed in the lower portions of the profiles with air concentration increasing with increased distance from the crest. Figure 5.22 shows the same type of data for h = 1.0 ft. Notice that grouping of the profiles again indicates that average air concentration remains approximately constant for a given discharge. However, a surprising difference is shown in the lower portions of the profiles where air concentration decreases, rather than increases, along the length of the spillway. The difference is only slight when comparing profile averages but is interesting to note, nonetheless. Remaining air concentration profiles versus discharge and station for all tests are given in Appendix A.

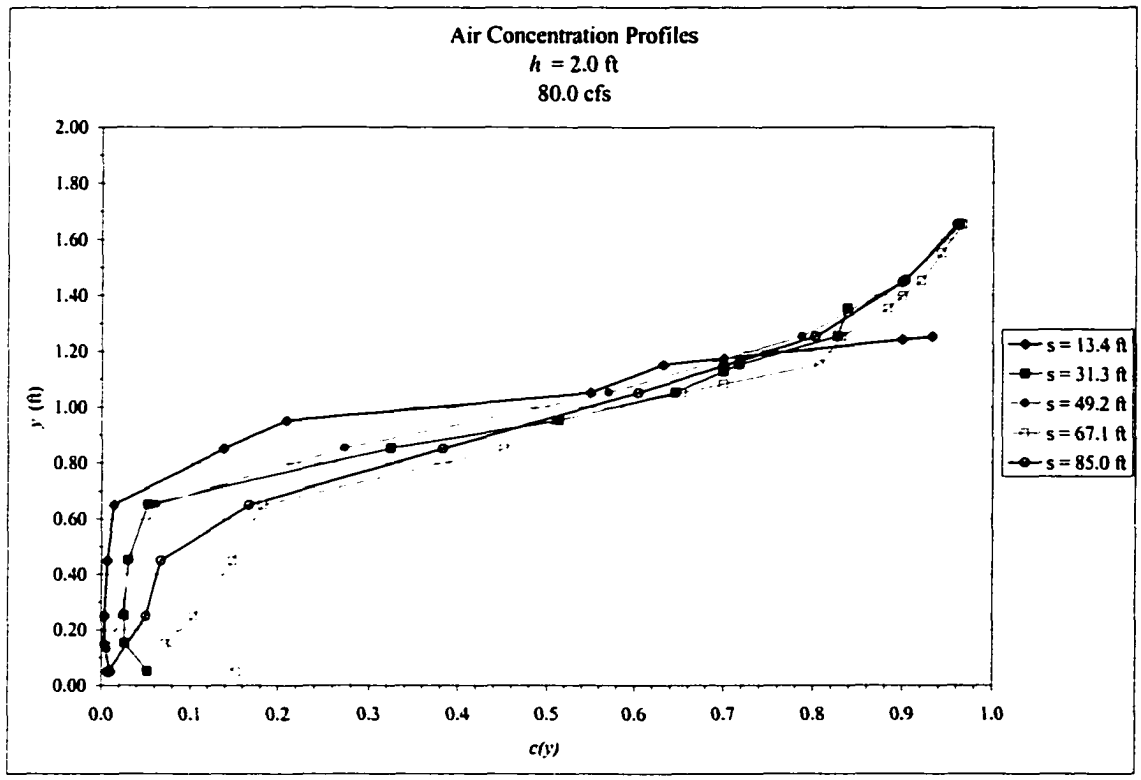

Figure 5.21 – Typical air concentration profiles (h = 2.0 ft, Q = 80.0 cfs).

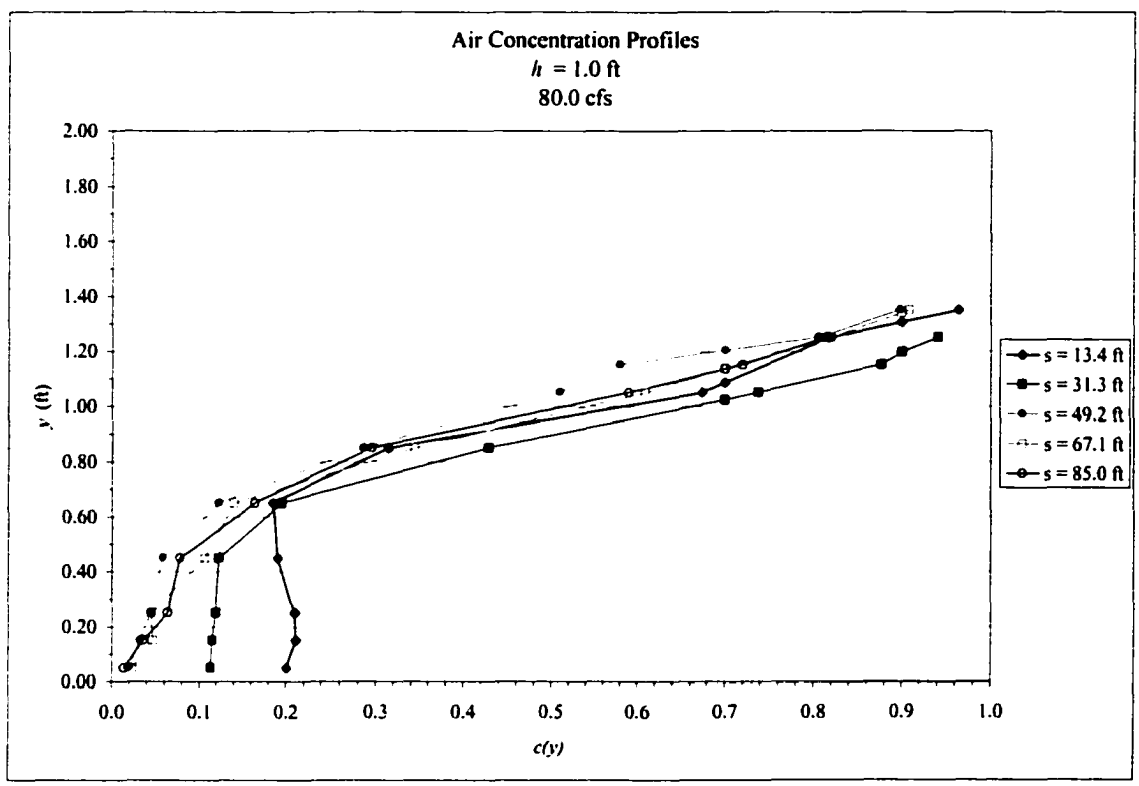

Figure 5.22 – Typical air concentration profiles (h = 1.0 ft, Q = 80.0 cfs).

5.3.2- Average Air Concentration

Lack of a definite free surface and the need to quantify attributes of the aerated flow requires definitions for average air concentration and characteristic depths. Given the profiles of local air concentration *c(y)*, average air concentration $\overline{C}$ can be defined as:

$$\overline{C} = \frac{\int_{y_l}^{y_u} c(y)dy}{\int_{y_l}^{y_u} dy} = \frac{1}{y_u - y_l}\int_{y_l}^{y_u} c(y)dy \tag{5-1}$$

where y_l and y_u are the lower and upper limits of the depth profile to be integrated. It is common to select a value for y_u at the depth where the local air concentration is 0.90, frequently defined as y_{90} (Wood, 1991; Boes and Hager, 1998; Chamani and Rajaratnam, 1999). In their classic work on aerated flow, Straub and Anderson (1958) used a depth where the air concentration is 0.99. For the present study, the integration depth was typically defined from the first point in the depth profile y_l to an upper depth where $y_u = y_{90}$.

As seen in Figures 5.18 through 5.22, most of the profiles begin just above the tip of the step and extend to a depth where the air concentration ranges from 0.70 to 0.98. During data collection, the air concentration probe was set at a distance of approximately 0.05 ft from the tip of the step. Upper depth readings were generally taken where the instrument measured data that was near the dry-air readings and visually appeared almost out of the flow. Applying the air probe calibration equation to the raw data reduced the higher air readings by a small percentage, often below 0.90. Where this occurred, the depth $y_u = y_{90}$ was linearly extrapolated from the uppermost data points. In profiles extending beyond 0.90, the depth y_{90} was linearly interpolated between data points. Data

at the lowest depth in the profile frequently showed very high air concentrations due to displacement of the probe into the separation area below the step tip (Figure 5.23). It was observed that this was caused by deflection of the probe support mechanism due to forces of the flowing water. Another concern was the existence of data that appeared suspect or unreasonable due to probe malfunction, such as loss of signal or zero balance. An example of this is shown in Figure 5.23 with the upper portion of station s = 13.4 ft profile.

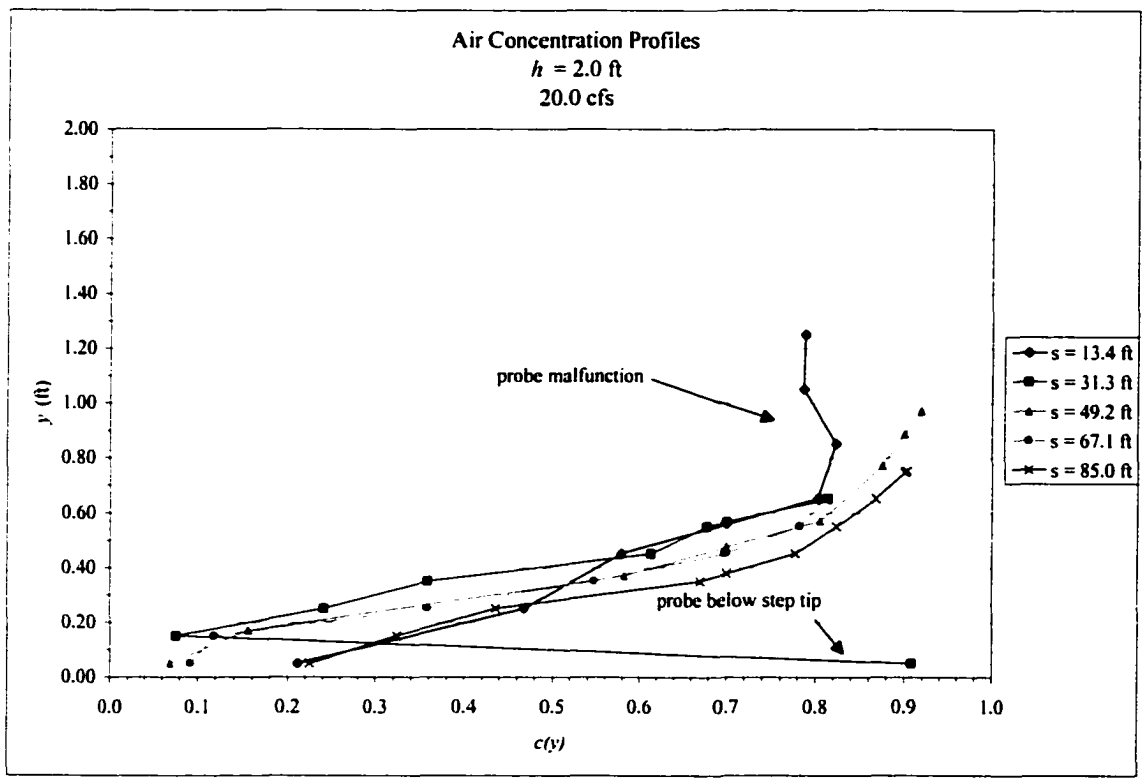

Figure 5.23 – Example of outlier air concentration data (h = 2.0 ft, Q = 20 cfs).

Selection of integration points within each profile was based on eliminating data with the problems mentioned above and integrating a representative air concentration profile. It should be noted that profiles with erroneous data were not the majority and that the entire profile depth was generally used for averaging. Most of the problems occurred in data from the h = 2.0 ft tests with only one profile modified in h = 1.0 ft tests

and none in smooth spillway tests. Figures 5.24, 5.25 and 5.26 show average air concentration values along the spillway for h = 2.0 ft, h = 1.0 ft, and the smooth spillway, respectively. Notice that, as shown previously (Figures 5.21 and 5.22), average air concentration appears to slightly increase with distance downstream from the crest for h = 2.0 ft and slightly decrease for h = 1.0 ft. Remaining profiles of average air concentration versus station for all tests are given in Appendix B.

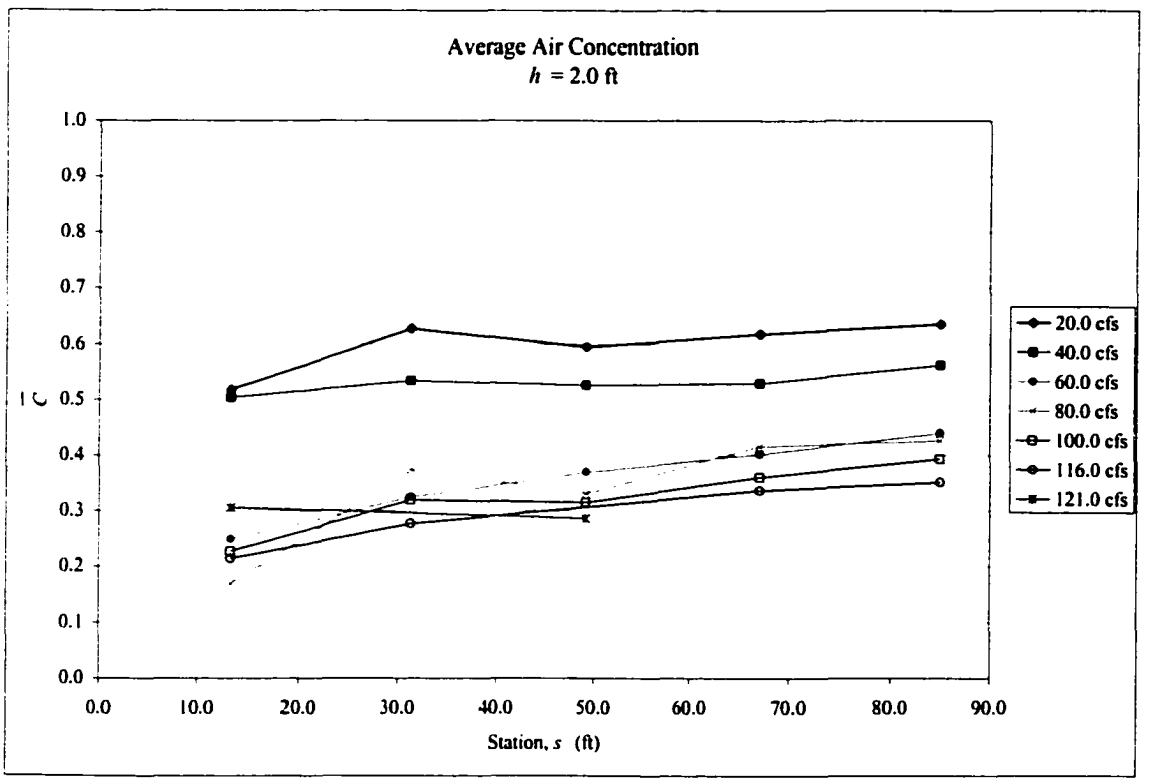

Figure 5.24 – Average air concentration, h = 2.0 ft.

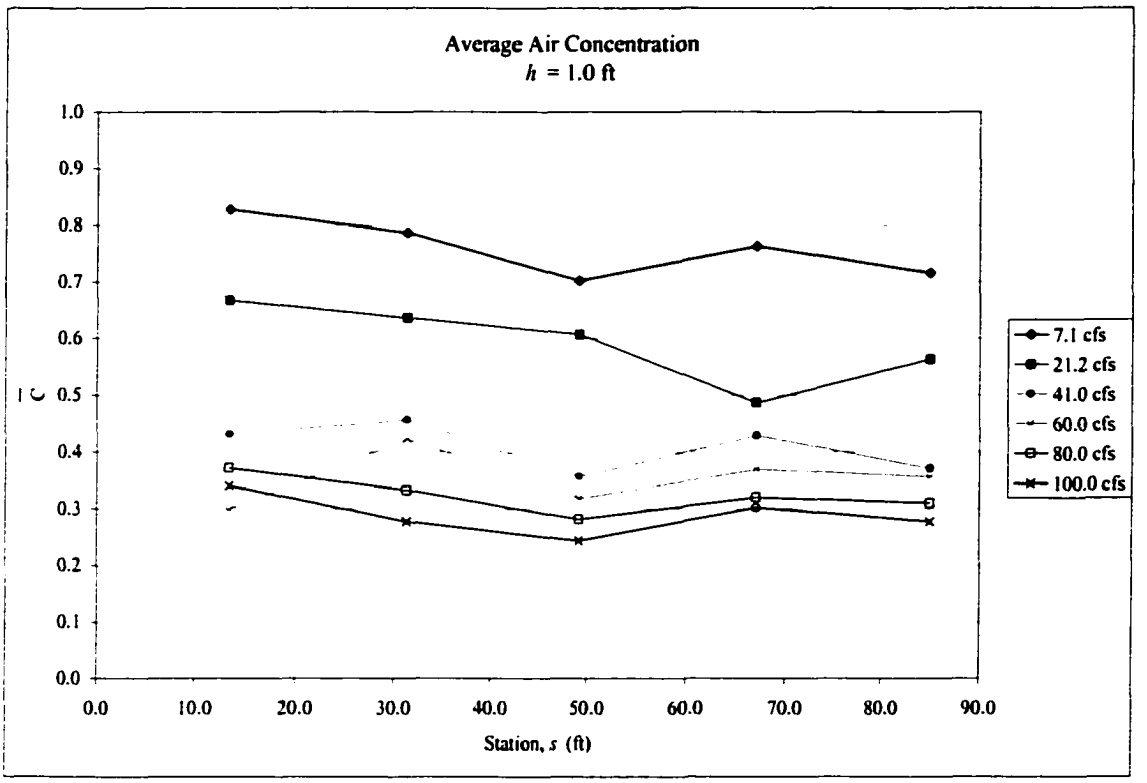

Figure 5.25 – Average air concentration, $h = 1.0$ ft.

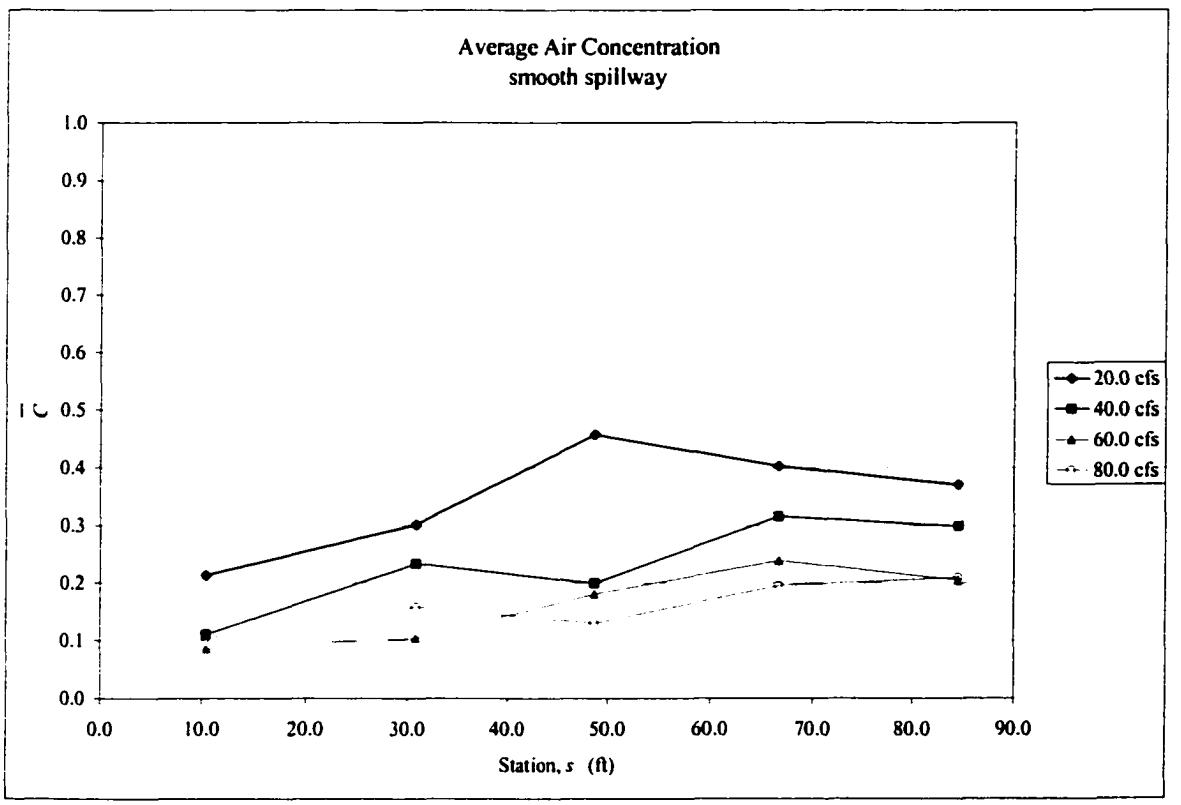

Figure 5.26 - Average air concentration, smooth spillway.

5.4 – Velocity

Velocity of the aerated flow was determined using the back-flushing Pitot tube described in Section 4.2. The Pitot tube provides a measurement of the difference in kinetic and static pressure heads while continuously back flushing to prevent air bubbles from entering the instrument. With the known local air concentration, a calibration coefficient is applied to the differential pressure measurement to compute the local velocity *u(y)* of the air-water flow.

5.4.1 – Velocity Profiles

Velocity profiles were obtained simultaneously with the air concentration profiles at the same intervals and stations. Figures 5.27, 5.28, and 5.29 show a typical set of velocity profiles at a given station over a range of discharges for $h = 2.0$ ft, $h = 1.0$ ft, and the smooth spillway, respectively. In general, for the stepped spillway, the profiles tend to have the same shape beginning with velocity gradually increasing from the bed until a maximum velocity gradient is reached. At some point in the upper region of the depth, an acute change is observed where the velocity abruptly increases or decreases. Velocity profiles similar to this shape have been observed in several studies of stepped spillway flow (Gaston, 1995; Chamani, 1997; Chamani and Rajaratnam, 1999; Matos and Frizell, 2000) and steep, rough-surfaced spillway flow (Straub and Lamb, 1956; Cain, 1978).

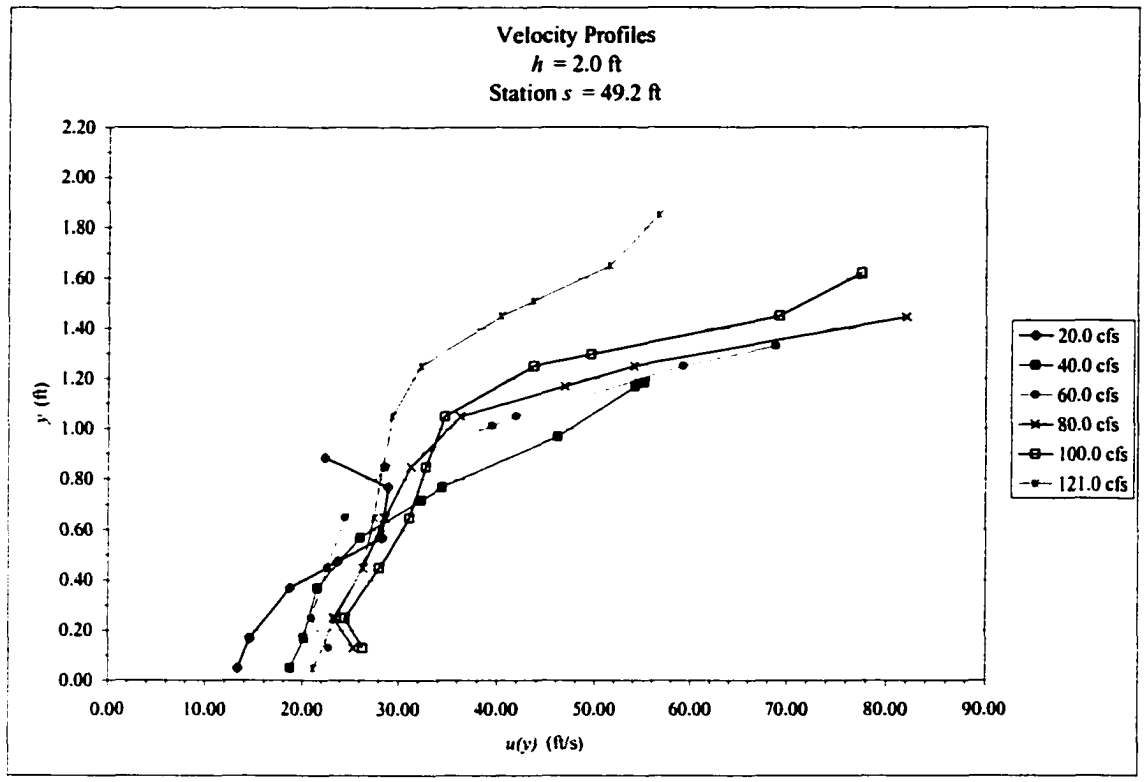

Figure 5.27 – Typical velocity profiles (h = 2.0 ft, Station s = 49.2 ft).

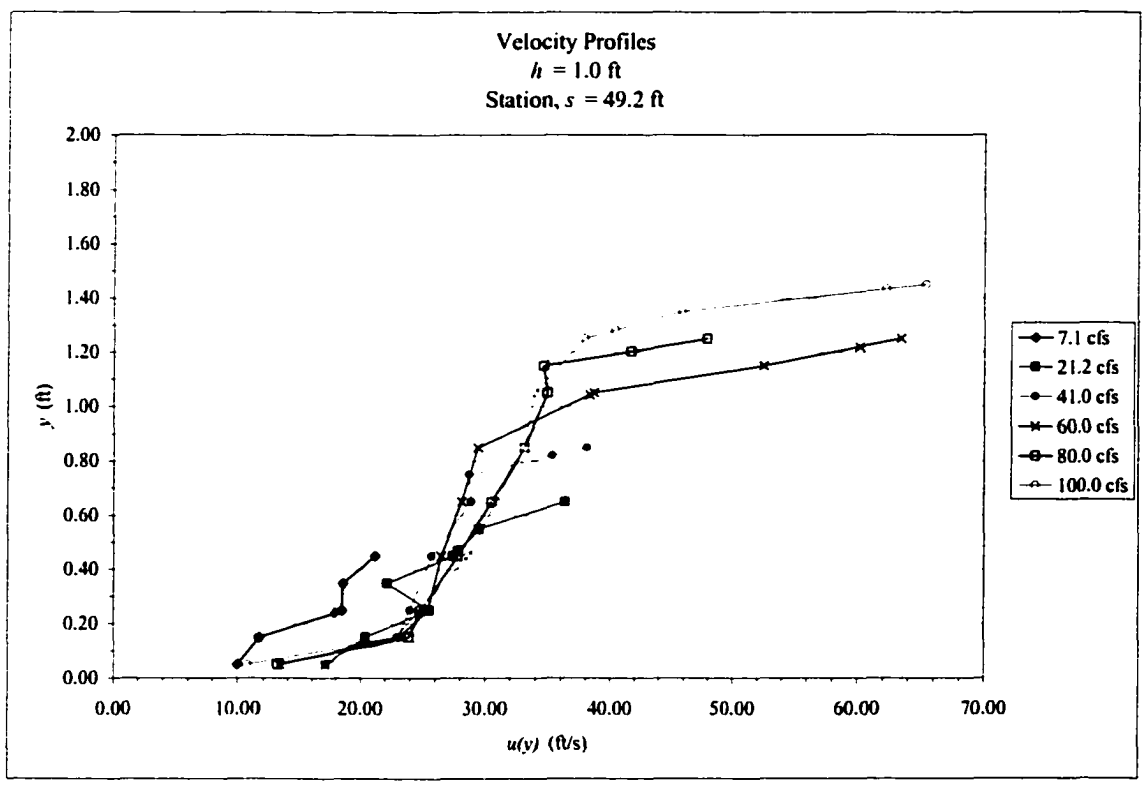

Figure 5.28 – Typical velocity profiles (h = 1.0 ft, Station s = 49.2 ft).

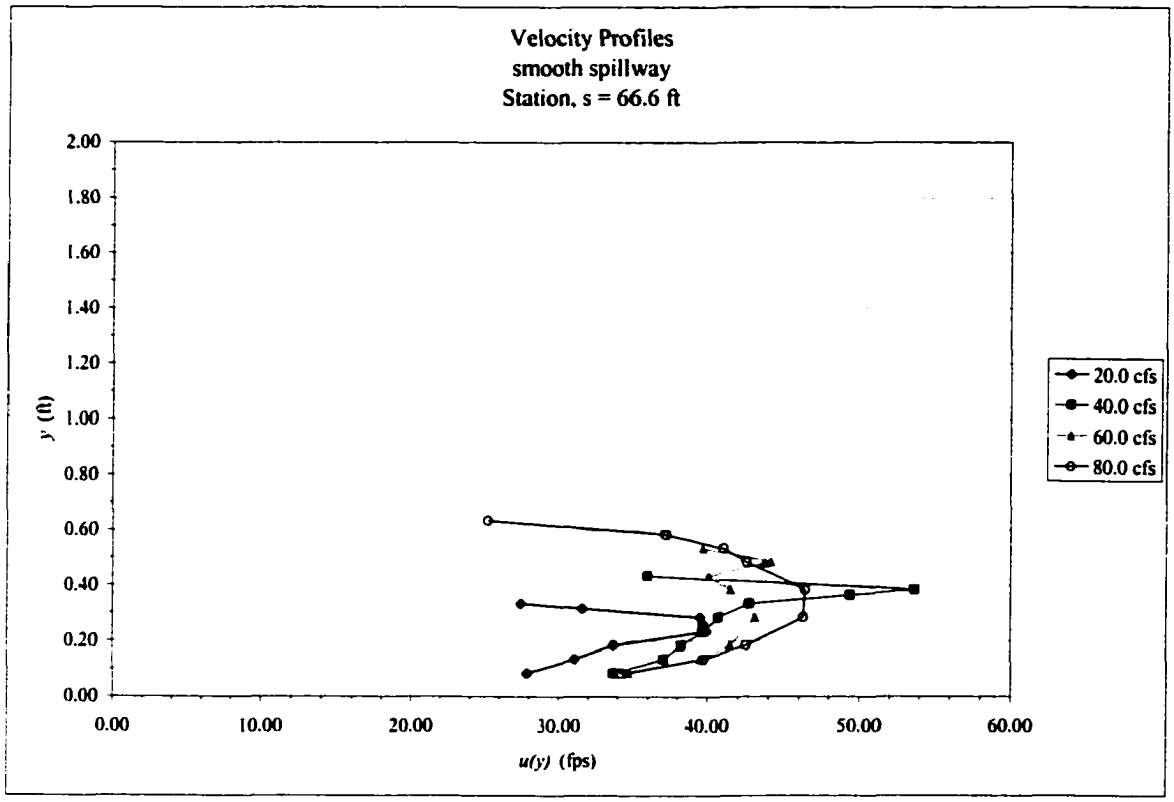

Figure 5.29 - Typical velocity profiles (smooth spillway, Station s = 52.8 ft)

As mentioned previously, in the upper portion of several profiles, near the surface or at the extent of data collection, an acute change is observed corresponding to a sudden decrease or increase in velocity. Straub and Lamb (1956) first noticed this phenomenon in velocity measurements of self-aerated flow on a steep, rough-surfaced spillway. Flow conditions in the upper region consisted of a highly irregular, wavy surface above which large particles or "clumps" of water ejected from the main flow, similar to that of stepped spillway flow. Velocity profiles in their study, obtained using an electrical conductivity probe and salt injection method, mainly decreased in the upper regions. It was hypothesized that shear stress develops from increased resistance on these particles due to atmospheric drag and the change in momentum and the return of particles back to the main flow results in a loss of velocity.

In the present study, the acute change in the profile was more often associated with an increase in velocity. A plausible explanation is the sensitivity of the Pitot tube to high air concentrations and low pressure differentials in this region. The backflushing flow maintained in the Pitot tube is determined by the necessity to overcome the maximum anticipated velocity head in the main flow. In highly aerated regions, the velocity of air alone may not provide sufficient differential pressure to overcome the flushing flow. In the upper region, it is possible that the Pitot tube recorded intermittent periods of high pressure, due to impacting water particles, followed by periods of little or no pressure, due to air velocity only. This condition was observed during calibration of the Pitot tube at high air concentrations and prevented calibration above approximately 80%. In addition, the Pitot tube coefficient λ in equation (4-5) increases as a power function with an increase in air concentration. Large values of air concentration (i.e. small values of pressure differential) may result in a large value for the coefficient, possibly returning an unreasonably high value of velocity.

Cain (1978) had similar results in aerated smooth spillway flow using a velocity probe that measured dynamic pressure. He showed that the sensitivity to errors in either dynamic pressure or air concentration could be demonstrated by differentiating an equation similar to equation (4-5):

$$u = \sqrt{\frac{2(p_d - p_s)}{\rho_w(1-c)}} = \left[\frac{2}{\rho_w}\left[\frac{p_d - p_s}{1-c}\right]\right]^{1/2} \tag{5-2}$$

$$du = \frac{1}{2}\left[\frac{2}{\rho_w}\left[\frac{p_d - p_s}{1-c}\right]\right]^{-1/2}\left[\frac{2dp_d}{\rho_w(1-c)} + \frac{2(p_d - p_s)dc}{\rho_w(1-c)^2}\right] \tag{5-3}$$

$$\frac{du}{u} = \frac{dp_d}{u^2 \rho (1-c)} + \frac{dc}{2(1-c)} \tag{5-4}$$

$$\frac{du}{u} = \frac{dp_d}{u^2 \rho (1-c)} + \frac{dc}{2(1-c)} \tag{5-5}$$

It is apparent from equation (5-5) that when c tends to 1.0, even small errors in dynamic pressure dp_d or air concentration dc will cause large errors in velocity du. As discussed in Chapter 4, the backflushing Pitot tube used in the present study is sensitive to low differential pressures corresponding to high air concentrations. During calibration, pressures encountered with air concentration above approximately 80% were below the range of pressure sensitivity for the Pitot tube. Analysis of local velocity data from both stepped spillway tests showed that the acute increase in velocity associated with low pressure differentials occurred at an average air concentration of approximately 0.70. Based on the above discussion, it is reasonable to assume that velocity data corresponding to air concentrations greater than 0.70 are unreliable.

It is interesting to note that earlier research conducted with an identical backflushing Pitot tube to the one used in the present study yielded similar results. Gaston (1995) determined velocity data above an air concentration of 0.65 to be invalid while Matos and Frizell (2000) found velocity data to be inaccurate at concentrations as low as 0.40 to 0.50. For the present study, velocities were deemed not valid for regions of flow with air concentrations greater than 70%. An exception is for the smooth spillway velocity profiles shown in Figure 5.29 where velocities in the upper region tended to decrease. The high velocity smooth spillway flow maintained higher dynamic pressures throughout the entire profile, even with air concentrations greater than 70%. In

addition, air concentration in general was less than approximately 80% throughout the profile until the last data point where the probe was essentially out of the water and registered 90% or greater. Velocities were not taken for the last data point. Differential pressures and corresponding velocities throughout the depth appeared valid even in areas greater than 70% air concentration.

Based on the above discussion, it is reasonable to assume a constant velocity of u_{70} for depths greater than y_{70}, where y_{70} and u_{70} are the linearly interpolated depth and velocity corresponding to an air concentration of 0.70. Another assumption is to define the upper limit of the profile at a linearly interpolated depth of y_{90}, or where the corresponding air concentration is 0.90. Figure 5.30 shows a typical set of modified velocity profiles for h = 2.0 ft. It should be noted that velocity profiles for the smooth spillway were not altered and were analyzed in their original form due to reasons discussed previously. All velocity profiles collected in this study, with modifications to the upper regions, are given in Appendix A.

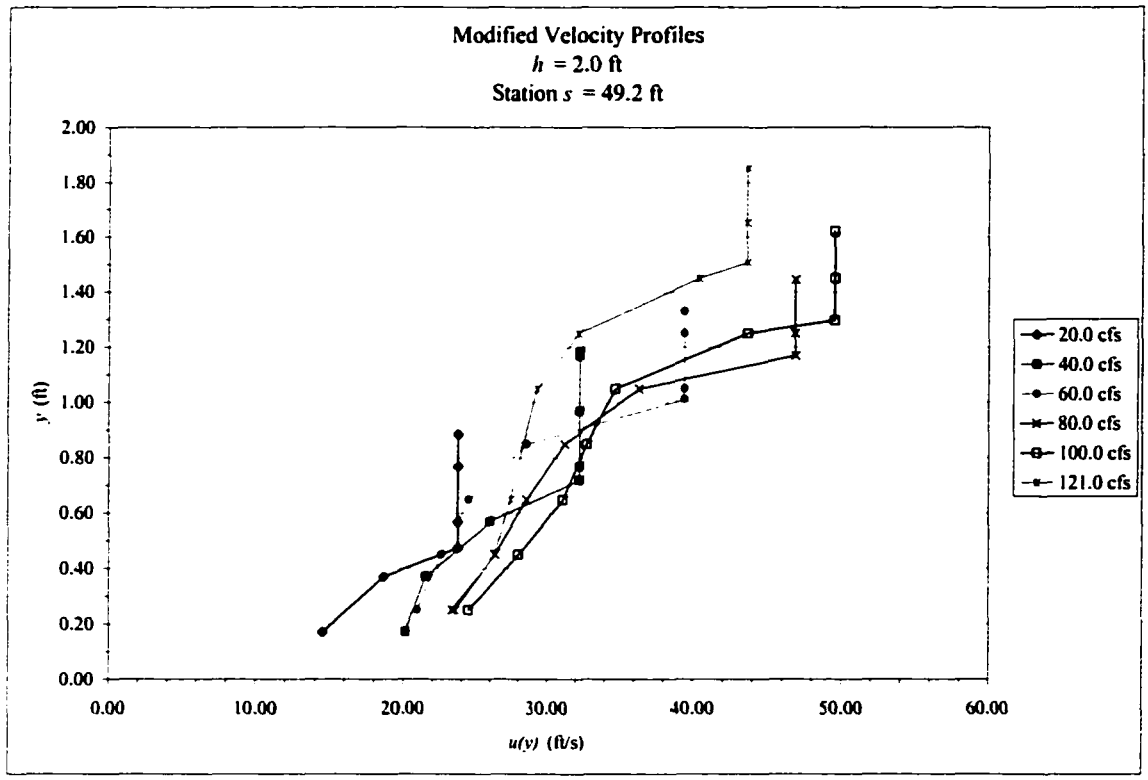

Figure 5.30 – Typical modified velocity profiles (h = 2.0 ft, Station, s = 49.2).

5.4.2 – Average Velocity

Average velocity of the aerated flow can be determined by integrating a given profile of local velocities over a certain depth. As with the air concentration profiles, selection of the lower and upper limits of integration, y_u and y_l, must be determined. Selection of the lower limit was generally equal to the starting depth of the corresponding air concentration profile. In addition, if an outlier point was removed from an air concentration profile, the corresponding local velocity at that depth was also removed. For the upper limit, the depth y_{90} was selected. Therefore, average velocity $\overline{U}$ is defined as:

$$\overline{U} = \frac{\int_{y_l}^{y_{90}} u(y)dy}{\int_{y_l}^{y_{90}} dy} = \frac{1}{y_{90} - y_l} \int_{y_l}^{y_{90}} u(y)dy \tag{5-6}$$

Figures 5.31, 5.32, and 5.33 show average velocity values along the spillway for h = 2.0 ft, h = 1.0 ft, and the smooth spillway, respectively. Notice that for h = 2.0 ft, average velocity is initially increasing with distance along the spillway indicating acceleration and nonuniform or gradually varying flow conditions. With the exception of profiles for Q = 100 and 116 cfs, average velocity begins to become constant approximately halfway down the slope, or station s = 50 ft, indicating nearly uniform flow conditions. For h = 1.0 ft, average velocity appears to be fairly constant along the full length of the spillway. Average velocities for the smooth spillway increase with distance and are consistently 10-40% greater than for the stepped spillway depending on total discharge and location along the slope. Remaining profiles of average velocity versus station for all tests are given in Appendix B.

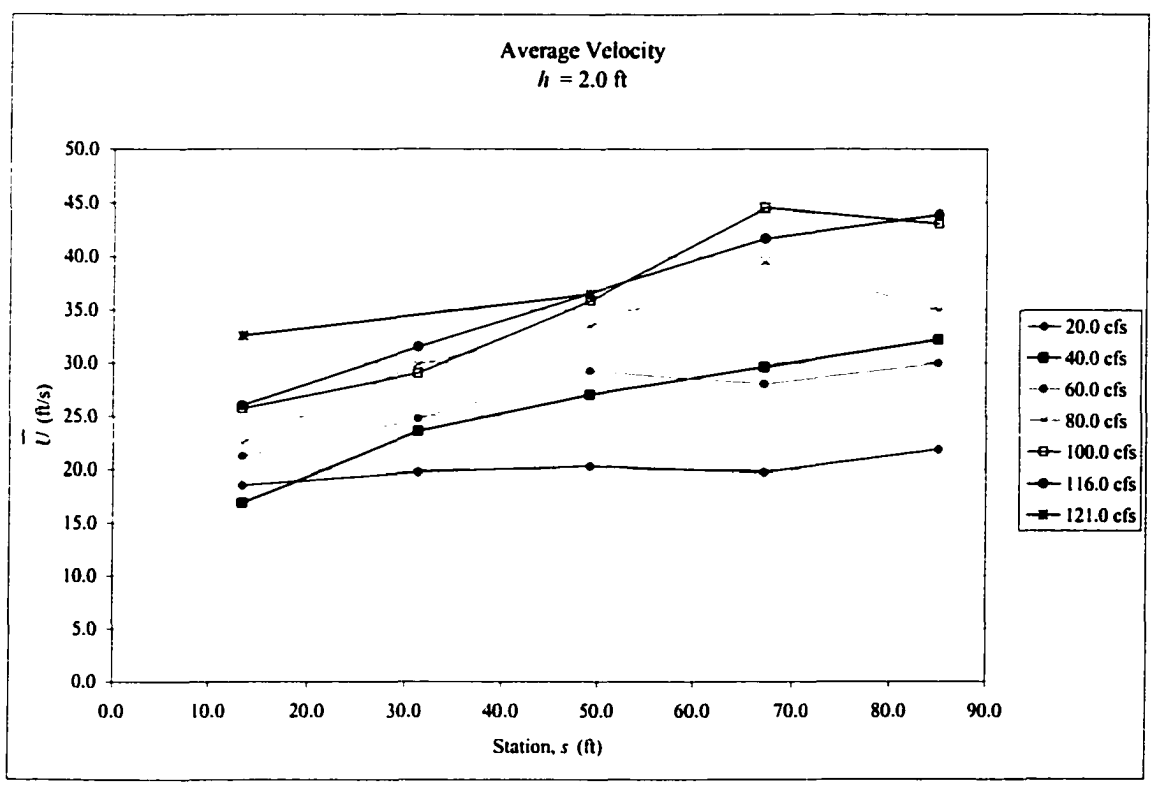

Figure 5.31 – Average velocity, h = 2.0 ft.

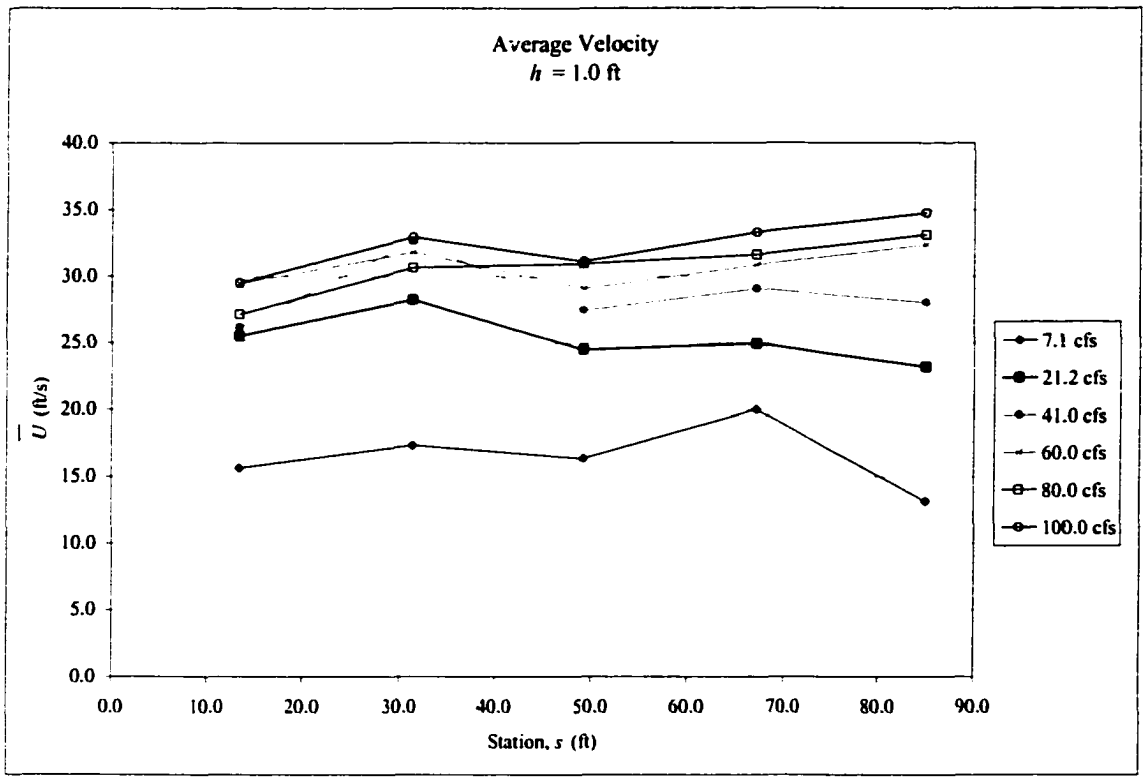

Figure 5.32 – Average velocity, h = 1.0 ft.

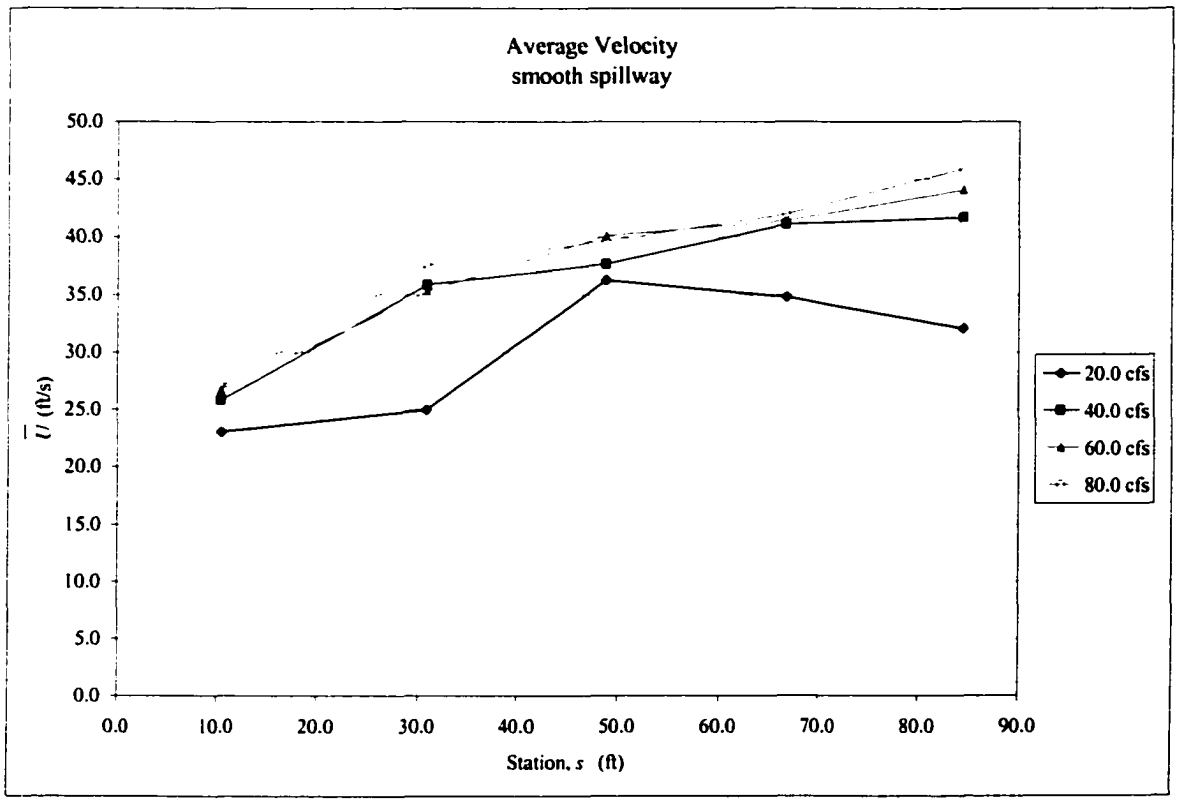

Figure 5.33 – Average velocity, smooth spillway.

5.5 Pressure Profiles

Pressure data were taken using flush-mounted pressure taps mounted along the longitudinal centerline of the steps at three locations as described in Section 4.5. Figures 5.34 and 5.35 show typical pressure profiles taken approximately at station s = 50 ft for h = 2.0 ft (step number 12) and h = 1.0 ft (step number 23), respectively. Figure 5.36 shows the pressure distribution for h = 1.0 ft, step number 23, and the upstream adjoining step number 22. It is interesting to note the similarity in the pressure profiles over the two steps. This pattern was repeated along the spillway, especially at the middle and bottom stations where the flow was considered developed and nearly uniform. Pressure profiles for stations near the crest and base of the spillway are given in Appendix C for both h = 1.0 ft and h = 2.0 ft. Values of pressure along the spillway ranged from approximately –0.433 psi (1.0 ft of water) on the vertical face just below the tip of the step, to over +2.3 psi (5.3 ft of water) on the horizontal face near the tip of the step, depending on discharge. Negative pressures normally occurred with the nappe flow regime in the separation zone just below the step tip. As anticipated, the overall magnitude of the pressures increased with flow rate.

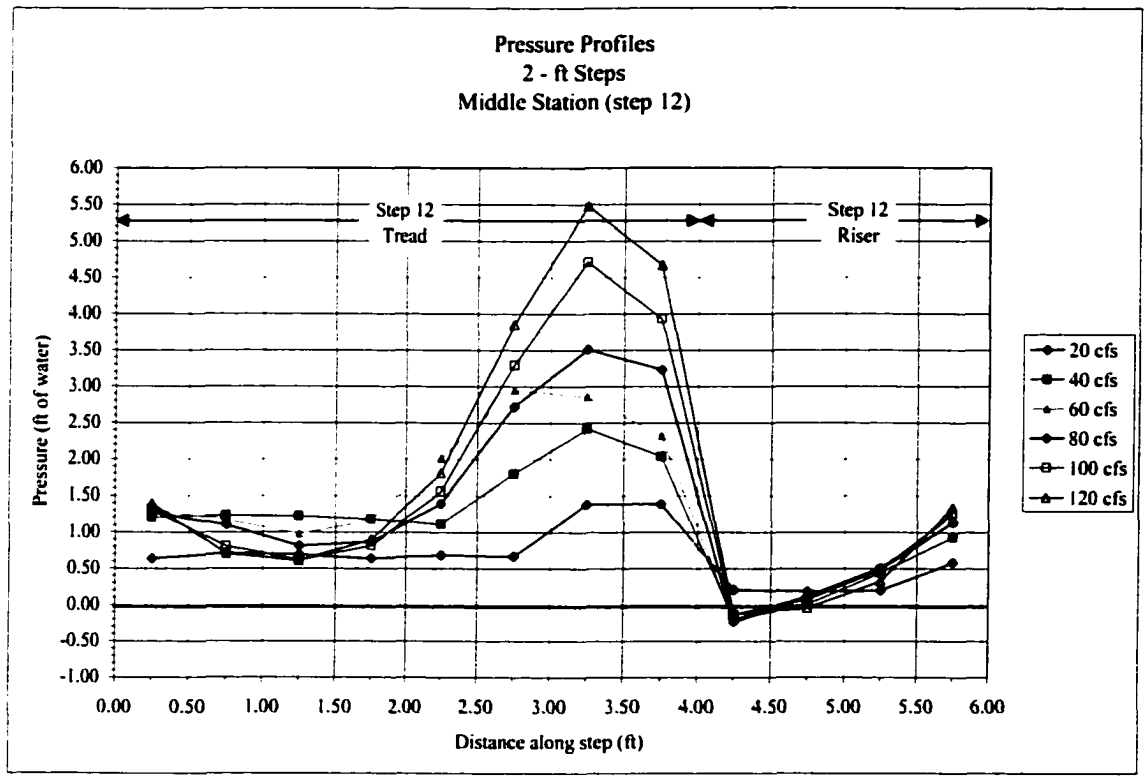

Figure 5.34 – Typical pressure profiles, h = 2.0 ft, step number 12.

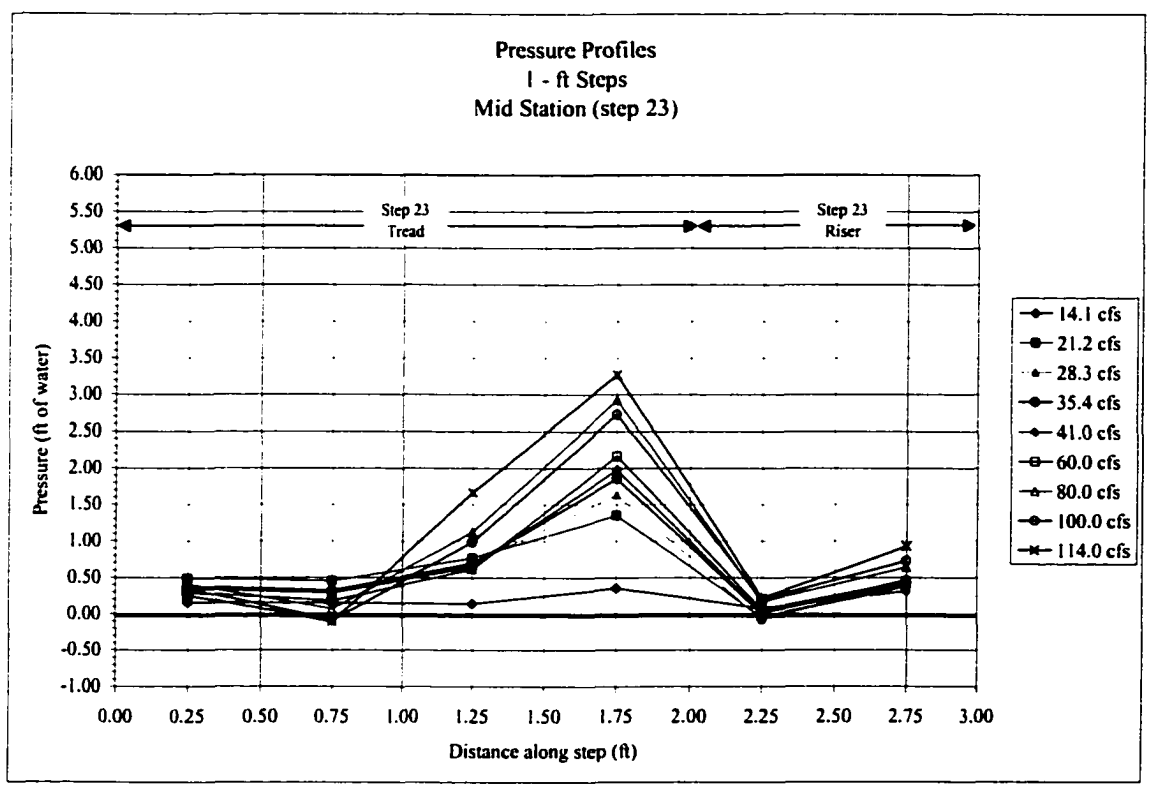

Figure 5.35 - Typical pressure profiles, h = 1.0 ft, step number 23.

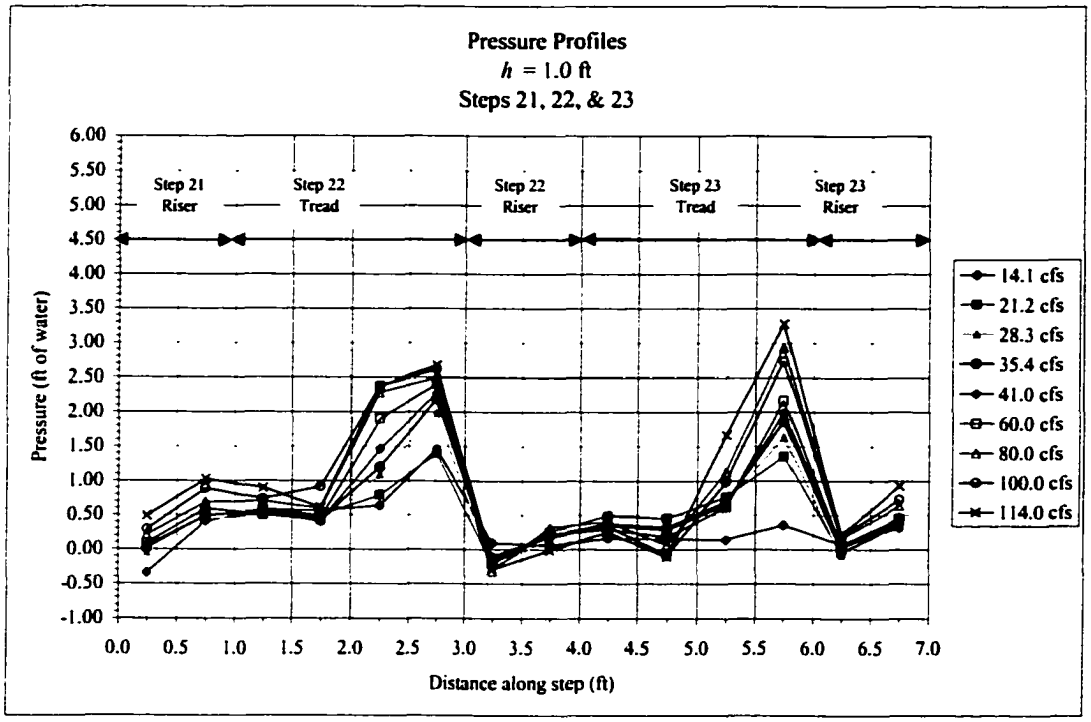

Figure 5.36 - Typical pressure profiles, h = 1.0 ft, steps number 21, 22, and 23.

CHAPTER 6

DATA ANALYSIS

6.1 Flow Depth and Continuity

6.1.1 Characteristic Flow Depth

A common difficulty associated with the study of highly turbulent, aerated, open channel flow is determining a characteristic flow depth. With the knowledge of air concentration variation with depth, it is possible to define both an aerated and non-aerated flow depth. As discussed previously, the depth at which air concentration equals 0.90, or y_{90}, is typically selected as a representative bulked flow depth for aerated flow. Several comparisons with flow depths observed through the viewing windows in the present study showed y_{90} to reasonably represent the aerated bulked flow depth.

Recalling equation (5-1) and defining the upper flow depth as $y_u = y_{90}$ and $y_l = 0$, defined as the psuedo-bottom formed by a plane passing through the tips of the steps, average air concentration is given as:

$$\overline{C} = \frac{\int_{y_l}^{y_u} c(y)dy}{\int_{y_l}^{y_u} dy} = \frac{1}{y_{90}} \int_{0}^{y_{90}} c(y)dy \qquad (6\text{-}1)$$

The non-aerated, clear water depth can be defined as:

$$d_w = \int_0^{y_{90}} (1 - c(y))dy \tag{6-2}$$

Combining equations (6-1) and (6-2), the non-aerated clear water flow depth is given as a function of the bulked flow depth and average air concentration:

$$d_w = y_{90}(1 - \overline{C}) \tag{6.3}$$

Plots of d_w versus distance down the stepped spillway for h = 2.0 ft, h = 1.0 ft, and the smooth spillway are given in Figures 6.1, 6.2, and 6.3, respectively. As with the average velocity profiles in Figures 5.31 and 5.32, the small variation in flow depth with distance shows that the flow appears to be approaching uniform conditions for both h =1.0 ft and h = 2.0 ft. For the 2.0 ft steps, clear water depth slightly decreases with distance, reflecting increasing portions of the velocity profiles shown in Figure 5.31, especially for higher flow rates. With the 1.0 ft steps, it appears that uniform flow is achieved approximately halfway down the slope, or at a slope distance of around 50 ft. The shallow, fairly constant clear water depths along the slope of the smooth spillway were clearly observed in the high velocity flow of the model study. Remaining clear water depth profiles versus station for all tests are given in Appendix B.

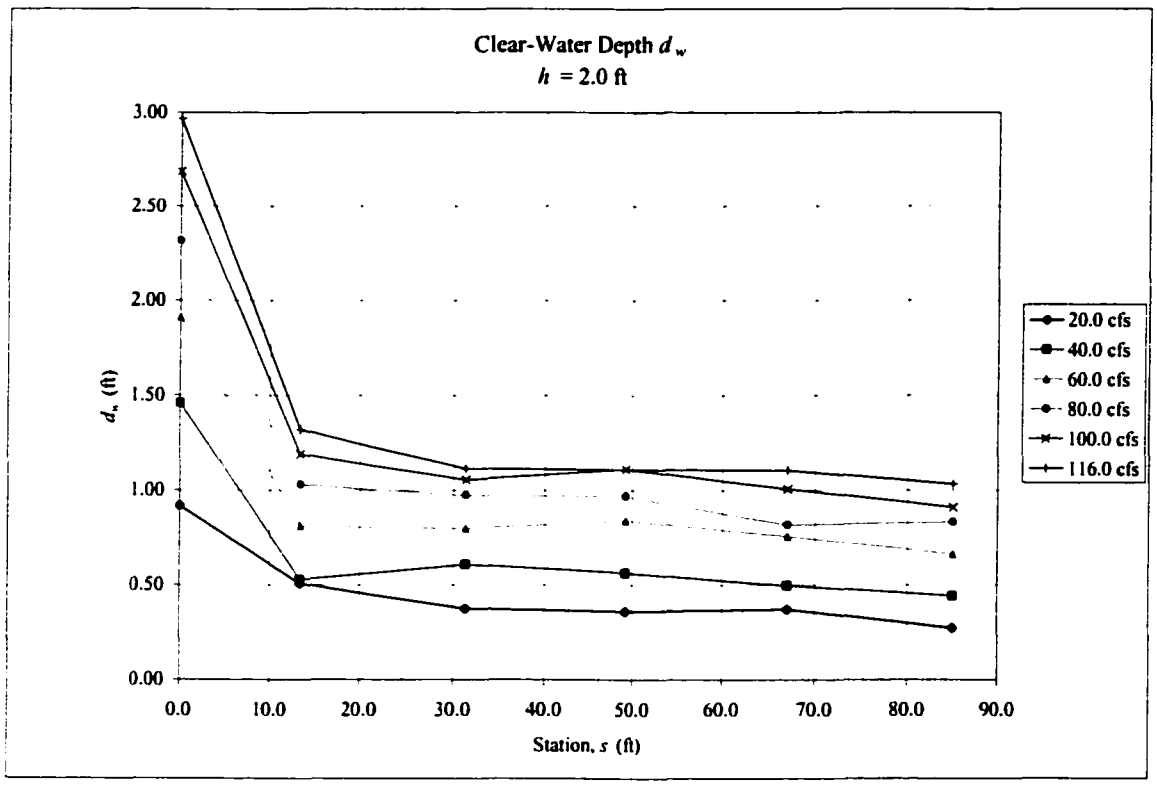

Figure 6.1 – Clear water depth d_w versus station, h = 2.0 ft.

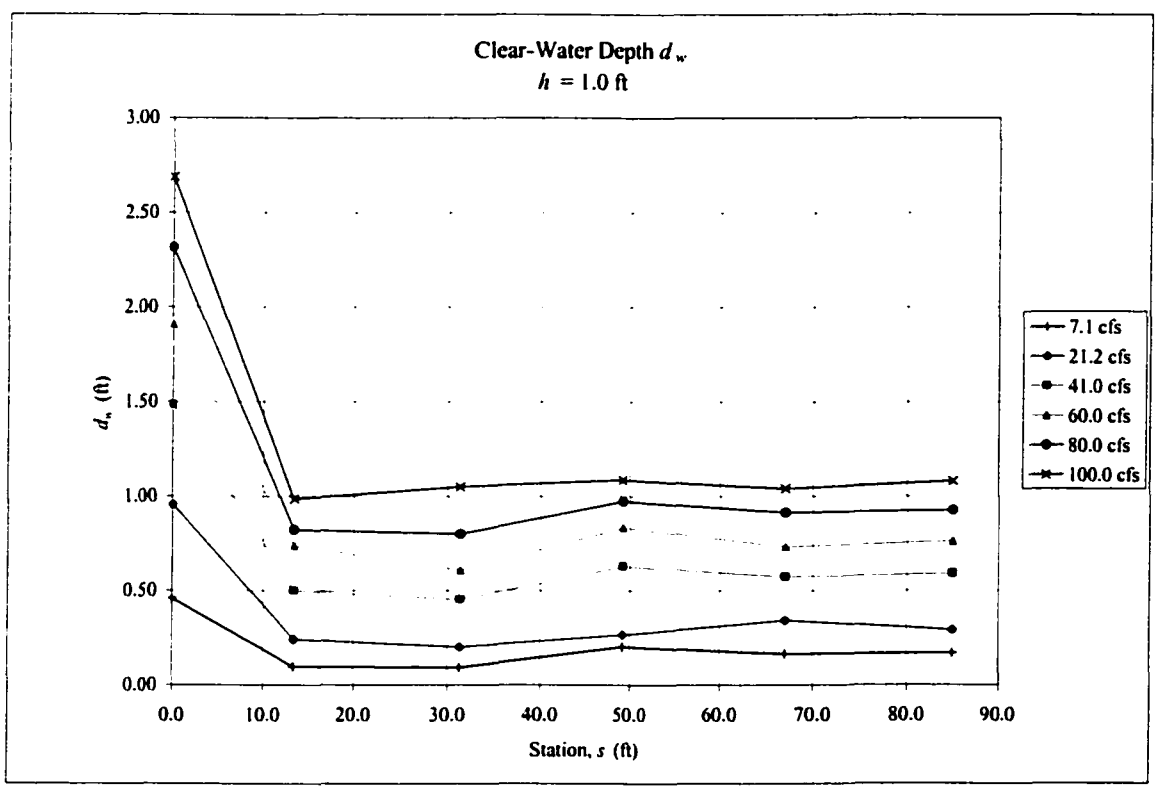

Figure 6.2 – Clear water depth d_w versus station, h = 1.0 ft.

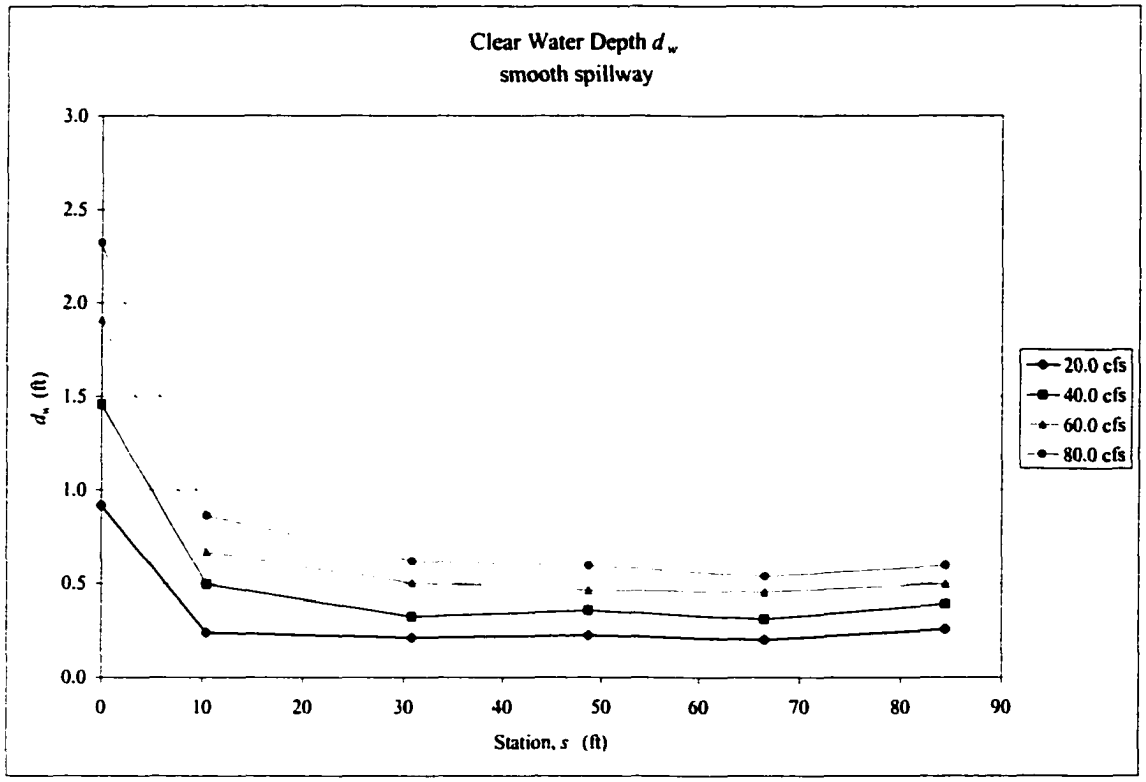

Figure 6.3 – Clear water depth d_w versus station, smooth spillway.

6.1.2 Bulking

The clear water depth d_w defined by equation (6-3) is an estimate of the compressed depth of flow with entrained air removed, while the depth y_{90} is the bulked depth of the aerated flow. The ratio of y_{90} to d_w is a measure of the amount of bulking due to entrained air and can be defined as a bulking coefficient, ε:

$$\varepsilon = \frac{y_{90}}{d_w} \tag{6-4}$$

The amount of bulking is important in determining sidewall or training wall heights along the length of the spillway. Figures 6.4 and 6.5 show bulking along the stepped spillway for the step heights h = 1 ft and h = 2 ft with the value of ε varying from approximately 1.20 to 1.80.

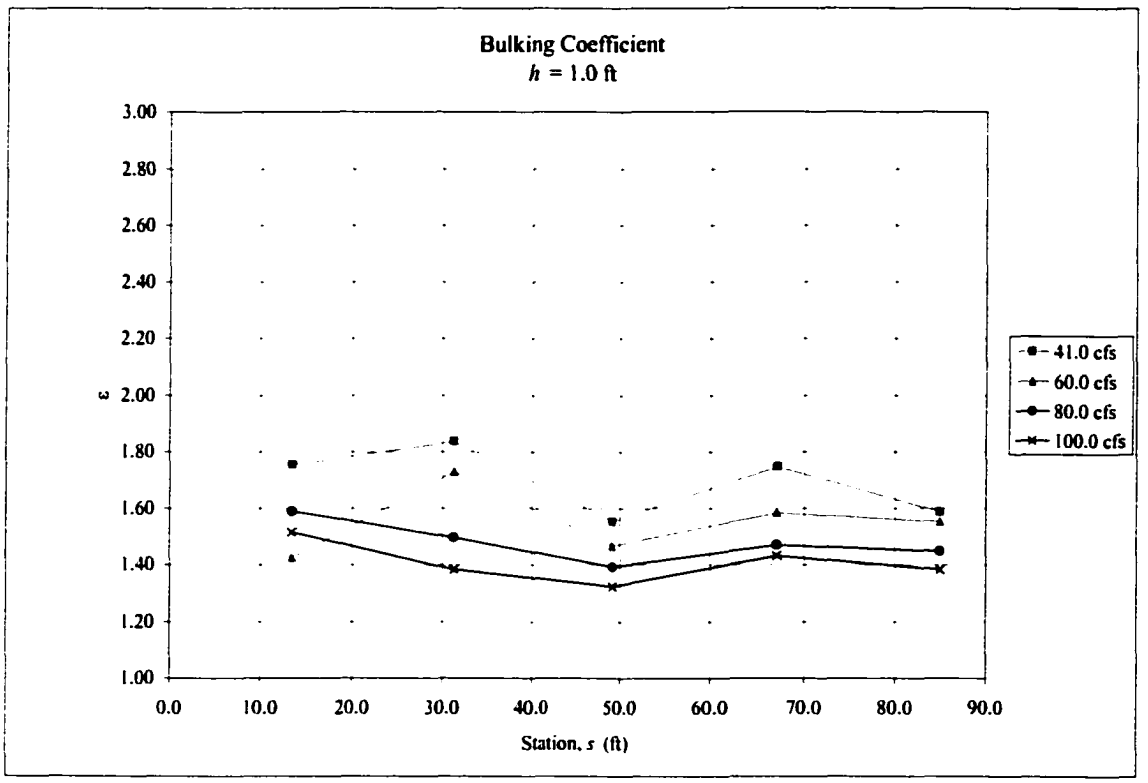

Figure 6.4 – Bulking coefficient, h = 1.0 ft

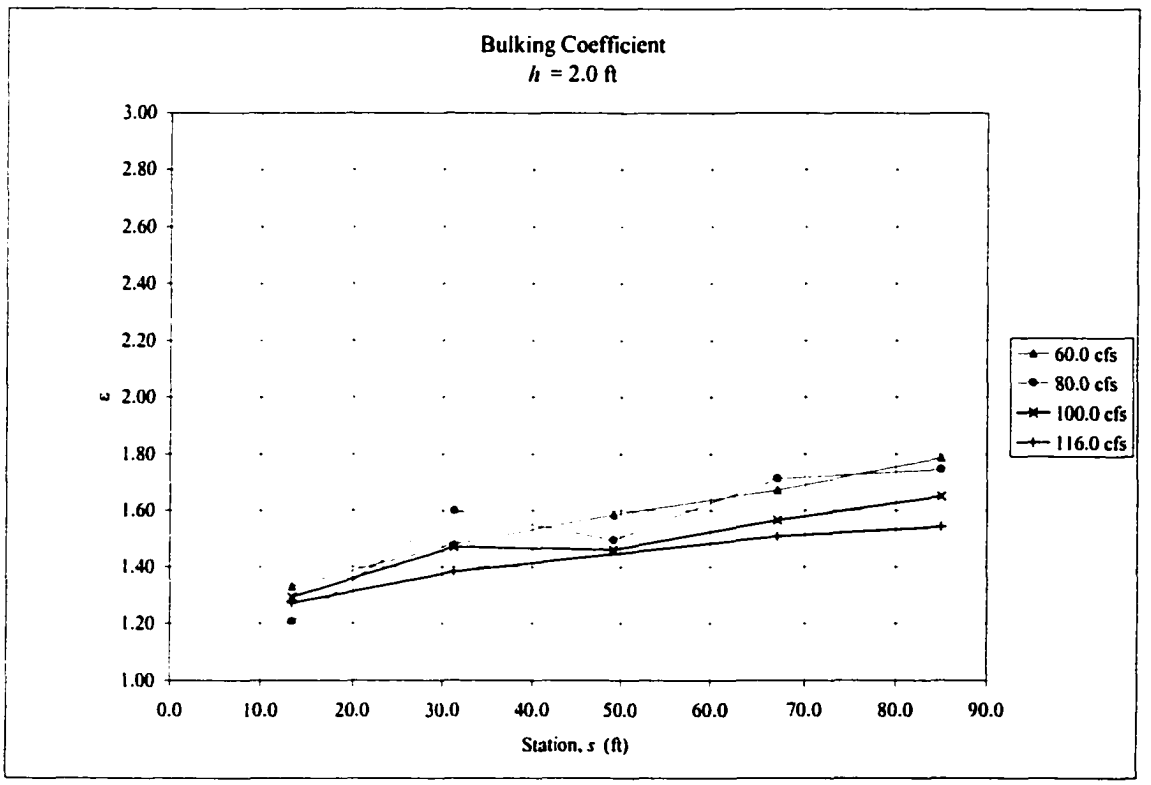

Figure 6.5 – Bulking Coefficient, h = 2.0 ft

6.1.3 Continuity

As an attempt to verify the data, measured flow rate q_m coming into the model was compared to computed flow rate using the experimental data. Volumetric clear water unit discharge q_w was estimated by integrating the air concentration and velocity profiles obtained at the centerline of a cross section in the flume:

$$q_w = \int_0^{y_{90}} (1 - c) u dy \tag{6-5}$$

Figures 6.6, 6.7, and 6.8 show the percent difference in q_w from q_m versus distance along the spillway, where q_m is the unit discharge provided to the test facility measured using a sonic flow meter installed in the delivery pipeline. It can be seen that the computed flow rate q_w is up to approximately 30% greater than the actual flow rate q_m for the stepped spillway and up to approximately 20% for the smooth spillway. Average overestimation of unit discharge was approximately 15% on the stepped spillway and 2% on the smooth spillway. It was also observed that overestimation was much less at the upstream stations with q_w within plus or minus 5% of q_m for the h = 1 ft and smooth spillway and approximately 10 – 20% for the h = 2 ft spillway. Closer comparison of the computed flow rate q_w to the measured flow rate q_m at the upstream stations is likely due to less entrained air and turbulence in this region.

Overestimation of unit discharge was initially a concern and was thoroughly investigated. As noted earlier in Section 5.2, observations of boundary effects from the sidewalls indicate a nonuniform transverse velocity profile with the maximum velocity along the centerline of the flume where data were collected. This alone could contribute to overestimation of unit discharge. The computation of unit discharge using equation (6-

5) assumes a velocity profile collected along the centerline of the flume is representative of the full cross section. This is rarely the case in any open channel flow with a narrow cross section and was clearly observed to be an inaccurate assumption in the present study. Figure 6.9 shows an exaggerated schematic of the error that could be introduced with this assumption. The actual average velocity of the cross section is potentially much less than the maximum. It was concluded that the average overestimation of 15% for the stepped spillway data is within a reasonable range of acceptance given the extremely turbulent conditions of the variable density two-phase flow and the observed nonuniform velocity distribution across the width of the flume. Prior studies using similar flume conditions and identical velocity and air concentration instruments reported overestimated unit discharge up to 30% (Gaston, 1995). Cain (1978) reported overestimation of velocity by 7 - 20% for a smooth spillway using a similar type stagnation pressure Pitot tube and resistivity air probe.

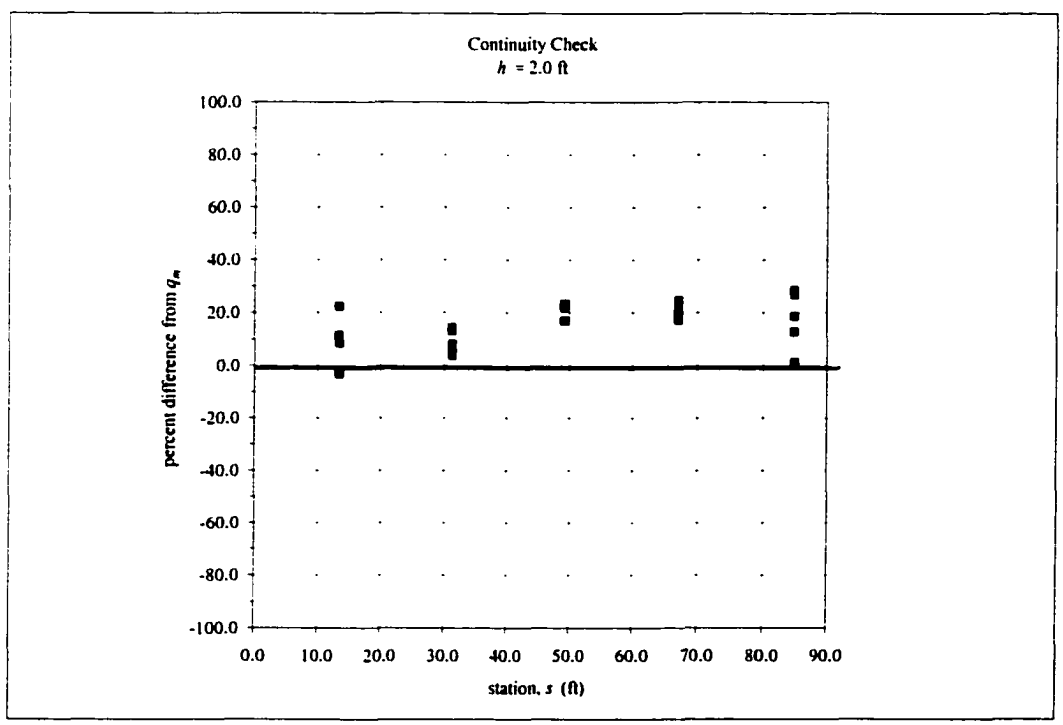

Figure 6.6 – Continuity check, h = 2.0 ft.

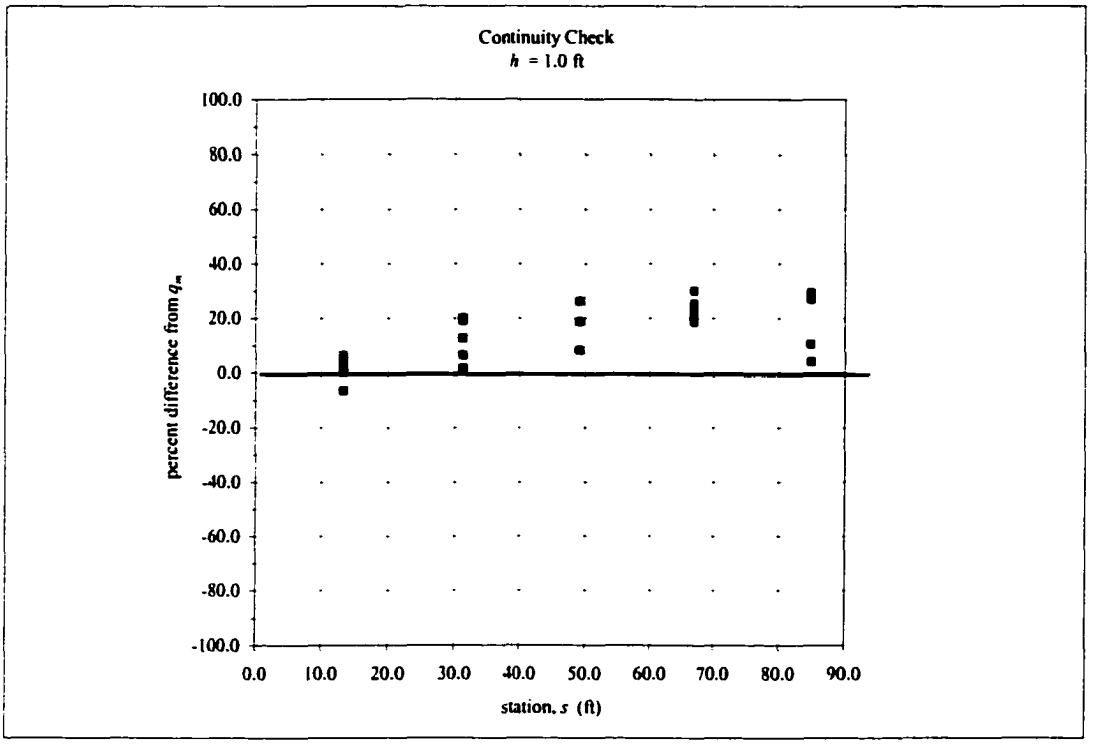

Figure 6.7 – Continuity check, h = 1.0 ft.

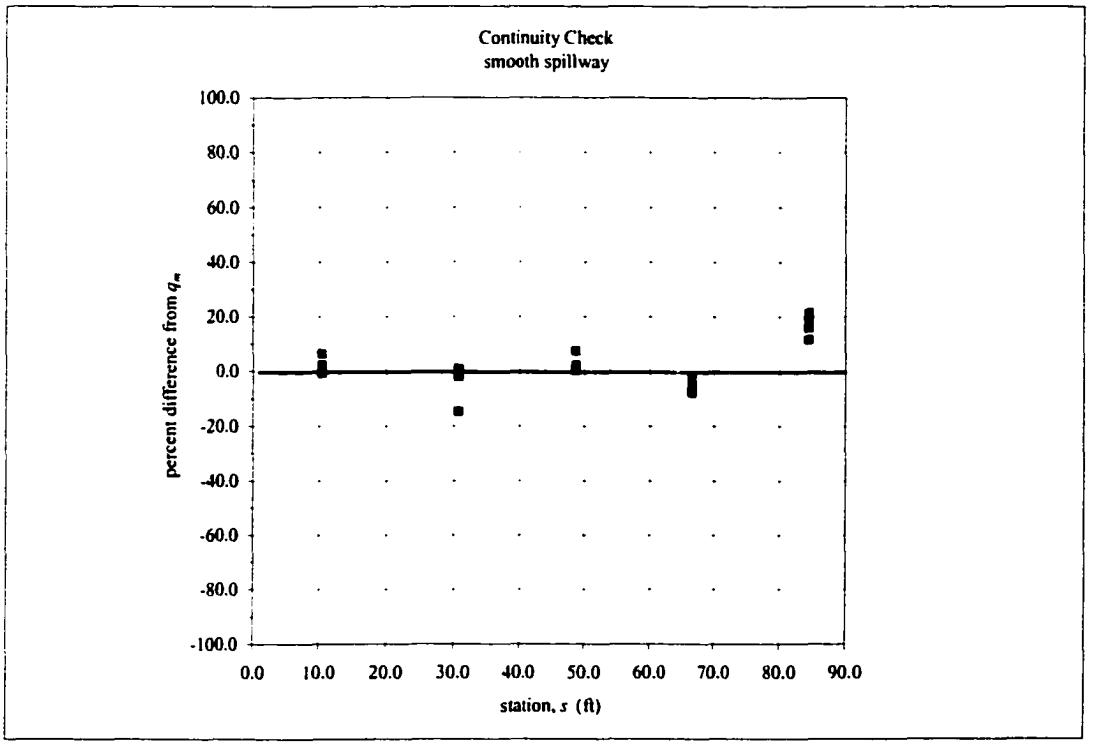

Figure 6.8 – Continuity check, smooth spillway.

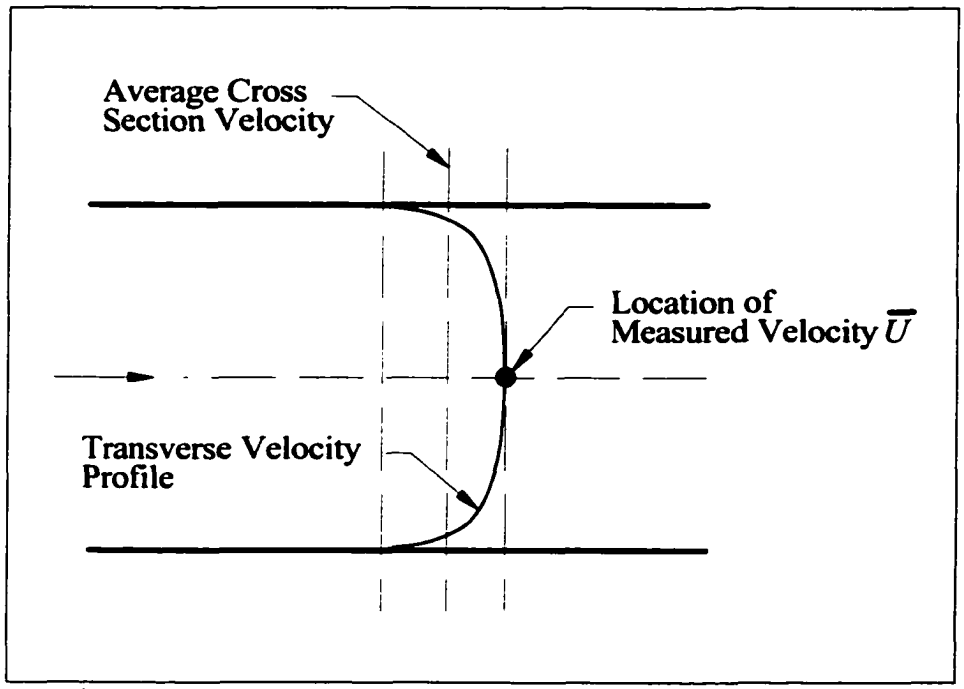

Figure 6.9 – Schematic of nonuniform transverse velocity profile.

In summary, the velocity data measured with the Pitot tube are felt to be accurate, however the local velocities u and the integrated velocity $\overline{U}$ are maximum values at the centerline of the cross section rather than representative average velocities. To continue the analysis, a representative average velocity was estimated using the measured unit discharge and computed clear water depth d_w given by:

$$U_{avg} = \frac{q_m}{d_w} \tag{6-6}$$

Results showed that U_{avg} ranged on the order of 5 to 30% percent lower than $\overline{U}$, the approximate amount unit discharge was overestimated. **Note that U_{avg} is used in all computations throughout the remainder of this analysis.**

6.2 Friction Factor

In skimming flow, the tips of the steps form a psuedo-bottom through which shear stresses are transmitted between the main flow and the recirculating flow. These shear stresses consume energy and induce friction contributing to the resistance of flow. Many methods have been developed to estimate the resistance of skimming flow over stepped spillways, usually in the form of the Darcy-Weisbach friction factor, f. Most methods assume fully developed, uniform flow conditions, and compute shear stress induced resistance based flow depth and velocity. For the present study, this method is used as the basis for determining friction factor in analyzing the stepped spillway data.

The friction factor f can be estimated by determining resistance of the main skimming stream due to shear stresses developed by the recirculating fluid between the steps. For computational purposes, uniform flow conditions must be assumed and are achieved when gravitational forces acting on an element of water are in balance with resisting forces. Applying the momentum equation for open channel flow to a section of skimming flow with dimensions of depth y_{90}, length L, and width w yields (Figure 6.10):

$$\beta\rho_m A_1 U_{avg}^2 + p_1 A_1 - \beta\rho_m A_2 U_{avg}^2 - p_2 A_2 = \gamma_m AL \sin\theta - \tau_b wL - \tau_w 2y_{90} L \qquad (6\text{-}7)$$

where β = momentum correction factor, ρ_m = density of the air-water mixture, U_{avg} = average velocity, A = cross-sectional area, p = hydrostatic pressure, γ_m = unit weight of the air-water mixture, θ = channel slope, τ_b = bed shear stress, and τ_w = wall shear stress. Assuming uniform conditions with $p_1A_1 = p_2A_2$ and $\beta\rho_m A_1 U_{avg}^2 = \beta\rho_m A_2 U_{avg}^2$ and

assuming the bed and wall shear stress equal to the total stress, τ_o, equation (6-7) reduces to:

$$\tau_o = \gamma_m \frac{A}{2y_{90} + w} \sin\theta = \gamma_m \frac{A}{P} \sin\theta = \gamma_m R_h \sin\theta \tag{6-8a}$$

where the hydraulic radius $R_h = A/P$ is the ratio of the cross-sectional area $A = wy_{90}$ to the wetted perimeter $P = 2y_{90}+w$. Replacing bed slope $S_o = \sin\theta$ with friction slope S_f, shear stress can be written as the following:

$$\tau_o = \gamma_m R_h S_f \tag{6-8b}$$

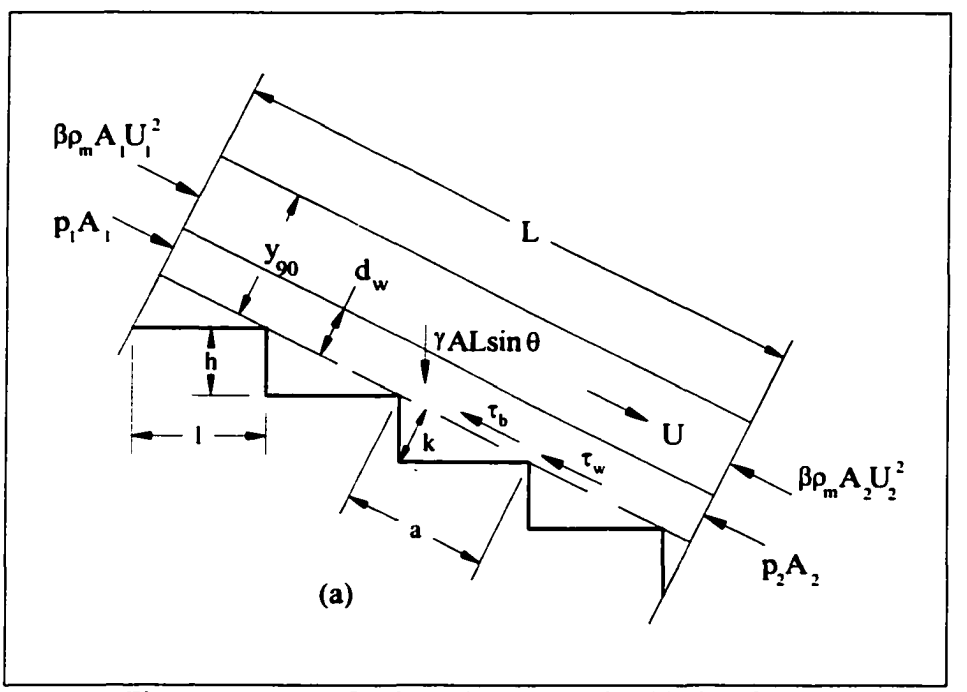

Figure 6.10 – Definition of variables for friction factor.

The Darcy-Weisbach friction formula for pipe-flow is commonly used for open-channel flow:

$$h_f = f \frac{L}{D} \frac{U_{avg}^2}{2g} \tag{6-9}$$

in which h_f = head loss due to friction and D = pipe diameter. Combing equations (6-8b) and (6-9) and noting that pipe diameter is equivalent to $4R_h$ and the hydraulic radius R_h can be assumed as the uniform flow depth y_{90}, the Darcy friction factor due to surface friction can be defined as:

$$f = \frac{8gy_{90}S_f}{U_{avg}^2} \tag{6-10}$$

Notice that equation (6-10) is a function of the bulked flow depth y_{90}. Use of this depth in computing the friction factor has been a matter of question in recent literature. In their recent work, Chamani and Rajaratnam (1999) used y_{90} in calculating skin friction while Chanson (1993) suggest using the clear water depth d_w. However, Matos and Quintela (1995) note that Chanson (1995) used the bulked flow depth in calculating f. Other researchers such as Sorenson (1985) and Christodoulou (1993) conducted studies at small scales and used the observed water depth in which there was very little or no aeration. Close inspection of equation (6-10) shows that the friction factor is proportional to the inverse of the Froude number F_r squared, where $F_r = U_{avg} / \sqrt{d_w g}$. By definition, Froude number is defined as the ratio of inertial to gravitational forces, the latter being a function of water depth. Therefore, it is the author's opinion that the clear water depth d_w be used in computing the friction factor, or:

$$f = \frac{8gd_wS_f}{U_{avg}^2} \tag{6-11}$$

Friction slope, velocity, and depth in equation (6-11) were taken as the average values of a section between stations, or:

$$S_f = (E_i + E_{i+1})/\Delta x \quad ; \tag{6-12}$$

$$U_{avg} = \left(U_{avg_i} + U_{avg_{i+1}}\right)/2 \quad ; \tag{6-13}$$

$$d_w = \left(d_{wi} + d_{wi+1}\right)/2 \tag{6-14}$$

where station i is upstream of station $i+1$.

Friction factor f is a function of clear water depth d_w, critical depth y_c, average velocity U_{avg}, spillway slope θ, acceleration due to gravity g, spillway height H, and step height h. Dimensional analysis suggest that f is a function of the following relations:

$$f = \mathrm{f}\left(\theta, \frac{d_w}{y_c}, \frac{h}{y_c}, \frac{H}{y_c}\left(\text{or } \frac{Nh}{y_c}\right), F_r = \frac{U_{avg}}{\sqrt{d_w g}}\right) \tag{6-15}$$

where F_r is Froude number. In developing design charts, it is advantageous to present friction factor as a dimensionless function in terms of known design characteristic lengths, or the ratio H/y_c. Further refinement of this ratio can be achieved by expressing H as a function of step height h and step number N, or Nh/y_c where $H = Nh$. Figures 6.11 and 6.12 show friction factor for various unit discharges as a function Nh/y_c for h = 1.0 ft and h = 2.0 ft, respectively.

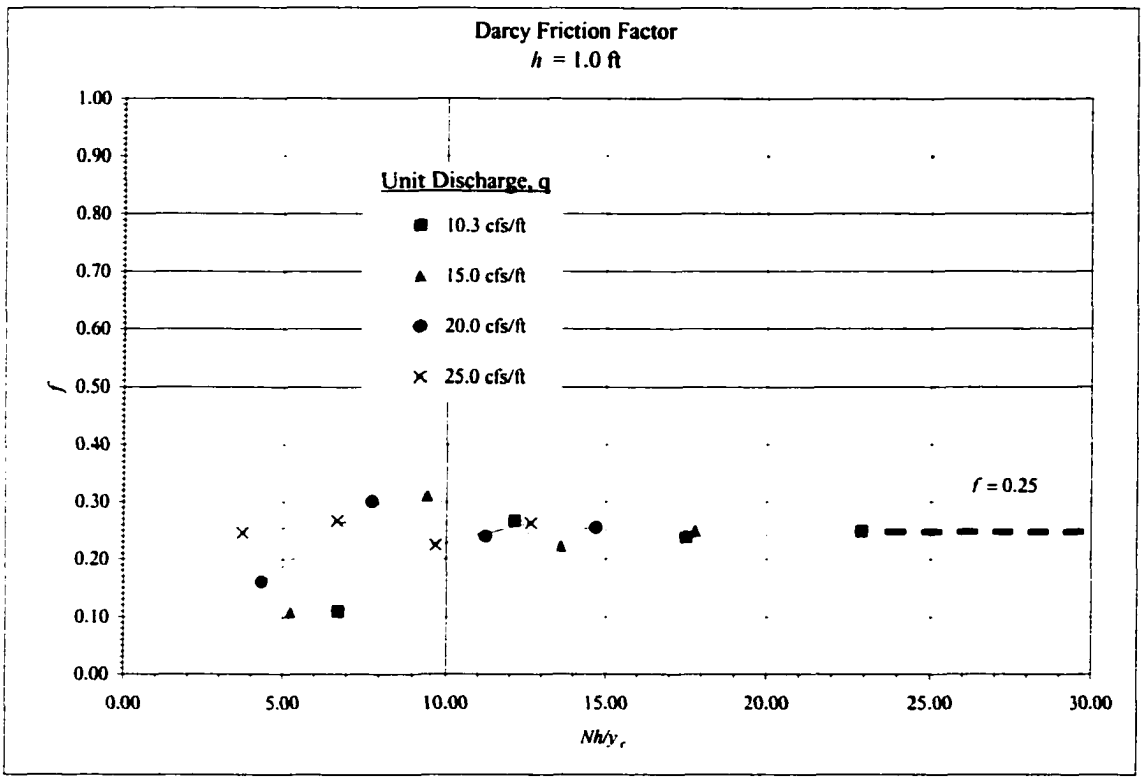

Figure 6.11 – Darcy Friction Factor versus NH/y_c, h = 1.0 ft

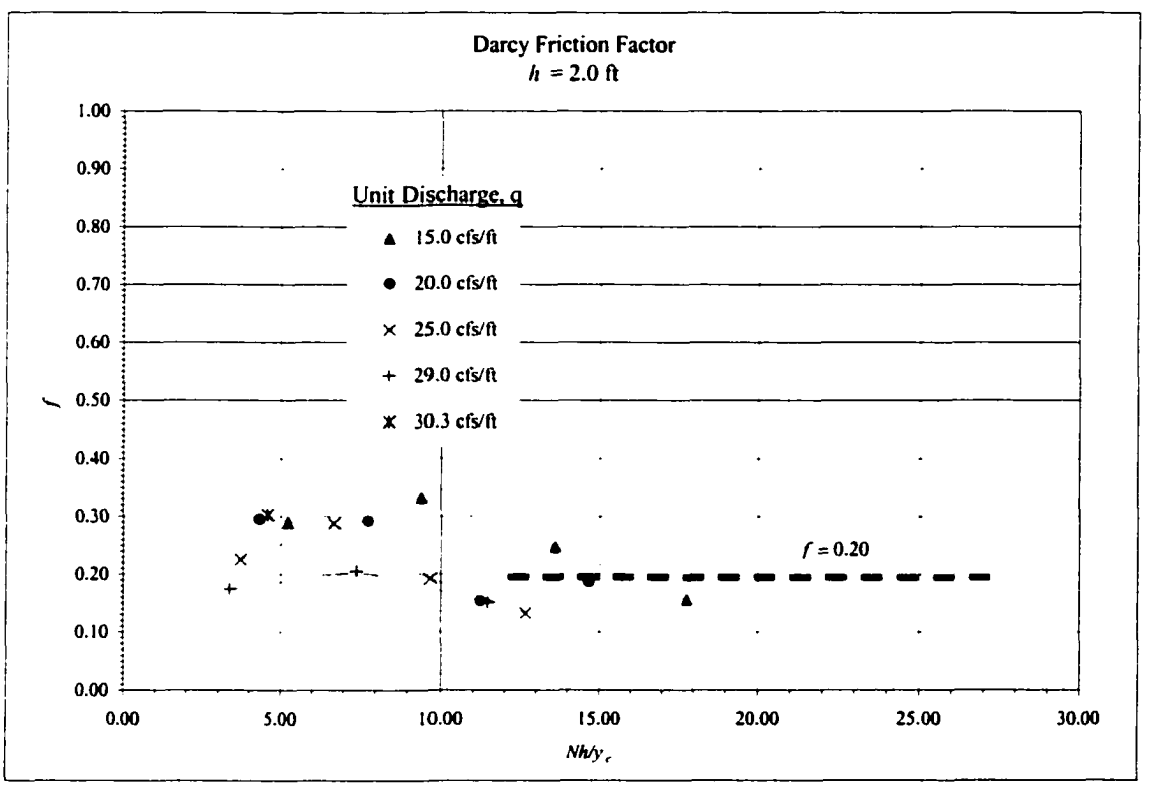

Figure 6.12 – Darcy Friction Factor versus NH/y_c, h = 2.0 ft

Due to the nature of the friction factor data and the lack of definite correlation with unit discharge and step height, general limitations and guidelines were made for selection of friction factor. For h = 1.0 ft at locations a greater distance down the spillway, i.e. Nh/y_c greater than approximately 10.0, friction factor becomes constant at approximately f = 0.25. For h = 2.0 ft, friction factor tends towards a value of approximately f = 0.20. The tendency for f to become constant is a reflection of the flow becoming fully developed and uniform. As discussed in Chapter 5, uniform flow conditions were more apparent for the h = 1 ft steps than for the h = 2 ft steps. However, values of f still appear to be converging for h = 2.0 ft. A difference in f of 0.05 used as a design value would produce minimal difference in the results of a backwater computation. Therefore, as a conservative approach, a constant value of f = 0.25 is suitable for both h = 1.0 ft and h = 2.0 ft.

Results from the present study along with data from Gaston (1995) and Chamani and Rajaratnam (1999) are shown in Figure 6.13 plotted against the ratio k/d_w, where k is a characteristic roughness height defined as $k = h\cos\theta$. Data from the present study are shown for the bottom two stations of the stepped spillway and the bottom station of the smooth spillway in regions where the flow is considered developed. For Gaston (1995) and Chamani and Rajaratnam (1999), friction factor was recalculated using equation (6-11) where S_f was assumed equal to $\sin\theta$ and clear water depth and average velocity were computed by equations (6-3) and (6-6), respectively. Data from these two investigations were chosen because of similarity in instrumentation to the present study. However, Gaston (1995) used a prototype-scale step height of 0.40 ft on a 2H:1V slope and Chamani and Rajaratnam used a scale model step height of 0.41 ft and 0.10 ft on a

0.8H:1V slope. Figure 6.13 shows a plot of equation (2-16) from Tozzi (1994) for a 2H:1V slope and equation (2-23) from Chamani and Rajaratnam (1999), where $f = 4c_f$ (reference Chapter 2). A similar equation was fit to the all of the data in Figure 6.13:

$$\frac{1}{\sqrt{f}} = 2.35 + 0.82 log\left(\frac{d_w}{k}\right) \tag{6-16}$$

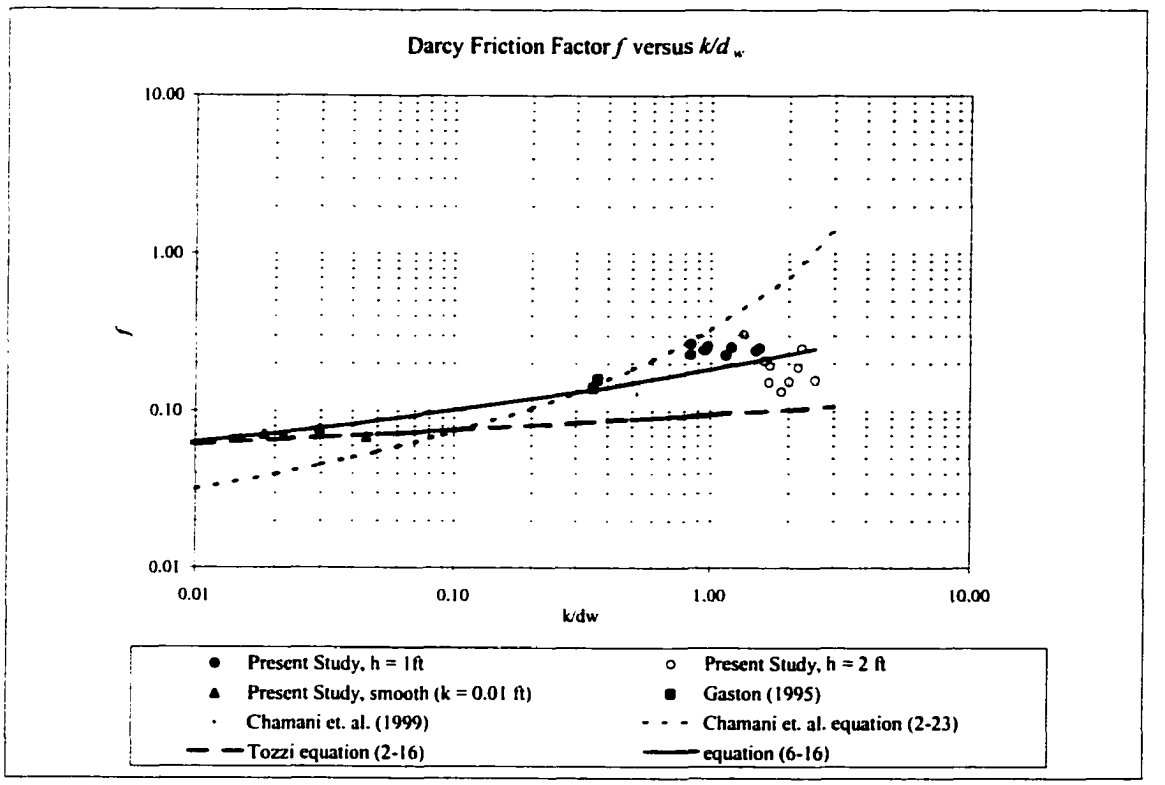

Figure 6.13 – Darcy friction factor for the bottom two stations of the present study, Gaston (1995), and Chamani and Rajaratnam (1999).

6.3 Dimensionless Comparison of Results

Dimensional analysis of friction factor in section 6.2 provided important relationships dependent on the hydraulic characteristics of stepped spillway flow. Skimming flow data from the present study are shown in Figures 6.14 and 6.15 in dimensionless form. It can be seen that as Nh/y_c increases, or as height and length of the spillway increases, both Froude number and the ratio d_w/y_c tend towards nearly constant values. The tendency for both the h = 1.0 ft and h = 2.0 ft data to collapse near the same values indicates little influence of scale effect between the two step heights. Potentially, if developed and skimming flow exists on a 2:1 (H:V) slope, stepped spillway, then the friction factor, Froude number, and ratio d_w/y_c become nearly constant with $d_w/y_c \cong 0.40$ and $F_r \cong 4.0$. For prototype conditions similar to the present study, these values may be used as guidelines for design.

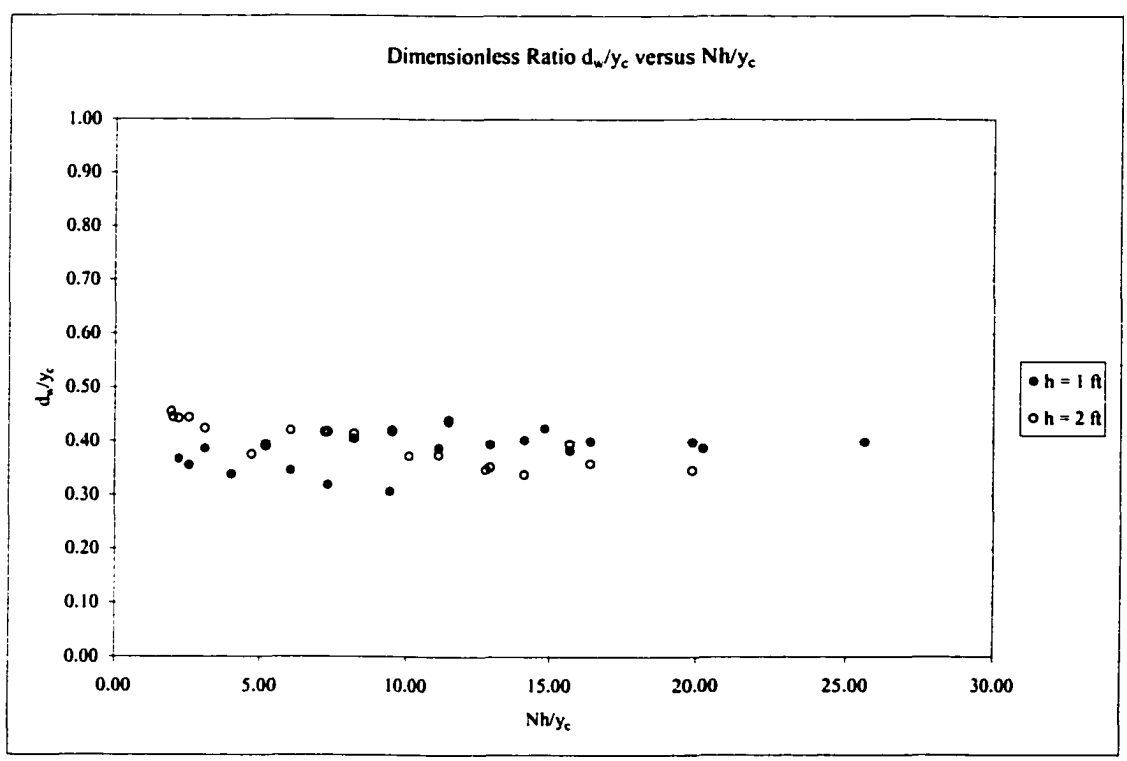

Figure 6.14 – Dimensionless ratio d_w/y_c versus Nh/y_c

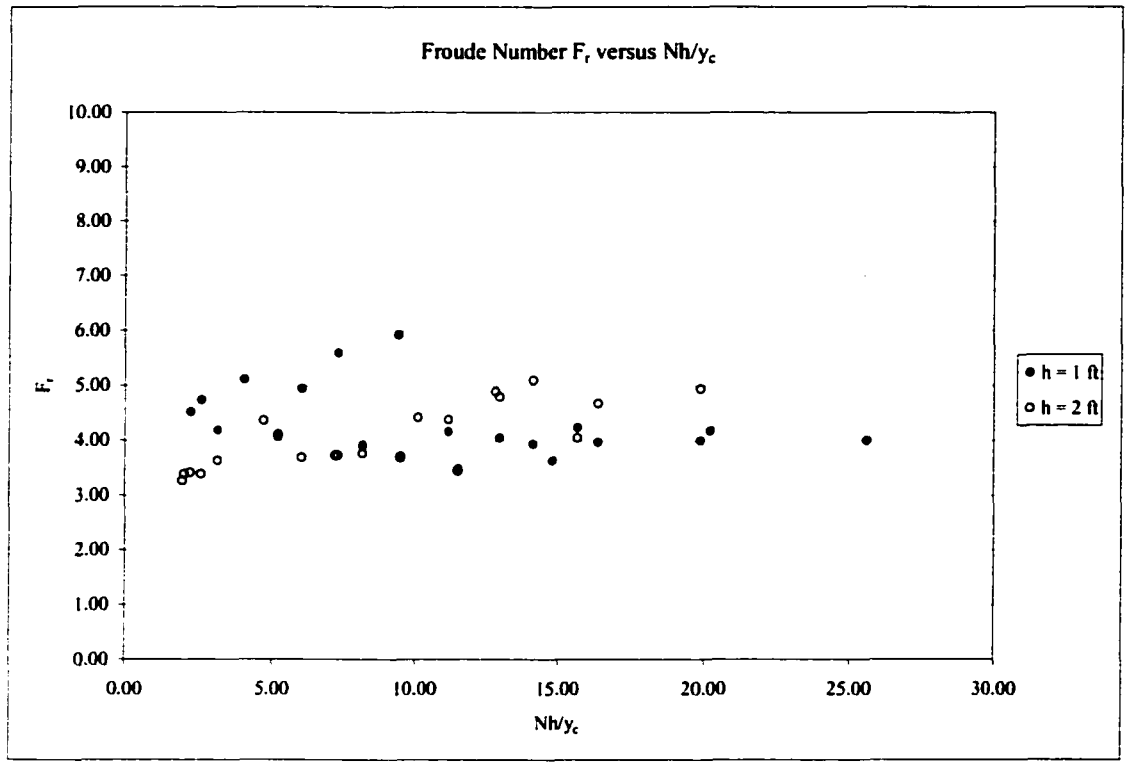

Figure 6.15 – Froude number F_r versus Nh/y_c

6.4 Energy Dissipation

Skimming flow over a stepped spillway is characterized by a coherent stream skimming over the steps supported by recirculating fluid trapped between the external edges of the steps. Energy dissipation is due to frictional shearing between the main flow and recirculating flow in addition to drag forces developed from local impact and separation pressures existing on the step surfaces. Nappe flow is distinguished by a series of plunging, free-falling jets cascading from one step to another with energy being dissipated by jet impact and breakup, jet mixing, and the formation of a partially or fully developed hydraulic jump on the step.

In general, energy dissipation can be interpreted as the ratio of energy loss to total available energy at a given location along the spillway. For the present study, energy

data (i.e. velocity, depth, and elevation) were collected at several elevations below the crest of the spillway. This allows energy dissipation to be computed as a function of spillway height from the crest to a downstream location. The method assigns a datum at the spillway crest and compares energy loss to total energy *at that location only*. Using a variable datum can be useful for design by computing energy dissipation assuming varying spillway heights.

With reference to Figure 6.16 and assuming a fixed datum at the crest of the stepped spillway, the total available head at a downstream location can be written as:

$$E_o = H_o + y_o + \frac{U_o^2}{2g} \tag{6-17}$$

The energy at any location along the stepped spillway can be approximated as:

$$E_1 = d_w \cos\theta + \frac{U_{avg}^2}{2g} + h_f \tag{6-18}$$

where h_f is the energy head loss. Note that for the aerated flow conditions over a stepped spillway, the hydrostatic pressure term in equation (6-18) is estimated with the clear water depth d_w defined by equation (6-3). Combining equations (6-17) and (6-18) and noting that $h_f = E_o - E_1$, and expressing E_o in terms of critical depth y_c, energy dissipation can be approximated as:

$$\frac{\Delta E}{E_o} = \frac{E_o - E_1}{E_o} = \frac{\left(H_o + \frac{3}{2}y_c\right) - \left(d_w \cos\theta + \frac{U_{avg}^2}{2g}\right)}{\left(H_o + \frac{3}{2}y_c\right)} \tag{6-19}$$

or simplifying:

$$\frac{\Delta E}{E_o} = 1 - \frac{d_w \cos\theta + \frac{U_{avg}^2}{2g}}{H_o + \frac{3}{2} y_c} \tag{6-20}$$

Energy dissipation along the spillway is given for h = 1.0 ft, h = 2.0 ft, and the smooth spillway in Figures 6.17, 6.18, and 6.19, respectively.

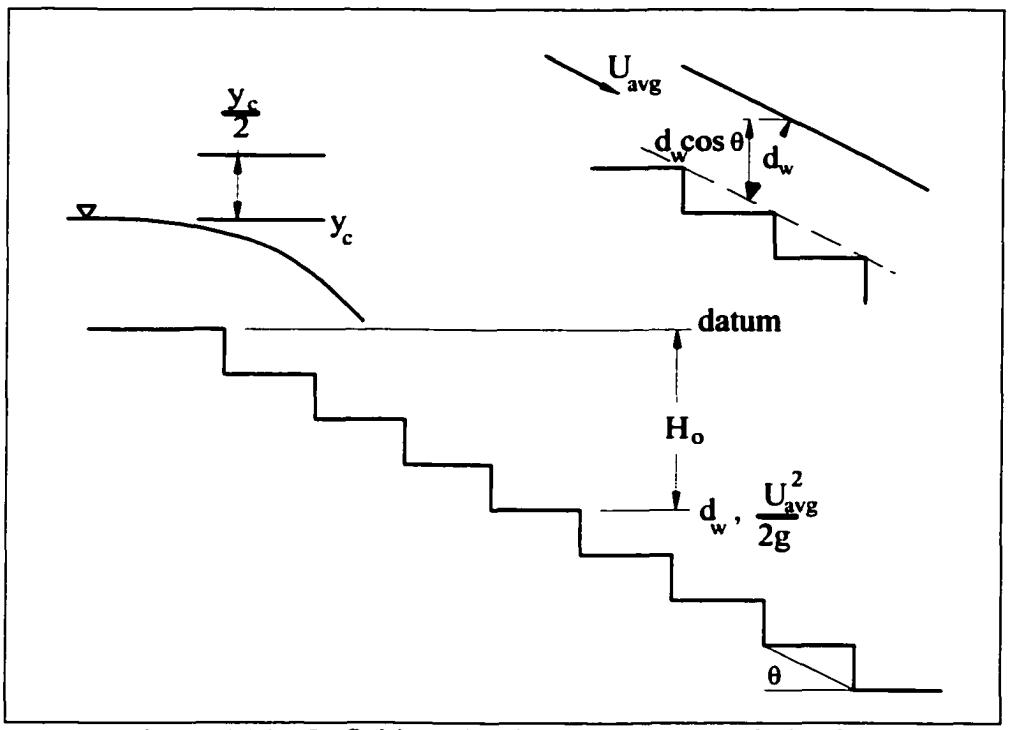

Figure 6.16 – Definition of variables for energy dissipation.

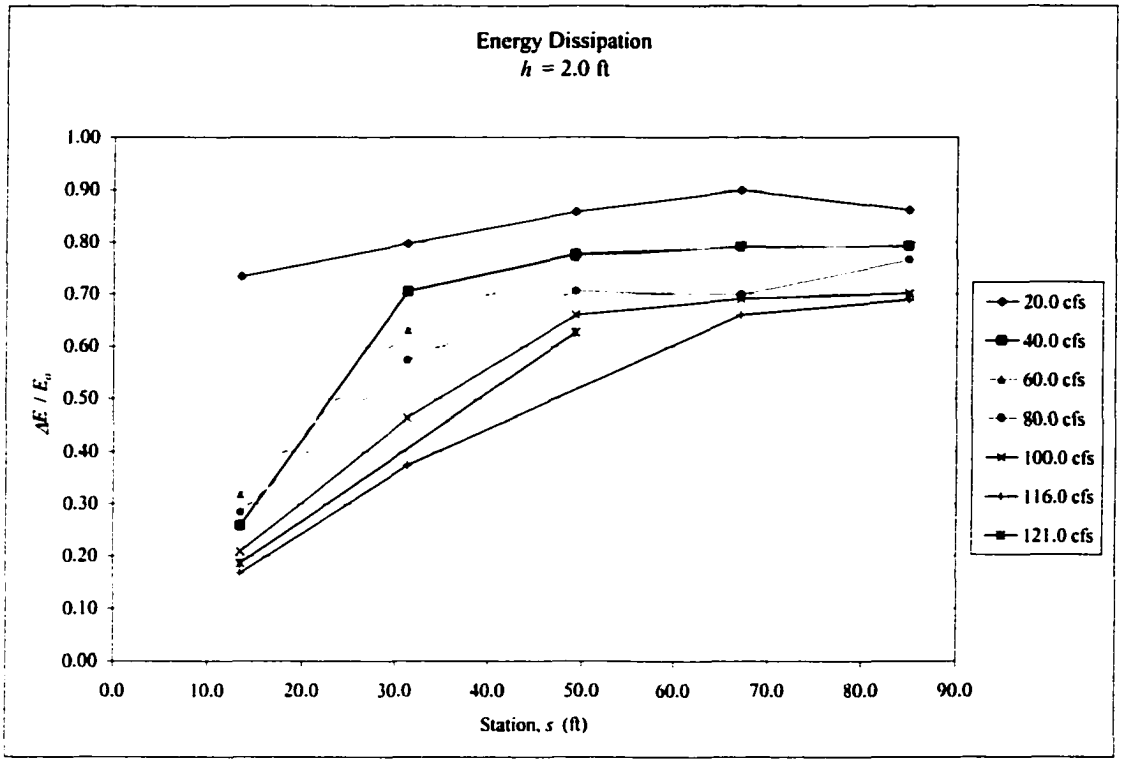

Figure 6.17 – Energy Dissipation along the spillway, h = 2.0 ft.

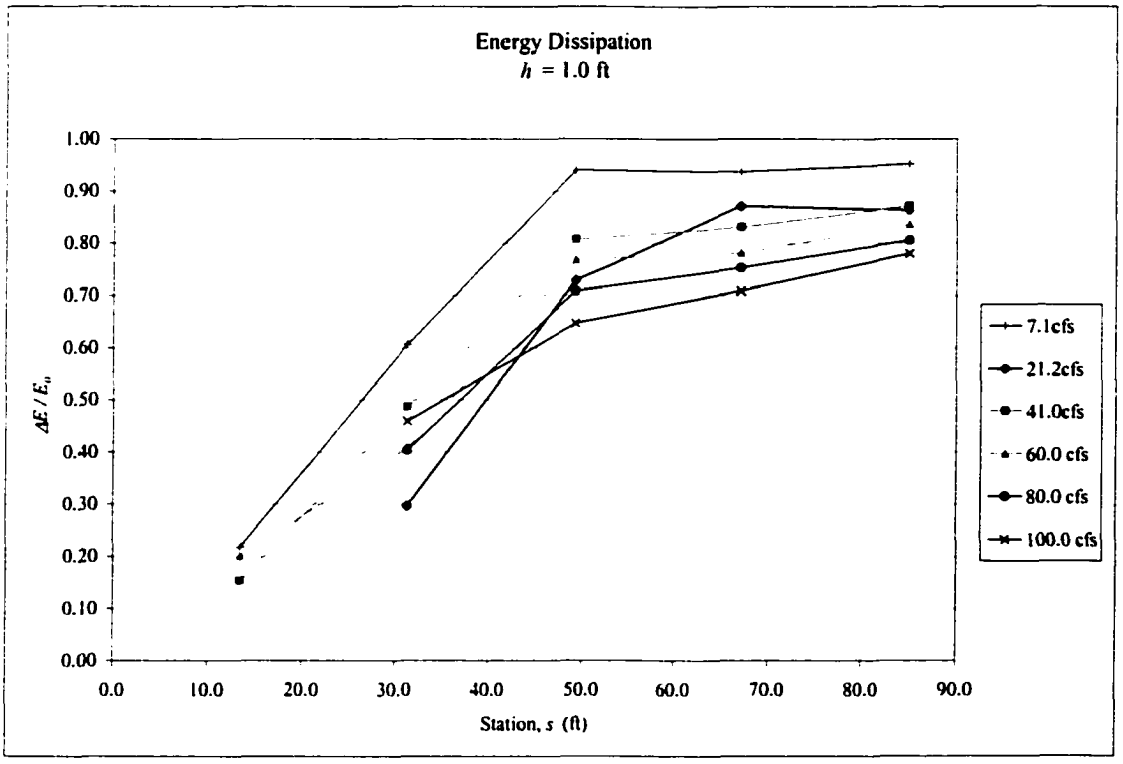

Figure 6.18 – Energy dissipation along the spillway, h = 1.0 ft.

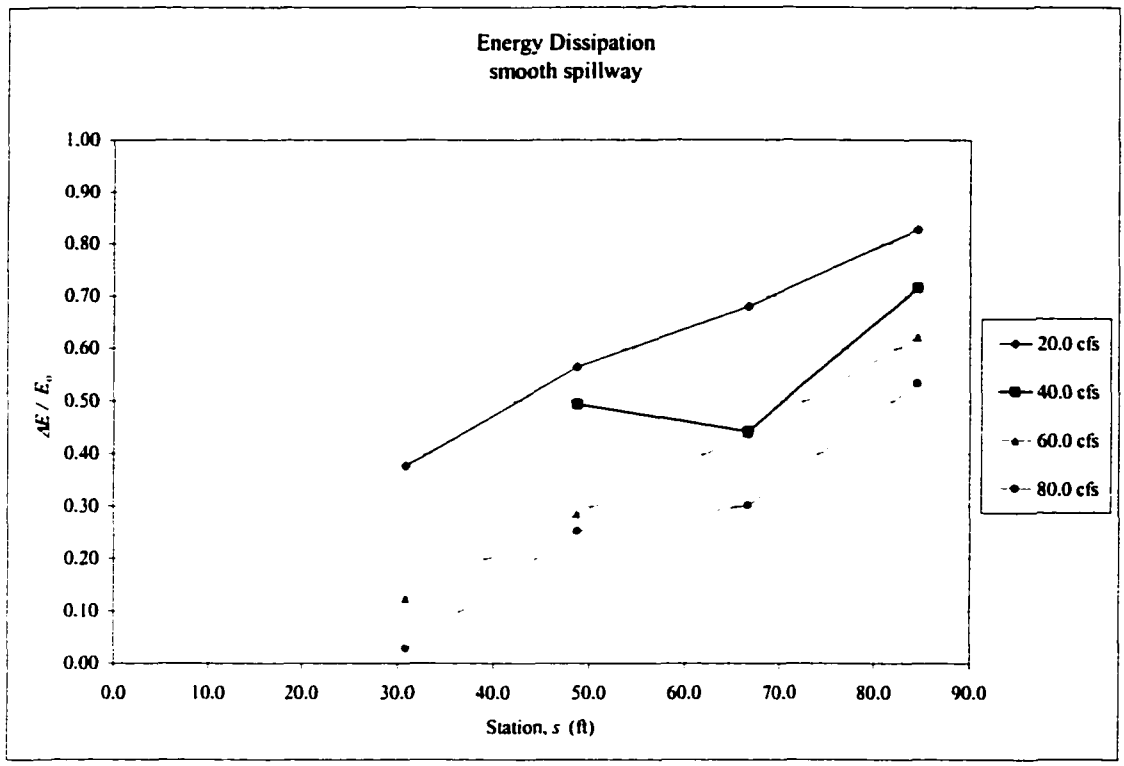

Figure 6.19 – Energy dissipation along the spillway, smooth spillway.

It has been shown that, assuming uniform flow conditions, the energy dissipation ratio in equation (6-20) can be written as a function of the Darcy friction factor f (Stephenson, 1991; Chanson,1994):

$$\frac{\Delta E}{E_o} = 1 - \frac{\left(\frac{f}{8\sin\theta}\right)^{\frac{1}{3}}\cos\theta + \frac{1}{2}\left(\frac{f}{8\sin\theta}\right)^{-\frac{2}{3}}}{\frac{Nh}{y_c} + \frac{3}{2}} \qquad (6\text{-}21)$$

Figure 6.20 shows energy dissipation data from the stepped spillway tests computed using equation (6-20). In addition, equation (6-21) is shown for $f = 0.25$, $f = 0.20$, and $f = 0.071$ representing estimated constant f-values for step heights h = 1.0 ft and h = 2.0 ft and the smooth spillway, respectively. It can be seen that the data are in good agreement

with equation (6-21) and the difference of 0.05 in friction factor for step heights h = 1.0 ft and h = 2.0 ft produces minimal difference in energy dissipation.

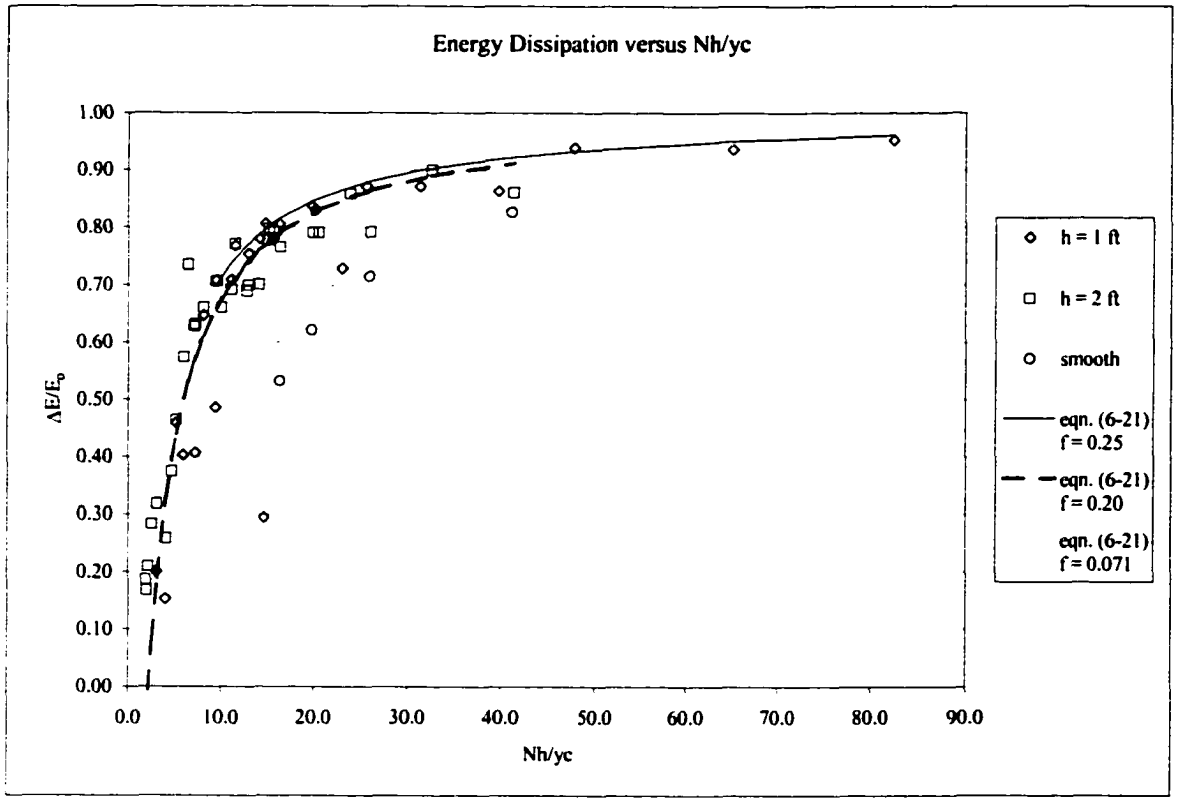

Figure 6.20 – Energy Dissipation versus Nh/y_c.

CHAPTER 7

HYDRAULIC DESIGN

The designer of a stepped spillway is typically provided with information on the design volume of water to be passed over the selected crest length b of the spillway (i.e. total discharge Q or unit discharge q), slope of the embankment θ, and height of the spillway H. If it is assumed that the designer has also selected the step height h, then it is desired to know certain hydraulic characteristics of the spillway flow to complete the design. Most importantly, these characteristics include velocities for stilling basin design and bulked flow depth for training wall design. A design procedure was developed using data from the present study to estimate velocity and bulked flow depth along the stepped spillway. Design examples for h = 1.0 ft and h = 2.0 ft are given in addition to a smooth spillway comparison example.

7.1 Hydraulic Design Procedure

Flow conditions in open channels are often described by water surface profiles determined from classical computational methods such as the standard step method. These methods yield the change in flow depth along the channel based on estimating changes in energy loss due to friction slope S_f. In a typical open channel, the methods require selection of a friction parameter such as Manning n or Darcy friction factor f, and carrying out the computations from a known boundary condition. The complication of

using these methods with stepped spillway flow is the existence of air entrainment and varying air-water density in the flow along the spillway. In addition, selection of an appropriate value for the friction parameter is unknown.

7.1.1 Design Charts

In Chapter 6, section 6.2, computation of the Darcy friction factor f was presented in terms of the dimensionless ratio Nh/y_c. Figure 7.1 is a design chart developed from the present study that may be used as a guideline for selecting the magnitude of friction factor and its variation with spillway height for a given unit discharge and step height. As mentioned in section 6.2, if fully developed skimming flow conditions are assumed, f tends to a constant value of approximately 0.25 for h = 1.0 ft and 0.20 for h = 2.0 ft. As a conservative approach, selecting a constant value of f = 0.25 is a good approximation for developed skimming flow for both h = 1.0 ft and h = 2.0 ft. Varying values of friction factor may also be selected from Figure 7.1 for low values of Nh near the spillway crest, if desired. However, for most spillway designs, the height and length of spillway will be sufficient for nearly uniform bulked flow conditions and a constant value of f = 0.25 is suggested.

For design purposes, it is also convenient to express the bulking coefficient ε in terms of Nh/y_c. Figure 7.2 is a design chart developed from the present study that may be used as a guideline for selecting the magnitude of the bulking coefficient and its variation with spillway height for a given unit discharge and step height. As with friction factor, the value of ε becomes constant for larger values of Nh/y_c, or as the skimming flow becomes developed and nearly uniform. Therefore, a conservative approximation is to select a constant value of ε = 1.75 for both h = 1.0 ft and h = 2.0 ft.

Darcy Friction Factor Design Charts

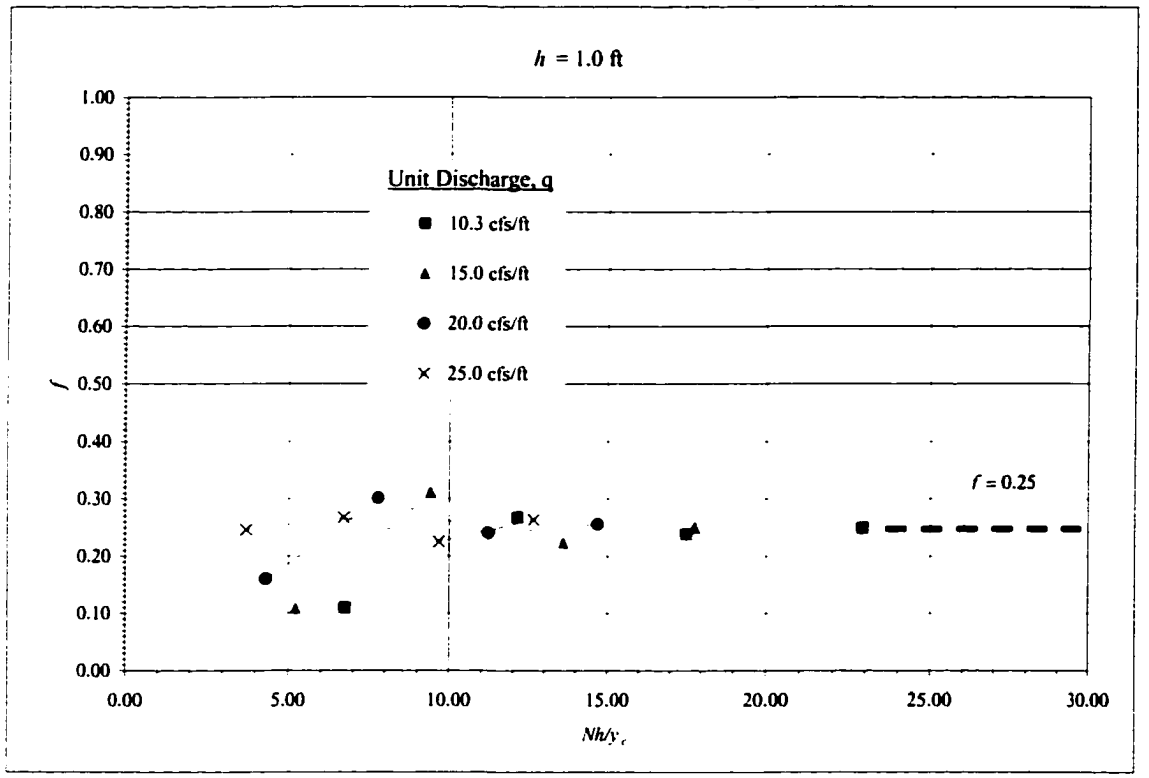

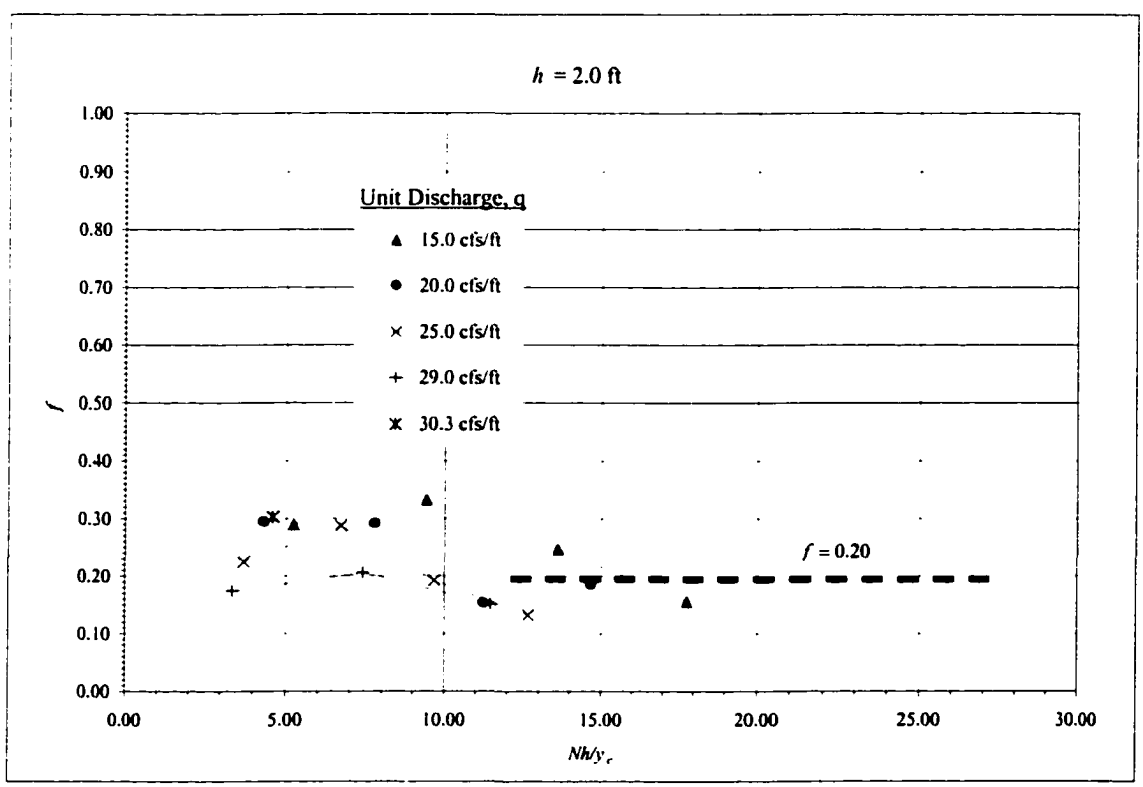

Figure 7.1 – Darcy Friction Factor Design Charts, $h = 1.0$ ft, $h = 2.0$ ft.

Bulking Coefficient Design Charts

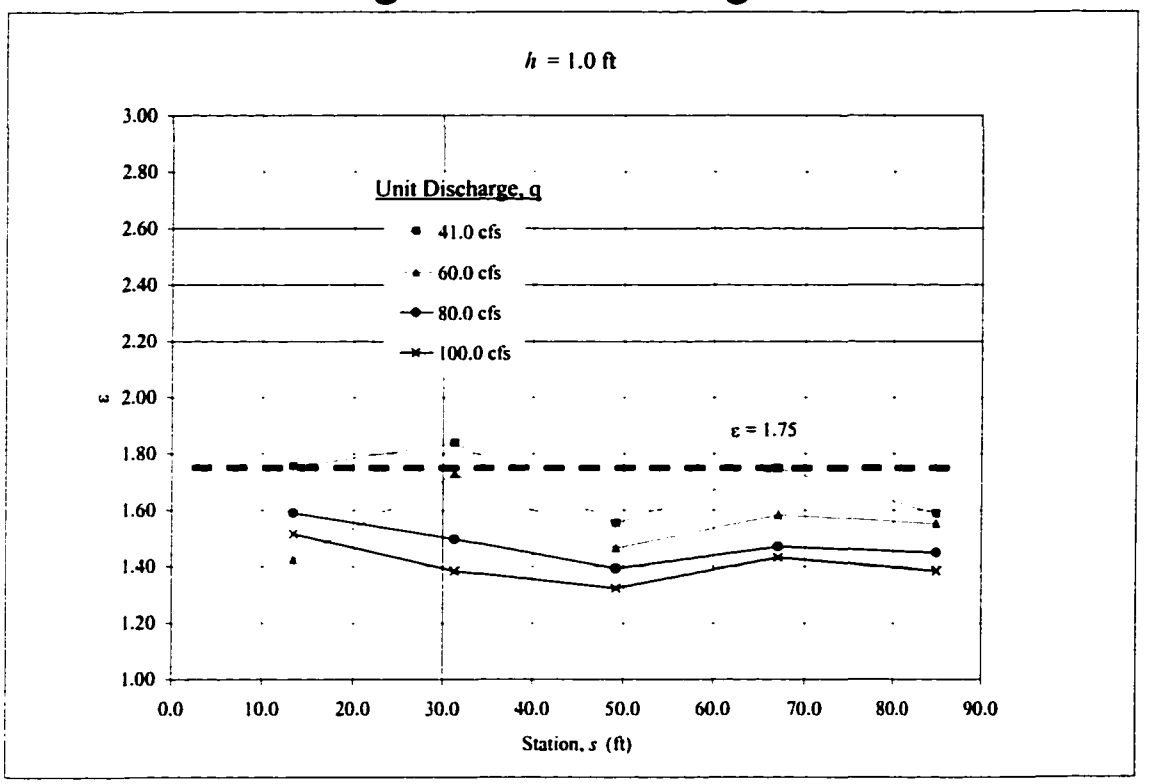

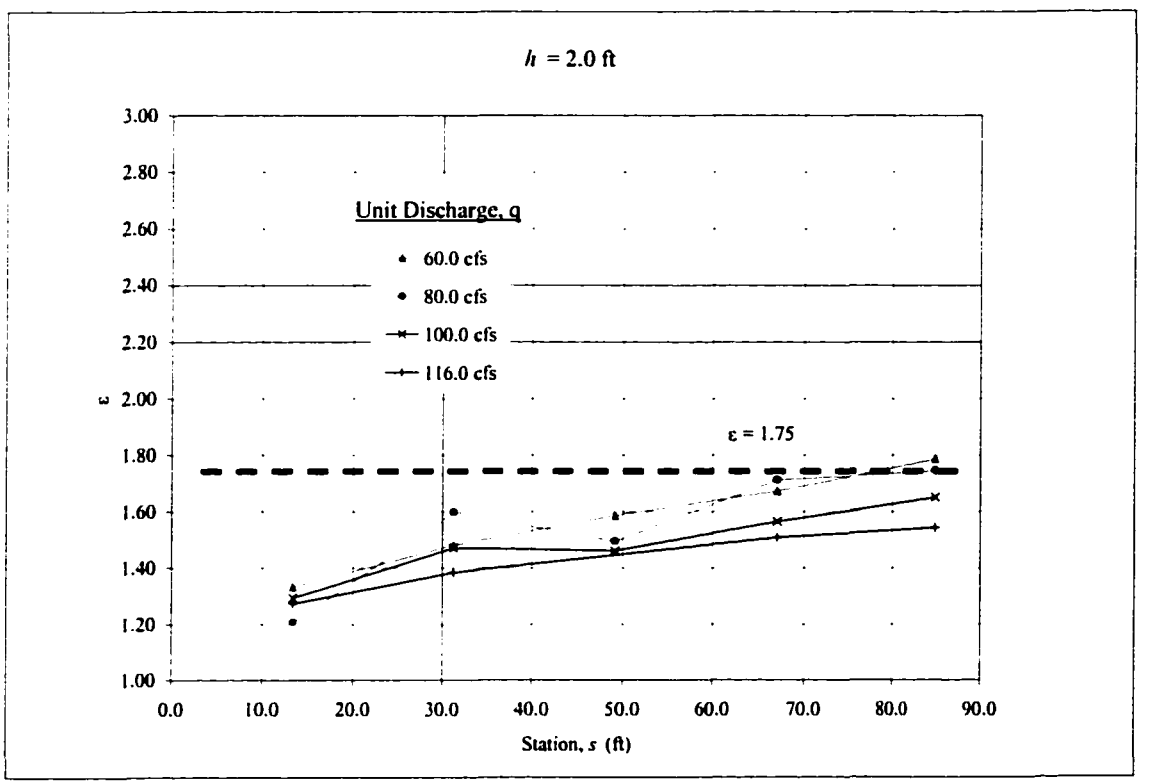

Figure 7.2 – Bulking Coefficient Design Charts, h = 1.0 ft, h = 2.0 ft

7.1.2 Training Wall Height

Bulked flow depth y_{90} is defined as the depth at which air concentration in the flow is 90% and can be found using clear water depth d_w, Equation (6-4), and Figure 7.2. It is assumed that a very small portion of the total discharge is carried above this depth. However, a considerable amount of splash may be projected above y_{90} with water particles ejected from the main spillway channel necessitating additional freeboard. At maximum flow rates tested in the present study, sidewall heights of approximately 5-ft above the tips of the steps, measured perpendicular to the spillway, provided freeboard of approximately $2.5y_{90}$, which essentially contained the entire splash within the test channel. Based on observations from the present study, it appears that a minimum of $2.0y_{90}$ is required to minimize splash over the wall and contain the majority of flow.

For values of Nh greater than approximately 10.0 ft measured vertically from the spillway crest (approximately station 22 ft for a 2:1 H:V slope), a freeboard of $2.0y_{90}$ is recommended where a small amount of splash over the wall is acceptable and $2.5y_{90}$ where minimizing splash over the wall is critical. Channel sidewalls upstream from this location should be increased in a tapered fashion to match a height of approximately $1.5y_c$ at the spillway crest.

7.1.3 Design Procedure

Based on the above discussion and the analysis outlined in Chapter 6, a hydraulic design procedure was developed. With knowledge of how f varies with spillway height, clear water depth and average velocity profiles along the length of the spillway can be found using the standard step method. From d_w, bulked flow depth y_{90} can be determined using the bulking ratio ε from equation (6-4) and Figure 7.2. Training wall heights are

then designed based on y_{90} and a factor of safety. Energy dissipation along the spillway can be found with H, d_w and U_{avg} using equation (6-20) or Figure 6.20. The hydraulic design procedure is summarized by the following steps:

Step 1: Known design variables:
Total discharge Q;
spillway width b;
spillway slope $\theta = 26.6°$;
spillway height H;
step height $h = 1.0$ ft or $h = 2.0$ ft.

Step 2: Select friction factor $f = 0.25$.

Step 3: Determine clear water depth d_w and average velocity U_{avg} profiles along the spillway length using a backwater computation, such as the Standard Step Method. Assume the starting boundary condition as critical depth at the spillway crest with the channel bed defined as the psuedo-bottom formed by the tips of the steps.

Step 4: Determine bulked flow depth y_{90} with $\varepsilon = 1.75$ and design for additional freeboard.

Step 5: Determine energy dissipation along the spillway from equation (6-20) or Figure 6.20.

7.2 Design Example

7.2.1 Stepped spillway example

Step 1: Given data:

Total discharge, $Q = 1250.0$ cfs

spillway width $b = 50.0$ ft

spillway height $H = 40.0$ ft

spillway slope $\theta = 26.6°$

Compute unit discharge q:

$$q = \frac{Q}{b} = \frac{1250.0\,\text{cfs}}{50.0\,\text{ft}} = 25.0\,\text{cfs/ft} \tag{7-1}$$

Compute critical depth y_c:

$$y_c = \left(\frac{q^2}{g}\right)^{1/3} = \left(\frac{25.0^2}{32.2}\right)^{1/3} = 2.69\,\text{ft} \tag{7-2}$$

Step 2: From Figure 7.1, find values of f for various Nh/y_c :

Compute Nh/y_c for full spillway height:

Step height $h = 1.0$ ft, $N = 40$ steps

$$Nh / y_c = \frac{40(1)}{2.69} = 14.9 \tag{7-3}$$

Step height $h = 2.0$ ft, $N = 20$ steps

$$Nh / y_c = \frac{20(2)}{2.69} = 14.9 \tag{7-4}$$

Since Nh/y_c is sufficiently large, select a constant $f = 0.25$ for both $h = 1.0$ ft and $h = 2.0$ ft.

Step 3: Figures 7.3 and 7.4 shows results of a Standard Step Method computation adapted from Chow (1959) resulting in a clear water depth of d_w = 1.07 ft and average velocity U_{avg} = 23.43 ft/s at the base of the stepped spillway. Appendix D provides results of the stepwise computations.

Step 4: Compute y_{90} with ε = 1.75 for both h = 1.0 ft and h = 2.0 ft resulting in a maximum value of y_{90} = 2.05 ft at Nh = 10 ft and y_{90} = 1.87 ft at the base of the stepped spillway. Design training wall heights of 4.10 ft based on $2.0y_{90}$, using the maximum value of y_{90} along the slope. Transition training walls upstream to match a spillway crest wall height of $1.5y_c$ = 1.5(2.69) = 4.04 ft.

Step 5: Compute energy dissipation at base of the spillway using clear water depth d_w = 1.07 ft, average velocity U_{avg} = 23.43 ft/s and equation (6.20):

$$\frac{\Delta E}{E_o} = 1 - \frac{d_w \cos\theta + \frac{U_{avg}^2}{2g}}{H_o + \frac{3}{2}y_c} = 1 - \frac{1.07\cos 26.6 + \frac{(23.43)^2}{2(32.2)}}{40 + \frac{3}{2}(2.69)} = 0.79 \Rightarrow 79\% \quad (7\text{-}5)$$

7.2.2 Smooth Spillway Comparison

Conditions from the design example were applied to the smooth spillway for comparison purposes. A friction factor of f = 0.071 was selected for the smooth surface based on results from the present study (reference Figure 6.13). Results of the backwater computations are shown in Figure 7.5 with clear water depth d_w = 0.72 ft and average velocity U_{avg} = 34.64 ft/s found at the base of the spillway.

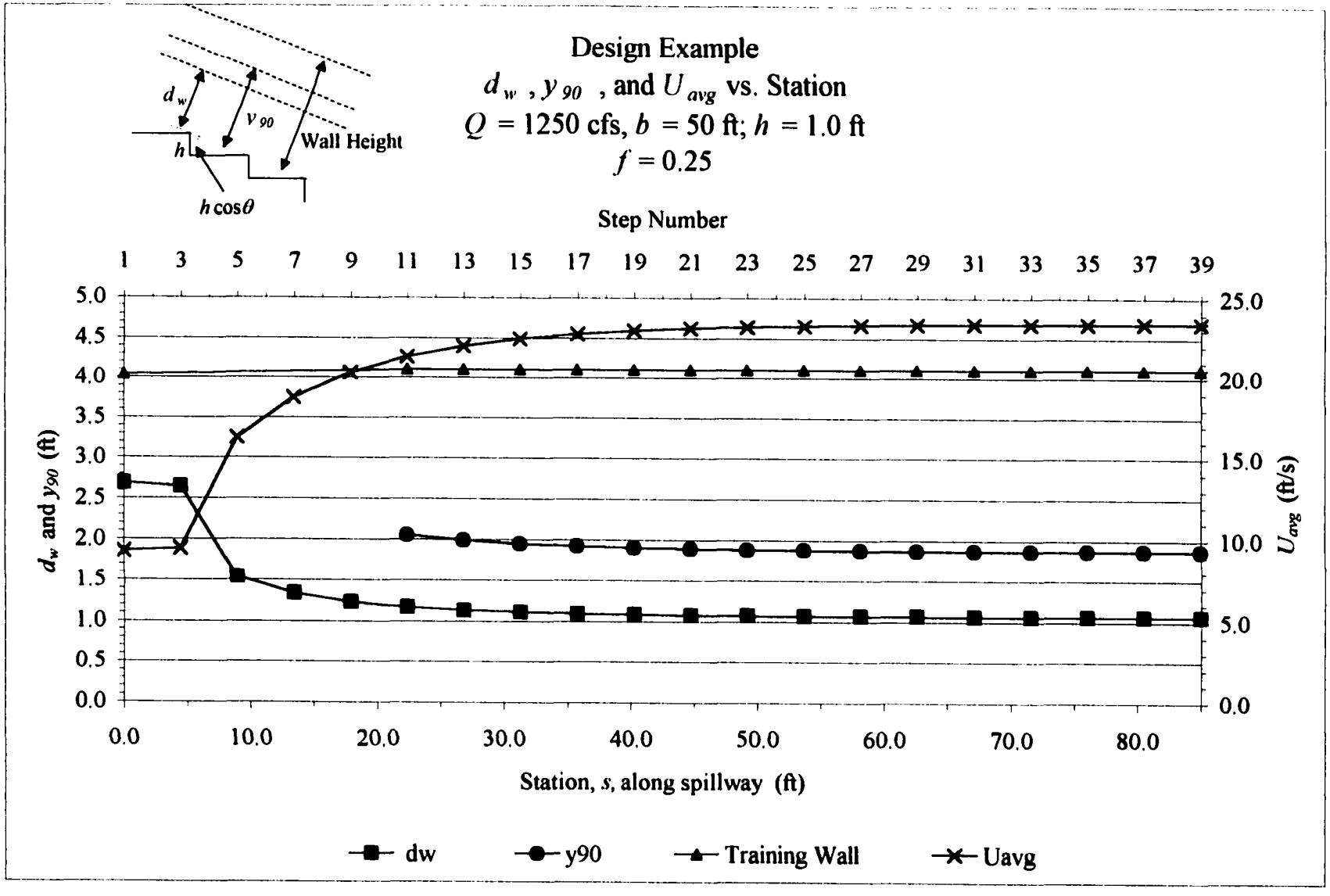

Figure 7.3 – Design Example Results, h = 1.0 ft.

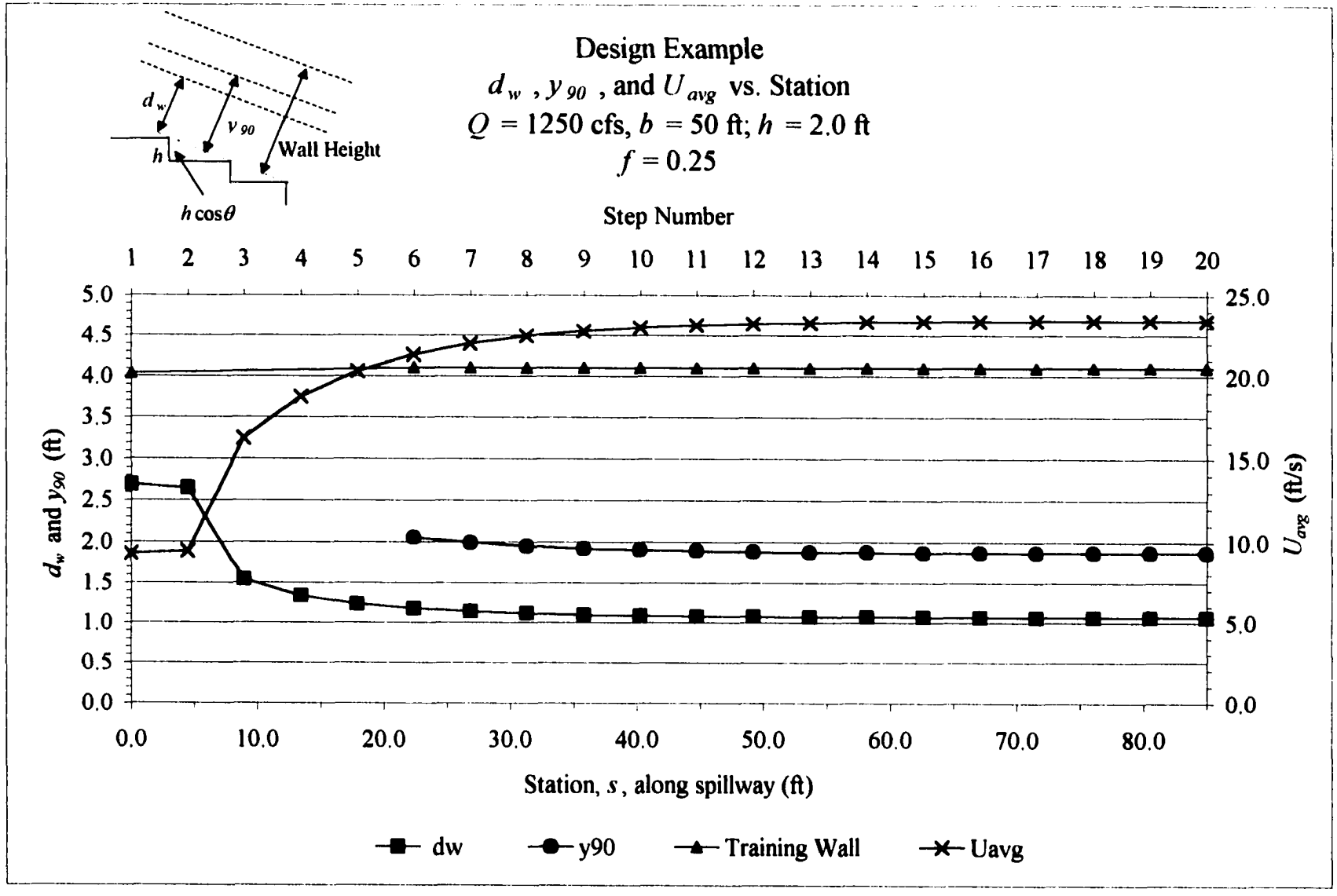

Figure 7.4 – Design Example Results, h = 2.0 ft.

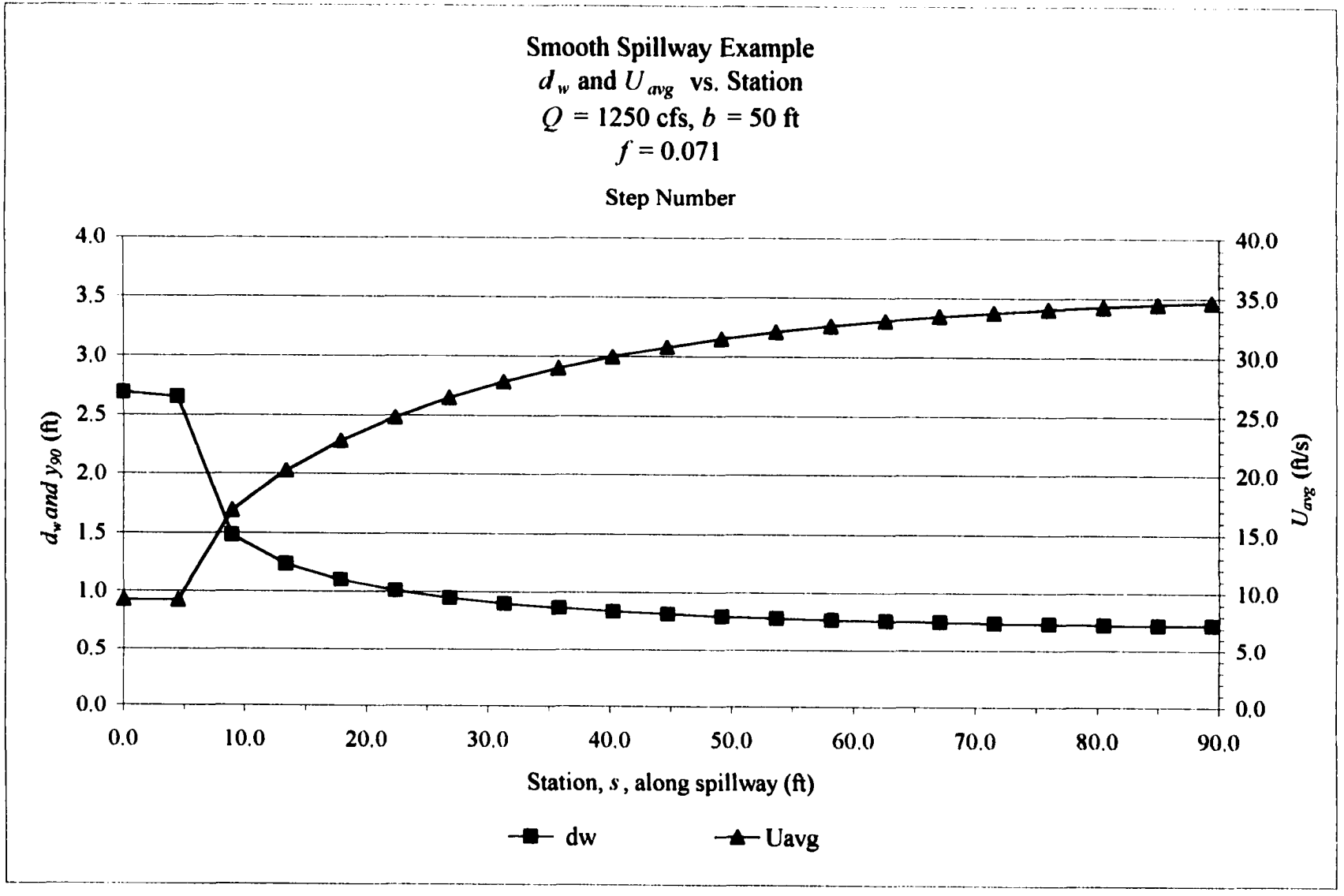

Figure 7.5 – Design Example smooth spillway.

7.2.3 Summary and Discussion of Results

Results of the stepped spillway example using h = 1.0 ft and h = 2.0 ft are identical due to selection of f = 0.25 for both step heights. This is consistent with the conclusions found in the present study. For a given unit discharge q, velocity and clear water depth varied only slightly. As shown in section 6.3, the data collapse to dimensionless values of $d_w/y_c \cong 0.40$ and Froude number $F_r \cong 4.0$, reflecting that, for a given skimming flow unit discharge, velocity and depth were independent of step height.

Note that in the example results, d_w and y_{90} are measured from the psuedo-bottom formed by a plane passing through the tips of the steps. Therefore, an additional height of $h\cos\theta$ perpendicular to the slope would need to be accounted for in the training wall design. The economic implications of this additional height as well as the number of steps to be constructed should be considered when selecting step height.

If it is assumed that for both stepped and smooth spillways, the hydraulic jump produced at the base of the spillway is contained in a USBR Type I stilling basin, then a comparison of required basin lengths L can be made (Peterka, 1983). Velocity and clear water depth entering the basin for the stepped and smooth spillway were used to calculate Froude numbers of F_r = 4.0 and 7.2, respectively. From Figure 6 of USBR Monograph 25 (Peterka, 1983), the ratio of hydraulic jump length (basin length L) to depth entering the basin can be determined. Table 7.1 gives a summary and comparison of velocities, flow depths, and stilling basin lengths. By using a stepped spillway, velocity entering the stilling basin is reduced by 32% compared to that of the smooth spillway, resulting in a 23% increase in energy dissipation. In addition, the stilling basin length of the stepped

spillway is 27% shorter than for the smooth spillway, a potentially significant cost savings.

Table 7.1 – Stepped spillway to smooth spillway comparison for q = 25.0 cfs/ft.

Step height h (ft)	Unit Discharge q (cfs/ft)	clear water depth entering basin d_w (ft)	average velocity entering basin U_{avg} (ft/s)	Energy dissipation at base of spillway	Froude number entering basin F_r	Length of hydraulic jump (basin length) L (ft)
1.0	25.0	1.07	23.4	79%	4.0	29.9
2.0	25.0	1.07	23.4	79%	4.0	29.9
smooth	25.0	0.72	34.6	56%	7.2	41.1

CHAPTER 8

SUMMARY, CONCLUSIONS, AND FUTURE RESEARCH

8.1 Summary

The objective of this study was to collect and interpret data on the hydraulic characteristics of flow over a stepped spillway. In addition, it was desired to develop a procedure from which a designer could estimate the flow characteristics for a given design discharge and step height. Numerous tests were conducted on a simulated stepped spillway at the near-prototype scale overtopping research facility located at Colorado State University's Engineering Research Center. Construction and testing spanned two full years and resulted in a large amount of data from which conclusions and a design procedure were obtained.

Prior to testing, an extensive review of existing literature pertaining to stepped spillway flow was conducted. Selection of literature focused on research conducted with physical scale models and on other studies having significantly contributed to the knowledge of stepped spillway flow. In addition, literature was reviewed covering the subject of self-aerated flow and the measurement of air concentration. As a result of the review, the need for further research was clearly established including the need for accurate measurement of air concentration, flow depth, velocity, and energy dissipation. In addition, the lack of existing prototype scale data was evident.

Steps fabricated from plywood and lumber were placed in the 2:1 (H:V) slope, 4 ft wide, 100 ft long chute of the overtopping facility and tested over a range of unit discharges up to 30 cfs/ft. Two different step configurations were tested with an additional test conducted on the smooth concrete spillway with the steps removed. The first stepped spillway consisted of twenty-five steps of height h = 2.0 ft. The addition of an infill comprised the second test with fifty steps of height h = 1.0 ft.

Instrumentation used to collect data in this study included an air concentration probe and a velocity probe. The probe for measuring air concentration is based on the difference in electrical resistivity between air and water. A square electronic waveform is produced indicating the ratio of air to water in the flow mixture. Velocity measurements were made using a back flushing Pitot tube designed to prevent air from entering the system.

Air concentration and velocity depth profiles were obtained at five locations along the spillway for each series of tests over a range of discharges. Detailed analyses were performed in order to reduce the data into a useable format. Statistical methods as well as subjective observations were used to remove outliers and other suspect data. Final data sets included averages of air concentration, clear water depth, bulked water depth, and velocity along the length of the spillway. Using this data, energy dissipation and Darcy friction factor were computed resulting in a design procedure based on selecting an appropriate value of friction factor for use in a water surface profile calculation. The procedure yields clear water flow depth and velocity at any location along the spillway for a given unit discharge and step height. A bulking ratio is then applied to the clear water depth to obtain a bulked depth profile for use in spillway training wall design. A

design example of a stepped spillway was provided along with a comparison to a smooth spillway design.

8.2 Conclusions

The present study is the first of its kind to gather data on the hydraulic characteristics of stepped spillway flow at near-prototype conditions. Step heights of h = 1.0 ft and h = 2.0 ft, which are typical of most RCC and conventional concrete stepped spillways, were modeled. Data were collected and analyzed that resulted in a design procedure important for those considering a stepped spillway. With limited required information, a designer can predict the hydraulic characteristics of the stepped spillway flow using this procedure. Design charts of Darcy friction factor f and bulking coefficient ε (Figures 7.1 and 7.2) were produced that provide information on the relative magnitude of these important parameters.

Analysis of the results in dimensionless form revealed minimal scaling effects between the h = 1.0 ft and h = 2.0 ft data. Near the base of the spillway where the flow is considered fully developed and nearly uniform, the data from both step heights tended towards approximately constant values of Froude number F_r = 4.0, d_w/y_c = 0.40, and f = 0.25. For prototype conditions similar to the present study, these values may be used as guidelines for design.

Stepped spillways have the advantage over smooth spillways by significantly reducing velocities and increasing energy dissipation. Data from the present study showed average velocities near the base of the smooth spillway reduced by 30 – 40% using the steps resulting in an increase in energy dissipation by approximately 20% on

average. A design example was given with results showing a 32% reduction in stilling basin length using a stepped spillway versus a traditional smooth surface spillway.

8.3 Recommendations for Future Research

As stated previously, this study is the first of such to model steps heights of this size at near prototype scale. Although not addressed in this dissertation, the effects of scaling in small scale models have been a matter of concern in much of the literature on stepped spillways. Comparison of data from this study to scale model data would be of great value in verifying previous works. In addition, combining other data sets can be used to reinforce as well as improve upon existing information.

Specialized instrumentation used for measuring air concentration and velocity was used in this study and provided data with a reasonable level of confidence. However, several complications concerning calibration and limitations of the instruments were encountered during the study. Refinement of the instruments themselves and procedures involving their use and calibration are of utmost importance for future model studies.

The design procedure presented herein is based on computation of Darcy friction factor and the resulting design charts are adequate for use as a guideline. Preliminary analysis revealed that the calculation of friction factor is sensitive to all of the variables used in determining its value, particularly energy slope. A rigorous study of friction factor including a sensitivity analysis to air concentration, flow depth, and other important variables may be of value.

REFERENCES

REFERENCES

1. American Society of Civil Engineers, ACSE (1994), *Roller-Compacted Concrete from the U.S. Army Corps of Engineers*, ASCE Press, New York.

2. American Society of Mechanical Engineers, ASME (1959), *Fluid Meters, Their Theory and Application*, Report of the ASME Research Committee on Fluid Meters, 5th Edition, New York.

3. Bindo, M., Gautier, J., and Lacroix, F (1993). "The Stepped Spillway of M'Bali Dam." International Water Power and Dam Construction, vol. 45, issue 1, January.

4. Boes, R. M. and Hager, W. H. (1998). "Fiber-Optical Experimentation in Two-Phase Cascade Flow." *Proceedings of the International RCC Dams Seminar*, K. Hansen (ed), Denver.

5. Bradley, J.N., and Peterka, A.J. (1957). "The Hydraulic Design of Stilling Basins: Short Stilling Basin for Canal Structures, Small Outlet Works and Small Spillways (Basin III)." Journal of Hydraulics Division, vol. 83, no. HY5, paper 1403, October.

6. Cain, P. (1978). *Measurements within Self-Aerated Flow on a Large Spillway*, Dissertation, University of Canterbury, Christchurch New Zealand.

7. Cain, P. and Wood, I. R. (1981). "Instrumentation for Aerated Flow on Spillways." Journal of the Hydraulics Division, Vol. 107, No. HY11, November.

8. Chamani M.R. (1997). *Skimming Flow in a Large Model of a Stepped Spillway*, Dissertation, University of Alberta, Canada.

9. Chamani, M. R. and Rajaratnam, N. (1994). "Jet Flow on Stepped Spillways." Journal of Hydraulic Engineering, vol. 120, no. 2, February.

10. Chamani, M. R. and Rajaratnam, N. (1999). "Characteristics of Skimming Flow Over Stepped Spillways." Journal of Hydraulic Engineering, vol. 125, no. 4, April.

11. Chanson, H. (1993). "Stepped Spillway Flows and Air Entrainment." Canadian Journal of Civil Engineering, vol. 20, no. 3, June.

12. Chanson, Hubert (1994). *Hydraulic Design of Stepped Cascades, Channels, Weirs and Spillways*. Pergamon, Oxford, England.

13. Christodoulou, G. C. (1993). "Energy Dissipation on Stepped Spillways." Journal of Hydraulic Engineering, vol 119, no. 5, May.

14. Chow, V.T. (1959). *Open Channel Hydraulics*, McGraw-Hill, New York, 1959.

15. Diez-Cascon, J., Blanco, J. L., Revilla, J. and Garcia, R. (1991). "Studies of the Hydraulic Behaviour of Stepped Spillways." International Water Power and Dam Construction, vol. 43, September.

16. Ehrenberger, R. (1926). "Flow of Water in Steep Chutes with Special Reference to Self-Aeration." Wasservewegung in steilen Rinnen (Schusstennen) mit besonderer Berucksichtigung der Selbstbeluftung, Osterreichischen Ingenieurund Architektenvereines, nos. 15/16 and 17/18, translated by E.F. Wilsey, United States Bureau of Reclamation.

17. Essery, I. T. S., and Horner, M. W. (1978). "The Hydraulic Design of Stepped Spillways." Report 33, Construction Industry Research and Information Association, London, England, January.

18. Falvey, H.T. (2001). Personal communications.

19. Falvey, H.T. (1979). "Mean Air Concentration of Self-Aerated Flows." Journal of the Hydraulics Division, vol. 105, no. HY1, January.

20. Frizell, K. H. (1992). "Hydraulics of Stepped Spillways for RCC Dams and Dam Rehabilitations." Proceedings, 1992 ASCE Roller Compacted Concrete III Conference, San Diego, CA, February.

21. Frizell, K. H., Ehler, D. G., Mefford, B. W. (1994) "Developing Air Concentration and Velocity Probes for Measuring Highly-Aerated, High-Velocity Flow", *Proceedings Hydraulic Engineering Conference, ASCE*, Buffalo, NY.

22. Gaston M. L.(1995) *Air Entrainment and Energy Dissipation on a Stepped Block Spillway*, Thesis, Colorado State University, USA.

23. Hewlett et. al. (1997) *Design of Stepped-Block Spillways*, Construction Industry Research and Information Association, CIRIA Special Punlication 142, London.

24. Houston, K. L. (1987) "Stepped Spillway Design with a RCC Dam." ASCE Hydraulic Engineering Proceedings.

25. Jacobs, M. L. (1997), "Air Concentration Meter Electronics Package Manual" *U.S. Bureau of Reclamation Technical Service Center, Project Notes 8450-98-01*, October.

26. Johnson, B. and Cowan, G. (1997). "Hydraulic Model for a New Dam Significant Savings." Public Works, vol. 128, no. 8, July.

27. Lamb, O.P. and Killen, J.M. (1950). "An Electrical Method for Measuring Air Concentration in Flowing Air-Water Mixtures." Technical Paper Number 2, Series B, University of Minnesota, St. Anthony Falls Hydraulic Laboratory, Minneapolis, Minn.

28. Lejeune, M. and Lejeune, A. (1994). "About the Energy Dissipation of Skimming Flows Over Stepped Spillways." Proceedings of the First Conference on Hydroinformatics, Deflt, Netherlands, vol 2, September.

29. Matos, J. and Frizell, K. (2000). "Air Concentration and Velocity Measurements on Self-aerated Flow down Stepped Chutes." Project notes, Technical University of Lisbon, Lisbon, Portugal.

30. Matos, J. and Quintela, A. (1995). "Flow Resistance and Energy Dissipation in Skimming Flow over Stepped Spillways." Proceedings of the First International Conference on Water Resources, ASCE Water Resources Engineering Division, San Antonio, TX, vol. 2, August.

31. McKenna (2001) *Air-Water Gas Transfer on Stepped Spillways*, Thesis, Colorado State University, USA.

32. Montgomery, D.C. and Runger, G. C. (1999) *Applied Statistics and Probability for Engineers*, John Wiley & Sons, 2nd Edition, New York.

33. Omega Instruments (1995) *The Flow and Level Handbook*, Vol. 29, Omega Engineering, Inc. Stamford, CT.

34. Perterka, A.J. (1983). *Hydraulic Design of Stilling Basins and Energy Dissipators*, Engineering Monograph No. 25, U.S. Bureau of Reclamation, Denver, Colorado.

35. Peyras, L., Royet, P. and Degoutte, G. (1992). "Flow and Energy Dissipation Over Stepped Gabion Weirs." Journal of Hydraulic Engineering, vol 118, no. 5, May.

36. Rajaratnam, N. (1990). "Skimming Flow in Stepped Spillways." Journal of Hydraulic Engineering, vol 116, no. 4, April.

37. Rand, W. (1955). "Flow Geometry at Straight Drop Spillways." Proceedings, ASCE, vol. 108, no. 791, September.

38. Rice, C. E. and Kadavy, K. C. (1996). "Model Study of a Roller Compacted Concrete Stepped Spillway." Journal of Hydraulic Engineering, vol. 122, no. 6, June.

39. Rice, C. E. and Kadavy, K. C. (1997). "Physical Model Study of the Proposed Spillway For Cedar Run Site 6, Faquier County, Virginia." ASAE Applied Engineering in Agriculture, vol. 13, no. 6.

40. Robinson, K. M., Rice, C.E., Kadavy, K. C., and Talbot, J. R. (1998). "Energy Losses on a Roller Compacted Concrete Stepped Spillway." ASCE Water Resources Engineering Division, Proceedings of the 1998 International Water Resources Engineering Conference, Memphis, TN, vol. 2, August.

41. Ruff, J. F. and Frizell, K. H. (1994). "Air Concentration in Highly Turbulent Flow on a Steeply-Sloping Chute." *Hydraulic Engineering '94: Proceedings of the 1994 Conference.*

42. Schnitter, N.J. (1994). *A history of Dams: the Useful Pyramids.* Balkema Publications, Rotterdam, The Netherlands.

43. Schuyler, J.D. (1912). *Reservoirs for Irrigation, Water Power and Domestic Water Supply.* John Wiley & Sons, 2nd Edition, New York.

44. Smith, N. (1972). *A History of Dams.* The Citadel Press, Secaucus, New Jersey.

45. Sorensen, R. M. (1985). "Stepped Spillway Hydraulic Model Investigations." Journal of Hydraulic Engineering, vol. 111, no. 12, December.

46. Stephenson, D. (1991). "Energy Dissipation Down Stepped Spillways." International Water Power and Dam Construction, vol. 43, September.

47. Straub, L.G. and Lamb, O.P. (1956). "Experimental Studies of Air Entrainment in Open Channel Flow." Proceedings, Minnesota International Hydraulics Convention, Minneapolis, Minnesota, September.

48. Straub, L. G. and Anderson. A. G. (1958). "Experiments on Self-Aerated Flow in Open Channels." Journal of the Hydraulics Division, vol. 84, no. HY7, December.

49. Tozzi, M. J. (1994). "Residual Energy in Stepped Spillways." International Water Power and Dam Construction, vol 46, May.

50. White, M. P. (1943). "Energy Loss at the Base of a Free Overfall – Discussion." *Transactions*, ASCE, vol. 108.

51. Wilhelms, S. C. (1994). Self-aerated Flow on Corps Engineers Spillways, Technical Report No. W-94-2, U.S. Army Engineers Waterways Experiment Station, Vicksburg, Miss.

52. Wood, I. R. (1983) "Uniform Flow Region of Self-Aerated Flow." Journal of Hydraulic Engineering, vol. 109, no. 3.

53. Wood, I. R. (1991) "Air Entrainment in Free-Surface Flows." *IAHR Hydraulic Strucutres Design Manual No. 4*, Hydraulic Design Considerations, Balkema Publications, Rotterdam, The Netherlands.

54. Zhou, H.; Wu, S.; and Jang, S. (1997). "Hydraulic Performances of Skimming Flow over Stepped Spillway." Journal of Hydrodynamics, vol. 9, no. 3.

APPENDIX A

AIR CONCENTRATION AND VELOCITY PROFILES

Profiles of local air concentration c(y) and velocity u(y) are given in this appendix for the stepped spillway tests and the smooth spillway test. Results are given in tabular and graphical form. Note that tabulated values of depth and velocity corresponding to c(y) = 0.70 and 0.90 are interpolated or extrapolated as discussed in Chapter 5.

Stepped Spillway Tests, h = 1.0 ft

Discharge (cfs)	Step Number	Depth y (ft)	Air Conc. c(y)	Velocity u(y) (ft/s)
7.1	7	0.05	0.5996	11.96
		0.10	0.7000	15.78
		0.15	0.8171	15.78
		0.25	0.8467	15.78
		0.35	0.8448	15.78
		0.45	0.8665	15.78
		0.55	0.8966	15.78
		0.56	0.9000	15.78
7.1	15	0.05	0.5117	14.72
		0.14	0.7000	17.65
		0.15	0.7321	17.65
		0.25	0.8453	17.65
		0.35	0.8775	17.65
		0.43	0.9000	17.65
		0.45	0.9053	
		0.55	0.9059	
7.1	23	0.05	0.1428	9.98
		0.15	0.4339	11.69
		0.24	0.7000	17.93
		0.25	0.7255	17.93
		0.35	0.7788	17.93
		0.45	0.8422	17.93
		0.55	0.8618	17.93
		0.65	0.8924	17.93
		0.67	0.9000	17.93
7.1	31	0.05	0.3721	12.73
		0.15	0.6856	19.91
		0.17	0.7000	20.66
		0.25	0.7801	20.66
		0.35	0.7683	20.66
		0.45	0.8073	20.66
		0.69	0.9000	20.66
7.1	39	0.05	0.1731	8.49
		0.15	0.5490	10.88
		0.22	0.7000	14.17
		0.25	0.7590	14.17
		0.35	0.8135	14.17
		0.45	0.8486	14.17
		0.55	0.8927	14.17
		0.59	0.9000	14.17
		0.65	0.9123	

Discharge (cfs)	Step Number	Depth y (ft)	Air Conc. c(y)	Velocity u(y) (ft/s)
21.2	7	0.05	0.4088	18.91
		0.15	0.3735	20.20
		0.25	0.4517	21.57
		0.35	0.7000	28.35
		0.35	0.7075	28.35
		0.45	0.7944	28.35
		0.55	0.8586	28.35
		0.65	0.8719	28.35
		0.73	0.9000	28.35
21.2	15	0.05	0.2641	19.95
		0.15	0.2835	21.39
		0.25	0.4853	24.73
		0.34	0.7000	33.75
		0.35	0.7224	33.75
		0.45	0.8157	33.75
		0.55	0.8968	33.75
		0.55	0.9000	33.75
		0.65	0.9625	
21.2	23	0.05	0.4459	17.12
		0.15	0.3760	20.41
		0.25	0.5370	25.53
		0.35	0.5257	22.12
		0.45	0.6814	27.41
		0.47	0.7000	27.80
		0.55	0.7819	27.80
		0.65	0.8743	27.80
		0.68	0.9000	27.80
21.2	31	0.05	0.0784	16.60
		0.15	0.1359	19.59
		0.25	0.2770	21.16
		0.35	0.5073	24.46
		0.45	0.6897	29.94
		0.46	0.7000	30.18
		0.55	0.7723	30.18
		0.65	0.8865	30.18
		0.66	0.9000	30.18
21.2	39	0.05	0.1319	15.67
		0.15	0.3602	21.02
		0.25	0.4325	22.67
		0.35	0.5330	21.99
		0.45	0.6898	25.72
		0.46	0.7000	26.08
		0.55	0.7996	26.08
		0.65	0.8867	26.08
		0.67	0.9000	26.08

Stepped Spillway Tests, h = 1.0 ft

Discharge (cfs)	Step Number	Depth y (ft)	Air Conc. c(y)	Velocity u(y) (ft/s)
41.0	7	0.05	0.1913	18.92
		0.15	0.2037	14.41
		0.25	0.2228	23.81
		0.45	0.2845	24.26
		0.65	0.6148	27.64
		0.71	0.7000	31.83
		0.85	0.8798	31.83
		0.88	0.9000	31.83
		0.95	0.9533	
41.0	15	0.05	0.1837	23.28
		0.15	0.1965	26.80
		0.25	0.1917	26.89
		0.35	0.2813	28.21
		0.45	0.4118	29.87
		0.64	0.7000	41.12
		0.65	0.7197	41.12
		0.75	0.8060	41.12
		0.83	0.9000	41.12
		0.85	0.9199	
41.0	23	0.05	0.0344	17.14
		0.15	0.0808	23.03
		0.25	0.0837	23.96
		0.45	0.2005	25.68
		0.65	0.4548	28.89
		0.75	0.5807	28.70
		0.82	0.7000	35.26
		0.85	0.7507	35.26
		0.95	0.8707	35.26
		0.97	0.9000	35.26
41.0	31	0.05	0.0656	19.57
		0.15	0.0981	23.14
		0.25	0.1447	25.25
		0.45	0.3045	27.45
		0.65	0.5123	29.37
		0.78	0.7000	35.64
		0.85	0.8030	35.64
		0.95	0.8649	35.64
		1.00	0.9000	35.64
41.0	39	0.05	0.0256	18.65
		0.15	0.0783	22.98
		0.25	0.1127	24.89
		0.45	0.2421	26.68
		0.65	0.4565	26.49
		0.75	0.7000	36.05
		0.75	0.7030	36.05
		0.85	0.8172	36.05
		0.94	0.9000	36.05
		0.95	0.9142	

Discharge (cfs)	Step Number	Depth y (ft)	Air Conc. c(y)	Velocity u(y) (ft/s)
60.0	7	0.05	0.1977	19.67
		0.15	0.1704	21.30
		0.25	0.1993	24.05
		0.45	0.2160	27.00
		0.65	0.3135	27.83
		0.85	0.6761	39.00
		0.87	0.7000	39.23
		1.05	0.9073	39.23
60.0	15	0.05	0.1523	21.92
		0.15	0.1623	25.23
		0.25	0.1654	26.79
		0.45	0.1881	28.51
		0.65	0.3439	29.50
		0.85	0.6390	34.78
		0.90	0.7000	41.30
		1.05	0.8912	41.30
		1.15	0.9430	41.30
		0.00	0.0000	0.00
60.0	23	0.05	0.0352	13.34
		0.15	0.0542	23.21
		0.25	0.0635	25.44
		0.45	0.0986	26.49
		0.65	0.1983	28.14
		0.85	0.4256	29.38
		1.04	0.7000	38.31
		1.05	0.7110	38.31
		1.15	0.8488	38.31
		1.22	0.9000	38.31
		1.25	0.9216	
60.0	31	0.05	0.0448	19.84
		0.15	0.0709	22.92
		0.25	0.0980	24.77
		0.45	0.1901	27.39
		0.65	0.2980	29.31
		0.85	0.5696	34.88
		0.96	0.7000	41.08
		1.05	0.8103	41.08
		1.15	0.8956	41.08
		1.16	0.9000	41.08
60.0	39	0.05	0.0139	20.67
		0.15	0.0525	23.23
		0.25	0.0789	25.90
		0.45	0.1170	27.98
		0.65	0.2756	29.90
		0.85	0.5425	34.09
		0.95	0.7000	45.00
		1.05	0.8458	45.00
		1.15	0.8789	45.00
		1.18	0.9000	45.00
		1.25	0.9519	

Stepped Spillway Tests, h = 1.0 ft

Discharge (cfs)	Step Number	Depth y (ft)	Air Conc. c(y)	Velocity u(y) (ft/s)
80.0	7	0.05	0.2011	18.79
		0.15	0.2115	20.01
		0.25	0.2102	25.21
		0.45	0.1906	26.51
		0.65	0.1855	27.20
		0.85	0.3148	28.26
		1.05	0.6740	30.63
		1.09	0.7000	30.82
		1.25	0.8174	30.82
		1.31	0.9000	30.82
		1.35	0.9643	
80.0	15	0.05	0.1134	24.22
		0.15	0.1152	27.13
		0.25	0.1191	26.35
		0.45	0.1229	30.40
		0.65	0.1958	31.83
		0.85	0.4287	32.06
		1.02	0.7000	33.97
		1.05	0.7377	33.97
		1.15	0.8764	33.97
		1.20	0.9000	33.97
		1.25	0.9405	
80.0	23	0.05	0.0207	13.14
		0.15	0.0324	23.95
		0.25	0.0449	24.83
		0.45	0.0578	27.79
		0.65	0.1229	30.51
		0.85	0.2862	33.10
		1.05	0.5098	34.92
		1.15	0.5799	34.58
		1.20	0.7000	41.68
		1.25	0.8054	41.68
		1.35	0.8980	41.68
		1.35	0.9000	41.68
80.0	31	0.05	0.0245	19.49
		0.15	0.0472	22.29
		0.25	0.0451	23.27
		0.45	0.1065	27.76
		0.65	0.1407	29.17
		0.85	0.3445	32.61
		1.05	0.6090	39.18
		1.14	0.7000	42.59
		1.25	0.8194	42.59
		1.34	0.9000	42.59
		1.35	0.9086	

Discharge (cfs)	Step Number	Depth y (ft)	Air Conc. c(y)	Velocity u(y) (ft/s)
80.0	39	0.05	0.0139	20.75
		0.15	0.0365	22.41
		0.25	0.0635	25.67
		0.45	0.0777	29.84
		0.65	0.1648	32.60
		0.85	0.2958	34.28
		1.05	0.5900	40.19
		1.13	0.7000	42.25
		1.15	0.7196	42.25
		1.25	0.8149	42.25
		1.34	0.9000	42.25
100.0	7	0.05	0.2146	19.19
		0.15	0.2072	20.40
		0.25	0.1764	23.26
		0.45	0.2027	26.10
		0.65	0.1729	28.37
		0.85	0.2012	30.56
		1.05	0.2901	31.66
		1.25	0.6781	36.02
		1.27	0.7000	37.62
		1.45	0.8638	37.62
		1.49	0.9000	37.62
		1.55	0.9503	
100.0	15	0.05	0.0743	21.45
		0.15	0.0727	24.17
		0.25	0.0566	26.09
		0.45	0.0485	29.70
		0.65	0.0882	32.74
		0.85	0.3021	34.15
		1.05	0.6718	41.25
		1.07	0.7000	43.38
		1.25	0.9094	43.38
		1.35	0.9723	
		1.45	0.9690	
		0.00	0.0000	
100.0	23	0.05	0.0059	10.73
		0.15	0.0273	22.95
		0.25	0.0243	24.69
		0.45	0.0435	28.67
		0.65	0.0754	30.86
		0.85	0.1659	33.10
		1.05	0.3151	33.90
		1.25	0.6432	37.86
		1.28	0.7000	40.34
		1.35	0.8268	40.34
		1.43	0.9000	40.34
		1.45	0.9140	

Stepped Spillway Tests, h = 1.0 ft

Discharge (cfs)	Step Number	Depth y (ft)	Air Conc. c(y)	Velocity u(y) (ft/s)
100.0	**31**	0.05	0.0203	20.30
		0.15	0.0531	21.83
		0.25	0.0478	23.99
		0.45	0.0573	29.07
		0.65	0.1604	31.20
		0.85	0.2081	33.43
		1.05	0.4234	36.65
		1.25	0.6464	40.43
		1.30	0.7000	46.45
		1.45	0.8733	46.45
		1.49	0.9000	46.45
		1.55	0.9447	
100.0	**39**	0.05	0.0196	18.27
		0.15	0.0582	25.08
		0.25	0.0475	27.77
		0.45	0.0587	31.19
		0.65	0.0855	33.60
		0.85	0.1963	38.42
		1.05	0.3474	37.80
		1.25	0.6174	39.73
		1.31	0.7000	42.95
		1.35	0.7543	42.95
		1.45	0.8569	42.95
		1.49	0.9000	42.95

Stepped Spillway Tests, $h = 2.0$ ft

Discharge (cfs)	Step Number	Depth y (ft)	Air Conc. c(y)	Velocity u(y) (ft/s)
20.0	4	0.05	0.2109	10.71
		0.25	0.4682	12.42
		0.45	0.5784	14.82
		0.56	0.7000	21.96
		0.65	0.8024	21.96
		0.85	0.8231	21.96
		1.05	0.7862	21.96
		1.25	0.7873	21.96
20.0	8	0.05	0.9080	36.35
		0.15	0.0756	14.91
		0.25	0.2411	16.43
		0.35	0.3584	17.16
		0.45	0.6134	21.64
		0.55	0.6781	20.06
		0.57	0.7000	21.11
		0.65	0.8134	21.11
		1.00	0.9000	21.11
20.0	12	0.05	0.0691	13.31
		0.17	0.1553	14.49
		0.37	0.5820	18.67
		0.48	0.7000	23.72
		0.57	0.8050	23.72
		0.77	0.8747	23.72
		0.89	0.9000	23.72
		0.97	0.9185	
20.0	16	0.05	0.0919	11.04
		0.15	0.1178	14.80
		0.25	0.3580	17.11
		0.35	0.5469	18.24
		0.45	0.6970	22.07
		0.45	0.7000	22.07
		0.55	0.7813	22.07
		0.65	0.8097	22.07
		0.97	0.9000	22.07
20.0	20	0.05	0.2246	15.93
		0.15	0.3234	17.31
		0.25	0.4358	18.35
		0.35	0.6707	23.46
		0.38	0.7000	24.46
		0.45	0.7768	24.46
		0.55	0.8231	24.46
		0.65	0.8677	24.46
		0.74	0.9000	24.46
		0.75	0.9018	
40.0	4	0.05	0.2262	14.89
		0.25	0.0914	15.58
		0.45	0.1686	15.78
		0.65	0.5273	16.59
		0.77	0.7000	18.88
		0.85	0.8050	18.88
		1.05	0.8951	18.88
		1.06	0.9000	18.88

Discharge (cfs)	Step Number	Depth y (ft)	Air Conc. c(y)	Velocity u(y) (ft/s)
40.0	4	0.05	0.0634	31.43
		0.25	0.1089	32.39
		0.45	0.1858	34.21
		0.65	0.5585	47.97
		0.75	0.7000	79.34
		0.85	0.8399	79.34
		1.03	0.9000	79.34
		1.05	0.9085	
		1.25	0.9378	
40.0	8	0.05	0.9030	24.61
		0.15	0.0456	17.44
		0.25	0.0660	18.55
		0.35	0.1160	20.54
		0.45	0.1235	20.70
		0.55	0.3383	21.85
		0.65	0.5001	
		0.75	0.6992	
		0.75	0.7000	26.07
		0.85	0.8230	26.07
		0.95	0.8327	26.07
		1.30	0.9000	26.07
40.0	12	0.05	0.0371	18.69
		0.17	0.0808	20.14
		0.37	0.2280	21.57
		0.57	0.5636	26.00
		0.72	0.7000	32.27
		0.77	0.7462	32.27
		0.97	0.8540	32.27
		1.17	0.8969	32.27
		1.19	0.9000	32.27
		1.37	0.9377	
40.0	16	0.05	0.1197	18.72
		0.15	0.0850	20.31
		0.25	0.1129	22.23
		0.35	0.1642	23.69
		0.45	0.3295	24.47
		0.55	0.4620	24.85
		0.65	0.6602	32.12
		0.72	0.7000	30.38
		0.75	0.7157	30.38
		0.85	0.7370	30.38
		0.95	0.8244	30.38
		1.05	0.8949	30.38
		1.06	0.9000	30.38
40.0	16	0.05	0.1073	21.28
		0.15	0.2041	24.55
		0.25	0.2231	25.98
		0.35	0.3118	25.62
		0.45	0.4708	28.94
		0.55	0.6030	32.06
		0.61	0.7000	36.06
		0.65	0.7565	36.06
		0.75	0.7978	36.06
		0.85	0.8251	36.06
		0.95	0.8628	36.06
		1.05	0.9000	36.06

Stepped Spillway Tests, $h = 2.0$ ft

Discharge (cfs)	Step Number	Depth y (ft)	Air Conc. c(y)	Velocity u(y) (ft/s)
40.0	20	0.05	0.1875	23.00
		0.15	0.1900	24.14
		0.25	0.2428	26.31
		0.35	0.3514	28.71
		0.45	0.5411	32.61
		0.55	0.6483	34.15
		0.60	0.7000	36.81
		0.65	0.7561	36.81
		0.75	0.7978	36.81
		0.85	0.8228	36.81
		0.95	0.8730	36.81
		1.00	0.9000	36.81
60.0	4	0.05	0.0255	20.26
		0.25	0.0173	20.68
		0.45	0.0583	22.32
		0.65	0.0916	21.13
		0.85	0.5254	21.13
		0.94	0.7000	21.13
		1.05	0.8951	21.13
		1.08	0.9000	21.13
		1.25	0.9294	
60.0	4	0.05	0.1245	28.15
		0.15	0.0276	32.35
		0.25	0.0256	31.25
		0.45	0.0646	34.18
		0.65	0.2644	37.99
		0.85	0.6557	60.86
		0.89	0.7000	74.59
		1.05	0.8623	74.59
		1.25	0.8767	74.59
		1.30	0.9000	74.59
60.0	8	0.05	0.4010	9.17
		0.15	0.0354	19.93
		0.25	0.0400	21.45
		0.45	0.0492	21.67
		0.65	0.1209	24.87
		0.75	0.3446	25.63
		0.85	0.4729	27.29
		0.95	0.6800	27.21
		0.97	0.7000	28.33
		1.05	0.7922	28.33
		1.15	0.8760	28.33
		1.18	0.9000	28.33
60.0	12	0.05	0.3074	8.39
		0.13	0.0103	22.81
		0.25	0.0289	20.98
		0.45	0.0479	22.59
		0.65	0.1346	24.48
		0.85	0.4603	28.57
		1.01	0.7000	39.41
		1.05	0.7556	39.41
		1.25	0.8725	39.41
		1.33	0.9000	39.41
		1.45	0.9415	

Discharge (cfs)	Step Number	Depth y (ft)	Air Conc. c(y)	Velocity u(y) (ft/s)
60.0	16	0.05	0.0617	9.82
		0.15	0.0465	18.28
		0.25	0.0495	19.88
		0.45	0.0727	22.31
		0.65	0.1975	25.18
		0.75	0.4129	27.76
		0.85	0.5979	31.64
		0.94	0.7000	31.12
		0.95	0.7078	31.12
		1.05	0.7853	31.12
		1.15	0.8444	31.12
		1.25	0.8826	31.12
		1.30	0.9000	31.12
60.0	16	0.05	0.0794	24.03
		0.15	0.1069	22.40
		0.25	0.1094	23.57
		0.45	0.1440	25.69
		0.65	0.3495	29.03
		0.75	0.4705	29.13
		0.85	0.6569	37.75
		0.90	0.7000	38.78
		0.95	0.7512	38.78
		1.05	0.8352	38.78
		1.15	0.8729	38.78
		1.22	0.9000	38.78
60.0	20	0.05	0.1104	21.97
		0.15	0.1531	22.96
		0.25	0.1625	24.13
		0.45	0.1796	26.17
		0.65	0.3495	28.50
		0.75	0.5648	32.58
		0.84	0.7000	36.90
		0.85	0.7143	36.90
		0.95	0.7978	36.90
		1.05	0.8531	36.90
		1.15	0.8897	36.90
		1.18	0.9000	36.90
60.0	20	0.05	0.1232	4.66
		0.25	0.0300	18.83
		0.45	0.0550	21.21
		0.65	0.2691	24.06
		0.85	0.6159	31.47
		0.95	0.7000	37.57
		1.05	0.7877	37.57
		1.25	0.8773	37.57
		1.32	0.9000	37.57
		1.45	0.9467	

Stepped Spillway Tests, $h = 2.0$ ft

Discharge (cfs)	Step Number	Depth y (ft)	Air Conc. c(y)	Velocity u(y) (ft/s)
80.0	**4**	0.05	0.0106	14.21
		0.15	0.0037	20.65
		0.25	0.0044	22.11
		0.45	0.0073	23.65
		0.65	0.0144	23.59
		0.85	0.1383	24.60
		0.95	0.2094	22.21
		1.05	0.5499	23.90
		1.15	0.6320	17.59
		1.17	0.7000	22.91
		1.24	0.9000	22.91
		1.25	0.9332	
80.0	**4**	0.05	0.0284	18.61
		0.25	0.0026	20.01
		0.45	0.0058	24.39
		0.65	0.0505	21.60
		0.85	0.0752	21.83
		1.05	0.3555	26.94
		1.44	0.9000	
80.0	**8**	0.05	0.0520	
		0.15	0.0264	21.33
		0.25	0.0267	22.31
		0.45	0.0304	25.09
		0.65	0.0527	27.27
		0.85	0.3242	29.85
		0.95	0.5138	31.41
		1.05	0.6458	34.76
		1.13	0.7000	35.08
		1.15	0.7177	35.08
		1.25	0.8276	35.08
		1.35	0.8382	35.08
		1.55	0.9000	35.08
80.0	**12**	0.05	0.0809	9.10
		0.13	0.0065	25.31
		0.25	0.0236	23.35
		0.45	0.0329	26.34
		0.65	0.0622	28.57
		0.85	0.2721	31.21
		1.05	0.5707	36.30
		1.17	0.7000	46.86
		1.25	0.7879	46.86
		1.44	0.9000	46.86
		1.45	0.9032	
		1.65	0.9598	

Discharge (cfs)	Step Number	Depth y (ft)	Air Conc. c(y)	Velocity u(y) (ft/s)
80.0	**16**	0.05	0.1533	5.36
		0.15	0.0714	25.37
		0.25	0.1045	28.64
		0.45	0.1487	31.32
		0.65	0.1825	33.23
		0.85	0.4510	40.61
		0.95	0.5111	38.45
		1.05	0.6533	47.89
		1.08	0.7000	53.25
		1.15	0.8069	53.25
		1.25	0.8316	53.25
		1.35	0.8835	53.25
		1.39	0.9000	53.25
		1.45	0.9209	
		1.55	0.9436	
		1.65	0.9669	
80.0	**20**	0.05	0.1163	27.45
		0.15	0.1719	27.81
		0.25	0.1561	31.46
		0.45	0.1886	34.26
		0.65	0.2715	39.05
		0.85	0.4533	42.03
		0.95	0.5803	47.63
		1.05	0.6894	52.52
		1.06	0.7000	53.58
		1.15	0.7910	53.58
		1.25	0.8320	53.58
		1.35	0.8860	53.58
		1.38	0.9000	53.58
		1.45	0.9329	
		1.55	0.9597	
80.0	**20**	0.05	0.0080	23.16
		0.25	0.0506	23.87
		0.45	0.0669	26.91
		0.65	0.1677	31.32
		0.85	0.3831	33.91
		1.05	0.6045	40.95
		1.15	0.7000	49.30
		1.25	0.8030	49.30
		1.45	0.9000	49.30
		1.45	0.9025	
		1.65	0.9631	
100.0	**4**	0.05	0.0029	18.72
		0.15	0.0014	21.56
		0.25	0.0019	21.66
		0.45	0.0026	24.06
		0.65	0.0085	24.62
		0.85	0.0173	25.77
		0.95	0.1114	25.91
		1.05	0.2375	27.02
		1.15	0.4835	28.38
		1.25	0.5680	26.32
		1.32	0.7000	31.41
		1.35	0.7541	31.41
		1.45	0.8322	31.41
		1.54	0.9000	31.41

Stepped Spillway Tests, $h = 2.0$ ft

Discharge (cfs)	Step Number	Depth y (ft)	Air Conc. c(y)	Velocity u(y) (ft/s)
100.0	**8**	0.05	0.0654	
		0.15	0.0096	21.85
		0.25	0.0209	23.26
		0.45	0.0132	25.68
		0.65	0.0248	27.98
		0.85	0.1069	29.49
		0.95	0.4568	36.12
		1.05	0.4358	27.99
		1.15	0.5121	27.26
		1.24	0.7000	33.33
		1.25	0.7247	33.33
		1.35	0.7856	33.33
		1.45	0.8431	33.33
		1.55	0.9000	33.33
100.0	**12**	0.05	0.0513	9.47
		0.13	0.0056	26.33
		0.25	0.0158	24.49
		0.45	0.0204	28.00
		0.65	0.0297	31.13
		0.85	0.0905	32.75
		1.05	0.3671	34.70
		1.25	0.6564	43.66
		1.30	0.7000	49.56
		1.45	0.8454	49.56
		1.62	0.9000	49.56
		1.65	0.9092	
		1.85	0.9560	
100.0	**16**	0.05	0.0740	27.61
		0.15	0.0655	28.54
		0.25	0.0781	28.91
		0.45	0.0782	32.82
		0.65	0.1027	36.22
		0.85	0.2814	40.28
		1.05	0.4280	41.32
		1.15	0.6525	52.42
		1.20	0.7000	56.46
		1.25	0.7437	56.46
		1.35	0.7982	56.46
		1.45	0.8753	56.46
		1.55	0.8860	56.46
		1.57	0.9000	56.46
		1.65	0.9532	
100.0	**20**	0.05	0.1308	28.38
		0.15	0.1356	30.11
		0.25	0.1522	32.77
		0.45	0.1701	37.51
		0.65	0.2082	41.98
		0.85	0.3170	43.59
		1.05	0.5131	45.09
		1.15	0.6555	51.80
		1.20	0.7000	54.87
		1.25	0.7541	54.87
		1.35	0.8436	54.87
		1.45	0.8787	54.87
		1.50	0.9000	54.87
		1.55	0.9249	

Discharge (cfs)	Step Number	Depth y (ft)	Air Conc. c(y)	Velocity u(y) (ft/s)
100.0	**20**	0.05	0.0045	25.23
		0.25	0.0446	27.09
		0.45	0.0500	30.43
		0.65	0.0713	33.62
		0.85	0.1900	35.31
		1.05	0.4225	37.47
		1.25	0.6803	47.29
		1.27	0.7000	50.04
		1.45	0.8488	50.04
		1.51	0.9000	50.04
116.0	**4**	0.05	0.0015	19.01
		0.15	0.0009	20.23
		0.25	0.0015	21.40
		0.45	0.0014	23.74
		0.65	0.0010	24.98
		0.85	0.0106	25.68
		0.95	0.0329	26.43
		1.05	0.0449	26.48
		1.15	0.2554	28.39
		1.25	0.3072	26.54
		1.35	0.5839	31.24
		1.43	0.7000	31.01
		1.45	0.7316	31.01
		1.55	0.8247	31.01
		1.65	0.8843	31.01
		1.68	0.9000	31.01
116.0	**8**	0.05	0.0751	
		0.15	0.0057	22.53
		0.25	0.0047	23.17
		0.45	0.0062	26.44
		0.65	0.0169	28.62
		0.85	0.0973	31.08
		0.95	0.1526	30.57
		1.05	0.3017	31.51
		1.15	0.5426	33.63
		1.25	0.6908	36.91
		1.26	0.7000	37.51
		1.35	0.7962	37.51
		1.45	0.8079	37.51
		1.54	0.9000	37.51
		1.55	0.9122	
116.0	**16**	0.05	0.0842	18.56
		0.15	0.0519	29.35
		0.25	0.0574	29.68
		0.45	0.0782	35.34
		0.65	0.0638	37.15
		0.85	0.1293	38.94
		1.05	0.3335	42.41
		1.25	0.5803	47.75
		1.35	0.6898	52.41
		1.36	0.7000	52.94
		1.45	0.7739	52.94
		1.55	0.8770	52.94
		1.65	0.8974	52.94
		1.66	0.9000	52.94
		1.75	0.9190	

Stepped Spillway Tests, $h = 2.0$ ft

Discharge (cfs)	Step Number	Depth y (ft)	Air Conc. c(y)	Velocity u(y) (ft/s)
116.0	**20**	0.05	0.1584	27.80
		0.15	0.1392	31.48
		0.25	0.1249	33.20
		0.45	0 1315	38.38
		0.65	0.1318	41.94
		0.85	0.2062	43.32
		1.05	0.3864	45.07
		1.25	0.6568	54.24
		1.33	0.7000	50.91
		1.35	0.7092	50.91
		1.45	0.8146	50.91
		1.55	0.8812	50.91
		1.59	0.9000	50.91
		1.65	0.9296	
		1.75	0.9495	
121.0	**4**	0.05	0.0003	21.10
		0.25	0.0008	23.56
		0.45	0.0007	26.26
		0.65	0.0009	27.45
		0.85	0.0065	28.32
		1.05	0.0480	29.30
		1.25	0.3675	32.19
		1.45	0.6590	40.37
		1.51	0.7000	43.59
		1.65	0.8001	43.59
		1.85	0.8675	43.59
		2.00	0.9000	43.59
121.0	**12**	0.05	0.0325	10.40
		0.13	0.0027	25.94
		0.25	0.0075	26.55
		0.45	0.0157	28.96
		0.65	0.0151	32.27
		0.85	0.0335	34.03
		1.05	0.1651	34.56
		1.25	0.4226	36.04
		1.44	0.7000	49.06
		1.45	0.7104	49.06
		1.65	0.8460	49.06
		1.78	0.9000	49.06
		1.85	0.9284	
121.0	**12**	0.05	0.1149	7.28
		0.26	0.0387	29.38
		0.46	0.0398	33.22
		0.66	0.0465	34.77
		0.86	0.0980	37.01
		1.06	0.2603	38.03
		1.26	0.5806	43.90
		1.38	0.7000	51.62
		1.46	0.7838	51.62
		1.65	0.9000	51.62
		1.66	0.9043	
		1.86	0.9480	
		2.06	0.9787	

Smooth Spillway Tests

Discharge (cfs)	Station s (ft)	Depth y (ft)	Air Conc. c(y)	Velocity u(y) (ft/s)
20.0	10.5	0.08	0.0012	23.02
		0.13	0.0027	24.17
		0.18	0.0995	24.53
		0.23	0.1961	20.18
		0.28	0.7000	23.19
		0.28	0.7370	23.41
		0.30	0.9000	
20.0	30.9	0.08	0.0070	26.15
		0.13	0.0285	28.07
		0.18	0.2104	23.69
		0.23	0.4428	17.32
		0.27	0.7000	29.18
		0.28	0.8303	35.19
		0.29	0.9000	
20.0	48.7	0.08	0.0184	27.57
		0.13	0.1070	31.32
		0.18	0.2984	35.92
		0.23	0.5025	39.18
		0.27	0.7000	44.74
		0.28	0.7378	45.80
		0.33	0.7589	28.66
		0.33	0.8125	16.97
		0.36	0.9000	
20.0	66.6	0.08	0.0643	27.86
		0.13	0.0923	31.10
		0.18	0.2109	33.74
		0.23	0.5789	39.97
		0.26	0.7000	39.76
		0.28	0.8046	39.58
		0.32	0.9000	31.59
		0.33	0.9494	27.46
20.0	84.5	0.08	0.0786	28.66
		0.13	0.0833	30.65
		0.18	0.1661	34.21
		0.23	0.3086	36.18
		0.28	0.4487	34.25
		0.33	0.7000	31.64
		0.33	0.7100	31.53
		0.38	0.8927	21.99
		0.38	0.9000	
40.0	10.5	0.08	0.0007	23.99
		0.13	0.0007	25.84
		0.18	0.0013	26.19
		0.23	0.0017	26.87
		0.28	0.0016	26.80
		0.33	0.0020	26.90
		0.38	0.0026	26.91
		0.43	0.0605	25.41
		0.48	0.3157	21.06
		0.53	0.7000	27.13
		0.53	0.7623	28.11
		0.55	0.9000	

Discharge (cfs)	Station s (ft)	Depth y (ft)	Air Conc. c(y)	Velocity u(y) (ft/s)
40.0	30.9	0.08	0.0013	29.32
		0.13	0.0013	32.35
		0.18	0.0018	34.43
		0.23	0.0026	35.50
		0.28	0.0503	35.33
		0.33	0.6058	42.24
		0.36	0.7000	40.79
		0.38	0.8126	39.07
		0.41	0.9000	35.97
		0.43	0.9789	33.18
40.0	48.7	0.08	0.0012	30.56
		0.13	0.0025	34.23
		0.18	0.0047	36.37
		0.23	0.0109	37.81
		0.28	0.0577	38.61
		0.33	0.1688	38.46
		0.38	0.5069	37.25
		0.42	0.7000	45.91
		0.43	0.7919	50.03
		0.45	0.9000	
40.0	66.6	0.08	0.0061	33.69
		0.13	0.0270	37.09
		0.18	0.0439	38.29
		0.23	0.0872	39.75
		0.28	0.2412	40.76
		0.33	0.5586	42.79
		0.36	0.7000	49.39
		0.38	0.7921	53.69
		0.43	0.9043	35.97
40.0	84.5	0.08	0.0127	32.33
		0.13	0.0265	36.99
		0.18	0.0505	38.72
		0.23	0.0672	40.10
		0.28	0.1200	41.92
		0.33	0.1927	42.06
		0.38	0.3654	42.07
		0.43	0.6107	48.72
		0.46	0.7000	46.35
		0.48	0.7941	43.85
		0.53	0.9019	48.03
60.0	10.5	0.08	0.0013	25.57
		0.13	0.0012	26.13
		0.18	0.0012	26.56
		0.28	0.0012	27.53
		0.38	0.0014	27.94
		0.43	0.0014	27.63
		0.48	0.0015	27.82
		0.53	0.0030	27.64
		0.58	0.0721	25.19
		0.63	0.1703	23.64
		0.68	0.6021	25.01
		0.72	0.9000	

Smooth Spillway Tests

Discharge (cfs)	Station s (ft)	Depth y (ft)	Air Conc. c(y)	Velocity u(y) (ft/s)
60.0	**30.9**	0.08	0.0012	29.00
		0.13	0.0012	31.88
		0.18	0.0012	33.81
		0.28	0.0012	36.38
		0.38	0.0012	37.61
		0.43	0.0040	37.87
		0.48	0.2732	34.40
		0.53	0.7000	37.20
		0.53	0.7201	37.33
		0.55	0.9000	
60.0	**48.7**	0.08	0.0011	31.41
		0.13	0.0012	34.81
		0.18	0.0014	37.35
		0.28	0.0053	42.12
		0.38	0.0662	42.94
		0.43	0.3678	42.43
		0.48	0.5270	40.72
		0.51	0.7000	42.59
		0.53	0.8139	43.82
		0.55	0.9000	
60.0	**66.6**	0.08	0.0009	34.77
		0.13	0.0027	39.58
		0.18	0.0096	41.58
		0.28	0.0376	43.16
		0.38	0.2049	41.54
		0.43	0.4448	40.11
		0.48	0.7000	43.78
		0.48	0.7263	44.16
		0.53	0.8694	39.74
		0.54	0.9000	
60.0	**84.5**	0.08	0.0017	35.49
		0.13	0.0042	38.49
		0.18	0.0098	40.25
		0.23	0.0130	42.14
		0.28	0.0321	43.49
		0.33	0.0553	44.63
		0.38	0.1015	45.45
		0.43	0.2245	46.26
		0.48	0.3638	46.89
		0.53	0.5467	47.26
		0.56	0.7000	52.31
		0.58	0.7870	55.17
		0.61	0.9000	
80.0	**10.5**	0.08	0.0010	23.89
		0.13	0.0010	27.15
		0.18	0.0010	26.52
		0.28	0.0011	28.02
		0.38	0.0019	28.30
		0.48	0.0011	28.49
		0.58	0.0016	28.82
		0.63	0.0108	28.69
		0.68	0.0086	28.55
		0.73	0.0626	26.90
		0.78	0.1122	22.22
		0.83	0.3596	13.74
		0.94	0.9000	

Discharge (cfs)	Station s (ft)	Depth y (ft)	Air Conc. c(y)	Velocity u(y) (ft/s)
80.0	**30.9**	0.08	0.0009	28.46
		0.13	0.0009	32.52
		0.18	0.0009	33.67
		0.28	0.0009	36.84
		0.38	0.0009	37.53
		0.48	0.0025	38.44
		0.53	0.0212	37.70
		0.58	0.2910	41.41
		0.63	0.4960	42.33
		0.73	0.9777	41.06
80.0	**48.7**	0.08	0.0012	31.20
		0.13	0.0011	35.11
		0.18	0.0010	38.04
		0.28	0.0009	42.52
		0.38	0.0016	43.43
		0.48	0.0067	42.95
		0.53	0.1786	39.42
		0.58	0.4193	35.16
		0.63	0.7000	33.43
		0.63	0.7081	33.38
		0.67	0.9000	
80.0	**66.6**	0.08	0.0013	34.25
		0.13	0.0014	39.81
		0.18	0.0018	42.58
		0.28	0.0038	46.33
		0.38	0.0308	46.43
		0.48	0.1116	42.59
		0.53	0.5779	41.11
		0.58	0.7000	37.23
		0.58	0.7023	37.16
		0.63	0.8563	25.21
		0.65	0.9000	
80.0	**84.5**	0.08	0.0008	35.09
		0.13	0.0010	39.48
		0.18	0.0019	43.49
		0.23	0.0031	45.00
		0.28	0.0075	45.95
		0.33	0.0173	48.51
		0.38	0.0409	48.89
		0.43	0.0748	48.89
		0.48	0.1440	48.59
		0.53	0.2230	47.69
		0.58	0.4298	46.02
		0.63	0.6322	48.29
		0.66	0.7000	46.90
		0.68	0.7759	45.33
		0.73	0.9000	

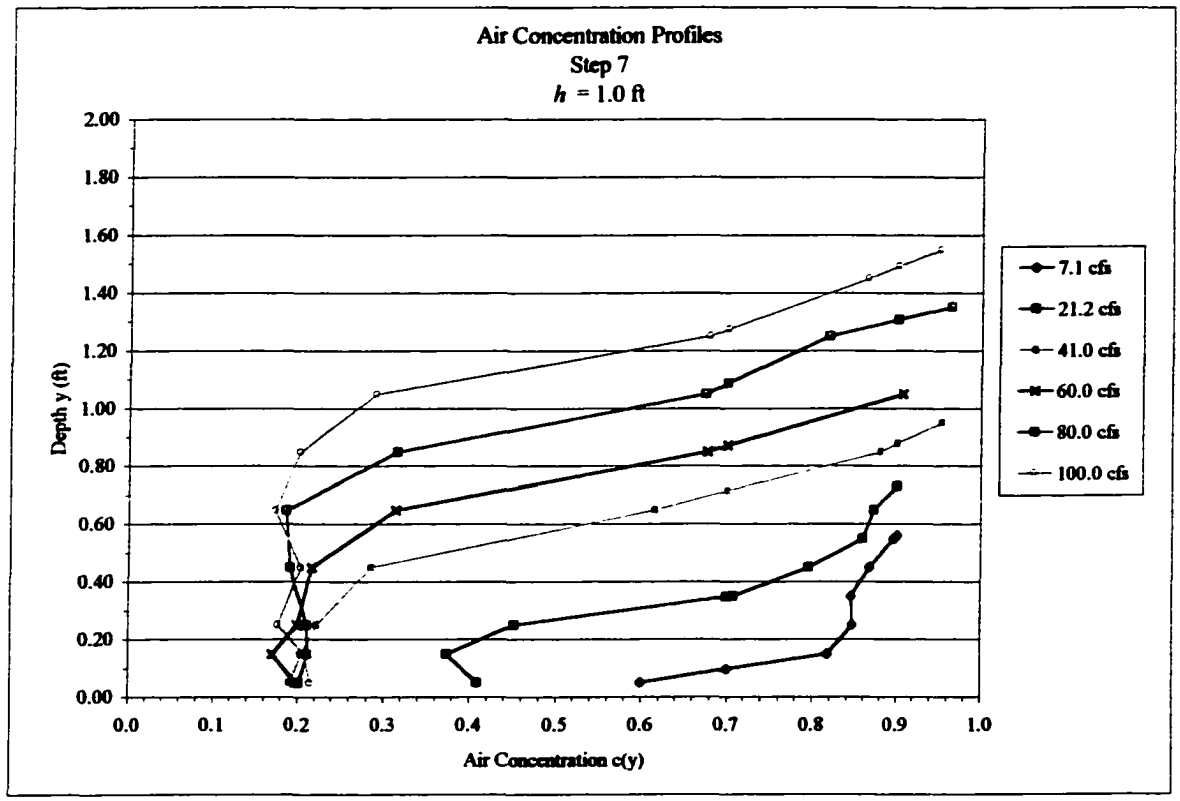

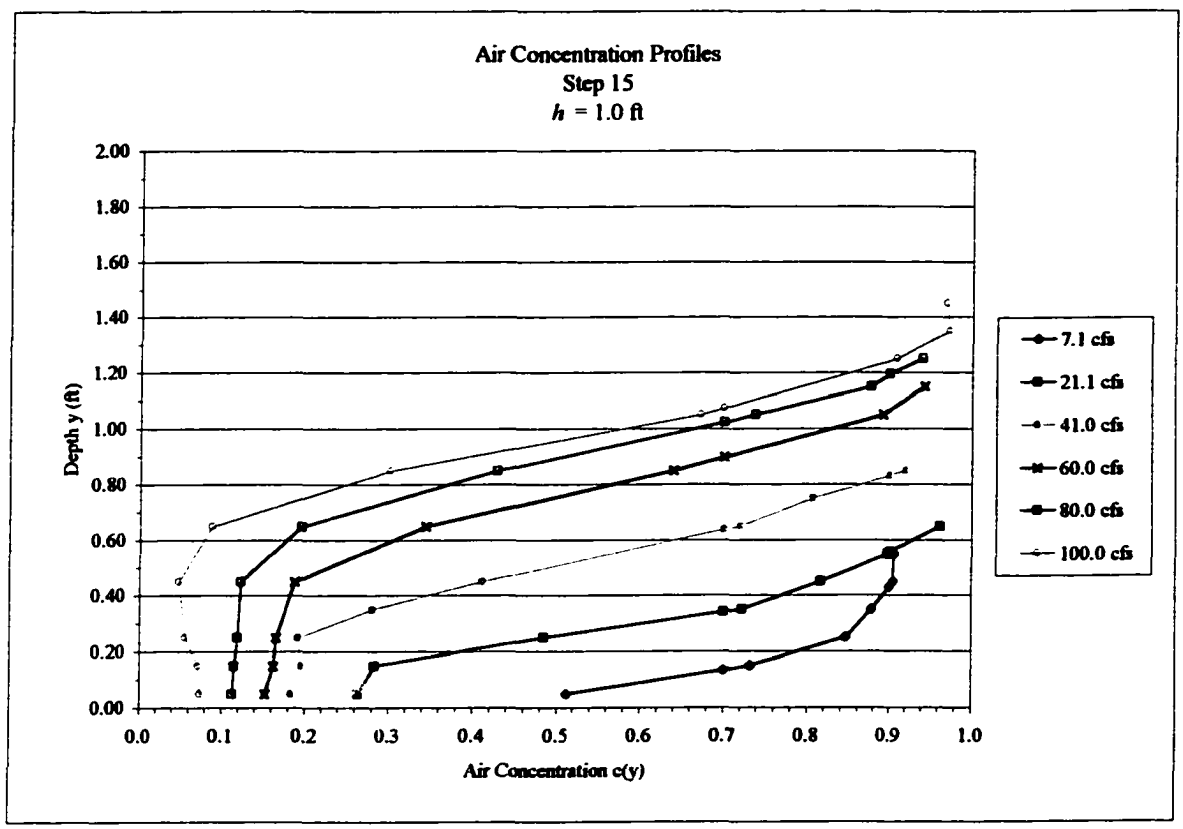

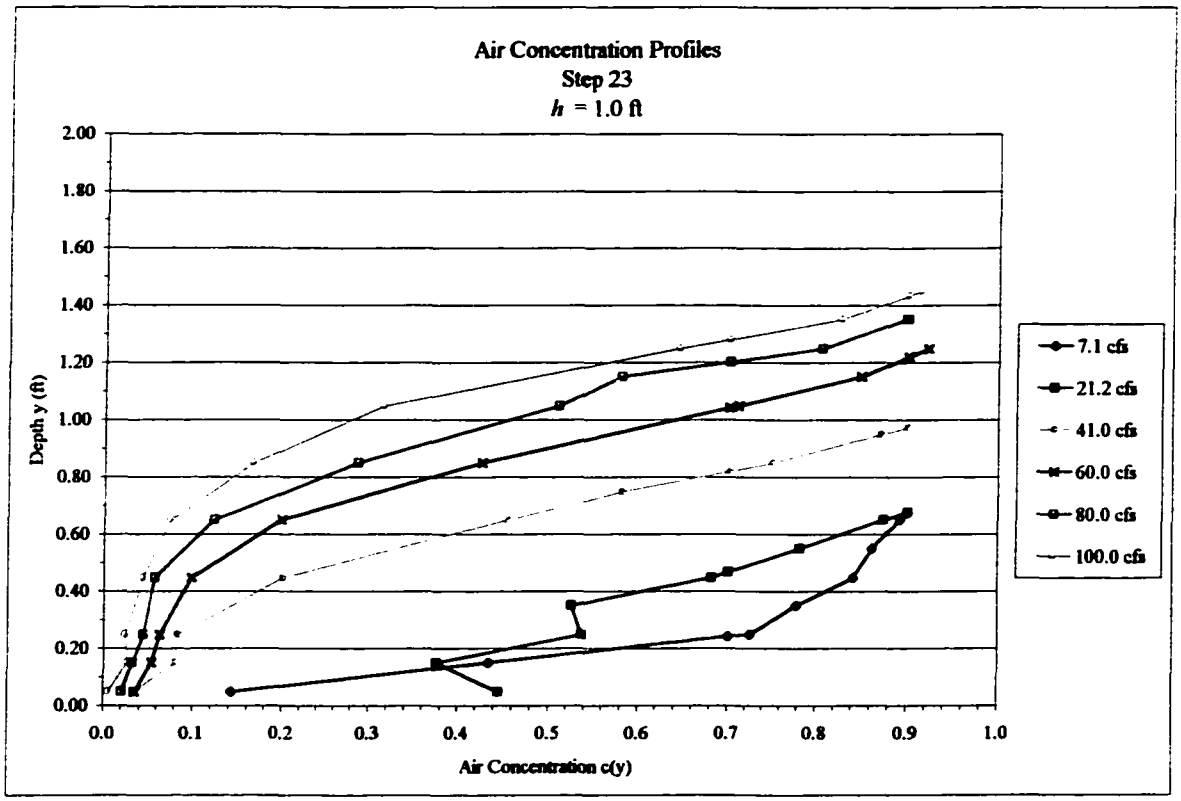

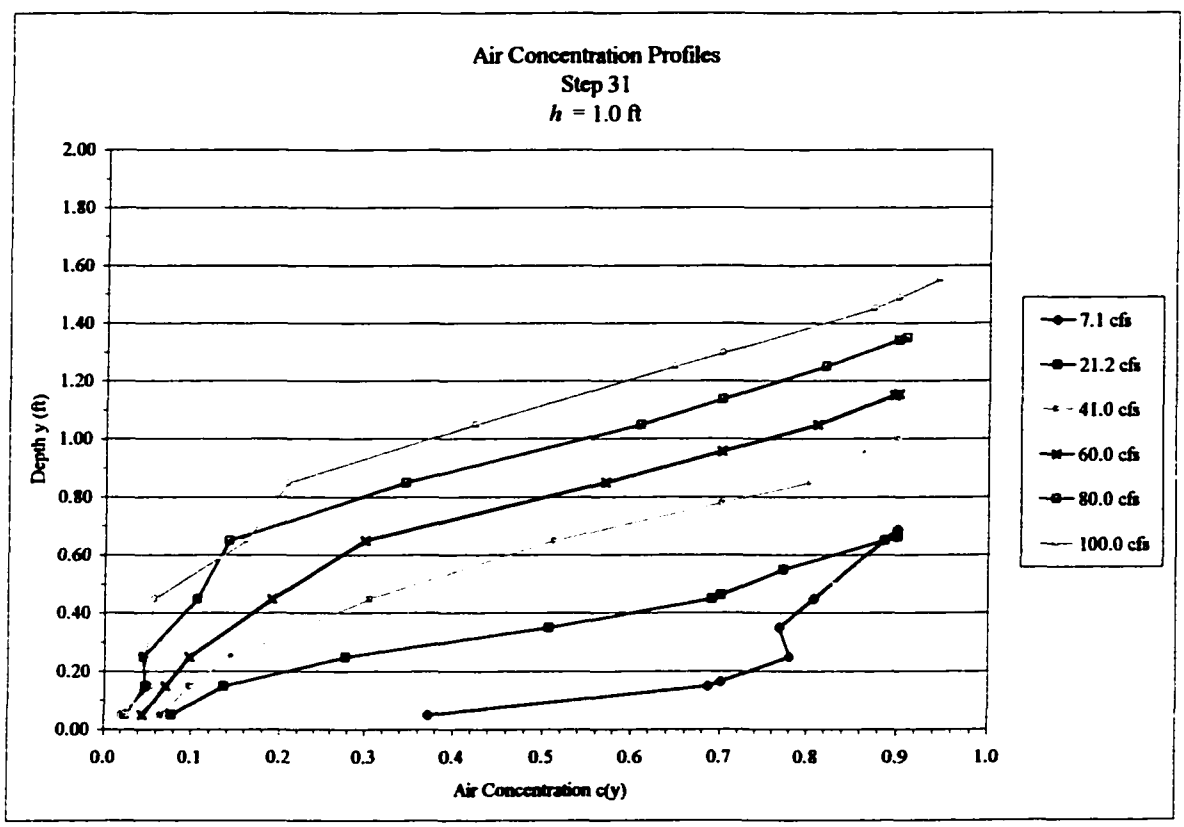

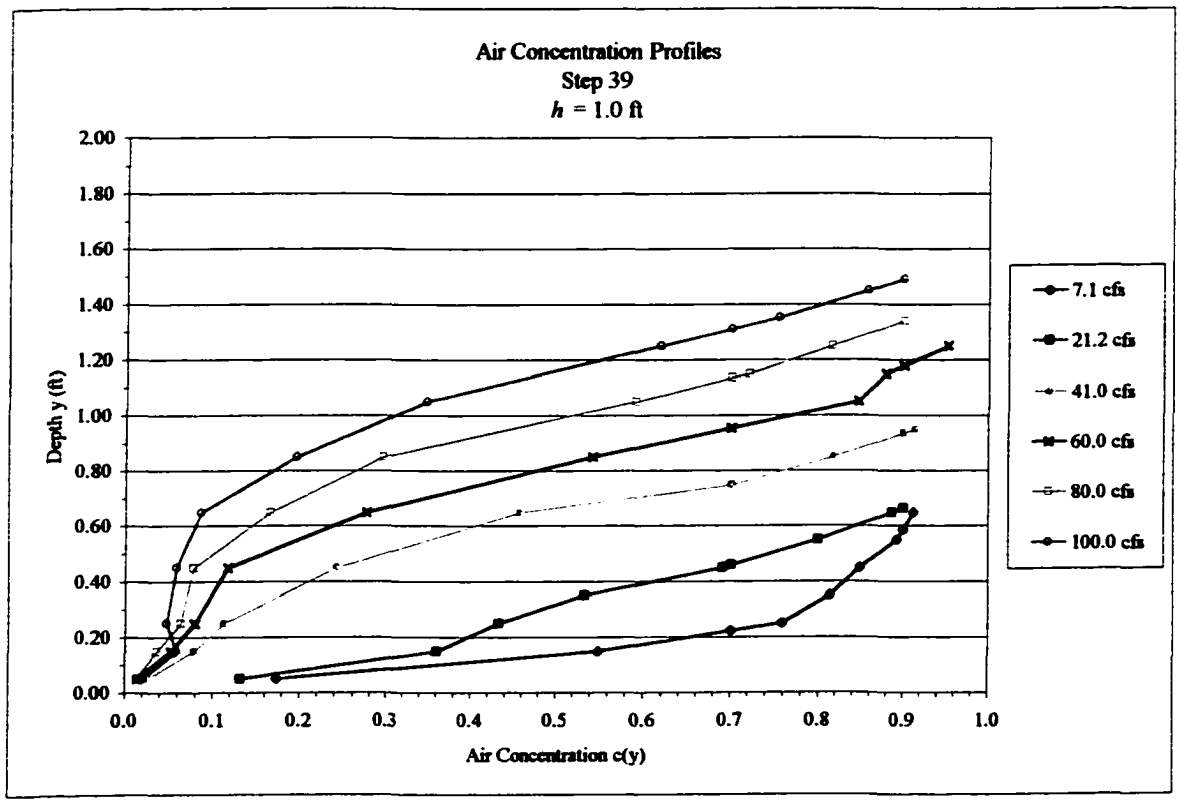

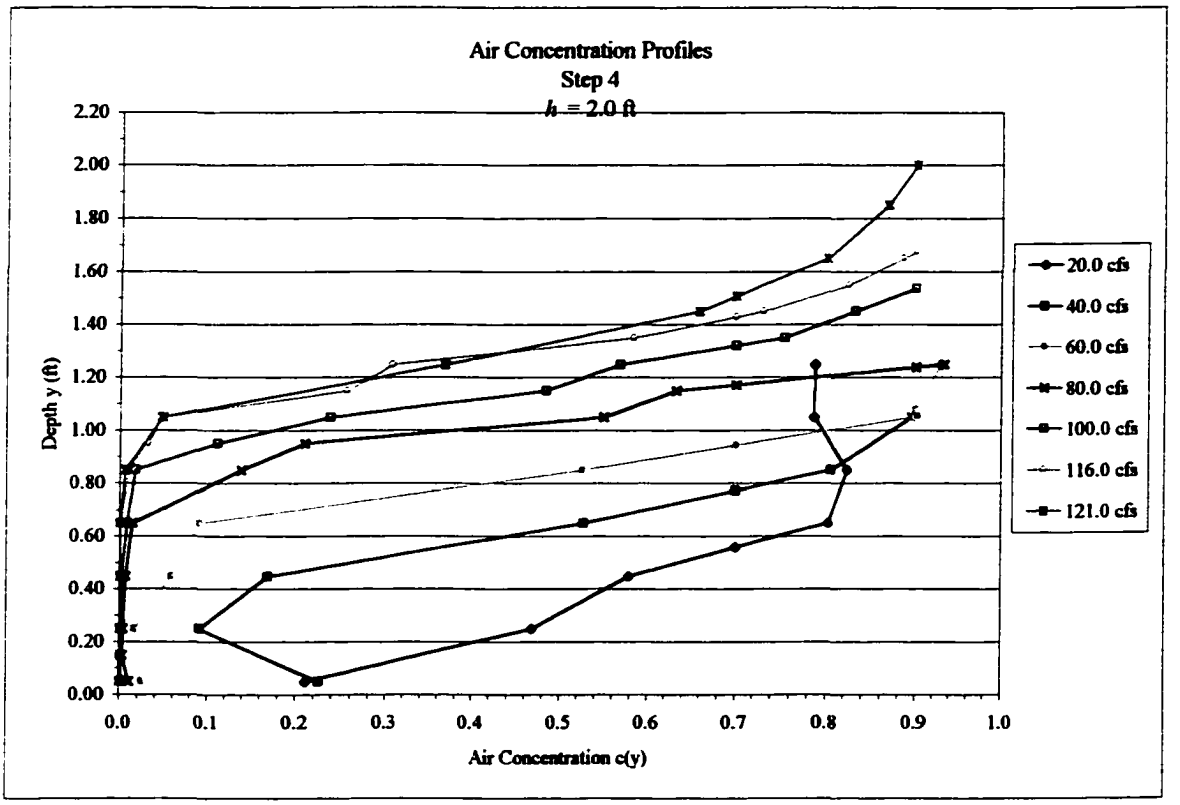

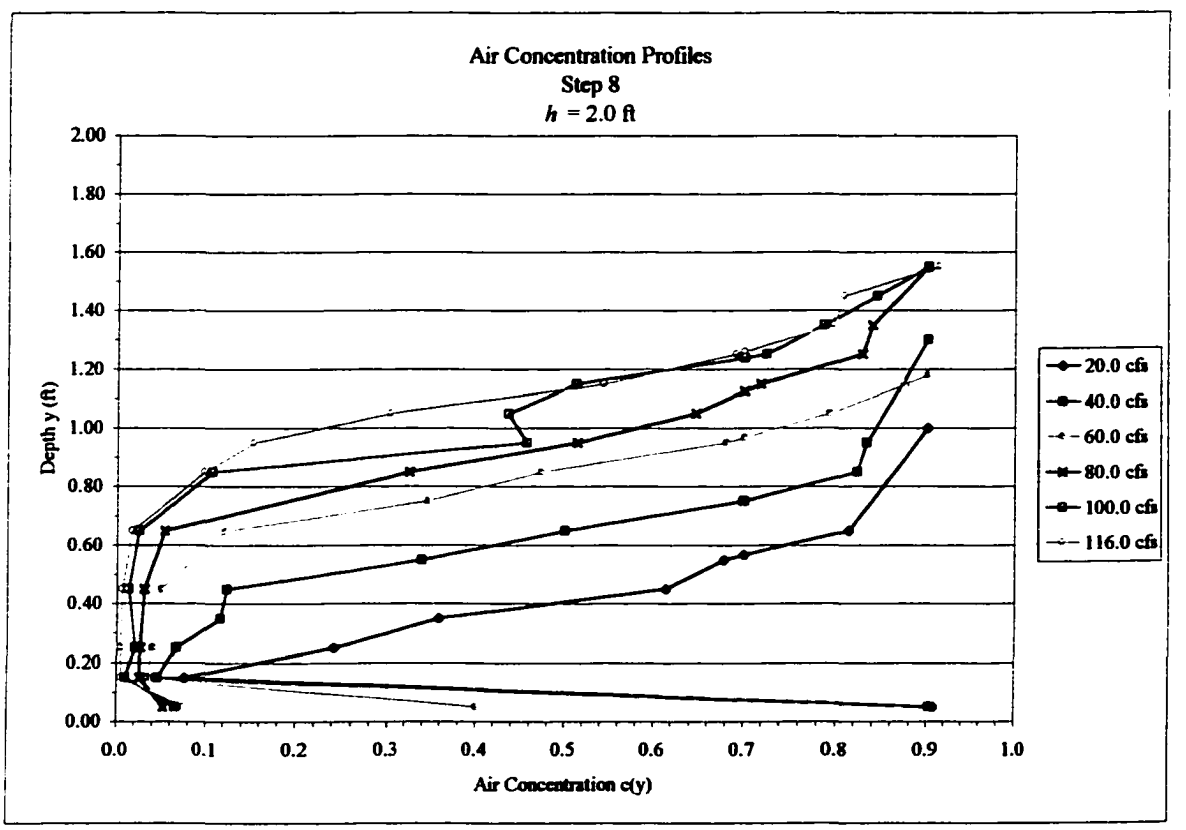

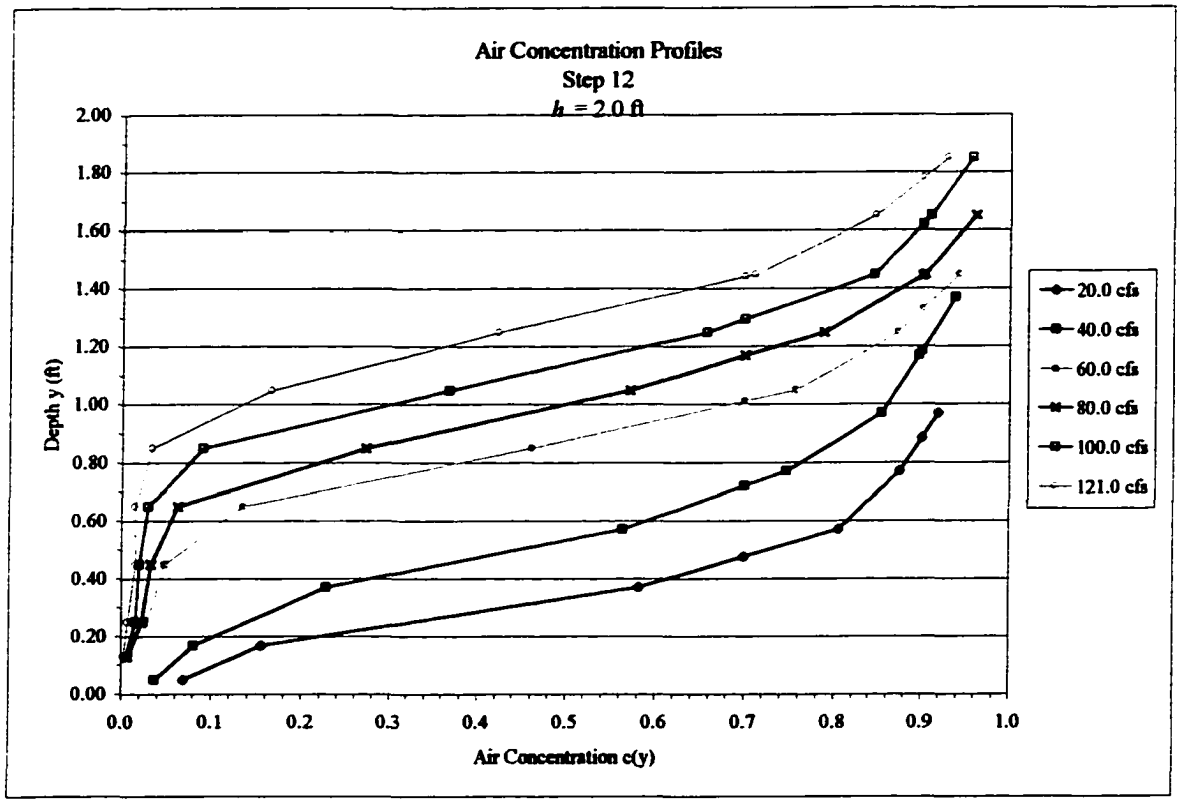

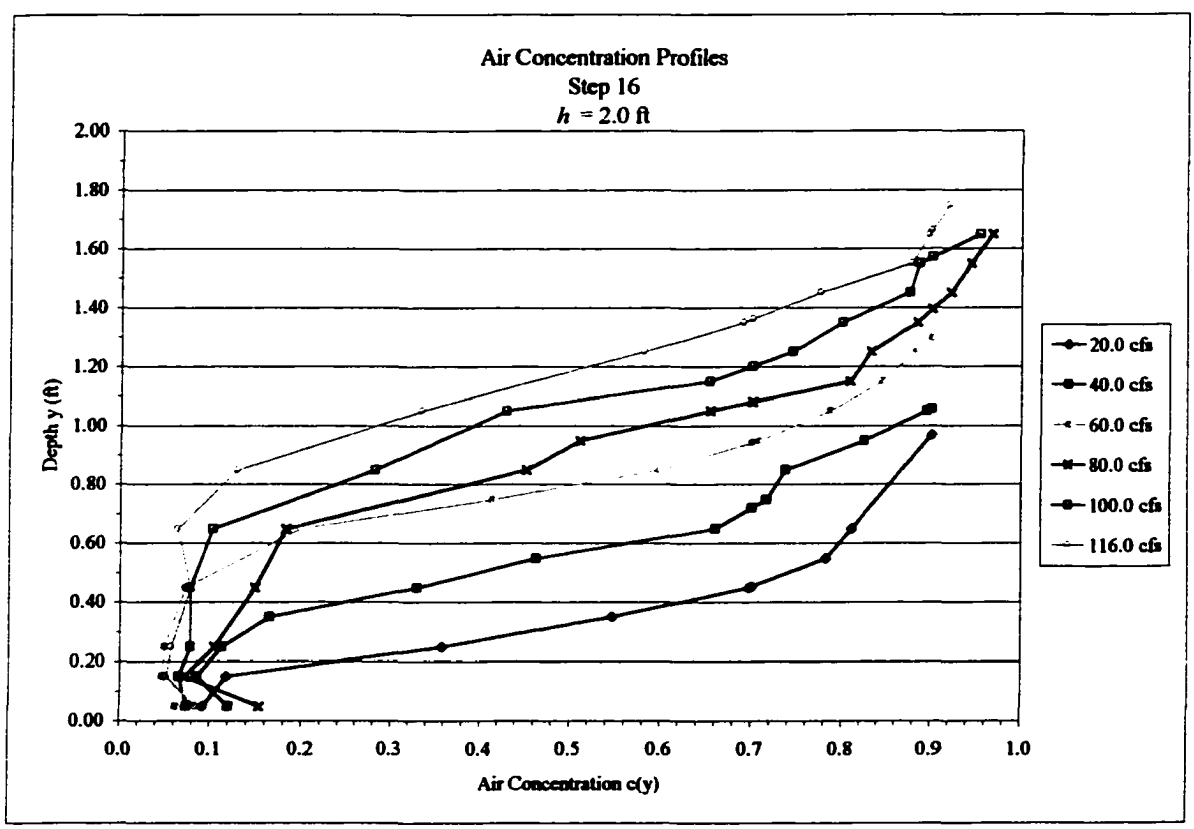

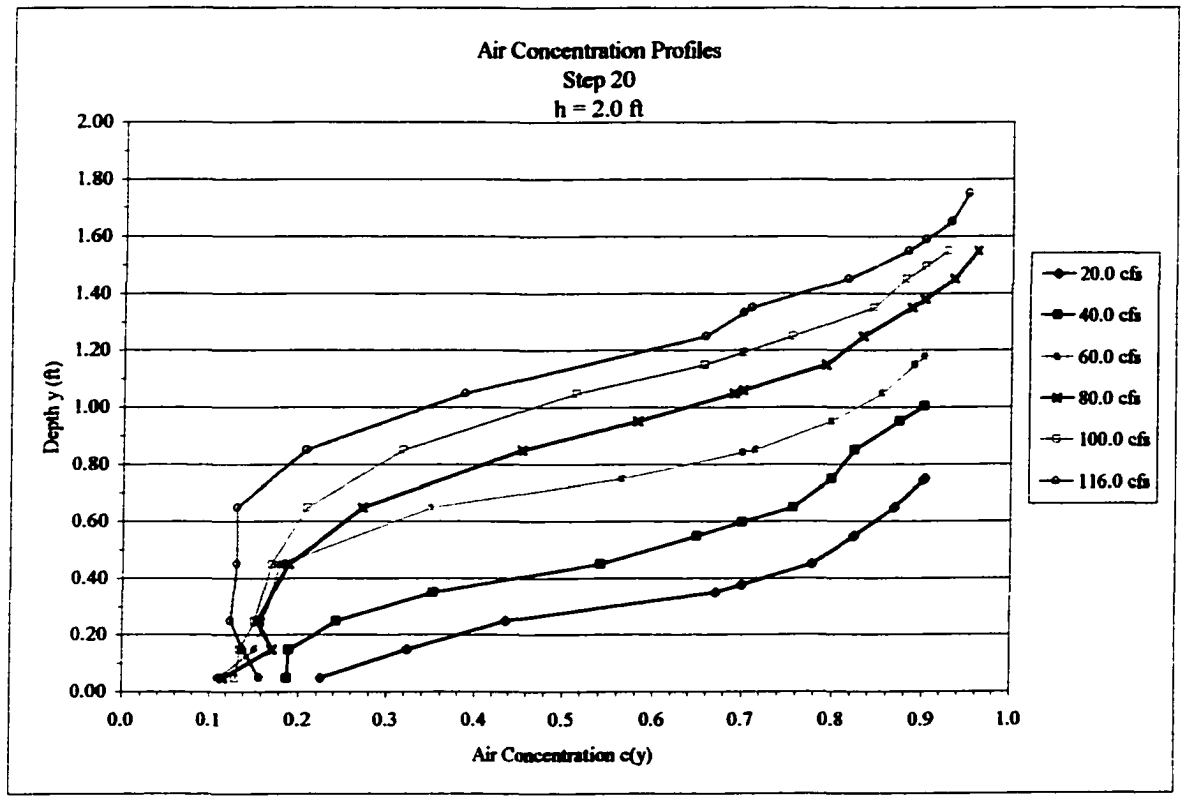

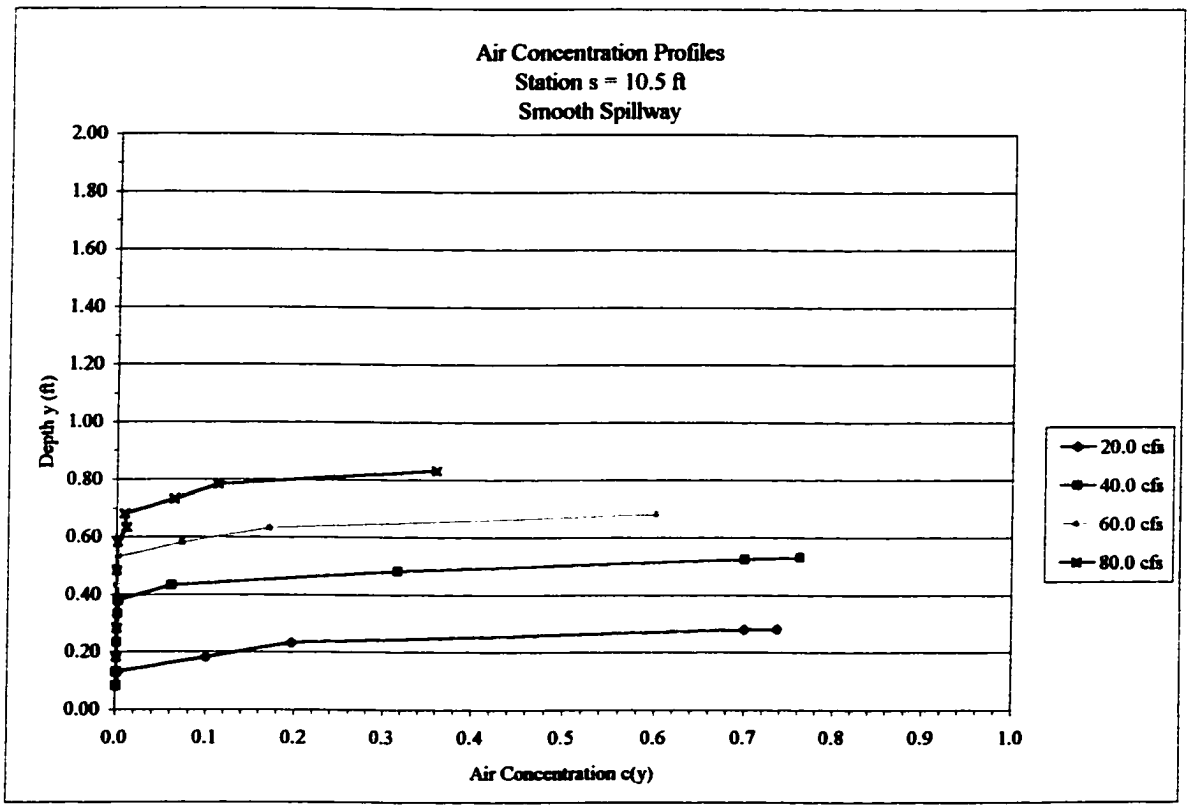

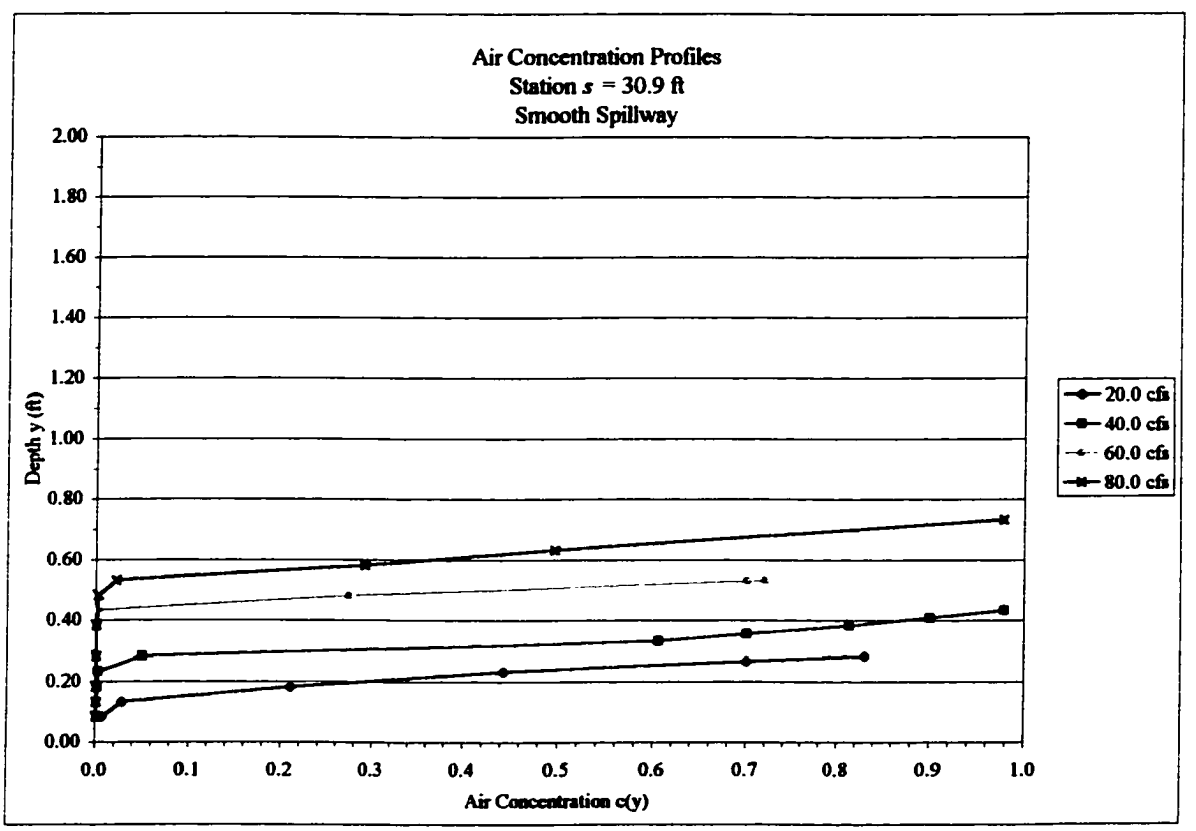

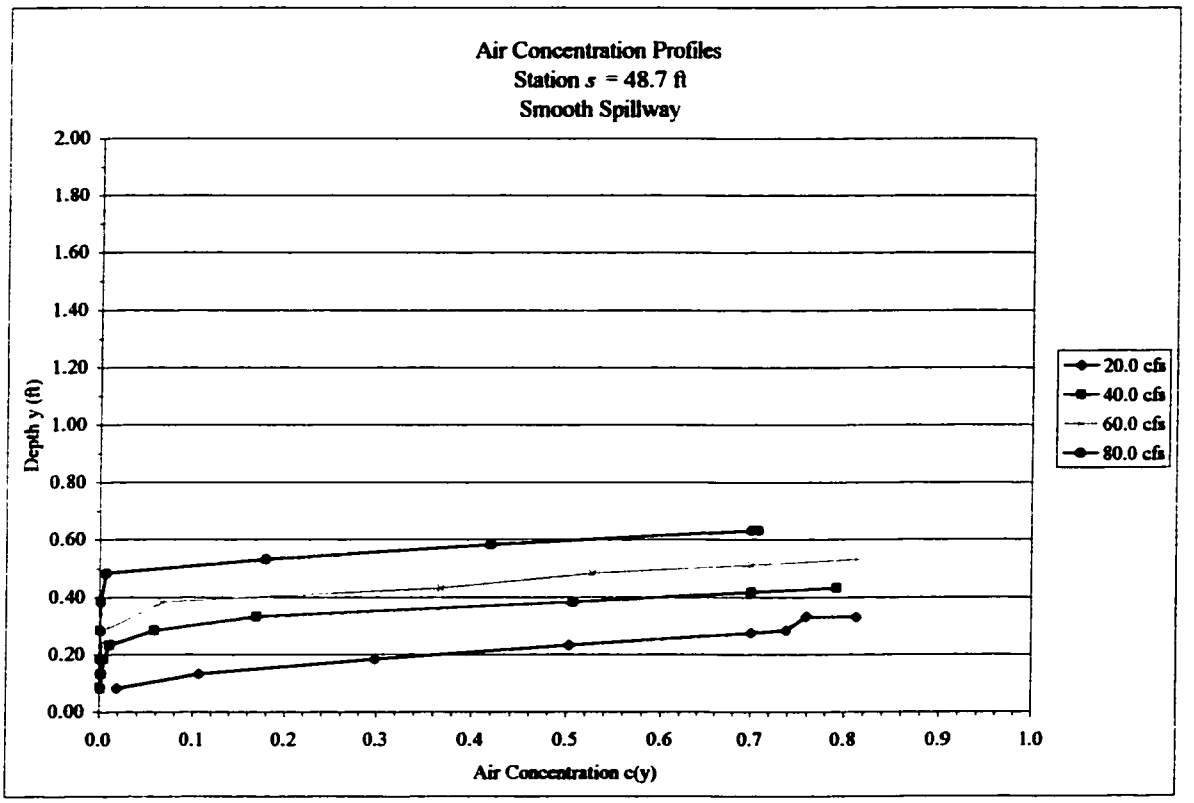

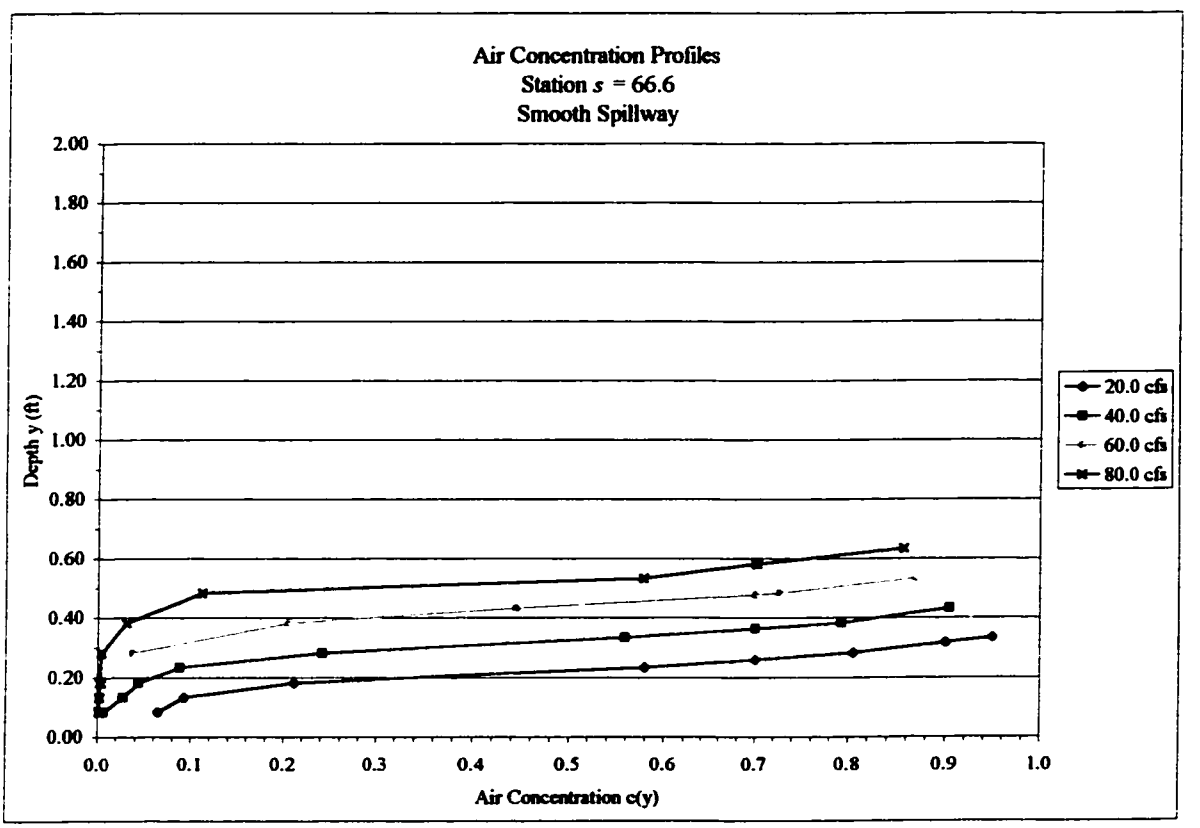

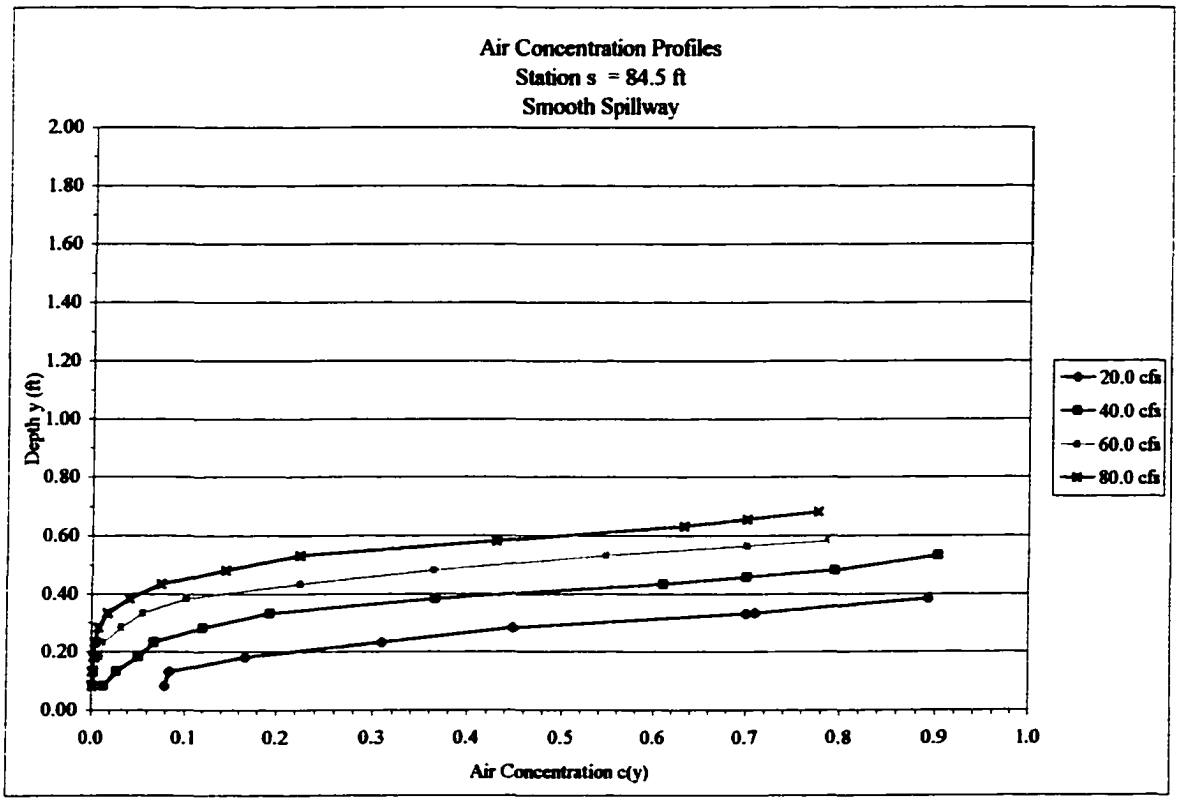

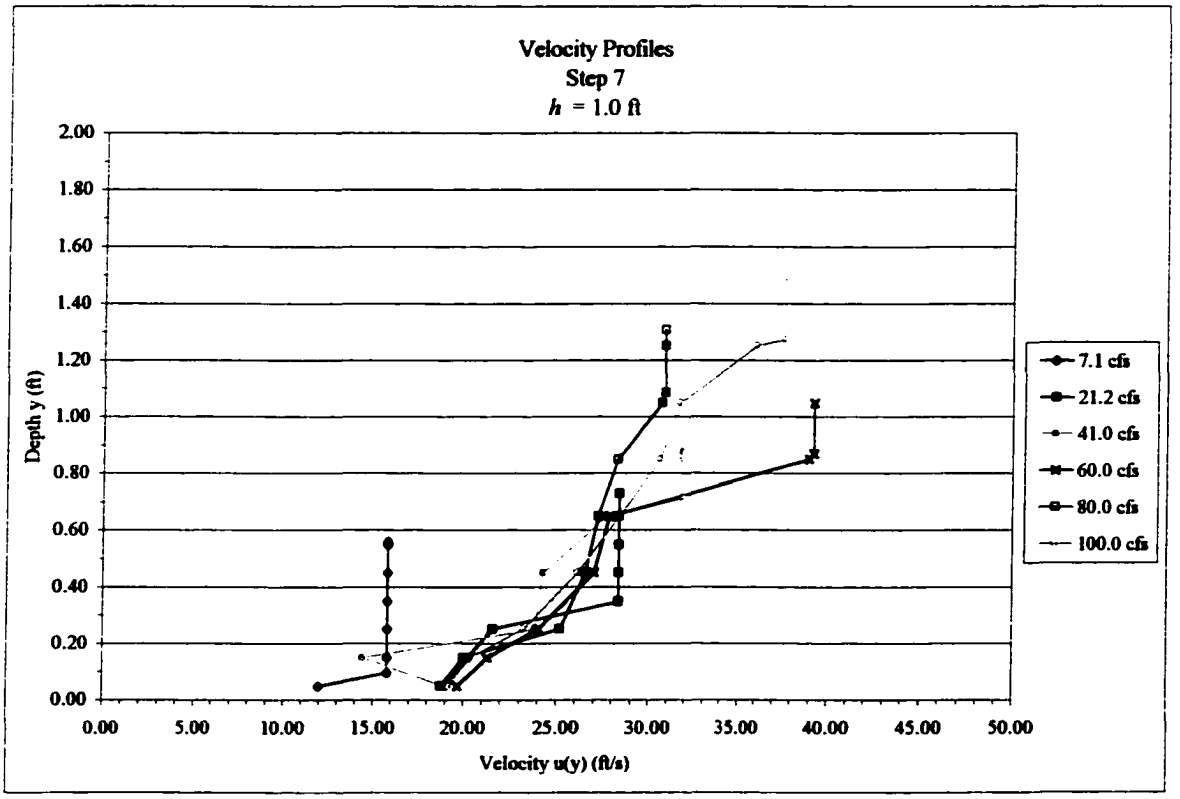

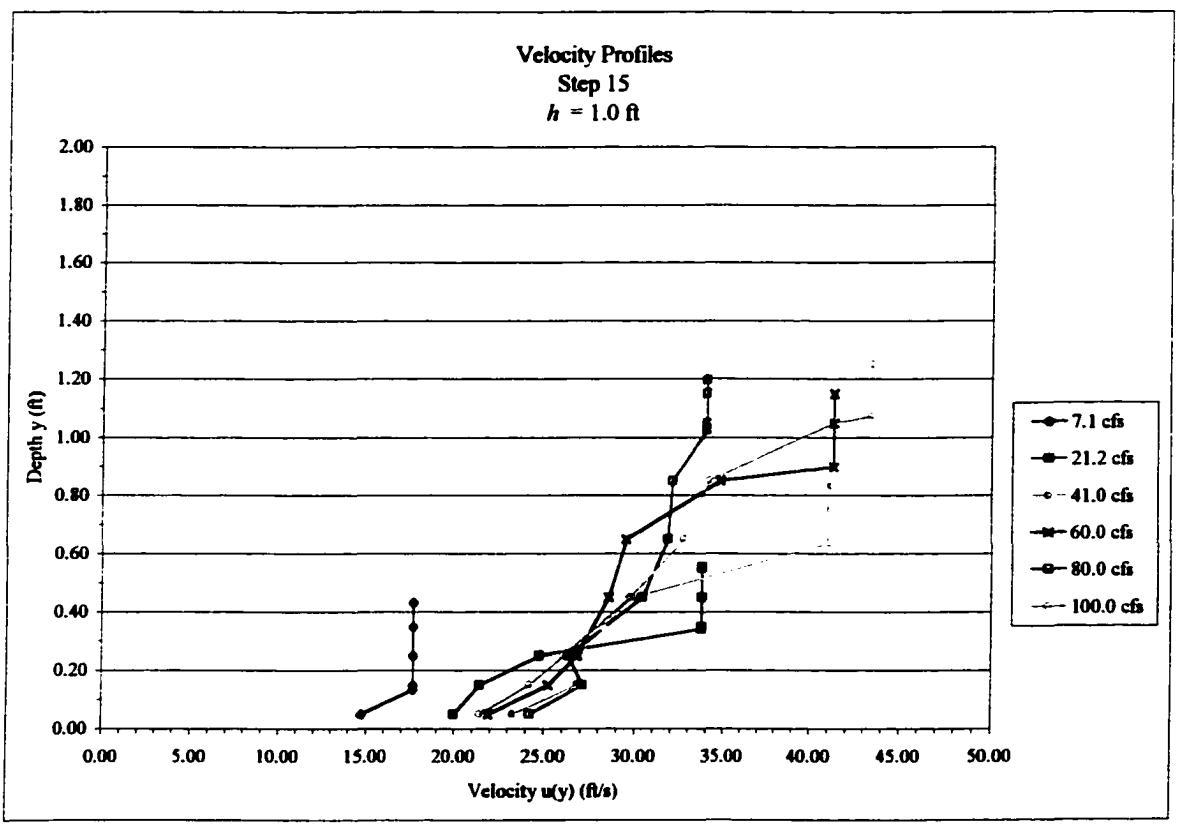

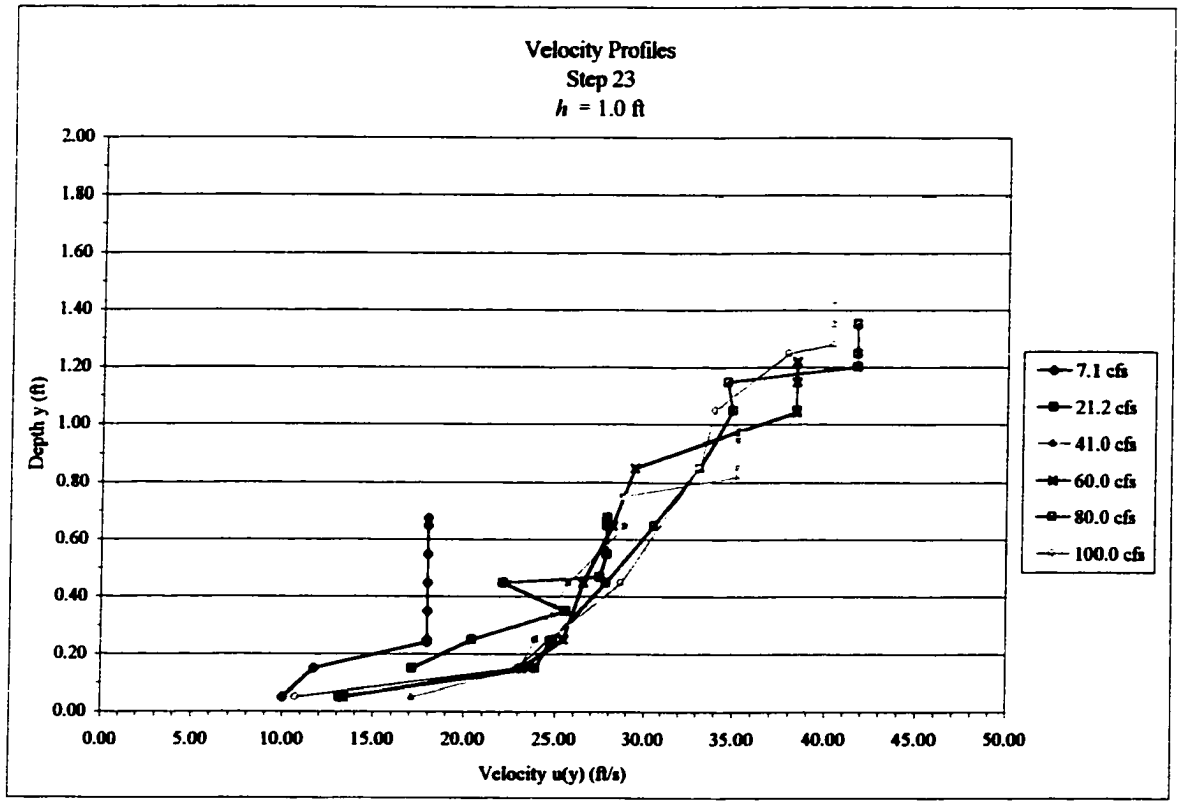

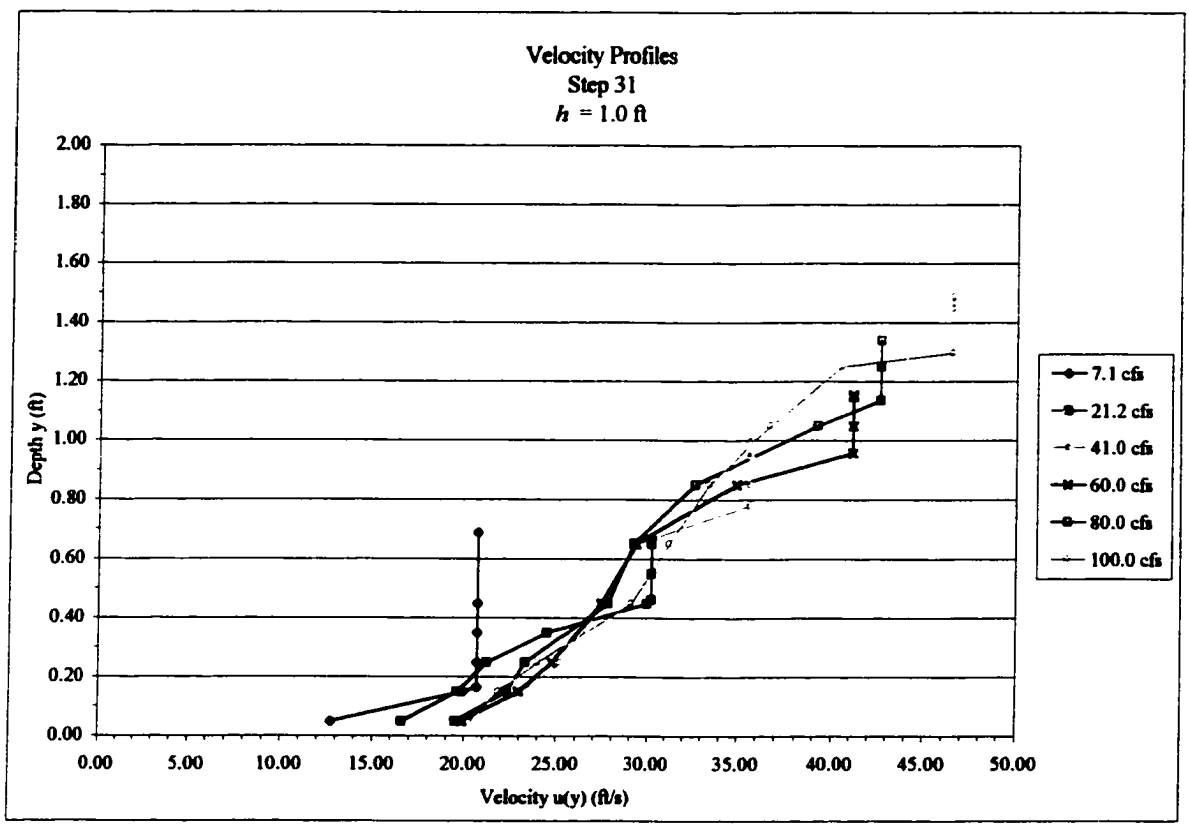

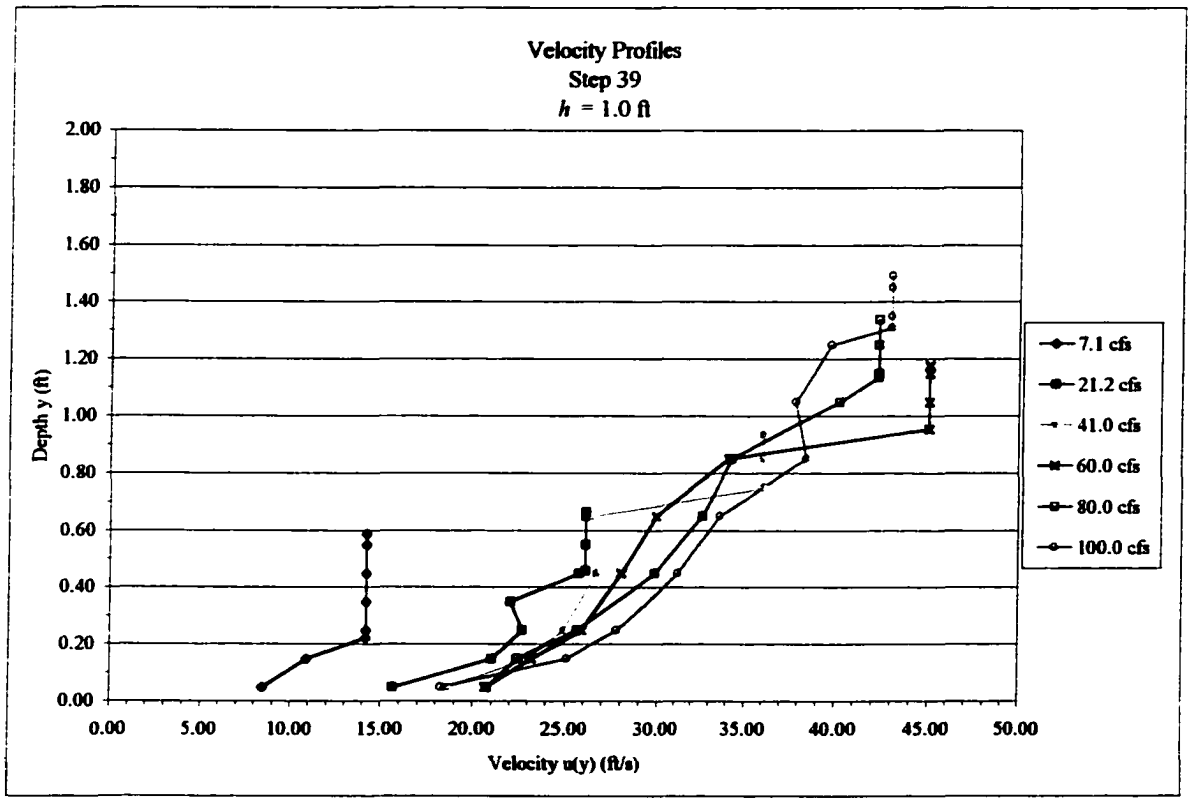

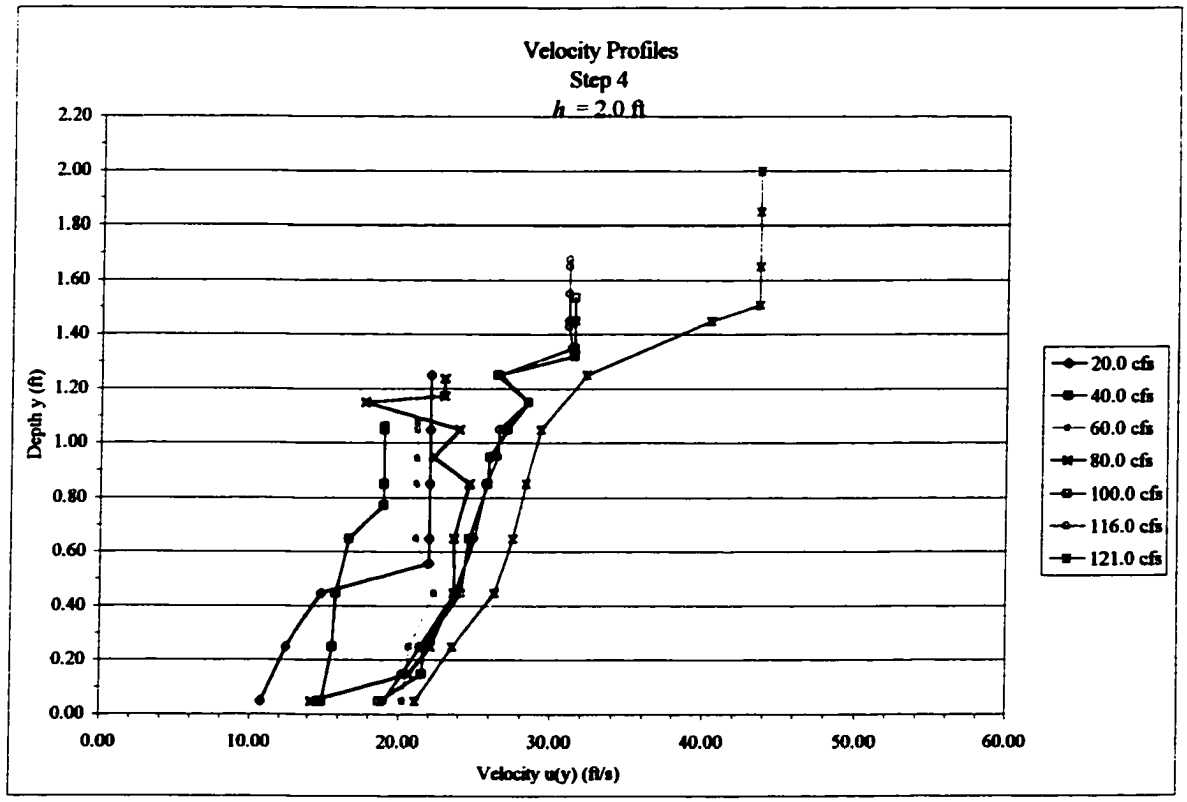

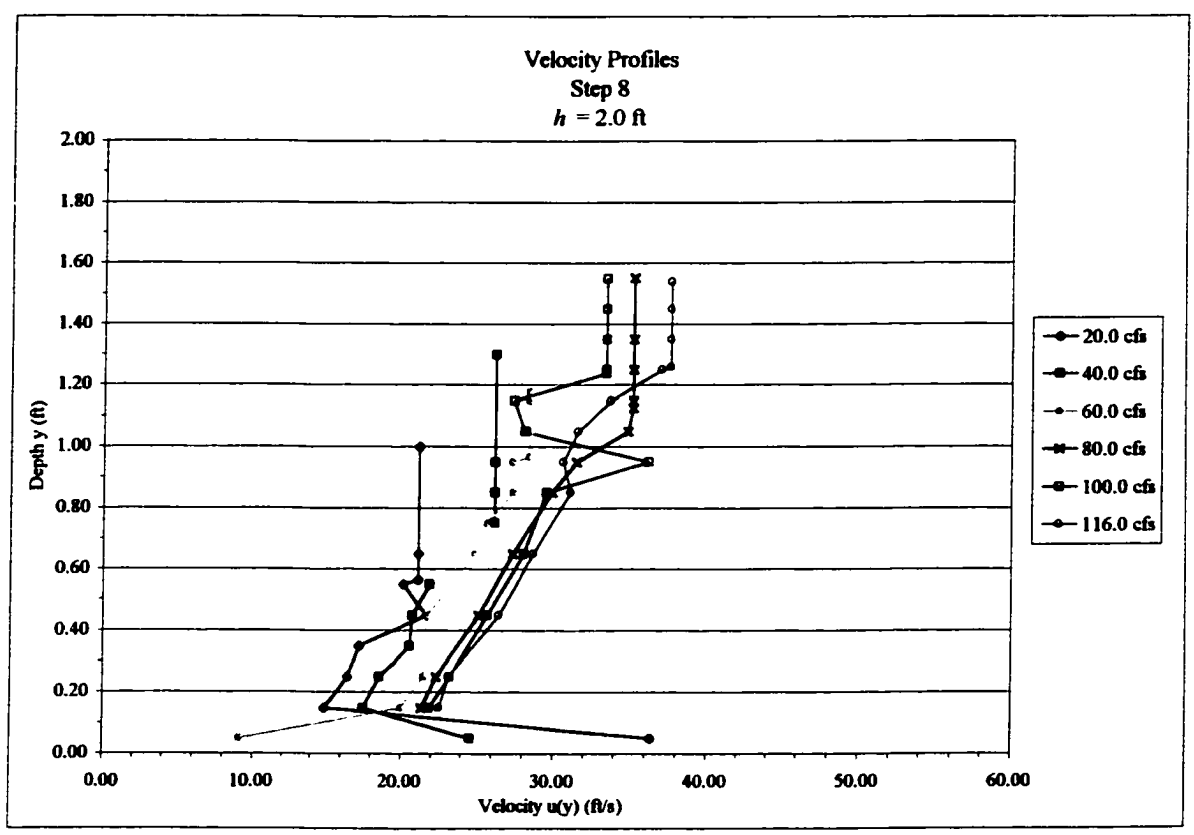

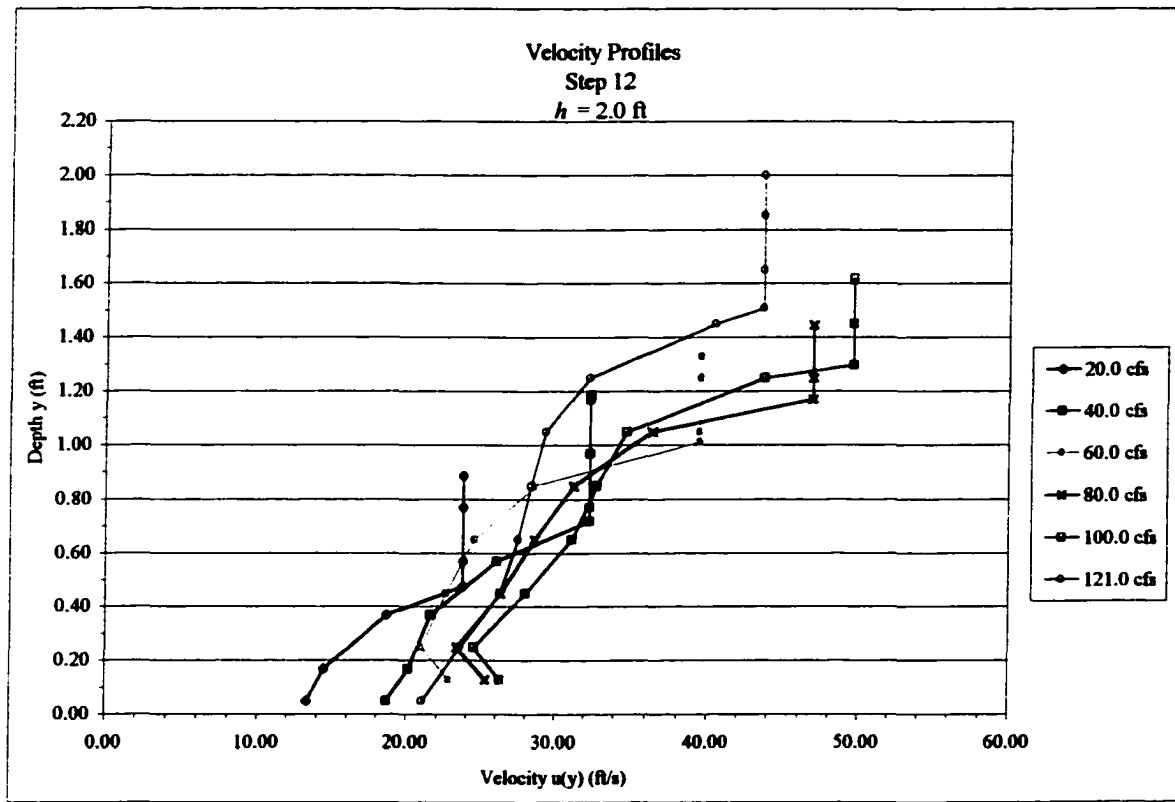

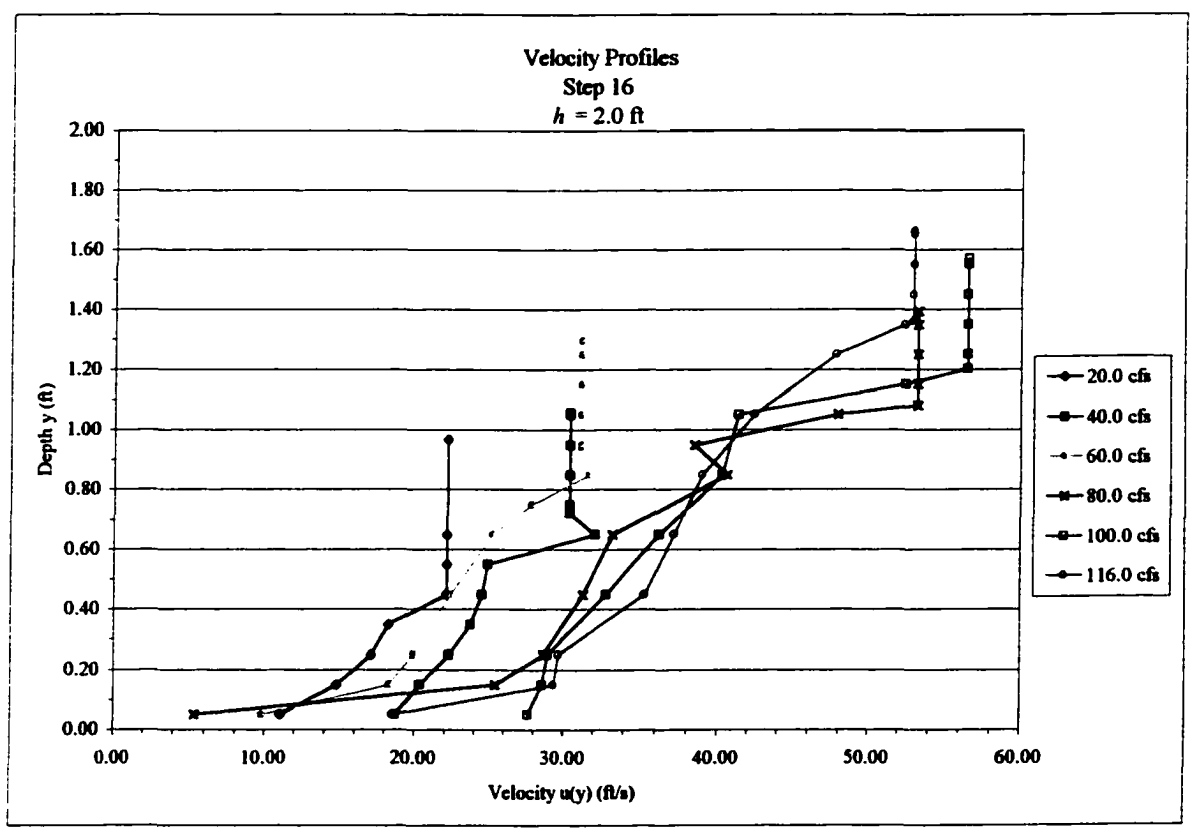

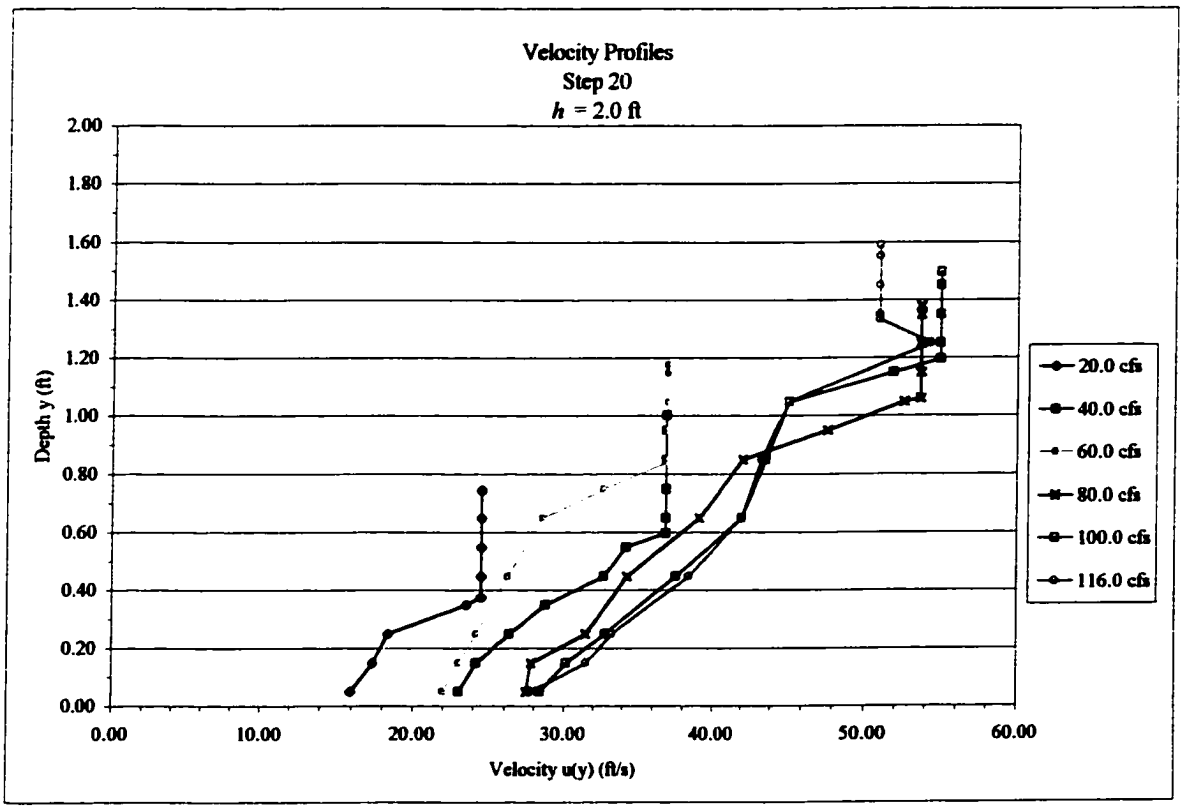

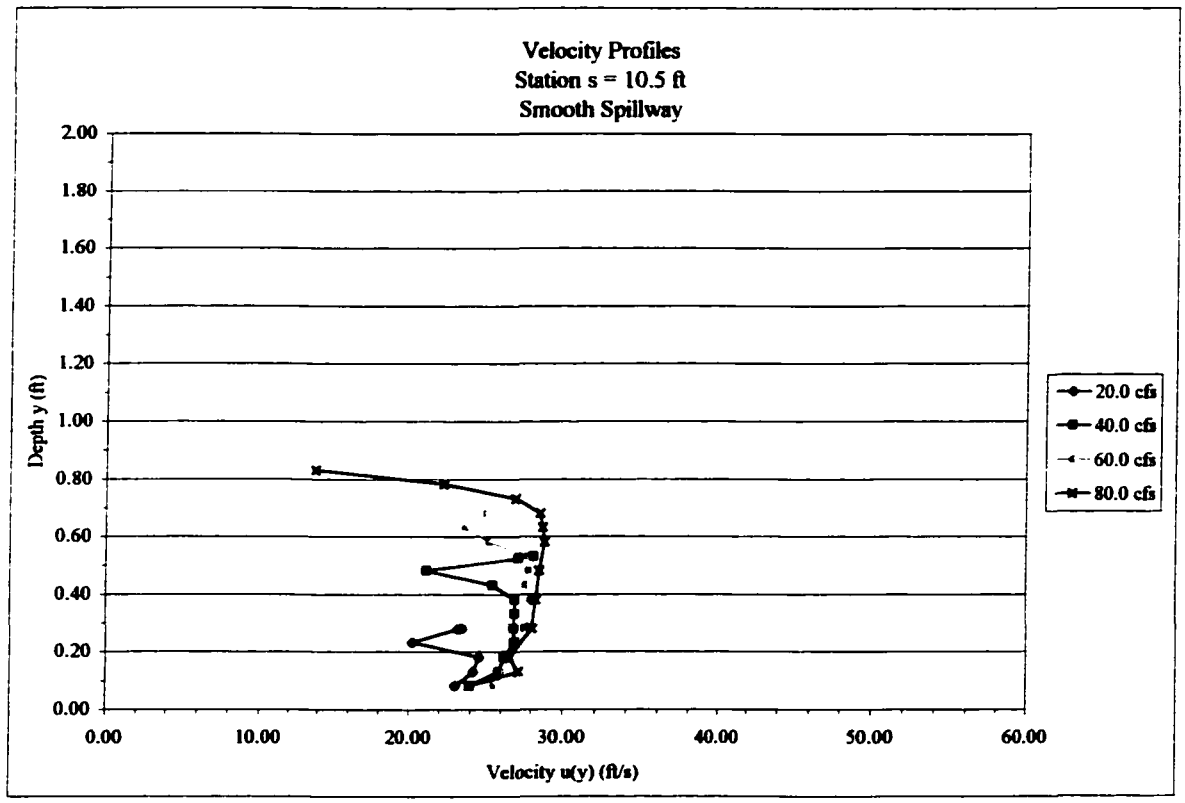

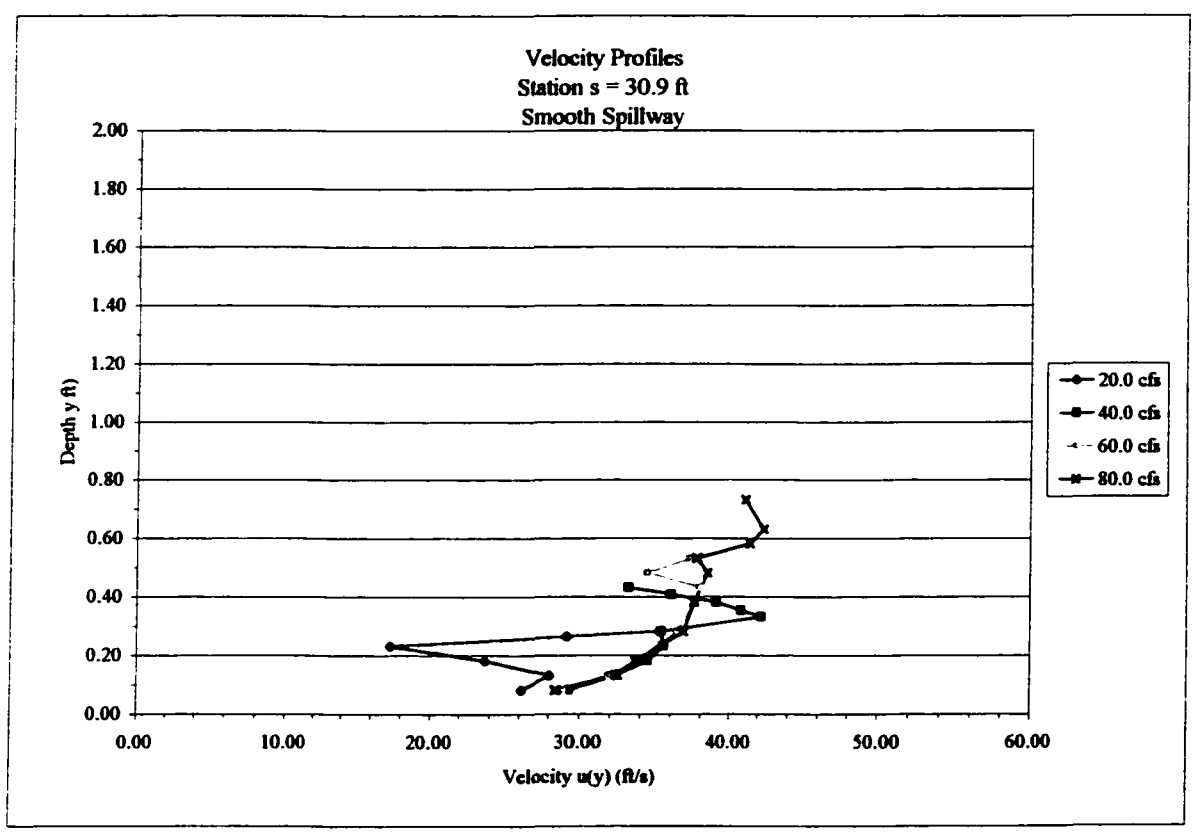

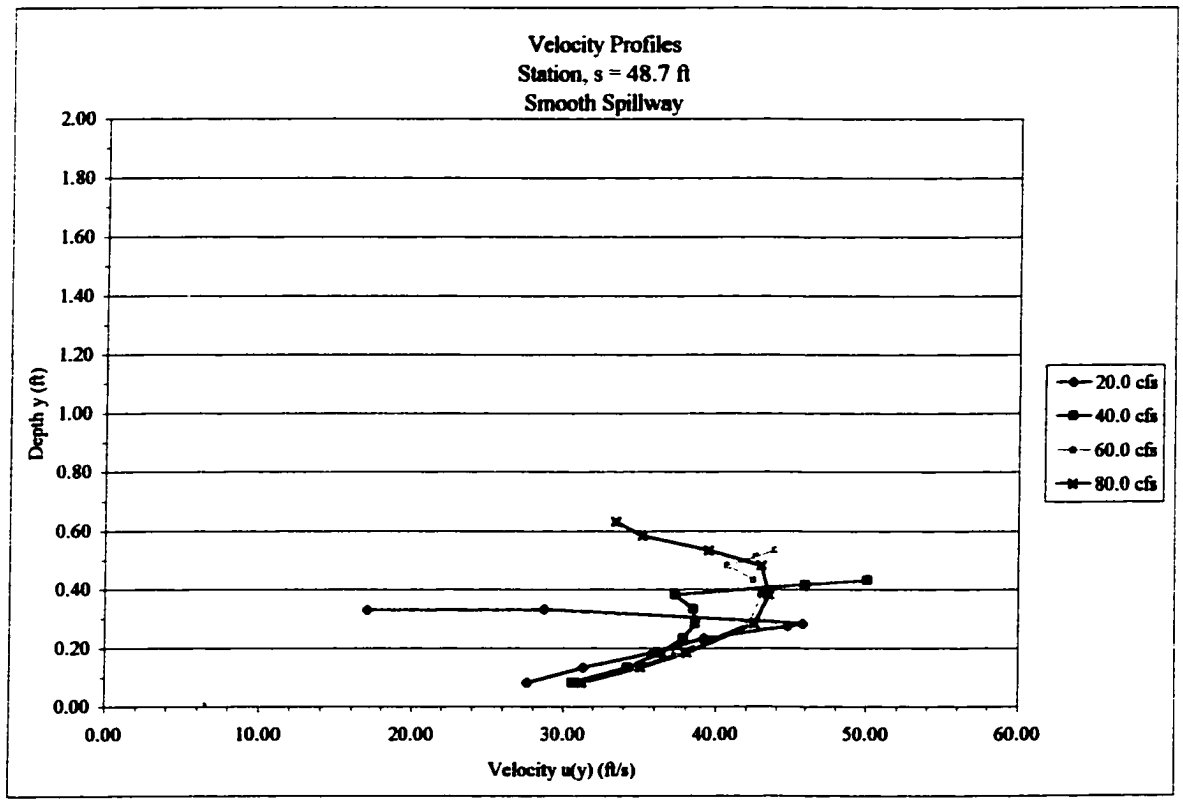

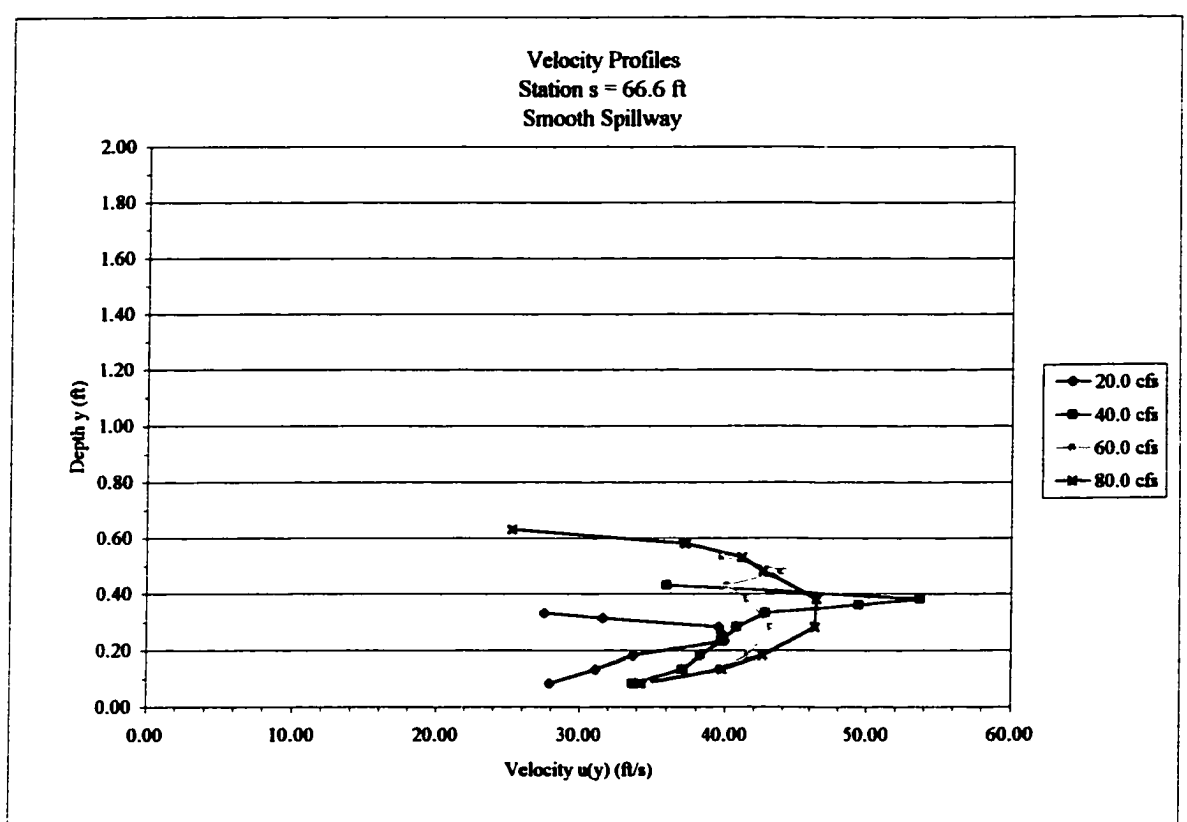

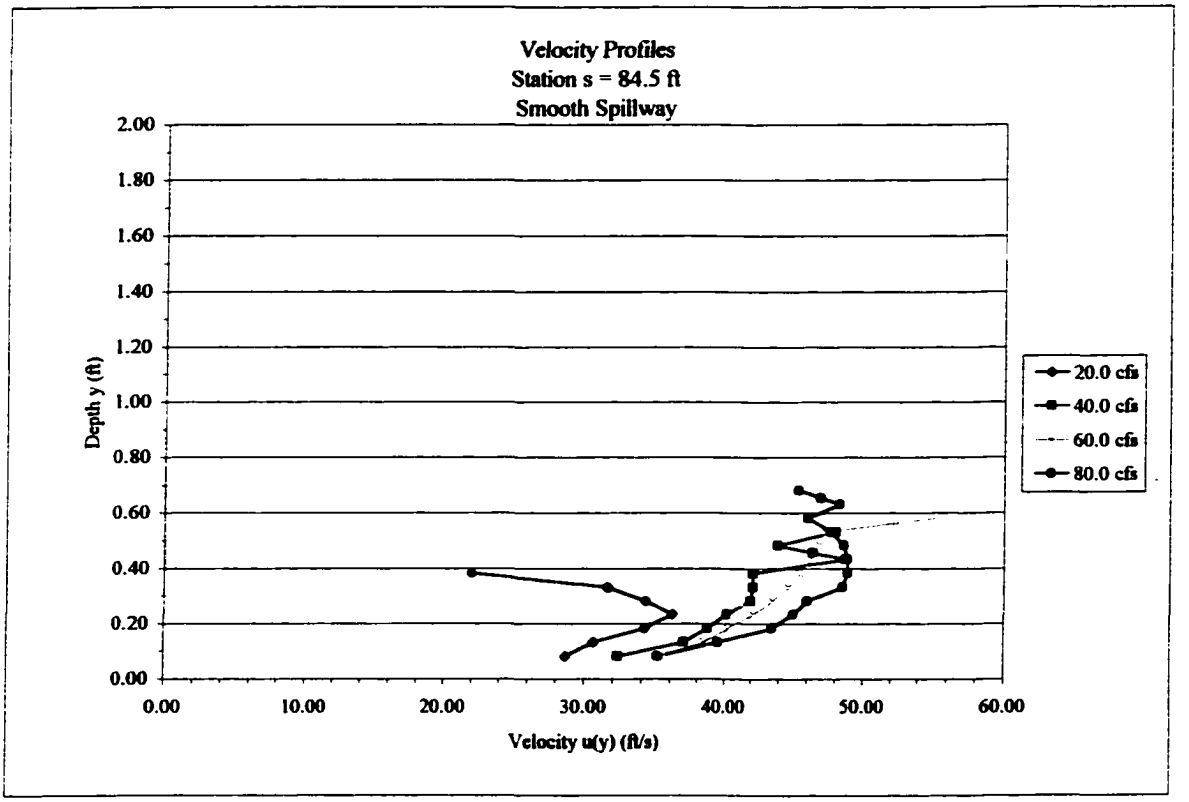

APPENDIX B

AVERAGE AIR CONCENTRATION, AVERAGE VELOCITY, AND CLEAR WATER DEPTH VERSUS STATION ALONG THE SPILLWAY

Profiles along the length of the spillway of average air concentration $\overline{C}$, average velocity U_{avg}, and clear water depth d_w are given in this appendix for the stepped spillway tests and the smooth spillway test. Results are given in tabular and graphical form versus step number and station along the spillway.

Stepped Spillway Tests, h = 1.0 ft

Discharge (cfs)	Unit Discharge (cfs/ft)	Critical Depth, yc (ft)	Step Number N	Station s (ft)	Elevation H (ft)	Average Air Conc. C	Average Velocity U_{avg} (ft/s)	Bulked Depth y_{90} (ft)	Clear Water Depth $d_w = y_{90}(1-C)$ (ft)
7.1	1.78	0.46	1	0.0	0	0.0000	3.85	0.46	0.46
7.1	1.78	0.46	7	13.4	6	0.8262	18.21	0.56	0.10
7.1	1.78	0.46	15	31.3	14	0.7853	19.18	0.43	0.09
7.1	1.78	0.46	23	49.2	22	0.7013	8.81	0.67	0.20
7.1	1.78	0.46	31	67.1	30	0.7610	10.80	0.69	0.16
7.1	1.78	0.46	39	85.0	38	0.7142	10.57	0.59	0.17
21.2	5.30	0.96	1	0.0	0	0.0000	5.55	0.96	0.96
21.2	5.30	0.96	7	13.4	6	0.6669	21.80	0.73	0.24
21.2	5.30	0.96	15	31.3	14	0.6361	26.25	0.55	0.20
21.2	5.30	0.96	23	49.2	22	0.6067	19.88	0.68	0.27
21.2	5.30	0.96	31	67.1	30	0.4855	15.56	0.66	0.34
21.2	5.30	0.96	39	85.0	38	0.5625	18.21	0.67	0.29
41.0	10.25	1.48	1	0.0	0	0.0000	6.91	1.48	1.48
41.0	10.25	1.48	7	13.4	6	0.4298	20.49	0.88	0.50
41.0	10.25	1.48	15	31.3	14	0.4557	22.62	0.83	0.45
41.0	10.25	1.48	23	49.2	22	0.3559	16.33	0.97	0.63
41.0	10.25	1.48	31	67.1	30	0.4273	17.90	1.00	0.57
41.0	10.25	1.48	39	85.0	38	0.3697	17.39	0.94	0.59
60.0	15.00	1.91	1	0.0	0	0.0000	7.85	1.91	1.91
60.0	15.00	1.91	7	13.4	6	0.2980	20.35	1.05	0.74
60.0	15.00	1.91	15	31.3	14	0.4215	24.70	1.05	0.61
60.0	15.00	1.91	23	49.2	22	0.3177	18.01	1.22	0.83
60.0	15.00	1.91	31	67.1	30	0.3678	20.54	1.16	0.73
60.0	15.00	1.91	39	85.0	38	0.3555	19.74	1.18	0.76
80.0	20.00	2.32	1	0.0	0	0.0000	8.64	2.32	2.32
80.0	20.00	2.32	7	13.4	6	0.3708	24.33	1.31	0.82
80.0	20.00	2.32	15	31.3	14	0.3319	25.03	1.20	0.80
80.0	20.00	2.32	23	49.2	22	0.2813	20.58	1.35	0.97
80.0	20.00	2.32	31	67.1	30	0.3196	21.93	1.34	0.91
80.0	20.00	2.32	39	85.0	38	0.3097	21.63	1.34	0.92
100.0	25.00	2.69	1	0.0	0	0.0000	9.30	2.69	2.69
100.0	25.00	2.69	7	13.4	6	0.3400	25.39	1.49	0.98
100.0	25.00	2.69	15	31.3	14	0.2771	23.85	1.45	1.05
100.0	25.00	2.69	23	49.2	22	0.2435	23.05	1.43	1.08
100.0	25.00	2.69	31	67.1	30	0.3013	24.06	1.49	1.04
100.0	25.00	2.69	39	85.0	38	0.2769	23.17	1.49	1.08

Stepped Spillway Tests, h = 2.0 ft

Discharge (cfs)	Unit Discharge (cfs/ft)	Critical Depth, yc (ft)	Step Number N	Station s (ft)	Elevation H (ft)	Average Air Conc. C	Average Velocity U_{avg} (ft/s)	Bulked Depth y_{90} (ft)	Clear Water Depth $d_w = y_{90}(1-C)$ (ft)
20.0	5.00	0.92	1	0.0	0	0.0000	5.44	0.92	0.92
20.0	5.00	0.92	4	13.4	6	0.5178	9.87	1.05	0.51
20.0	5.00	0.92	8	31.3	14	0.6275	13.42	1.00	0.37
20.0	5.00	0.92	12	49.2	22	0.5941	13.91	0.89	0.36
20.0	5.00	0.92	16	67.1	30	0.6180	13.50	0.97	0.37
20.0	5.00	0.92	20	85.0	38	0.6352	18.41	0.74	0.27
40.0	10.00	1.46	1	0.0	0	0.0000	6.85	1.46	1.46
40.0	10.00	1.46	4	13.4	6	0.5039	19.00	1.06	0.53
40.0	10.00	1.46	8	31.3	14	0.5337	16.50	1.30	0.61
40.0	10.00	1.46	12	49.2	22	0.5258	17.79	1.19	0.56
40.0	10.00	1.46	16	67.1	30	0.5291	20.17	1.05	0.50
40.0	10.00	1.46	20	85.0	38	0.5617	22.73	1.00	0.44
60.0	15.00	1.91	1	0.0	0	0.0000	7.85	1.91	1.91
60.0	15.00	1.91	4	13.4	6	0.2490	18.52	1.08	0.81
60.0	15.00	1.91	8	31.3	14	0.3247	18.84	1.18	0.80
60.0	15.00	1.91	12	49.2	22	0.3691	17.88	1.33	0.84
60.0	15.00	1.91	16	67.1	30	0.4018	19.92	1.26	0.75
60.0	15.00	1.91	20	85.0	38	0.4399	22.73	1.18	0.66
80.0	20.00	2.32	1	0.0	0	0.0000	8.64	2.32	2.32
80.0	20.00	2.32	4	13.4	6	0.1702	19.45	1.24	1.03
80.0	20.00	2.32	8	31.3	14	0.3738	20.61	1.55	0.97
80.0	20.00	2.32	12	49.2	22	0.3307	20.69	1.44	0.97
80.0	20.00	2.32	16	67.1	30	0.4155	24.55	1.39	0.81
80.0	20.00	2.32	20	85.0	38	0.4261	24.12	1.45	0.83
100.0	25.00	2.69	1	0.0	0	0.0000	9.30	2.69	2.69
100.0	25.00	2.69	4	13.4	6	0.2271	21.05	1.54	1.19
100.0	25.00	2.69	8	31.3	14	0.3196	23.72	1.55	1.05
100.0	25.00	2.69	12	49.2	22	0.3149	22.51	1.62	1.11
100.0	25.00	2.69	16	67.1	30	0.3607	24.89	1.57	1.00
100.0	25.00	2.69	20	85.0	38	0.3937	27.56	1.50	0.91
116.0	29.00	2.97	1	0.0	0	0.0000	9.77	2.97	2.97
116.0	29.00	2.97	4	13.4	6	0.2141	22.01	1.68	1.32
116.0	29.00	2.97	8	31.3	14	0.2769	26.07	1.54	1.11
116.0	29.00	2.97	16	67.1	30	0.3367	26.30	1.66	1.10
116.0	29.00	2.97	20	85.0	38	0.3518	28.16	1.59	1.03
121.0	30.25	3.05	1	0.0	0	0.0000	9.91	3.05	3.05
121.0	30.25	3.05	4	13.4	6	0.3057	21.78	2.00	1.39
121.0	30.25	3.05	12	49.2	22	0.2864	23.80	1.78	1.27

Smooth Spillway Tests

Discharge (cfs)	Unit Discharge (cfs/ft)	Critical Depth, yc (ft)	Station s (ft)	Elevation H (ft)	Average Air Conc. C	Average Velocity U_{avg} (ft/s)	Bulked Depth y_{90} (ft)	Clear Water Depth $d_w = y_{90}(1-C)$ (ft)
20	5.0	0.92	10.5	4.7	0.2125	21.30	0.30	0.23
20	5.0	0.92	30.9	13.8	0.3005	24.48	0.29	0.20
20	5.0	0.92	48.7	21.8	0.4579	25.30	0.36	0.20
20	5.0	0.92	66.6	29.8	0.4031	25.16	0.33	0.20
20	5.0	0.92	84.5	37.8	0.3705	20.63	0.38	0.24
40	10.0	1.46	10.5	3.6	0.1100	20.49	0.55	0.49
40	10.0	1.46	30.9	13.8	0.2327	30.10	0.43	0.33
40	10.0	1.46	48.7	21.8	0.1991	27.62	0.45	0.36
40	10.0	1.46	66.6	29.8	0.3150	33.72	0.43	0.30
40	10.0	1.46	84.5	37.8	0.2983	26.74	0.53	0.37
60	15.0	1.91	10.5	3.6	0.0848	22.84	0.72	0.66
60	15.0	1.91	30.9	13.8	0.1033	30.24	0.55	0.50
60	15.0	1.91	48.7	21.8	0.1799	33.38	0.55	0.45
60	15.0	1.91	66.6	29.8	0.2382	34.11	0.58	0.44
60	15.0	1.91	84.5	37.8	0.2045	31.09	0.61	0.48
80	20.0	2.32	10.5	3.6	0.1026	23.65	0.94	0.85
80	20.0	2.32	30.9	13.8	0.1572	32.38	0.73	0.62
80	20.0	2.32	48.7	21.8	0.1290	34.47	0.67	0.58
80	20.0	2.32	66.6	29.8	0.1949	38.38	0.65	0.52
80	20.0	2.32	84.5	37.8	0.2090	34.82	0.73	0.57

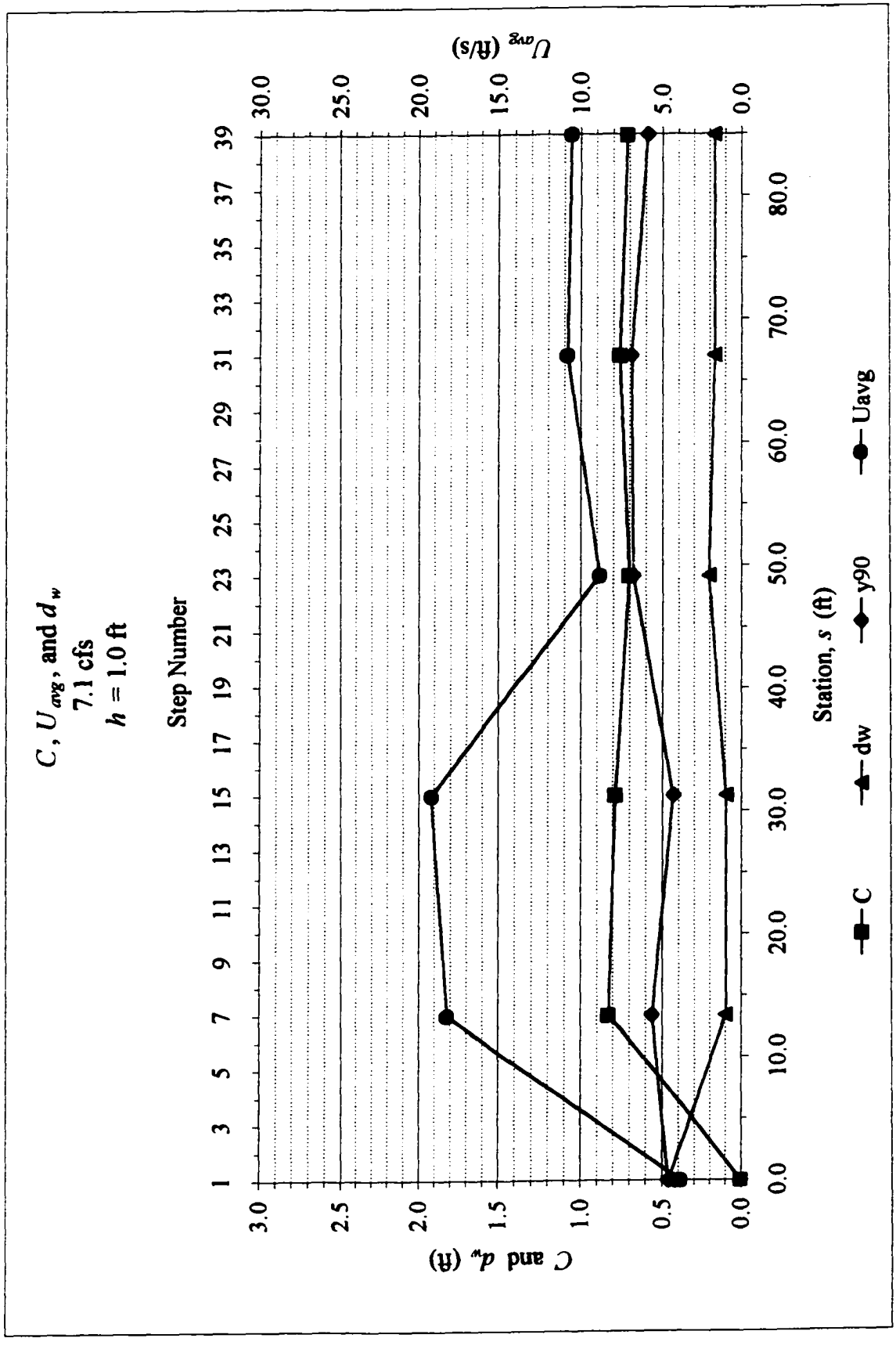

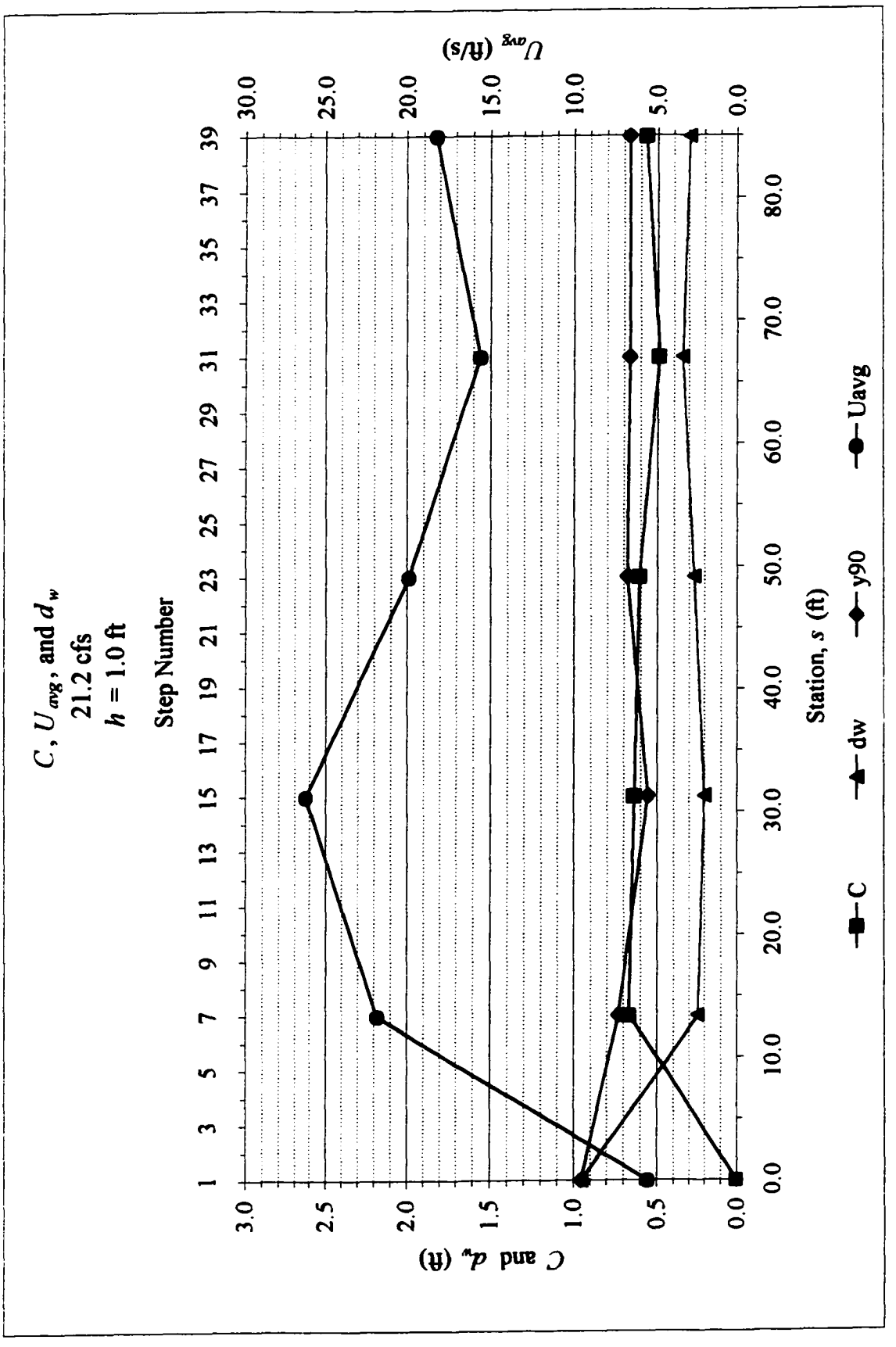

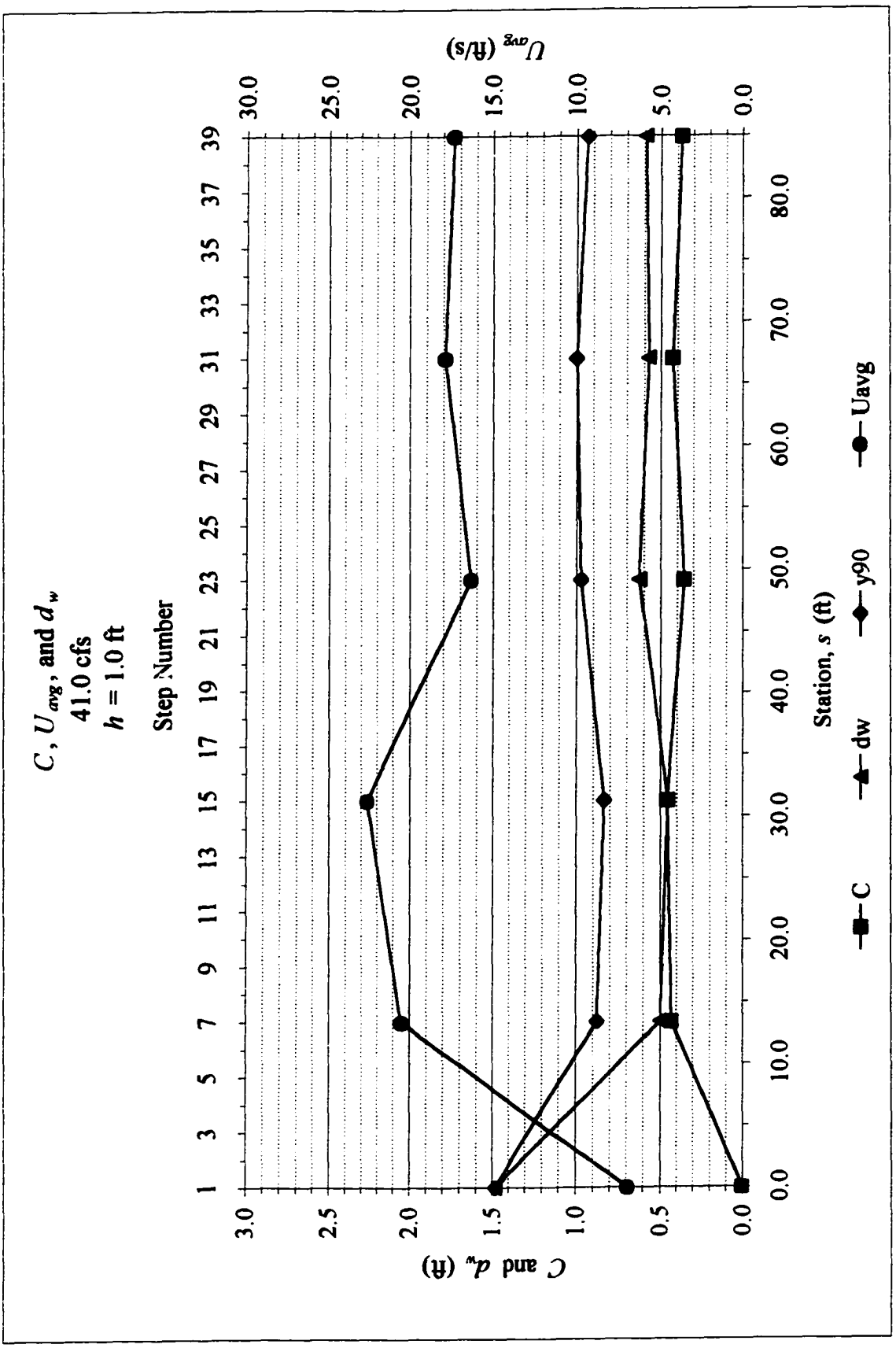

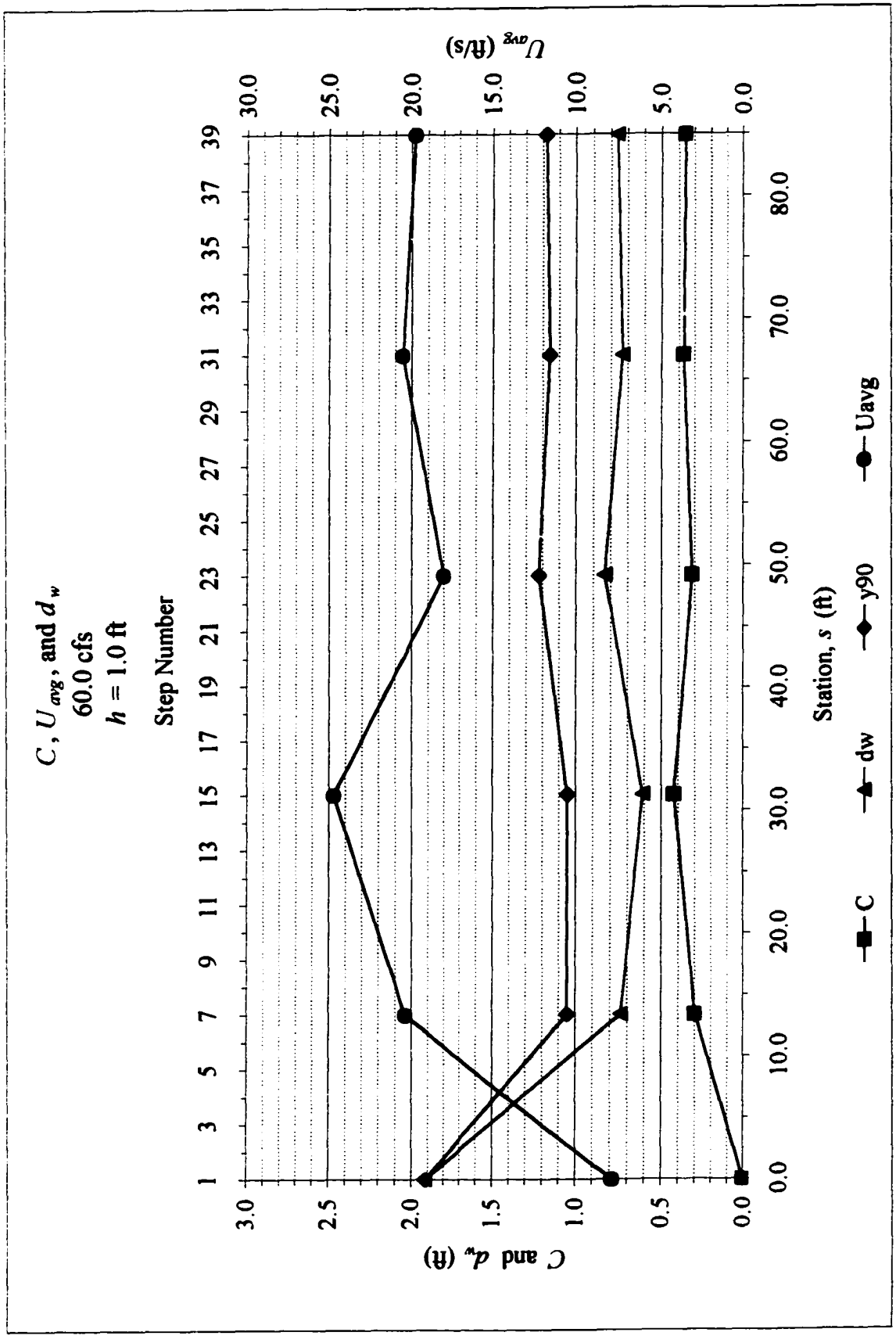

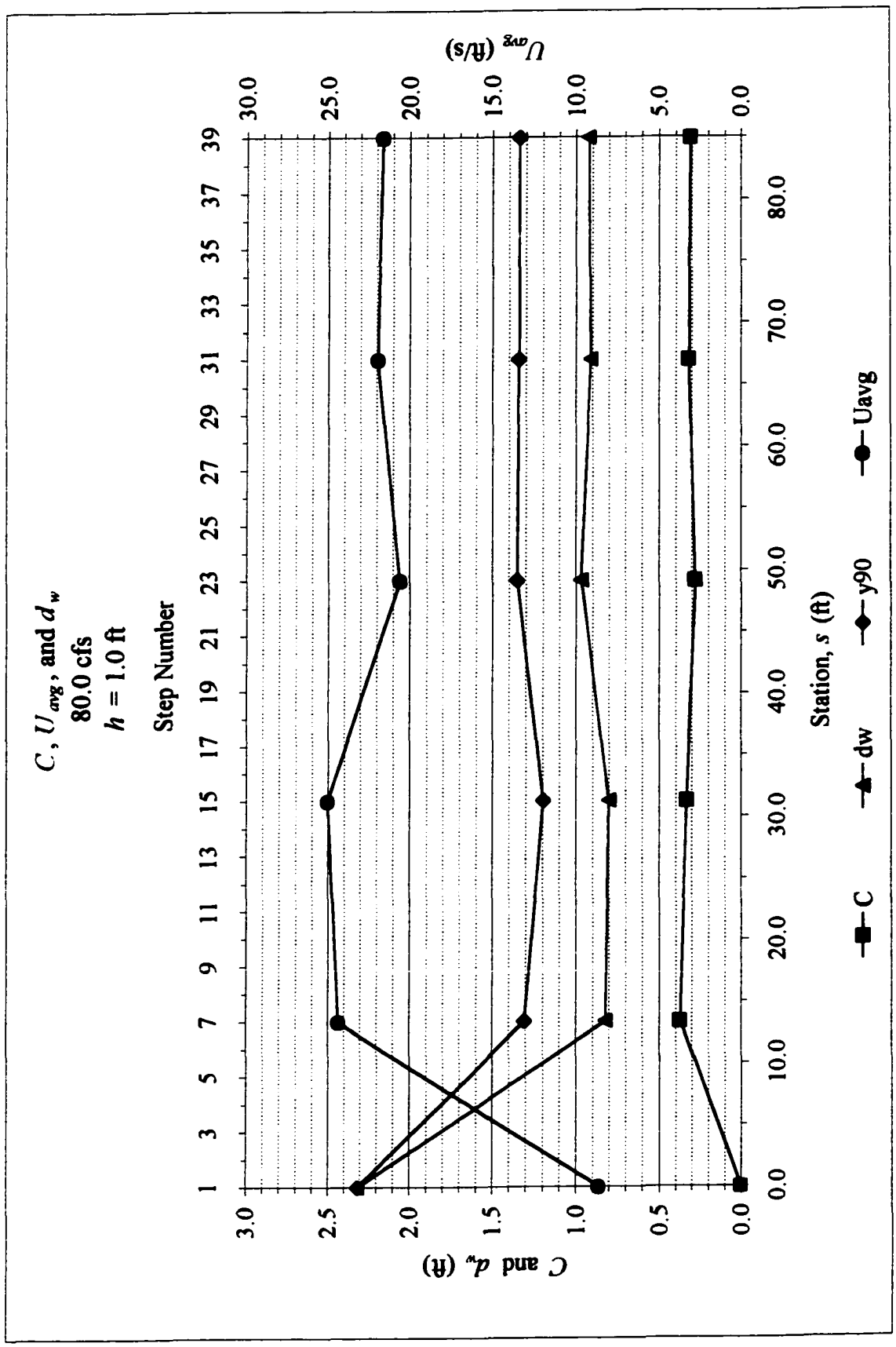

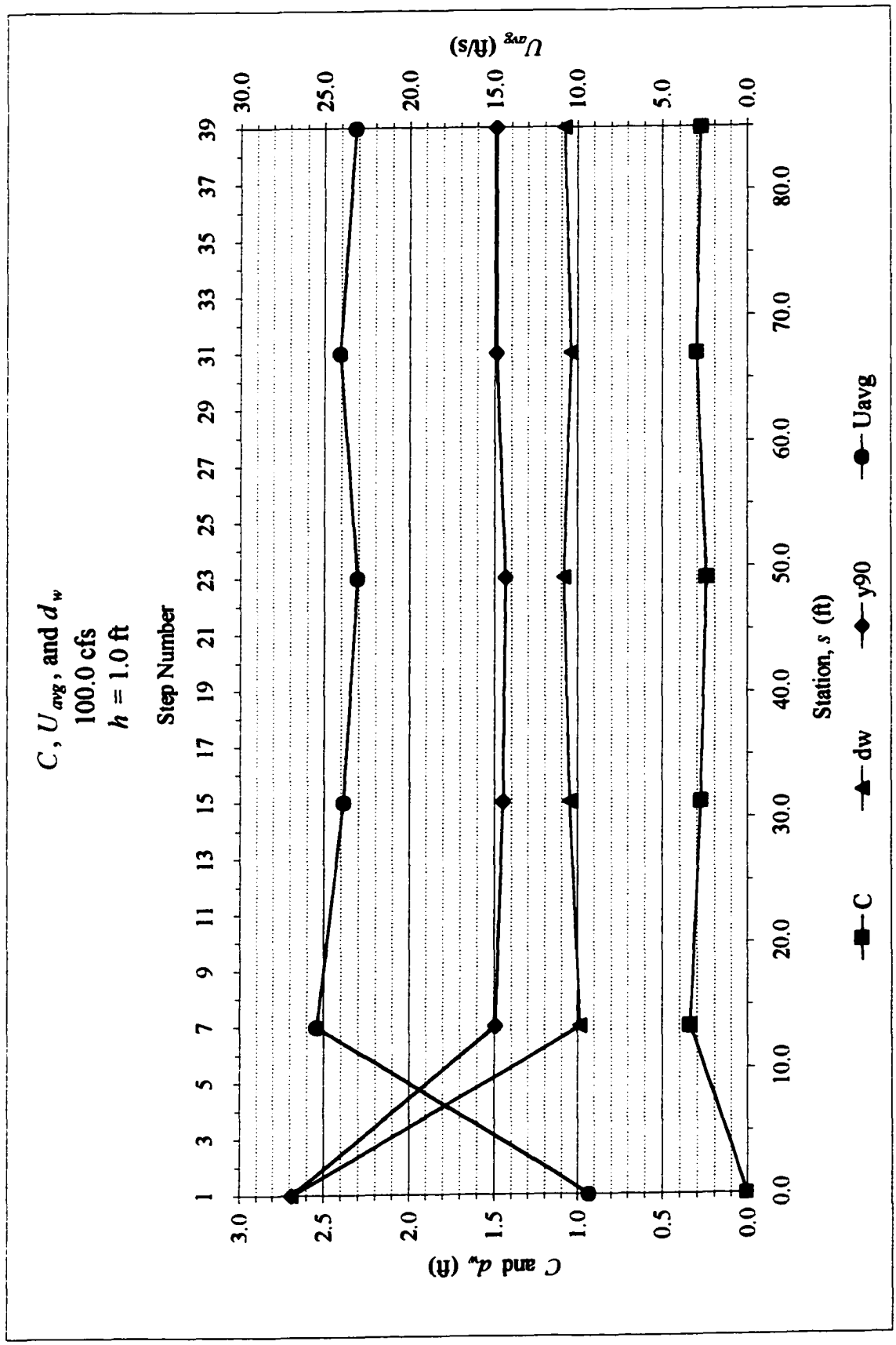

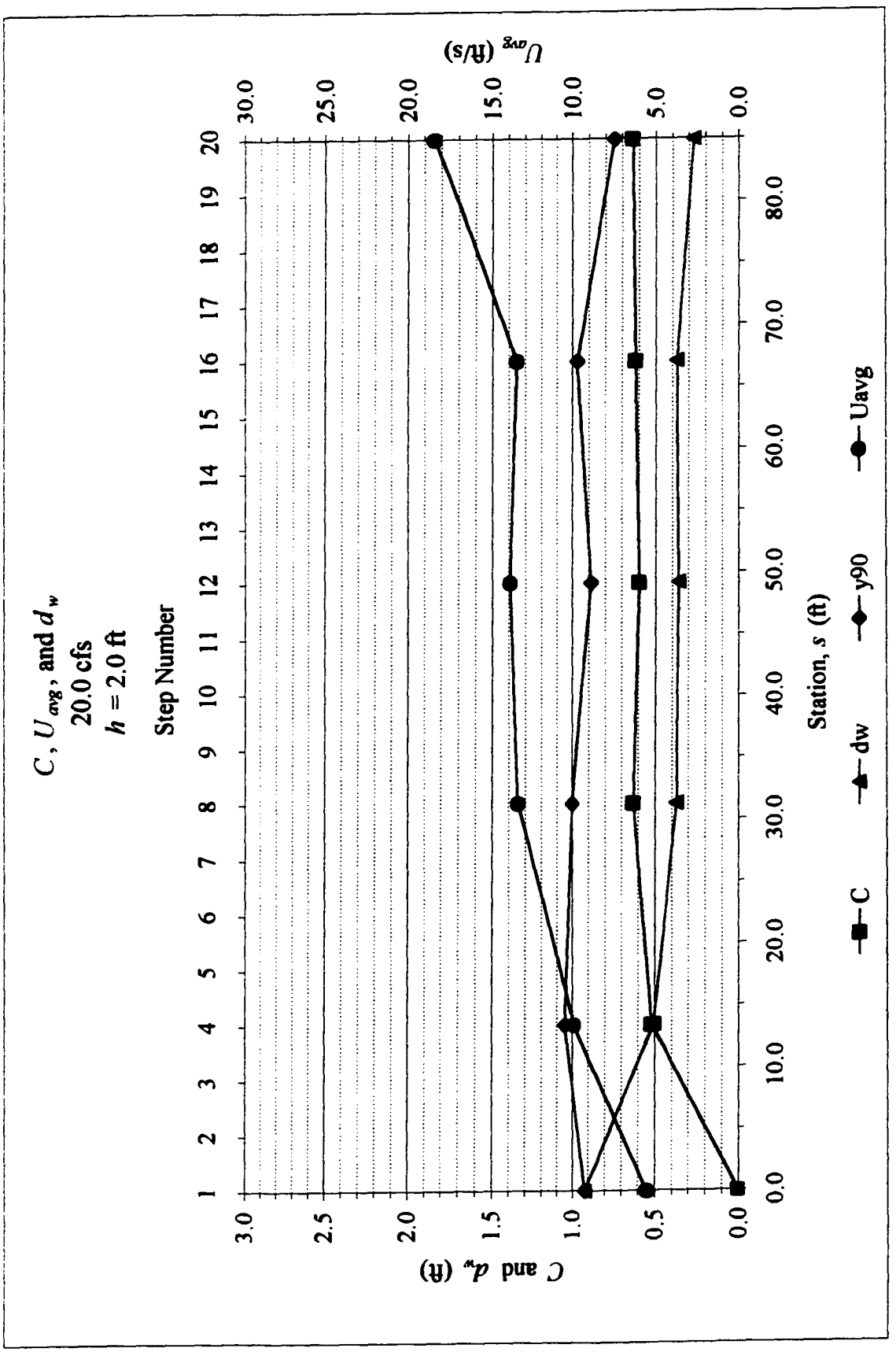

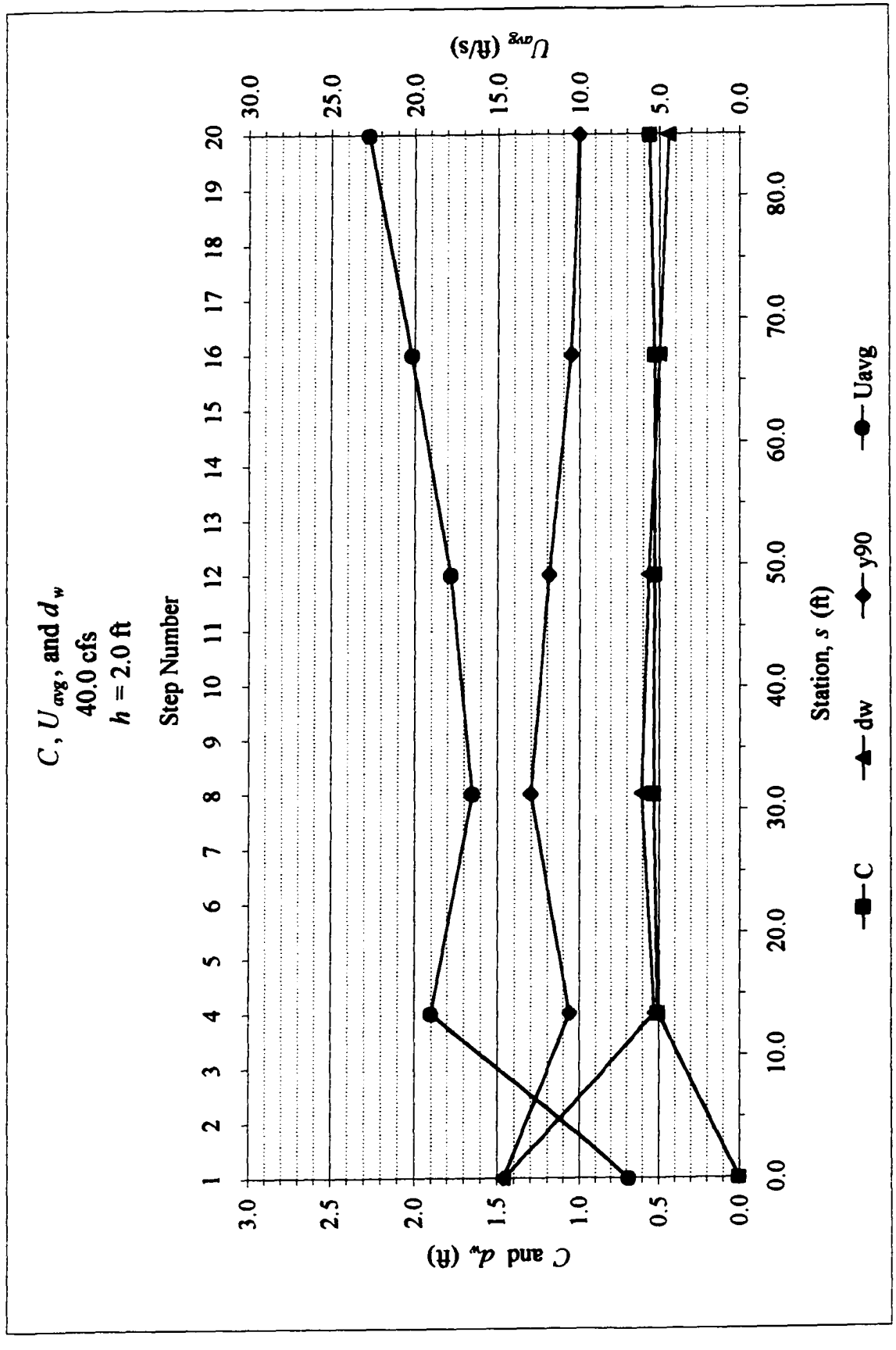

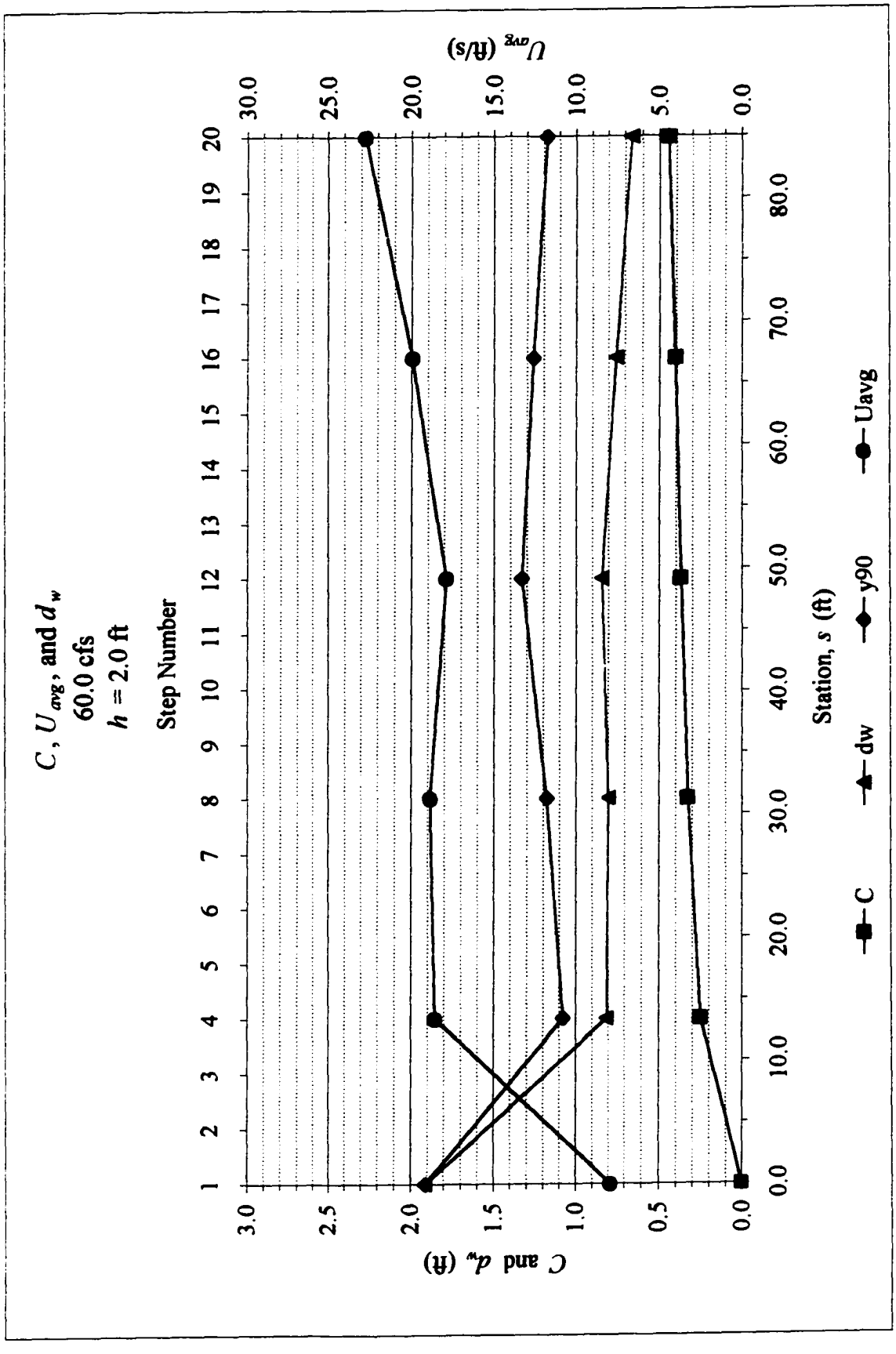

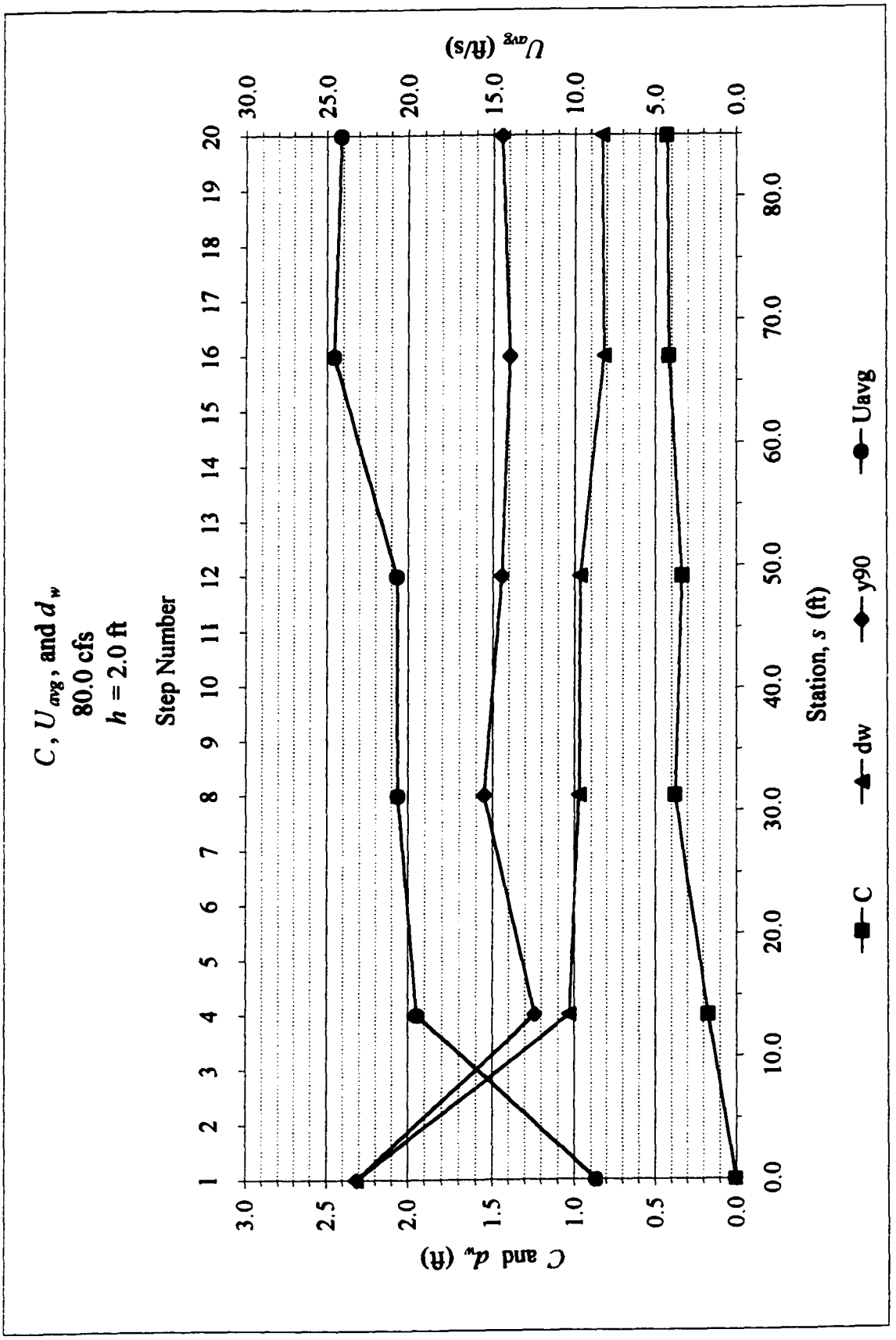

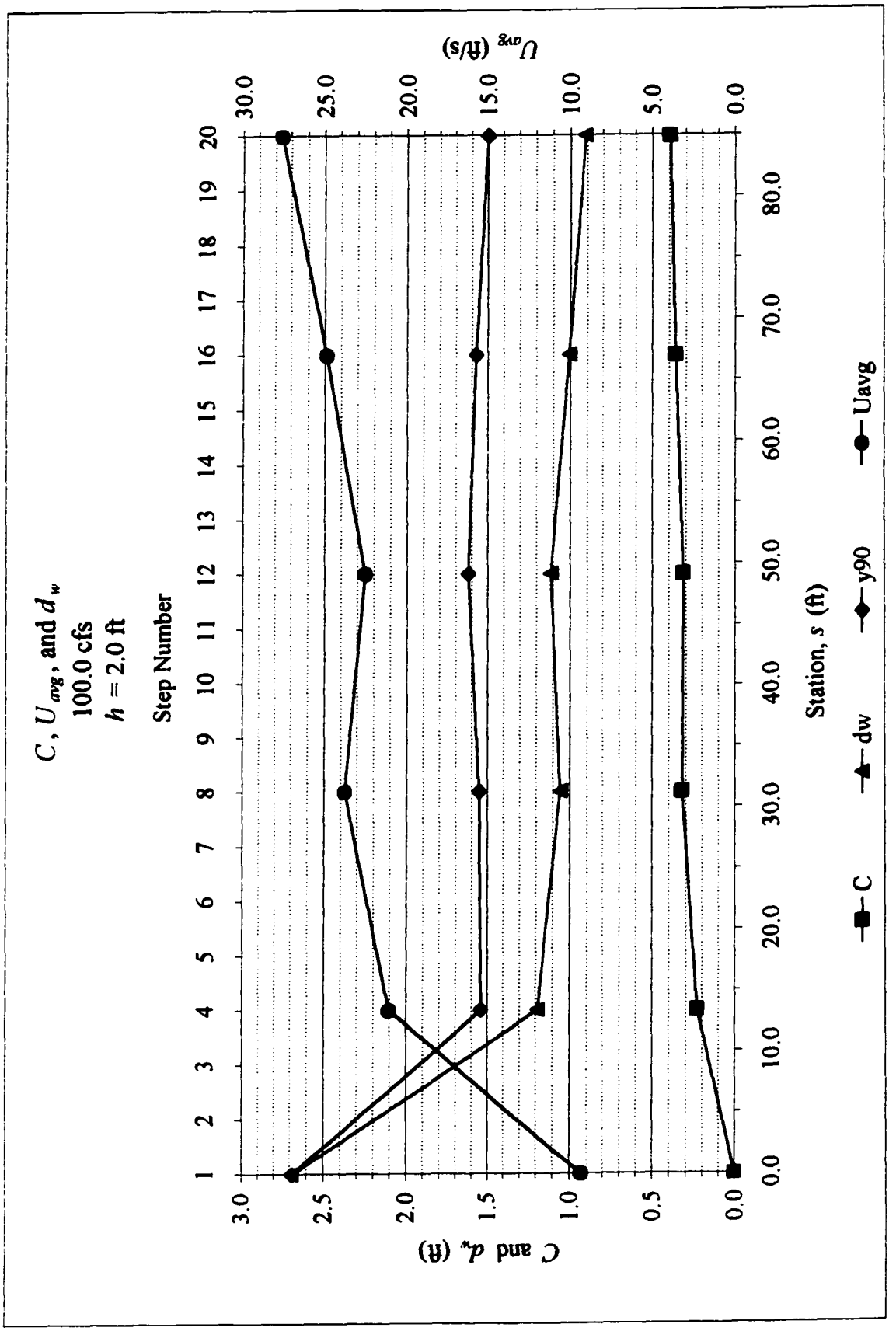

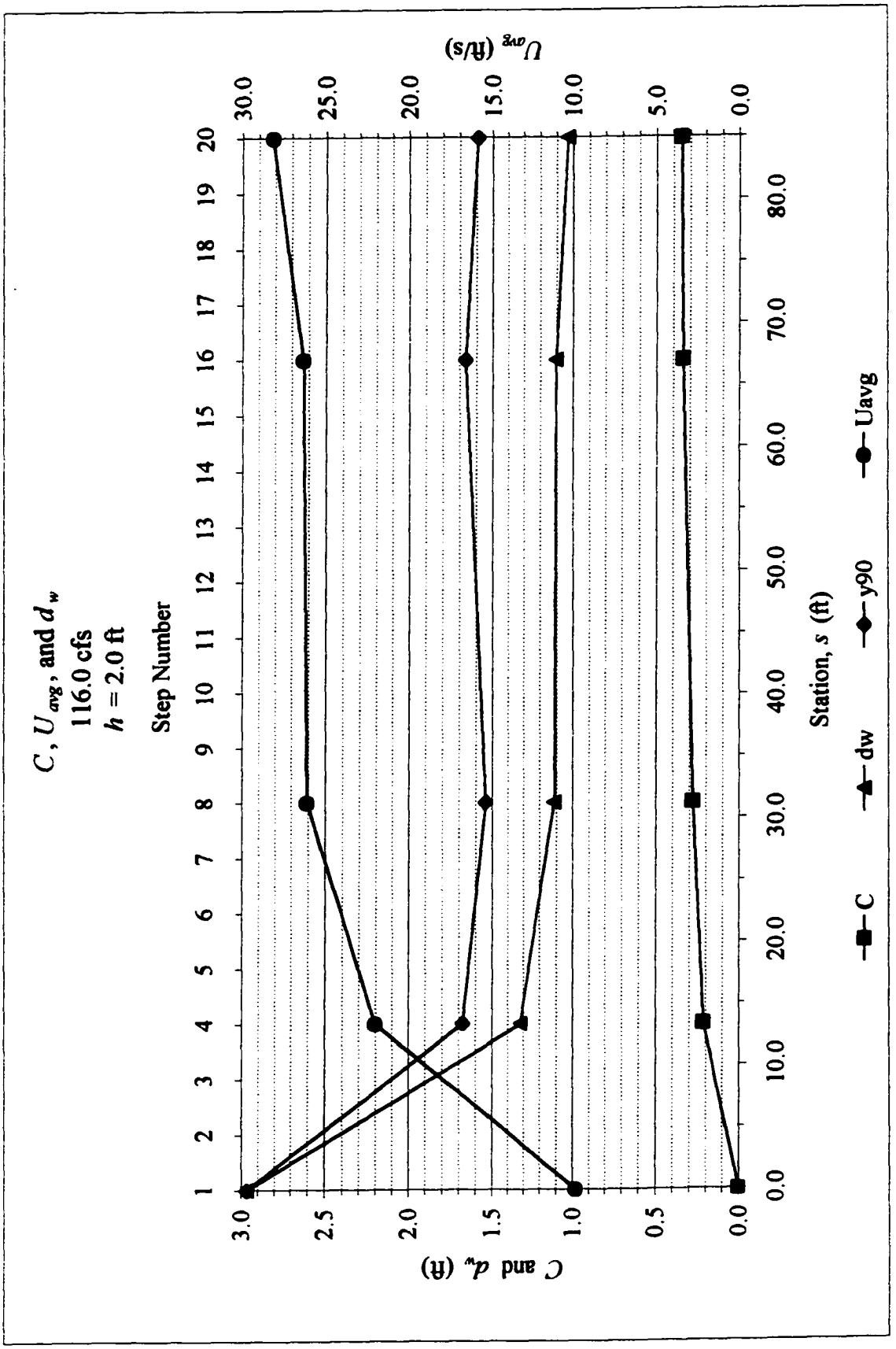

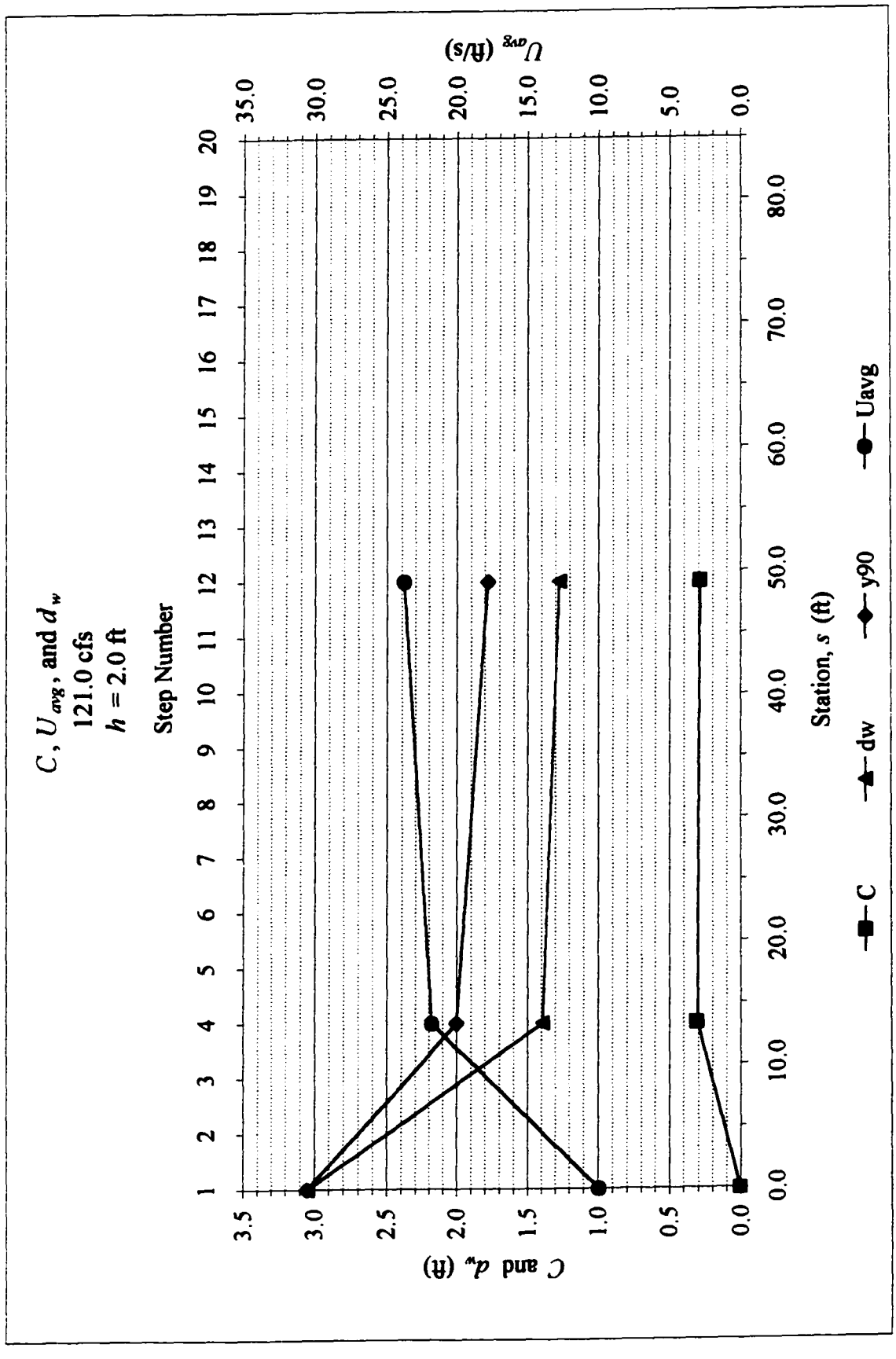

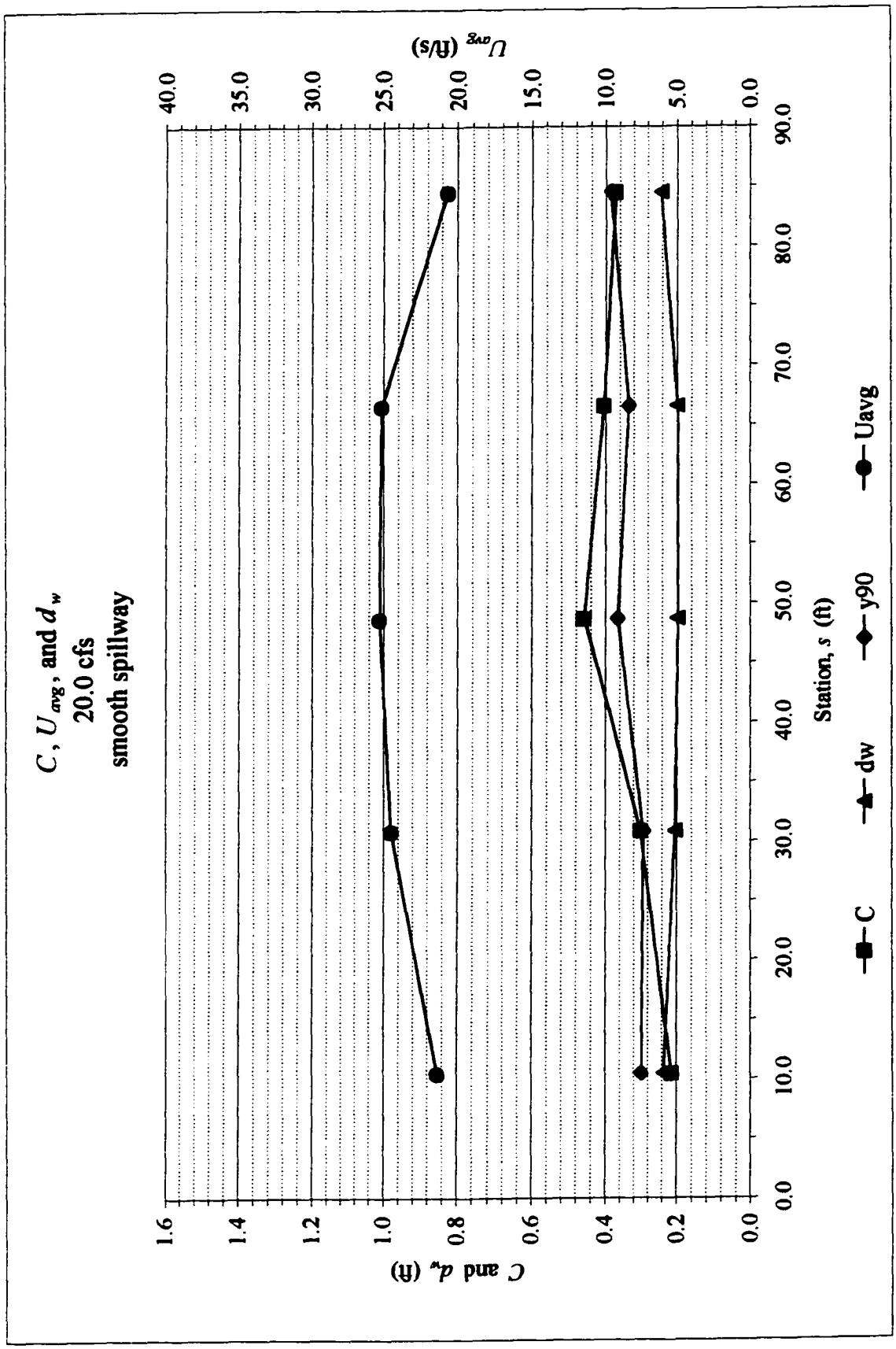

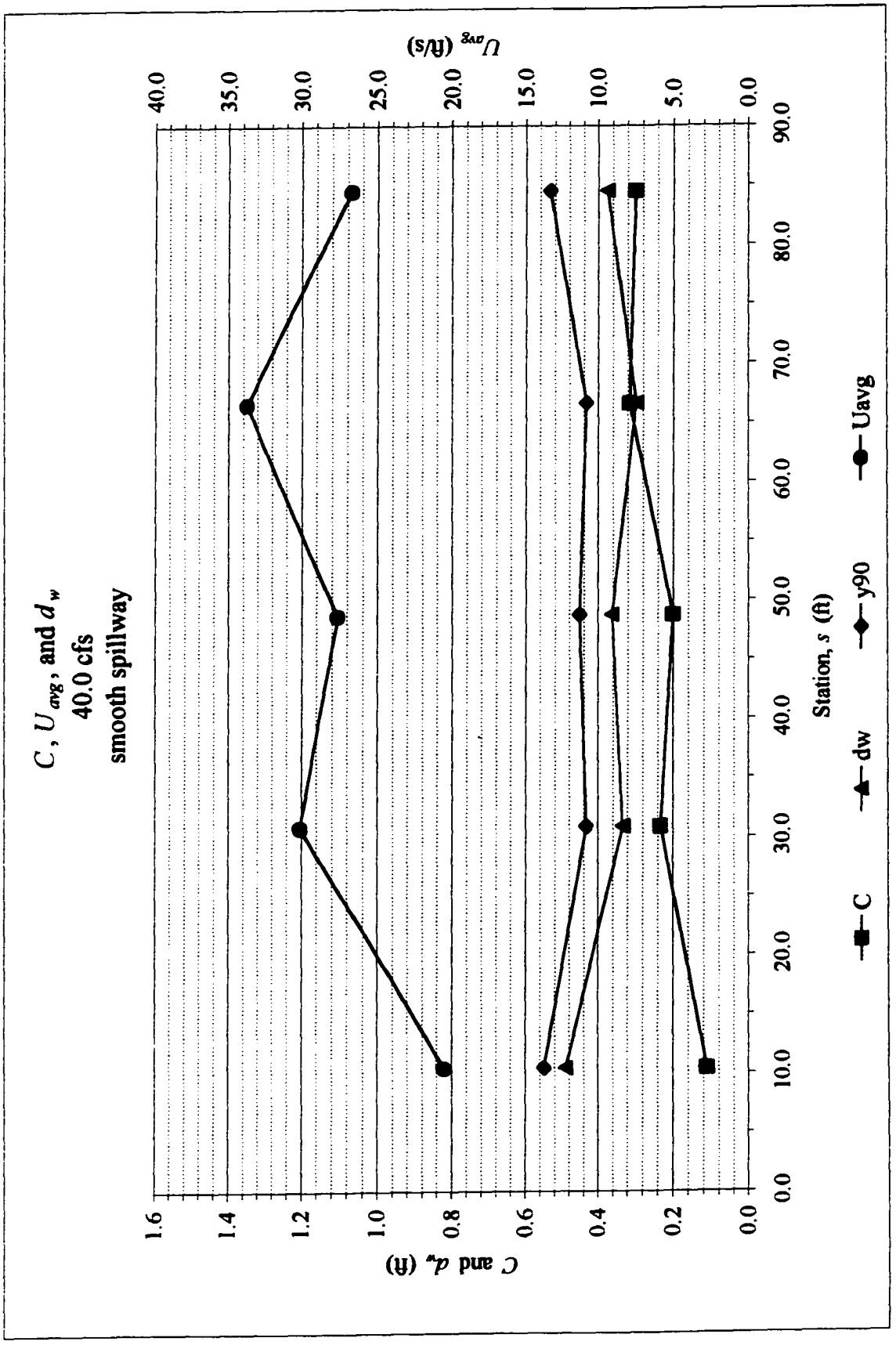

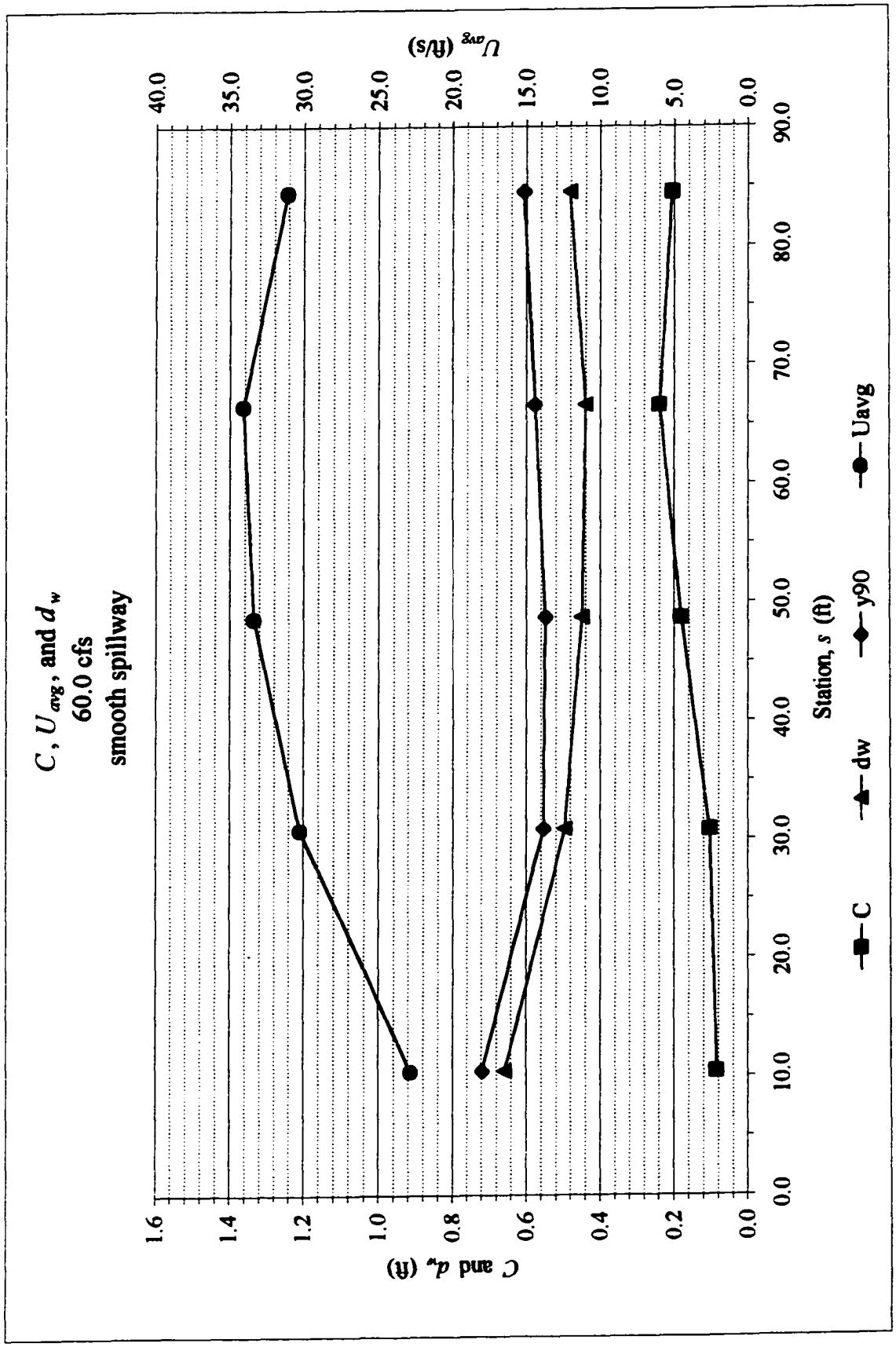

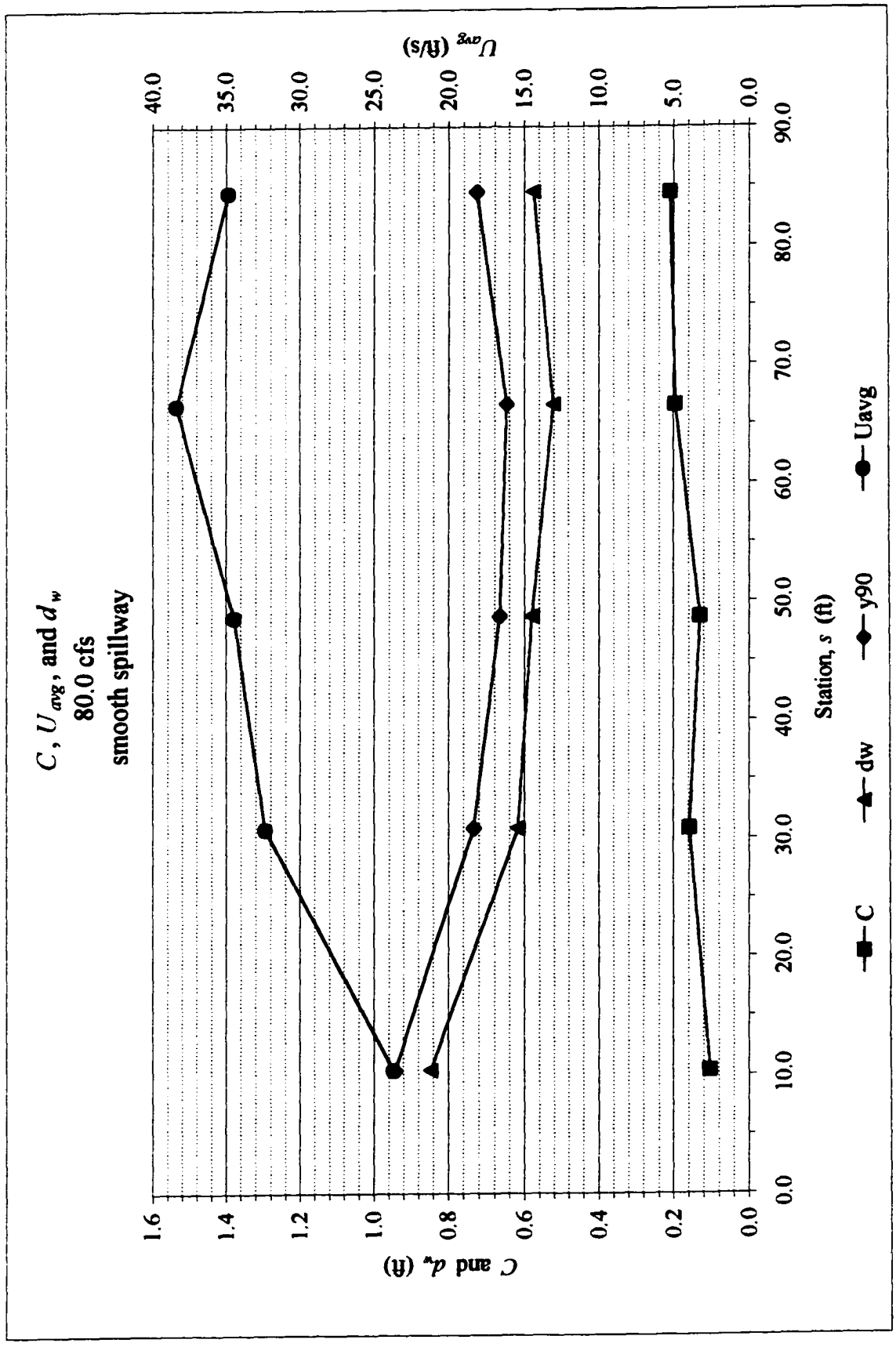

APPENDIX C

PRESSURE PROFILES

Pressure profiles taken along the spillway, as discussed in Chapter 5, are given in this appendix for the stepped spillway tests. Results are given in both tabular and graphical form.

Stepped Spillway Tests, h = 1 ft

Discharge (cfs)	Step Number	Tap Location	Tap Number	Distance along step (ft)	Total Pressure above trans. (psi)	Pressure at Step (psi)	Pressure at Step (ft of water)
7.1	1	Riser	1	0.25	1.45	-0.85	-1.95
	1	Riser	2	0.75	2.16	0.09	0.20
	2	Tread	3	1.25	2.14	0.16	0.38
	2	Tread	4	1.75	2.14	0.17	0.38
	2	Tread	5	2.25	2.16	0.18	0.42
	2	Tread	6	2.75	2.31	0.33	0.76
	2	Riser	7	3.25	1.87	0.02	0.03
	2	Riser	8	3.75	1.66	0.01	0.03
	3	Tread	9	4.25	1.67	0.13	0.30
	3	Tread	10	4.75	1.65	0.12	0.27
	3	Tread	11	5.25	1.97	0.43	1.00
	3	Tread	12	5.75	1.78	0.24	0.56
	3	Riser	13	6.25	1.43	0.00	0.01
	3	Riser	14	6.75	1.20	0.00	0.01
14.1	1	Riser	1	0.25	2.32	0.02	0.05
	1	Riser	2	0.75	2.09	0.02	0.04
	2	Tread	3	1.25	2.00	0.03	0.06
	2	Tread	4	1.75	2.00	0.03	0.06
	2	Tread	5	2.25	2.01	0.03	0.07
	2	Tread	6	2.75	2.00	0.02	0.05
	2	Riser	7	3.25	1.91	0.05	0.11
	2	Riser	8	3.75	1.91	0.26	0.61
	3	Tread	9	4.25	1.89	0.35	0.82
	3	Tread	10	4.75	1.85	0.31	0.72
	3	Tread	11	5.25	1.97	0.43	1.00
	3	Tread	12	5.75	2.42	0.88	2.03
	3	Riser	13	6.25	1.42	0.00	0.00
	3	Riser	14	6.75	1.20	0.00	0.00
21.2	1	Riser	1	0.25	2.27	-0.03	-0.08
	1	Riser	2	0.75	2.05	-0.03	-0.07
	2	Tread	3	1.25	1.96	-0.02	-0.04
	2	Tread	4	1.75	1.95	-0.03	-0.06
	2	Tread	5	2.25	1.95	-0.03	-0.06
	2	Tread	6	2.75	1.95	-0.03	-0.06
	2	Riser	7	3.25	1.91	0.05	0.12
	2	Riser	8	3.75	1.88	0.24	0.56
	3	Tread	9	4.25	1.88	0.34	0.80
	3	Tread	10	4.75	1.84	0.31	0.71
	3	Tread	11	5.25	1.86	0.33	0.75
	3	Tread	12	5.75	2.41	0.88	2.03
	3	Riser	13	6.25	1.36	-0.06	-0.14
	3	Riser	14	6.75	1.37	0.17	0.38

Stepped Spillway Tests, h = 1 ft

Discharge (cfs)	Step Number	Tap Location	Tap Number	Distance along step (ft)	Total Pressure above trans. (psi)	Pressure at Step (psi)	Pressure at Step (ft of water)
28.3	1	Riser	1	0.25	2.22	-0.08	-0.18
	1	Riser	2	0.75	2.01	-0.07	-0.16
	2	Tread	3	1.25	1.99	0.01	0.03
	2	Tread	4	1.75	1.98	0.00	0.00
	2	Tread	5	2.25	1.98	0.00	0.00
	2	Tread	6	2.75	1.98	0.00	0.01
	2	Riser	7	3.25	1.97	0.11	0.25
	2	Riser	8	3.75	1.96	0.32	0.74
	3	Tread	9	4.25	1.92	0.39	0.90
	3	Tread	10	4.75	1.91	0.37	0.86
	3	Tread	11	5.25	2.19	0.65	1.51
	3	Tread	12	5.75	2.45	0.91	2.10
	3	Riser	13	6.25	1.40	-0.02	-0.05
	3	Riser	14	6.75	1.41	0.21	0.48
35.4	1	Riser	1	0.25	2.15	-0.15	-0.35
	1	Riser	2	0.75	2.00	-0.08	-0.17
	2	Tread	3	1.25	2.00	0.02	0.05
	2	Tread	4	1.75	2.00	0.02	0.05
	2	Tread	5	2.25	2.00	0.02	0.05
	2	Tread	6	2.75	1.99	0.02	0.04
	2	Riser	7	3.25	2.03	0.17	0.40
	2	Riser	8	3.75	2.01	0.36	0.84
	3	Tread	9	4.25	1.98	0.45	1.03
	3	Tread	10	4.75	2.04	0.51	1.17
	3	Tread	11	5.25	2.49	0.96	2.21
	3	Tread	12	5.75	2.38	0.84	1.95
	3	Riser	13	6.25	1.41	-0.01	-0.03
	3	Riser	14	6.75	1.40	0.20	0.47
41.0	1	Riser	1	0.25	2.10	-0.20	-0.45
	1	Riser	2	0.75	2.10	0.03	0.06
	2	Tread	3	1.25	2.07	0.09	0.21
	2	Tread	4	1.75	2.05	0.07	0.16
	2	Tread	5	2.25	2.05	0.07	0.17
	2	Tread	6	2.75	2.48	0.50	1.15
	2	Riser	7	3.25	2.06	0.20	0.46
	2	Riser	8	3.75	2.04	0.40	0.93
	3	Tread	9	4.25	2.02	0.48	1.12
	3	Tread	10	4.75	1.97	0.43	1.00
	3	Tread	11	5.25	2.26	0.73	1.67
	3	Tread	12	5.75	2.31	0.77	1.79
	3	Riser	13	6.25	1.41	-0.01	-0.02
	3	Riser	14	6.75	1.43	0.23	0.52

Stepped Spillway Tests, h = 1 ft

Discharge (cfs)	Step Number	Tap Location	Tap Number	Distance along step (ft)	Total Pressure above trans. (psi)	Pressure at Step (psi)	Pressure at Step (ft of water)
60.0	1	Riser	1	0.25	1.97	-0.33	-0.75
	1	Riser	2	0.75	1.97	-0.10	-0.24
	2	Tread	3	1.25	1.92	-0.05	-0.12
	2	Tread	4	1.75	1.88	-0.10	-0.23
	2	Tread	5	2.25	1.93	-0.04	-0.10
	2	Tread	6	2.75	2.56	0.58	1.34
	2	Riser	7	3.25	2.18	0.32	0.73
	2	Riser	8	3.75	2.16	0.52	1.20
	3	Tread	9	4.25	2.15	0.62	1.42
	3	Tread	10	4.75	2.11	0.58	1.33
	3	Tread	11	5.25	2.43	0.89	2.06
	3	Tread	12	5.75	2.42	0.88	2.03
	3	Riser	13	6.25	1.47	0.04	0.10
	3	Riser	14	6.75	1.48	0.28	0.64
80.0	1	Riser	1	0.25	1.86	-0.44	-1.02
	1	Riser	2	0.75	1.83	-0.25	-0.57
	2	Tread	3	1.25	1.82	-0.16	-0.37
	2	Tread	4	1.75	1.74	-0.24	-0.55
	2	Tread	5	2.25	1.80	-0.18	-0.41
	2	Tread	6	2.75	2.50	0.52	1.20
	2	Riser	7	3.25	2.41	0.55	1.26
	2	Riser	8	3.75	2.36	0.71	1.65
	3	Tread	9	4.25	2.37	0.83	1.93
	3	Tread	10	4.75	2.31	0.78	1.80
	3	Tread	11	5.25	2.67	1.14	2.62
	3	Tread	12	5.75	2.65	1.12	2.58
	3	Riser	13	6.25	1.53	0.10	0.24
	3	Riser	14	6.75	1.53	0.32	0.75
100.0	1	Riser	1	0.25	1.79	-0.51	-1.17
	1	Riser	2	0.75	1.77	-0.31	-0.71
	2	Tread	3	1.25	1.72	-0.26	-0.60
	2	Tread	4	1.75	1.65	-0.33	-0.77
	2	Tread	5	2.25	1.67	-0.30	-0.70
	2	Tread	6	2.75	2.35	0.37	0.86
	2	Riser	7	3.25	2.50	0.64	1.47
	2	Riser	8	3.75	2.50	0.85	1.97
	3	Tread	9	4.25	2.45	0.92	2.12
	3	Tread	10	4.75	2.46	0.93	2.15
	3	Tread	11	5.25	2.79	1.25	2.89
	3	Tread	12	5.75	2.75	1.22	2.81
	3	Riser	13	6.25	1.58	0.16	0.36
	3	Riser	14	6.75	1.57	0.37	0.85

Stepped Spillway Tests, h = 1 ft

Discharge (cfs)	Step Number	Tap Location	Tap Number	Distance along step (ft)	Total Pressure above trans. (psi)	Pressure at Step (psi)	Pressure at Step (ft of water)
114.0	1	Riser	1	0.25	1.81	-0.49	-1.14
	1	Riser	2	0.75	1.79	-0.28	-0.65
	2	Tread	3	1.25	1.72	-0.25	-0.58
	2	Tread	4	1.75	1.71	-0.27	-0.62
	2	Tread	5	2.25	1.64	-0.34	-0.78
	2	Tread	6	2.75	2.22	0.24	0.55
	2	Riser	7	3.25	2.54	0.68	1.57
	2	Riser	8	3.75	2.52	0.88	2.03
	3	Tread	9	4.25	2.53	0.99	2.29
	3	Tread	10	4.75	2.50	0.96	2.22
	3	Tread	11	5.25	2.88	1.34	3.10
	3	Tread	12	5.75	2.83	1.29	2.98
	3	Riser	13	6.25	1.66	0.24	0.54
	3	Riser	14	6.75	1.65	0.45	1.04

Stepped Spillway Tests, h = 1 ft

Discharge (cfs)	Step Number	Tap Location	Tap Number	Distance along step (ft)	Total Pressure above trans. (psi)	Pressure at Step (psi)	Pressure at Step (ft of water)
7.1	21	Riser	1	0.25	0.21	-2.53	-5.84
	21	Riser	2	0.75	2.51	-0.02	-0.04
	22	Tread	3	1.25	2.59	0.13	0.30
	22	Tread	4	1.75	2.58	0.12	0.28
	22	Tread	5	2.25	2.66	0.20	0.47
	22	Tread	6	2.75	2.77	0.32	0.73
	22	Riser	7	3.25	2.28	-0.06	-0.14
	22	Riser	8	3.75	2.16	0.03	0.07
	23	Tread	9	4.25	2.08	0.06	0.13
	23	Tread	10	4.75	2.08	0.06	0.13
	23	Tread	11	5.25	2.08	0.06	0.14
	23	Tread	12	5.75	2.21	0.19	0.44
	23	Riser	13	6.25	1.94	0.04	0.08
	23	Riser	14	6.75	1.75	0.06	0.14
14.1	21	Riser	1	0.25	2.59	-0.15	-0.35
	21	Riser	2	0.75	2.71	0.17	0.40
	22	Tread	3	1.25	2.70	0.25	0.57
	22	Tread	4	1.75	2.70	0.24	0.56
	22	Tread	5	2.25	2.73	0.27	0.63
	22	Tread	6	2.75	3.09	0.63	1.46
	22	Riser	7	3.25	2.38	0.04	0.09
	22	Riser	8	3.75	2.15	0.02	0.05
	23	Tread	9	4.25	2.09	0.07	0.15
	23	Tread	10	4.75	2.08	0.06	0.14
	23	Tread	11	5.25	2.08	0.06	0.13
	23	Tread	12	5.75	2.17	0.15	0.35
	23	Riser	13	6.25	1.93	0.03	0.07
	23	Riser	14	6.75	1.82	0.13	0.31
21.2	21	Riser	1	0.25	2.75	0.01	0.02
	21	Riser	2	0.75	2.74	0.21	0.48
	22	Tread	3	1.25	2.70	0.24	0.55
	22	Tread	4	1.75	2.67	0.21	0.49
	22	Tread	5	2.25	2.80	0.34	0.79
	22	Tread	6	2.75	3.06	0.60	1.39
	22	Riser	7	3.25	2.24	-0.09	-0.22
	22	Riser	8	3.75	2.24	0.11	0.25
	23	Tread	9	4.25	2.23	0.21	0.48
	23	Tread	10	4.75	2.22	0.19	0.45
	23	Tread	11	5.25	2.35	0.33	0.76
	23	Tread	12	5.75	2.61	0.59	1.35
	23	Riser	13	6.25	1.88	-0.02	-0.05
	23	Riser	14	6.75	1.86	0.17	0.39

Stepped Spillway Tests, h = 1 ft

Discharge (cfs)	Step Number	Tap Location	Tap Number	Distance along step (ft)	Total Pressure above trans. (psi)	Pressure at Step (psi)	Pressure at Step (ft of water)
28.3	21	Riser	1	0.25	2.72	-0.02	-0.05
	21	Riser	2	0.75	2.71	0.18	0.42
	22	Tread	3	1.25	2.67	0.22	0.50
	22	Tread	4	1.75	2.64	0.18	0.42
	22	Tread	5	2.25	2.93	0.47	1.09
	22	Tread	6	2.75	3.31	0.86	1.98
	22	Riser	7	3.25	2.22	-0.12	-0.27
	22	Riser	8	3.75	2.20	0.07	0.15
	23	Tread	9	4.25	2.18	0.16	0.37
	23	Tread	10	4.75	2.16	0.13	0.31
	23	Tread	11	5.25	2.32	0.30	0.69
	23	Tread	12	5.75	2.73	0.71	1.63
	23	Riser	13	6.25	1.87	-0.04	-0.09
	23	Riser	14	6.75	1.85	0.16	0.37
35.4	21	Riser	1	0.25	2.75	0.01	0.02
	21	Riser	2	0.75	2.74	0.21	0.48
	22	Tread	3	1.25	2.69	0.24	0.55
	22	Tread	4	1.75	2.65	0.19	0.44
	22	Tread	5	2.25	2.98	0.52	1.20
	22	Tread	6	2.75	3.40	0.94	2.18
	22	Riser	7	3.25	2.29	-0.05	-0.12
	22	Riser	8	3.75	2.21	0.08	0.19
	23	Tread	9	4.25	2.18	0.16	0.36
	23	Tread	10	4.75	2.16	0.14	0.31
	23	Tread	11	5.25	2.32	0.30	0.68
	23	Tread	12	5.75	2.83	0.81	1.86
	23	Riser	13	6.25	1.91	0.00	0.00
	23	Riser	14	6.75	1.88	0.20	0.45
41.0	21	Riser	1	0.25	2.76	0.02	0.04
	21	Riser	2	0.75	2.74	0.21	0.48
	22	Tread	3	1.25	2.70	0.24	0.55
	22	Tread	4	1.75	2.63	0.17	0.40
	22	Tread	5	2.25	3.09	0.63	1.46
	22	Tread	6	2.75	3.44	0.98	2.26
	22	Riser	7	3.25	2.25	-0.09	-0.21
	22	Riser	8	3.75	2.22	0.09	0.21
	23	Tread	9	4.25	2.17	0.15	0.34
	23	Tread	10	4.75	2.15	0.12	0.28
	23	Tread	11	5.25	2.30	0.28	0.64
	23	Tread	12	5.75	2.88	0.86	1.97
	23	Riser	13	6.25	1.91	0.00	0.00
	23	Riser	14	6.75	1.87	0.18	0.42

Stepped Spillway Tests, h = 1 ft

Discharge (cfs)	Step Number	Tap Location	Tap Number	Distance along step (ft)	Total Pressure above trans. (psi)	Pressure at Step (psi)	Pressure at Step (ft of water)
60.0	21	Riser	1	0.25	2.78	0.03	0.08
	21	Riser	2	0.75	2.79	0.26	0.59
	22	Tread	3	1.25	2.67	0.21	0.50
	22	Tread	4	1.75	2.65	0.19	0.45
	22	Tread	5	2.25	3.28	0.82	1.90
	22	Tread	6	2.75	3.50	1.04	2.40
	22	Riser	7	3.25	2.25	-0.09	-0.21
	22	Riser	8	3.75	2.22	0.09	0.22
	23	Tread	9	4.25	2.15	0.12	0.29
	23	Tread	10	4.75	2.10	0.08	0.17
	23	Tread	11	5.25	2.29	0.26	0.61
	23	Tread	12	5.75	2.96	0.94	2.16
	23	Riser	13	6.25	1.92	0.02	0.04
	23	Riser	14	6.75	1.88	0.19	0.44
80.0	21	Riser	1	0.25	2.84	0.09	0.21
	21	Riser	2	0.75	2.83	0.30	0.69
	22	Tread	3	1.25	2.76	0.30	0.70
	22	Tread	4	1.75	2.71	0.26	0.59
	22	Tread	5	2.25	3.44	0.99	2.28
	22	Tread	6	2.75	3.53	1.08	2.49
	22	Riser	7	3.25	2.20	-0.14	-0.32
	22	Riser	8	3.75	2.27	0.14	0.32
	23	Tread	9	4.25	2.19	0.17	0.40
	23	Tread	10	4.75	2.05	0.03	0.06
	23	Tread	11	5.25	2.51	0.49	1.12
	23	Tread	12	5.75	3.29	1.27	2.92
	23	Riser	13	6.25	1.97	0.07	0.16
	23	Riser	14	6.75	1.96	0.27	0.63
100.0	21	Riser	1	0.25	2.87	0.13	0.29
	21	Riser	2	0.75	2.92	0.38	0.88
	22	Tread	3	1.25	2.77	0.32	0.73
	22	Tread	4	1.75	2.85	0.39	0.91
	22	Tread	5	2.25	3.48	1.03	2.37
	22	Tread	6	2.75	3.59	1.13	2.61
	22	Riser	7	3.25	2.27	-0.06	-0.15
	22	Riser	8	3.75	2.21	0.08	0.19
	23	Tread	9	4.25	2.17	0.15	0.34
	23	Tread	10	4.75	1.98	-0.04	-0.09
	23	Tread	11	5.25	2.45	0.43	0.98
	23	Tread	12	5.75	3.20	1.18	2.73
	23	Riser	13	6.25	1.99	0.08	0.19
	23	Riser	14	6.75	2.00	0.31	0.72

Stepped Spillway Tests, h = 1 ft

Discharge (cfs)	Step Number	Tap Location	Tap Number	Distance along step (ft)	Total Pressure above trans. (psi)	Pressure at Step (psi)	Pressure at Step (ft of water)
114.0	21	Riser	1	0.25	2.95	0.21	0.48
	21	Riser	2	0.75	2.97	0.44	1.02
	22	Tread	3	1.25	2.84	0.39	0.89
	22	Tread	4	1.75	2.72	0.26	0.61
	22	Tread	5	2.25	3.48	1.03	2.37
	22	Tread	6	2.75	3.61	1.15	2.66
	22	Riser	7	3.25	2.21	-0.13	-0.29
	22	Riser	8	3.75	2.12	-0.01	-0.02
	23	Tread	9	4.25	2.13	0.11	0.25
	23	Tread	10	4.75	1.97	-0.05	-0.11
	23	Tread	11	5.25	2.74	0.72	1.66
	23	Tread	12	5.75	3.44	1.42	3.27
	23	Riser	13	6.25	1.99	0.09	0.20
	23	Riser	14	6.75	2.09	0.40	0.92

Stepped Spillway Tests, h = 1 ft

Discharge (cfs)	Step Number	Tap Location	Tap Number	Distance along step (ft)	Total Pressure above trans. (psi)	Pressure at Step (psi)	Pressure at Step (ft of water)
7.1	39	Riser	1	0.25			
	39	Riser	2	0.75	2.25	0.02	0.05
	40	Tread	3	1.25	2.29	0.15	0.35
	40	Tread	4	1.75	2.28	0.14	0.32
	40	Tread	5	2.25	2.39	0.25	0.58
	40	Tread	6	2.75	2.39	0.25	0.58
	40	Riser	7	3.25	2.03	0.01	0.03
	40	Riser	8	3.75	1.67	-0.14	-0.33
	41	Tread	9	4.25	1.74	0.04	0.10
	41	Tread	10	4.75	1.74	0.04	0.09
	41	Tread	11	5.25	1.74	0.04	0.09
	41	Tread	12	5.75	1.86	0.15	0.35
	41	Riser	13	6.25	1.60	0.00	0.01
	41	Riser	14	6.75	1.39	0.02	0.04
14.1	39	Riser	1	0.25			
	39	Riser	2	0.75	2.33	0.09	0.22
	40	Tread	3	1.25	2.33	0.19	0.44
	40	Tread	4	1.75	2.33	0.19	0.43
	40	Tread	5	2.25	2.39	0.25	0.57
	40	Tread	6	2.75	2.62	0.48	1.10
	40	Riser	7	3.25	2.09	0.07	0.17
	40	Riser	8	3.75	1.80	-0.01	-0.02
	41	Tread	9	4.25	1.75	0.04	0.10
	41	Tread	10	4.75	1.74	0.04	0.10
	41	Tread	11	5.25	1.73	0.03	0.08
	41	Tread	12	5.75	1.86	0.16	0.37
	41	Riser	13	6.25	1.58	-0.01	-0.03
	41	Riser	14	6.75	1.46	0.08	0.19
21.2	39	Riser	1	0.25	2.45	0.00	0.01
	39	Riser	2	0.75	2.44	0.20	0.47
	40	Tread	3	1.25	2.41	0.27	0.62
	40	Tread	4	1.75	2.38	0.24	0.55
	40	Tread	5	2.25	2.57	0.43	1.00
	40	Tread	6	2.75	2.78	0.64	1.48
	40	Riser	7	3.25	2.16	0.14	0.31
	40	Riser	8	3.75	1.96	0.15	0.34
	41	Tread	9	4.25	1.95	0.25	0.58
	41	Tread	10	4.75	1.94	0.24	0.55
	41	Tread	11	5.25	2.02	0.32	0.73
	41	Tread	12	5.75	2.30	0.60	1.38
	41	Riser	13	6.25	1.58	-0.02	-0.04
	41	Riser	14	6.75	1.57	0.19	0.44

Stepped Spillway Tests, h = 1 ft

Discharge (cfs)	Step Number	Tap Location	Tap Number	Distance along step (ft)	Total Pressure above trans. (psi)	Pressure at Step (psi)	Pressure at Step (ft of water)
41.0	39	Riser	1	0.25	2.53	0.08	0.19
	39	Riser	2	0.75	2.51	0.27	0.63
	40	Tread	3	1.25	2.47	0.33	0.75
	40	Tread	4	1.75	2.42	0.28	0.65
	40	Tread	5	2.25	2.76	0.62	1.44
	40	Tread	6	2.75	3.17	1.03	2.37
	40	Riser	7	3.25	2.17	0.15	0.35
	40	Riser	8	3.75	1.95	0.14	0.33
	41	Tread	9	4.25	1.93	0.23	0.53
	41	Tread	10	4.75	1.89	0.19	0.44
	41	Tread	11	5.25	2.11	0.41	0.94
	41	Tread	12	5.75	2.62	0.92	2.13
	41	Riser	13	6.25	1.64	0.05	0.11
	41	Riser	14	6.75	1.59	0.21	0.50
60.0	39	Riser	1	0.25	2.56	0.11	0.24
	39	Riser	2	0.75	2.51	0.28	0.64
	40	Tread	3	1.25	2.44	0.30	0.70
	40	Tread	4	1.75	2.41	0.27	0.62
	40	Tread	5	2.25	2.98	0.84	1.95
	40	Tread	6	2.75	3.28	1.14	2.63
	40	Riser	7	3.25	2.10	0.08	0.18
	40	Riser	8	3.75	1.92	0.11	0.26
	41	Tread	9	4.25	1.90	0.19	0.45
	41	Tread	10	4.75	1.83	0.12	0.29
	41	Tread	11	5.25	2.16	0.46	1.05
	41	Tread	12	5.75	2.80	1.10	2.54
	41	Riser	13	6.25	1.64	0.05	0.11
	41	Riser	14	6.75	1.58	0.21	0.48
80.0	39	Riser	1	0.25	2.51	0.06	0.15
	39	Riser	2	0.75	2.54	0.31	0.71
	40	Tread	3	1.25	2.45	0.31	0.71
	40	Tread	4	1.75	2.48	0.34	0.78
	40	Tread	5	2.25	2.95	0.81	1.88
	40	Tread	6	2.75	3.37	1.23	2.83
	40	Riser	7	3.25	2.06	0.04	0.09
	40	Riser	8	3.75	1.89	0.08	0.19
	41	Tread	9	4.25	1.89	0.18	0.42
	41	Tread	10	4.75	1.80	0.10	0.23
	41	Tread	11	5.25	2.33	0.63	1.45
	41	Tread	12	5.75	2.92	1.22	2.81
	41	Riser	13	6.25	1.68	0.09	0.21
	41	Riser	14	6.75	1.62	0.24	0.55

Stepped Spillway Tests, h = 1 ft

Discharge (cfs)	Step Number	Tap Location	Tap Number	Distance along step (ft)	Total Pressure above trans. (psi)	Pressure at Step (psi)	Pressure at Step (ft of water)
100.0	39	Riser	1	0.25	2.58	0.13	0.30
	39	Riser	2	0.75	2.50	0.27	0.62
	40	Tread	3	1.25	2.44	0.30	0.70
	40	Tread	4	1.75	2.42	0.28	0.65
	40	Tread	5	2.25	3.15	1.01	2.33
	40	Tread	6	2.75	3.40	1.27	2.92
	40	Riser	7	3.25	2.10	0.08	0.19
	40	Riser	8	3.75	1.87	0.06	0.13
	41	Tread	9	4.25	1.83	0.12	0.29
	41	Tread	10	4.75	1.76	0.05	0.12
	41	Tread	11	5.25	2.29	0.59	1.36
	41	Tread	12	5.75	2.98	1.28	2.95
	41	Riser	13	6.25	1.69	0.09	0.21
	41	Riser	14	6.75	1.60	0.22	0.51

Stepped Spillway Tests, h = 2 ft

Discharge (cfs)	Step Number	Tap Location	Tap Number	Distance along step (ft)	Total Pressure above trans. (psi)	Pressure at Step (psi)	Pressure at Step (ft of water)
20.0	1	Riser	1	0.25	2.16	-0.13	-0.30
	1	Riser	2	0.75	1.66	-0.42	-0.96
	1	Riser	3	1.25	1.86	0.01	0.02
	1	Riser	4	1.75	1.84	0.20	0.47
	2	Tread	5	2.25	1.84	0.31	0.72
	2	Tread	6	2.75	1.82	0.29	0.68
	2	Tread	7	3.25	1.84	0.30	0.70
	2	Tread	8	3.75	1.84	0.31	0.71
	2	Tread	9	4.25	1.83	0.30	0.69
	2	Tread	10	4.75	1.84	0.31	0.71
	2	Tread	11	5.25	1.87	0.34	0.79
	2	Tread	12	5.75	2.20	0.67	1.53
	2	Riser	13	6.25	1.39	-0.03	-0.06
	2	Riser	14	6.75	1.17	-0.04	-0.09
	2	Riser	15	7.25	0.96	-0.02	-0.05
	2	Riser	16	7.75	1.03	0.26	0.60
40.0	1	Riser	1	0.25	2.08	-0.21	-0.48
	1	Riser	2	0.75	2.06	-0.02	-0.05
	1	Riser	3	1.25	2.02	0.16	0.38
	1	Riser	4	1.75	2.05	0.42	0.96
	2	Tread	5	2.25	2.05	0.52	1.20
	2	Tread	6	2.75	2.01	0.48	1.11
	2	Tread	7	3.25	2.01	0.48	1.10
	2	Tread	8	3.75	1.98	0.45	1.04
	2	Tread	9	4.25	2.07	0.54	1.24
	2	Tread	10	4.75	2.32	0.79	1.82
	2	Tread	11	5.25	2.46	0.93	2.16
	2	Tread	12	5.75	2.23	0.70	1.61
	2	Riser	13	6.25	1.26	-0.16	-0.37
	2	Riser	14	6.75	1.20	-0.01	-0.02
	2	Riser	15	7.25	1.17	0.19	0.43
	2	Riser	16	7.75	1.18	0.41	0.94
60.0	1	Riser	1	0.25	2.07	-0.22	-0.50
	1	Riser	2	0.75	2.03	-0.05	-0.10
	1	Riser	3	1.25	2.01	0.16	0.37
	1	Riser	4	1.75	2.04	0.40	0.92
	2	Tread	5	2.25	1.99	0.46	1.06
	2	Tread	6	2.75	1.98	0.45	1.03
	2	Tread	7	3.25	1.92	0.39	0.90
	2	Tread	8	3.75	1.90	0.37	0.84
	2	Tread	9	4.25	2.01	0.48	1.10
	2	Tread	10	4.75	2.30	0.77	1.78
	2	Tread	11	5.25	2.65	1.12	2.58
	2	Tread	12	5.75	2.49	0.96	2.20
	2	Riser	13	6.25	1.45	0.03	0.06
	2	Riser	14	6.75	1.39	0.18	0.42
	2	Riser	15	7.25	1.40	0.42	0.96
	2	Riser	16	7.75	1.47	0.70	1.63

Stepped Spillway Tests, h = 2 ft

Discharge (cfs)	Step Number	Tap Location	Tap Number	Distance along step (ft)	Total Pressure above trans. (psi)	Pressure at Step (psi)	Pressure at Step (ft of water)
80.0	1	Riser	1	0.25	2.07	-0.23	-0.52
	1	Riser	2	0.75	2.02	-0.06	-0.14
	1	Riser	3	1.25	2.00	0.15	0.34
	1	Riser	4	1.75	2.05	0.42	0.96
	2	Tread	5	2.25	2.00	0.47	1.07
	2	Tread	6	2.75	1.96	0.43	1.00
	2	Tread	7	3.25	1.87	0.34	0.78
	2	Tread	8	3.75	1.86	0.33	0.76
	2	Tread	9	4.25	1.94	0.41	0.94
	2	Tread	10	4.75	2.25	0.72	1.66
	2	Tread	11	5.25	2.75	1.22	2.82
	2	Tread	12	5.75	2.80	1.27	2.92
	2	Riser	13	6.25	1.61	0.19	0.43
	2	Riser	14	6.75	1.50	0.30	0.68
	2	Riser	15	7.25	1.54	0.55	1.28
	2	Riser	16	7.75	1.63	0.86	1.98
100.0	1	Riser	1	0.25	2.06	-0.24	-0.55
	1	Riser	2	0.75	1.98	-0.10	-0.23
	1	Riser	3	1.25	1.99	0.13	0.31
	1	Riser	4	1.75	2.03	0.39	0.90
	2	Tread	5	2.25	1.97	0.44	1.02
	2	Tread	6	2.75	1.93	0.40	0.93
	2	Tread	7	3.25	1.82	0.29	0.67
	2	Tread	8	3.75	1.80	0.27	0.62
	2	Tread	9	4.25	1.86	0.33	0.75
	2	Tread	10	4.75	2.14	0.61	1.41
	2	Tread	11	5.25	2.78	1.25	2.89
	2	Tread	12	5.75	2.92	1.39	3.21
	2	Riser	13	6.25	1.71	0.29	0.66
	2	Riser	14	6.75	1.66	0.46	1.05
	2	Riser	15	7.25	1.67	0.68	1.57
	2	Riser	16	7.75	1.78	1.02	2.35
120.0	1	Riser	1	0.25	2.06	-0.23	-0.53
	1	Riser	2	0.75	1.99	-0.08	-0.20
	1	Riser	3	1.25	2.00	0.15	0.34
	1	Riser	4	1.75	2.05	0.41	0.96
	2	Tread	5	2.25	1.98	0.45	1.05
	2	Tread	6	2.75	1.94	0.41	0.95
	2	Tread	7	3.25	1.85	0.32	0.73
	2	Tread	8	3.75	1.83	0.30	0.69
	2	Tread	9	4.25	1.87	0.34	0.79
	2	Tread	10	4.75	2.23	0.70	1.61
	2	Tread	11	5.25	2.81	1.28	2.95
	2	Tread	12	5.75	3.04	1.51	3.49
	2	Riser	13	6.25	1.86	0.44	1.01
	2	Riser	14	6.75	1.78	0.57	1.32
	2	Riser	15	7.25	1.71	0.72	1.67
	2	Riser	16	7.75	1.90	1.13	2.62

Stepped Spillway Tests, h = 2 ft

Discharge (cfs)	Step Number	Tap Location	Tap Number	Distance along step (ft)	Total Pressure above trans. (psi)	Pressure at Step (psi)	Pressure at Step (ft of water)
20.0	11	Riser	1	0.25	2.88	0.11	0.26
	11	Riser	2	0.75	2.66	0.11	0.26
	11	Riser	3	1.25	2.43	0.10	0.24
	11	Riser	4	1.75	2.32	0.21	0.48
	12	Tread	5	2.25	2.29	0.28	0.64
	12	Tread	6	2.75	2.32	0.31	0.71
	12	Tread	7	3.25	2.31	0.30	0.69
	12	Tread	8	3.75	2.29	0.28	0.64
	12	Tread	9	4.25	2.31	0.30	0.68
	12	Tread	10	4.75	2.31	0.29	0.67
	12	Tread	11	5.25	2.62	0.60	1.38
	12	Tread	12	5.75	2.63	0.60	1.39
	12	Riser	13	6.25	2.00	0.09	0.20
	12	Riser	14	6.75	1.78	0.08	0.18
	12	Riser	15	7.25	1.56	0.08	0.19
	12	Riser	16	7.75	1.51	0.25	0.58
40.0	11	Riser	1	0.25	2.67	-0.10	-0.22
	11	Riser	2	0.75	2.54	0.00	0.00
	11	Riser	3	1.25	2.53	0.20	0.46
	11	Riser	4	1.75	2.55	0.44	1.02
	12	Tread	5	2.25	2.53	0.52	1.20
	12	Tread	6	2.75	2.54	0.53	1.23
	12	Tread	7	3.25	2.54	0.53	1.22
	12	Tread	8	3.75	2.52	0.51	1.18
	12	Tread	9	4.25	2.50	0.48	1.11
	12	Tread	10	4.75	2.80	0.78	1.80
	12	Tread	11	5.25	3.07	1.05	2.41
	12	Tread	12	5.75	2.91	0.88	2.03
	12	Riser	13	6.25	1.83	-0.08	-0.20
	12	Riser	14	6.75	1.70	0.00	0.00
	12	Riser	15	7.25	1.67	0.19	0.44
	12	Riser	16	7.75	1.67	0.40	0.93
60.0	11	Riser	1	0.25	2.69	-0.08	-0.18
	11	Riser	2	0.75	2.55	0.01	0.02
	11	Riser	3	1.25	2.50	0.17	0.39
	11	Riser	4	1.75	2.50	0.38	0.89
	12	Tread	5	2.25	2.58	0.56	1.30
	12	Tread	6	2.75	2.52	0.51	1.17
	12	Tread	7	3.25	2.44	0.42	0.98
	12	Tread	8	3.75	2.52	0.51	1.17
	12	Tread	9	4.25	2.89	0.87	2.01
	12	Tread	10	4.75	3.29	1.28	2.95
	12	Tread	11	5.25	3.26	1.24	2.85
	12	Tread	12	5.75	3.03	1.00	2.32
	12	Riser	13	6.25	1.83	-0.09	-0.20
	12	Riser	14	6.75	1.75	0.05	0.12
	12	Riser	15	7.25	1.71	0.22	0.52
	12	Riser	16	7.75	1.76	0.50	1.15

Stepped Spillway Tests, h = 2 ft

Discharge (cfs)	Step Number	Tap Location	Tap Number	Distance along step (ft)	Total Pressure above trans. (psi)	Pressure at Step (psi)	Pressure at Step (ft of water)
80.0	11	Riser	1	0.25	2.70	-0.06	-0.14
	11	Riser	2	0.75	2.59	0.05	0.12
	11	Riser	3	1.25	2.54	0.21	0.48
	11	Riser	4	1.75	2.65	0.54	1.24
	12	Tread	5	2.25	2.56	0.55	1.27
	12	Tread	6	2.75	2.49	0.48	1.10
	12	Tread	7	3.25	2.36	0.35	0.81
	12	Tread	8	3.75	2.39	0.38	0.87
	12	Tread	9	4.25	2.62	0.60	1.39
	12	Tread	10	4.75	3.20	1.18	2.72
	12	Tread	11	5.25	3.54	1.52	3.51
	12	Tread	12	5.75	3.43	1.40	3.22
	12	Riser	13	6.25	1.81	-0.10	-0.24
	12	Riser	14	6.75	1.74	0.04	0.10
	12	Riser	15	7.25	1.69	0.21	0.49
	12	Riser	16	7.75	1.76	0.49	1.14
100.0	11	Riser	1	0.25	2.74	-0.02	-0.05
	11	Riser	2	0.75	2.59	0.05	0.11
	11	Riser	3	1.25	2.54	0.21	0.49
	11	Riser	4	1.75	2.71	0.60	1.37
	12	Tread	5	2.25	2.58	0.57	1.31
	12	Tread	6	2.75	2.36	0.35	0.81
	12	Tread	7	3.25	2.28	0.27	0.62
	12	Tread	8	3.75	2.37	0.35	0.81
	12	Tread	9	4.25	2.69	0.67	1.55
	12	Tread	10	4.75	3.44	1.43	3.29
	12	Tread	11	5.25	4.06	2.04	4.71
	12	Tread	12	5.75	3.73	1.70	3.93
	12	Riser	13	6.25	1.85	-0.06	-0.14
	12	Riser	14	6.75	1.73	0.03	0.07
	12	Riser	15	7.25	1.69	0.21	0.48
	12	Riser	16	7.75	1.81	0.54	1.25
120.0	11	Riser	1	0.25	2.76	0.00	0.00
	11	Riser	2	0.75	2.54	0.00	0.00
	11	Riser	3	1.25	2.48	0.15	0.34
	11	Riser	4	1.75	2.77	0.66	1.53
	12	Tread	5	2.25	2.62	0.61	1.40
	12	Tread	6	2.75	2.32	0.31	0.71
	12	Tread	7	3.25	2.28	0.26	0.61
	12	Tread	8	3.75	2.40	0.39	0.90
	12	Tread	9	4.25	2.80	0.78	1.81
	12	Tread	10	4.75	3.68	1.67	3.85
	12	Tread	11	5.25	4.39	2.37	5.47
	12	Tread	12	5.75	4.05	2.02	4.66
	12	Riser	13	6.25	1.86	-0.06	-0.13
	12	Riser	14	6.75	1.68	-0.02	-0.05
	12	Riser	15	7.25	1.62	0.14	0.32
	12	Riser	16	7.75	1.84	0.58	1.34

Stepped Spillway Tests, h = 2 ft

Discharge (cfs)	Step Number	Tap Location	Tap Number	Distance along step (ft)	Total Pressure above trans. (psi)	Pressure at Step (psi)	Pressure at Step (ft of water)
20.0	20	Riser	1	0.25	2.50	0.07	0.17
	20	Riser	2	0.75	2.30	0.09	0.20
	20	Riser	3	1.25	2.09	0.10	0.23
	20	Riser	4	1.75	2.05	0.28	0.64
	21	Tread	5	2.25	2.05	0.37	0.86
	21	Tread	6	2.75	2.05	0.38	0.87
	21	Tread	7	3.25	2.07	0.38	0.88
	21	Tread	8	3.75	2.06	0.37	0.86
	21	Tread	9	4.25	2.04	0.36	0.82
	21	Tread	10	4.75	2.21	0.52	1.21
	21	Tread	11	5.25	2.48	0.80	1.84
	21	Tread	12	5.75	2.33	0.64	1.48
	21	Riser	13	6.25	1.70	0.13	0.29
	21	Riser	14	6.75	1.48	0.13	0.29
	21	Riser	15	7.25	1.26	0.13	0.29
	21	Riser	16	7.75	1.08	0.15	0.36
40.0	20	Riser	1	0.25	2.45	0.03	0.06
	20	Riser	2	0.75	2.34	0.13	0.30
	20	Riser	3	1.25	2.33	0.34	0.78
	20	Riser	4	1.75	2.33	0.56	1.29
	21	Tread	5	2.25	2.33	0.65	1.50
	21	Tread	6	2.75	2.34	0.66	1.52
	21	Tread	7	3.25	2.33	0.65	1.50
	21	Tread	8	3.75	2.31	0.63	1.46
	21	Tread	9	4.25	2.31	0.62	1.44
	21	Tread	10	4.75	2.50	0.82	1.89
	21	Tread	11	5.25	2.94	1.25	2.89
	21	Tread	12	5.75	2.76	1.07	2.47
	21	Riser	13	6.25	1.62	0.05	0.11
	21	Riser	14	6.75	1.42	0.07	0.15
	21	Riser	15	7.25	1.39	0.25	0.58
	21	Riser	16	7.75	1.38	0.46	1.07
60.0	20	Riser	1	0.25	2.47	0.05	0.11
	20	Riser	2	0.75	2.38	0.17	0.40
	20	Riser	3	1.25	2.46	0.47	1.08
	20	Riser	4	1.75	2.48	0.70	1.61
	21	Tread	5	2.25	2.39	0.71	1.65
	21	Tread	6	2.75	2.31	0.63	1.46
	21	Tread	7	3.25	2.30	0.61	1.41
	21	Tread	8	3.75	2.37	0.69	1.59
	21	Tread	9	4.25	2.47	0.78	1.80
	21	Tread	10	4.75	2.69	1.01	2.33
	21	Tread	11	5.25	3.04	1.35	3.13
	21	Tread	12	5.75	2.79	1.10	2.53
	21	Riser	13	6.25	1.57	0.00	0.00
	21	Riser	14	6.75	1.52	0.17	0.39
	21	Riser	15	7.25	1.57	0.44	1.01
	21	Riser	16	7.75	1.57	0.65	1.50

Stepped Spillway Tests, h = 2 ft

Discharge (cfs)	Step Number	Tap Location	Tap Number	Distance along step (ft)	Total Pressure above trans. (psi)	Pressure at Step (psi)	Pressure at Step (ft of water)
80.0	20	Riser	1	0.25	2.49	0.07	0.16
	20	Riser	2	0.75	2.41	0.20	0.46
	20	Riser	3	1.25	2.46	0.47	1.08
	20	Riser	4	1.75	2.32	0.54	1.25
	21	Tread	5	2.25	2.31	0.64	1.47
	21	Tread	6	2.75	2.27	0.60	1.37
	21	Tread	7	3.25	2.23	0.55	1.27
	21	Tread	8	3.75	2.27	0.58	1.35
	21	Tread	9	4.25	2.49	0.81	1.87
	21	Tread	10	4.75	3.23	1.54	3.56
	21	Tread	11	5.25	3.49	1.80	4.17
	21	Tread	12	5.75	3.18	1.49	3.43
	21	Riser	13	6.25	1.65	0.08	0.18
	21	Riser	14	6.75	1.55	0.19	0.45
	21	Riser	15	7.25	1.56	0.42	0.97
	21	Riser	16	7.75	1.54	0.61	1.42
100.0	20	Riser	1	0.25	2.50	0.07	0.16
	20	Riser	2	0.75	2.40	0.19	0.43
	20	Riser	3	1.25	2.37	0.37	0.86
	20	Riser	4	1.75	2.45	0.67	1.55
	21	Tread	5	2.25	2.35	0.67	1.55
	21	Tread	6	2.75	2.21	0.53	1.22
	21	Tread	7	3.25	2.10	0.42	0.97
	21	Tread	8	3.75	2.14	0.46	1.06
	21	Tread	9	4.25	2.40	0.72	1.65
	21	Tread	10	4.75	3.02	1.33	3.08
	21	Tread	11	5.25	3.80	2.12	4.89
	21	Tread	12	5.75	3.57	1.88	4.33
	21	Riser	13	6.25	1.60	0.02	0.06
	21	Riser	14	6.75	1.48	0.13	0.30
	21	Riser	15	7.25	1.46	0.33	0.75
	21	Riser	16	7.75	1.53	0.61	1.40
120.0	20	Riser	1	0.25	2.54	0.11	0.27
	20	Riser	2	0.75	2.39	0.18	0.41
	20	Riser	3	1.25	2.36	0.37	0.85
	20	Riser	4	1.75	2.52	0.74	1.71
	21	Tread	5	2.25	2.40	0.72	1.67
	21	Tread	6	2.75	2.19	0.51	1.17
	21	Tread	7	3.25	2.06	0.38	0.87
	21	Tread	8	3.75	2.10	0.42	0.96
	21	Tread	9	4.25	2.43	0.75	1.72
	21	Tread	10	4.75	3.19	1.51	3.48
	21	Tread	11	5.25	4.03	2.35	5.42
	21	Tread	12	5.75	3.92	2.23	5.16
	21	Riser	13	6.25	1.62	0.05	0.12
	21	Riser	14	6.75	1.48	0.12	0.28
	21	Riser	15	7.25	1.42	0.28	0.66
	21	Riser	16	7.75	1.58	0.66	1.53

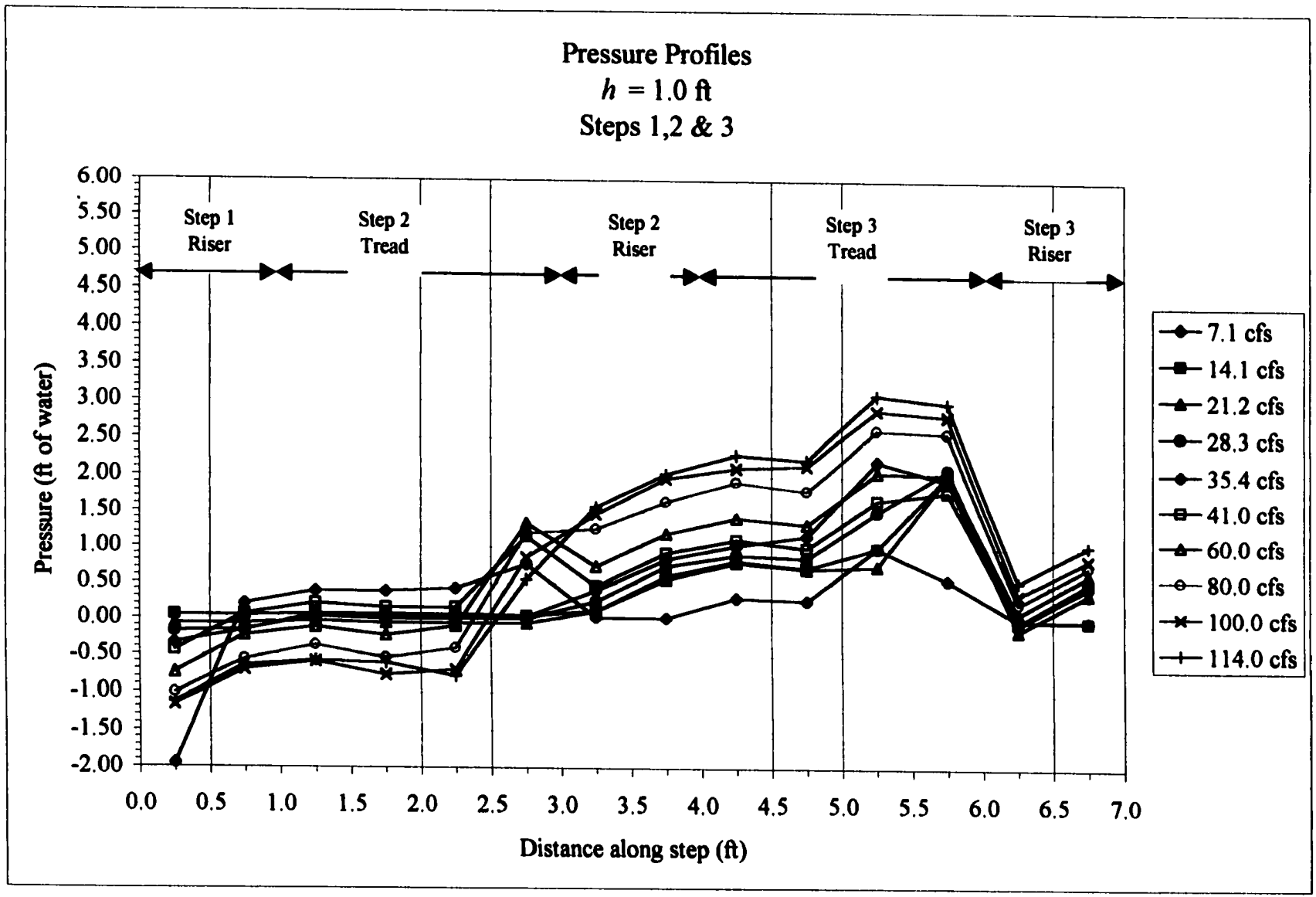

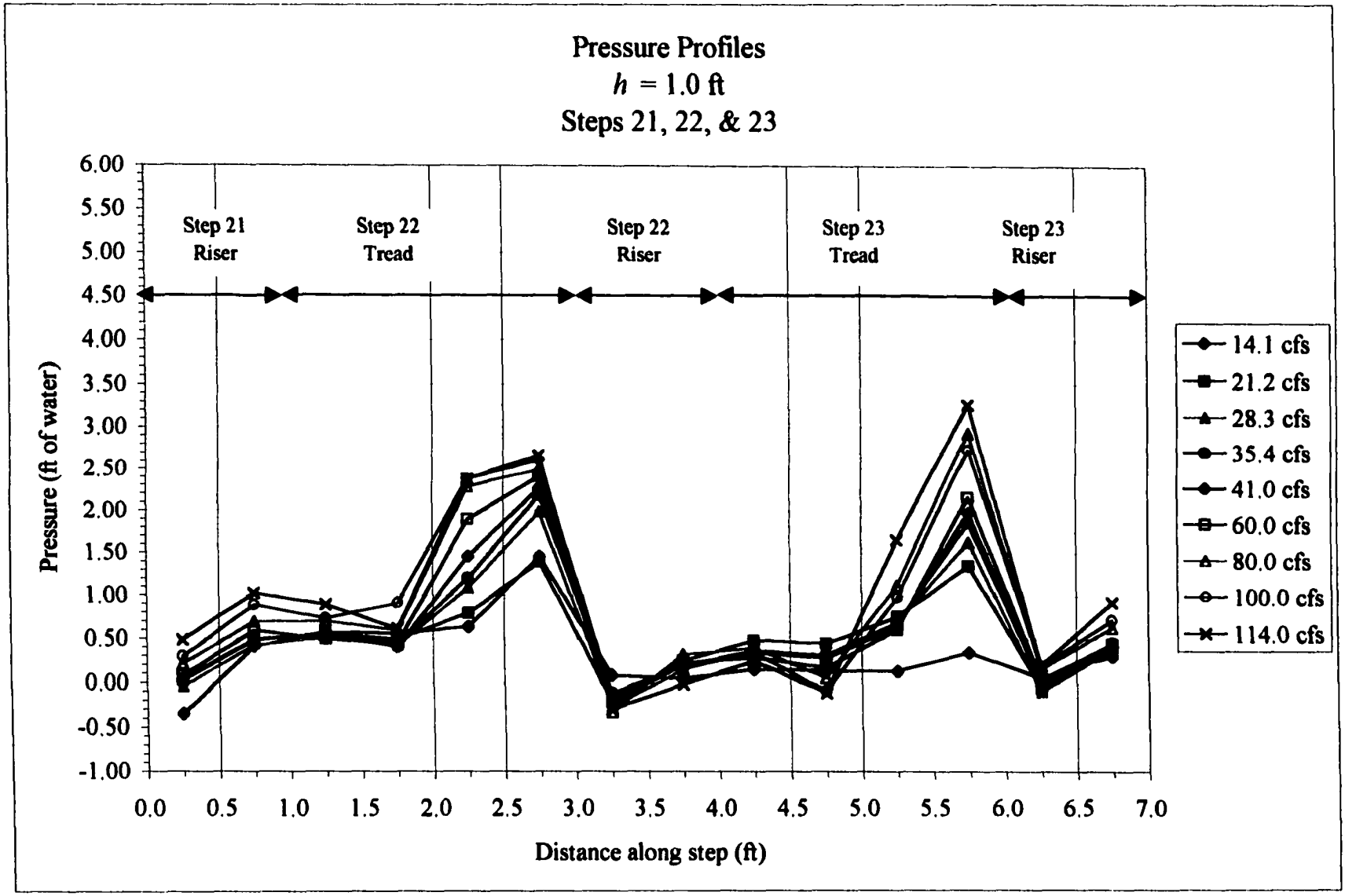

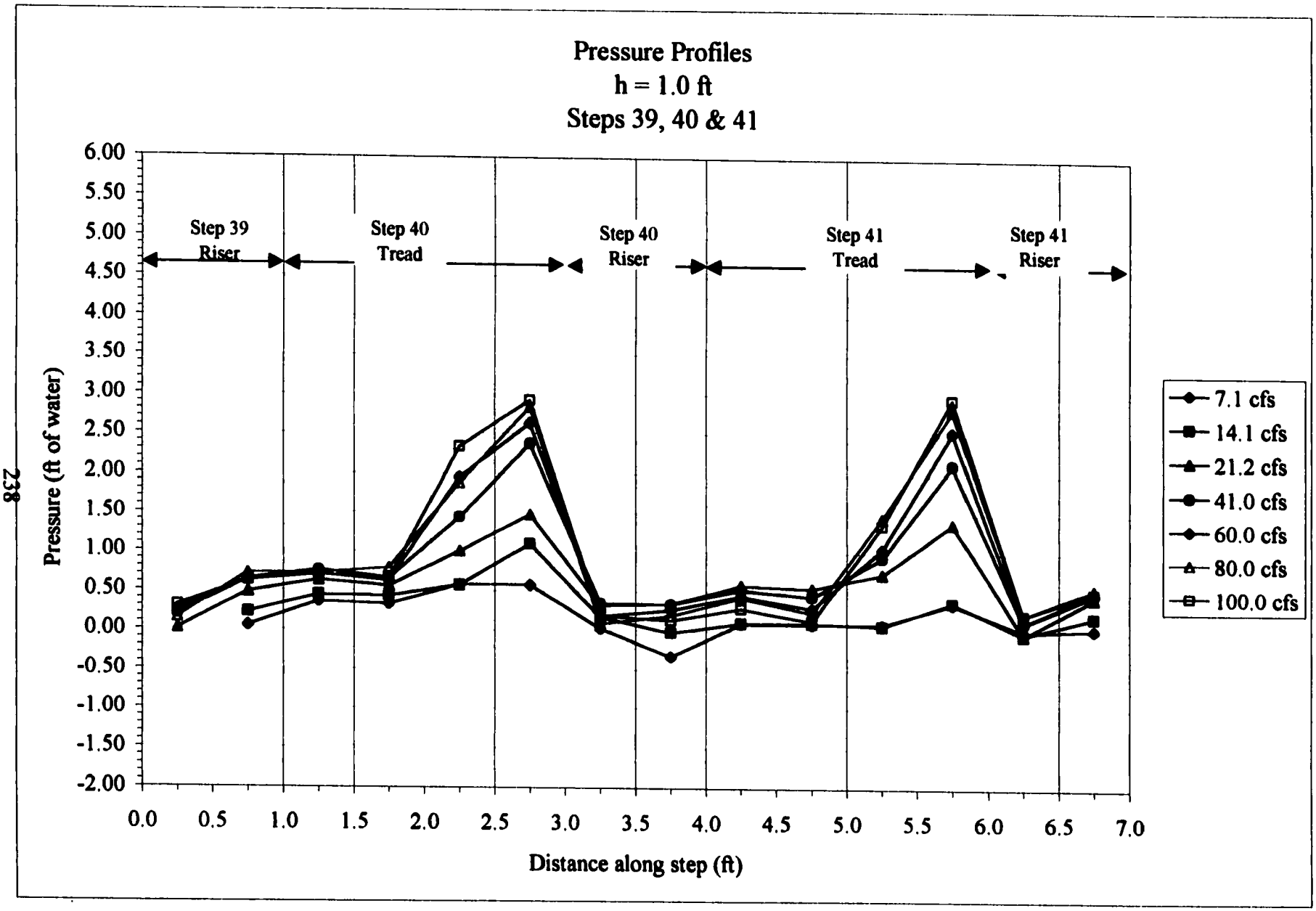

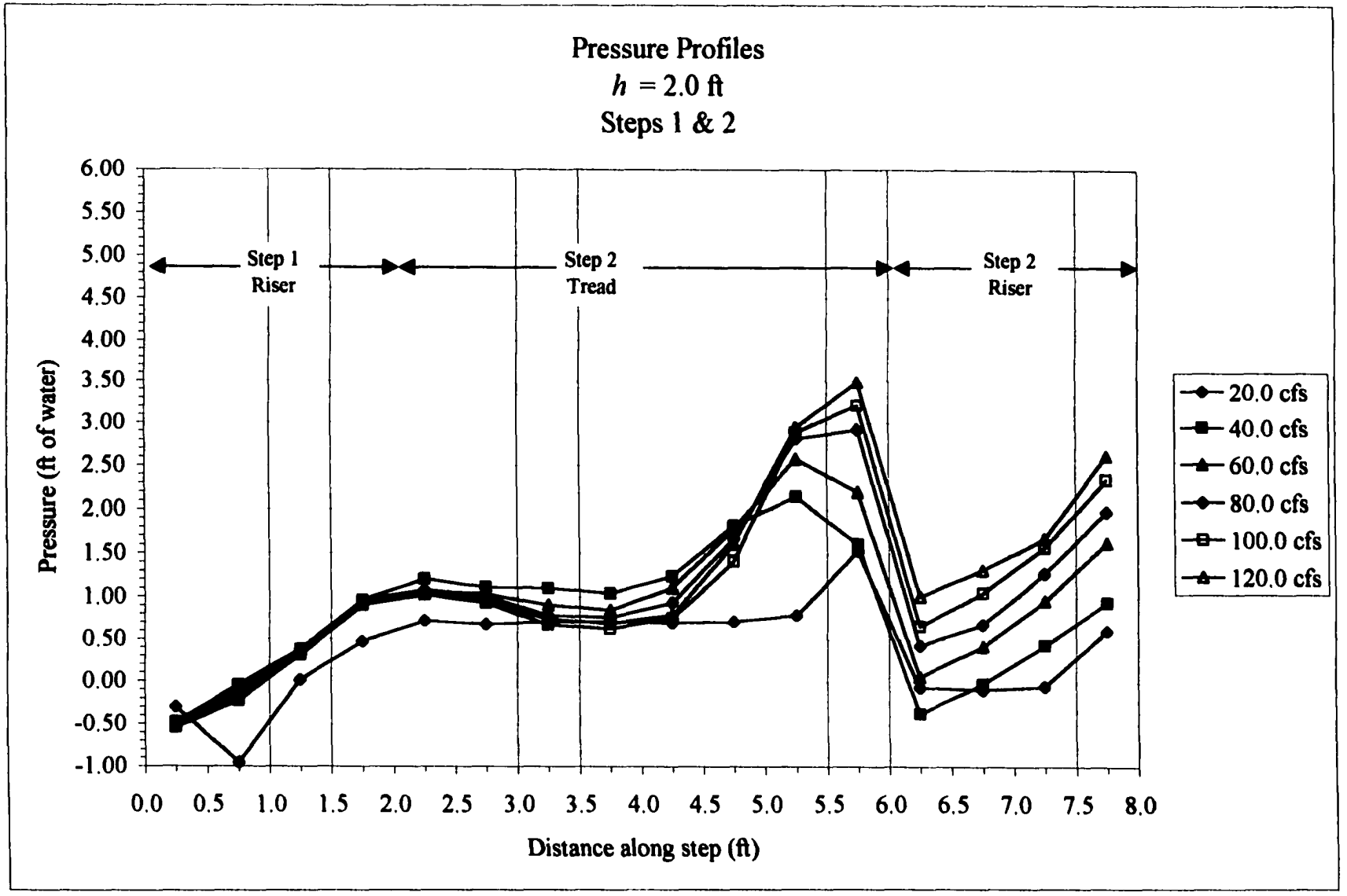

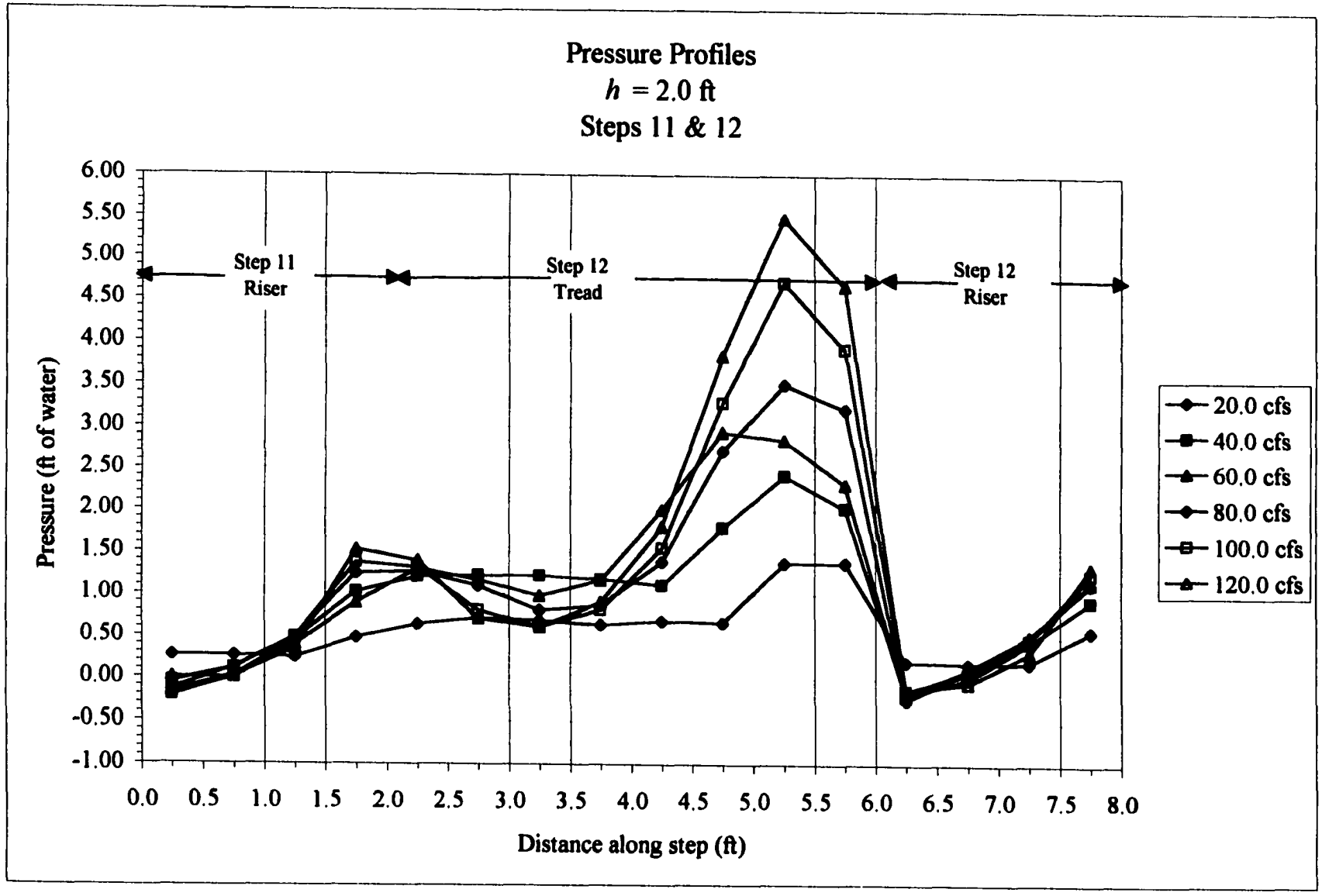

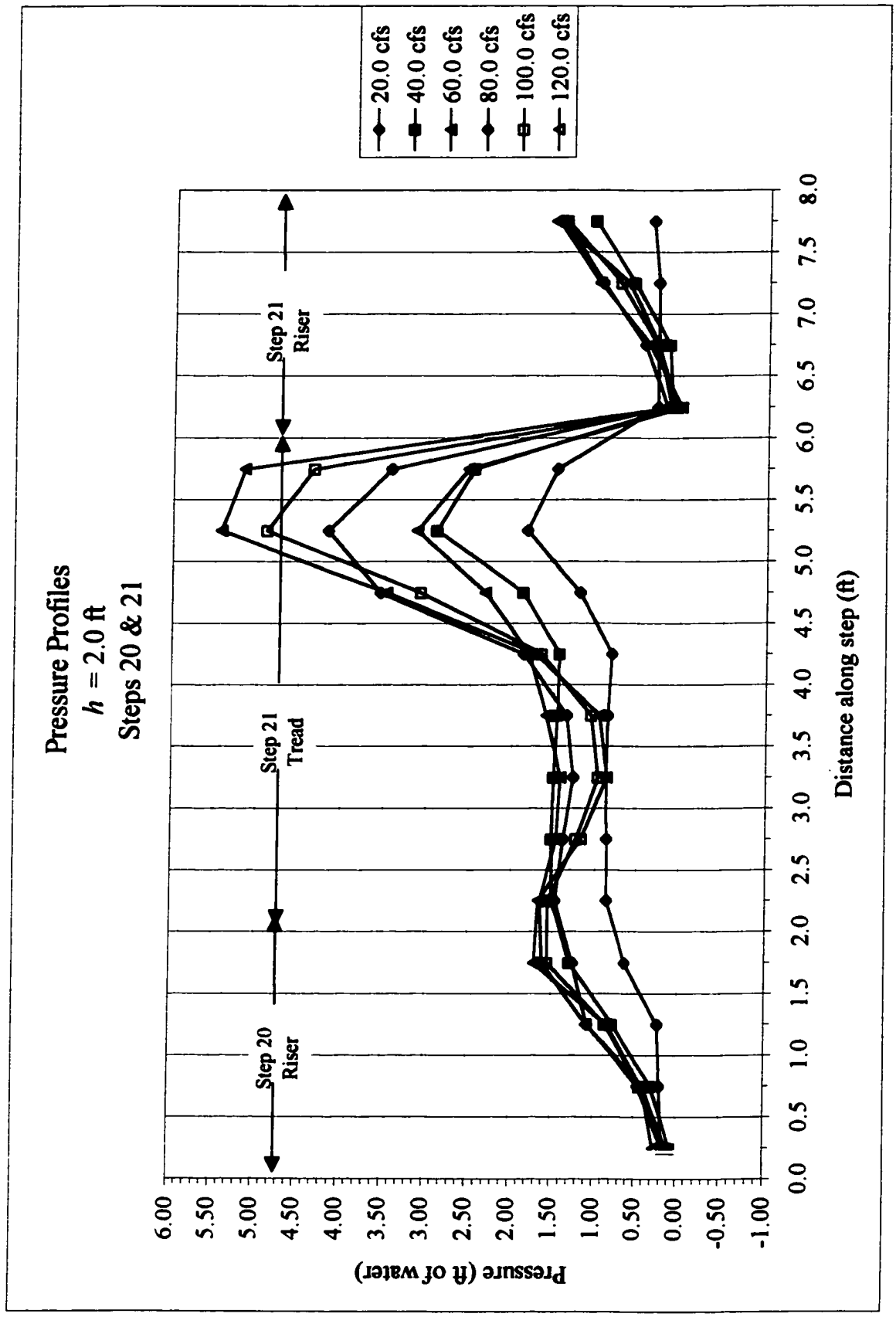

APPENDIX D

DESIGN EXAMPLE

STANDARD STEP METHOD COMPUTATIONS

Standard Step Method; Stepped Spillway Design Example

q = 25 cfs/ft θ = 26.6° step height h = 1.0 ft

Step Number N	Height H (ft)	Nh/yc	friction factor f	Station s (ft)	Δs (ft)	d_w (ft)	U_{avg} (ft/s)	U_{avg}^2/2g (ft)	S_f	Avg. S_f	S_o	E	h_f	E	ΔE
1	0	0.00	0.25	0.0	0.0	2.69	9.29	1.34	0.03		0.50	4.03			
3	2	0.74	0.25	4.5	4.0	2.65	9.43	1.38	0.03	0.03	0.50	6.03	0.13	4.16	-0.13
5	4	1.49	0.25	8.9	4.0	1.54	16.25	4.10	0.17	0.10	0.50	7.64	0.40	6.04	-0.01
7	6	2.23	0.25	13.4	4.0	1.33	18.75	5.46	0.26	0.21	0.50	8.79	0.85	7.64	0.00
9	8	2.97	0.25	17.9	4.0	1.23	20.30	6.40	0.32	0.29	0.50	9.63	1.16	8.79	0.00
11	10	3.72	0.25	22.4	4.0	1.17	21.32	7.06	0.38	0.35	0.50	10.23	1.40	9.63	0.00
13	12	4.46	0.25	26.8	4.0	1.14	22.00	7.51	0.41	0.39	0.50	10.65	1.58	10.23	0.00
15	14	5.20	0.25	31.3	4.0	1.11	22.46	7.83	0.44	0.43	0.50	10.94	1.71	10.65	0.00
17	16	5.95	0.25	35.8	4.0	1.10	22.77	8.05	0.46	0.45	0.50	11.15	1.80	10.94	0.00
19	18	6.69	0.25	40.2	4.0	1.09	22.98	8.20	0.47	0.46	0.50	11.29	1.86	11.15	0.00
21	20	7.43	0.25	44.7	4.0	1.08	23.13	8.31	0.48	0.48	0.50	11.39	1.90	11.29	0.00
23	22	8.18	0.25	49.2	4.0	1.08	23.23	8.38	0.49	0.48	0.50	11.45	1.93	11.39	0.00
25	24	8.92	0.25	53.7	4.0	1.07	23.29	8.43	0.49	0.49	0.50	11.50	1.95	11.45	0.00
27	26	9.66	0.25	58.1	4.0	1.07	23.34	8.46	0.49	0.49	0.50	11.53	1.97	11.50	0.00
29	28	10.41	0.25	62.6	4.0	1.07	23.37	8.48	0.50	0.49	0.50	11.55	1.98	11.53	0.00
31	30	11.15	0.25	67.1	4.0	1.07	23.39	8.50	0.50	0.50	0.50	11.57	1.98	11.55	0.00
33	32	11.89	0.25	71.6	4.0	1.07	23.41	8.51	0.50	0.50	0.50	11.58	1.99	11.57	0.00
35	34	12.63	0.25	76.0	4.0	1.07	23.42	8.52	0.50	0.50	0.50	11.58	1.99	11.58	0.00
37	36	13.38	0.25	80.5	4.0	1.07	23.43	8.52	0.50	0.50	0.50	11.59	1.99	11.58	0.00
39	38	14.12	0.25	85.0	4.0	1.07	23.43	8.52	0.50	0.50	0.50	11.59	2.00	11.59	0.00
41	40	14.86	0.25	89.4	4.0	1.07	23.43	8.53	0.50	0.50	0.50	11.59	2.00	11.59	0.00

Bulking Coefficent; Stepped Spillway Design Example

Step Number N	Height H (ft)	Nh/yc	d_w (ft)	Bulking Coefficient s	y_{90} (ft)
1	0	0.00	2.69		
3	2	0.74	2.65		
5	4	1.49	1.54		
7	6	2.23	1.33		
9	8	2.97	1.23		
11	10	3.72	1.17	1.75	2.05
13	12	4.46	1.14	1.75	1.99
15	14	5.20	1.11	1.75	1.95
17	16	5.95	1.10	1.75	1.92
19	18	6.69	1.09	1.75	1.90
21	20	7.43	1.08	1.75	1.89
23	22	8.18	1.08	1.75	1.88
25	24	8.92	1.07	1.75	1.88
27	26	9.66	1.07	1.75	1.87
29	28	10.41	1.07	1.75	1.87
31	30	11.15	1.07	1.75	1.87
33	32	11.89	1.07	1.75	1.87
35	34	12.63	1.07	1.75	1.87
37	36	13.38	1.07	1.75	1.87
39	38	14.12	1.07	1.75	1.87
41	40	14.86	1.07	1.75	1.87

Energy Dissipation; Stepped Spillway Design Example

Step Number N	Height H (ft)	d_w (ft)	U_{avg} (ft/s)	Eo (ft)	E1 (ft)	Eo-E1 (ft)	Eo-E1 / Eo
1	0	2.69	9.29	4.04	4.04	0.00	0.00
3	2	2.65	9.43	6.04	3.75	2.29	0.38
5	4	1.54	16.25	8.04	5.48	2.56	0.32
7	6	1.33	18.75	10.04	6.65	3.38	0.34
9	8	1.23	20.30	12.04	7.50	4.53	0.38
11	10	1.17	21.32	14.04	8.11	5.93	0.42
13	12	1.14	22.00	16.04	8.53	7.51	0.47
15	14	1.11	22.46	18.04	8.83	9.21	0.51
17	16	1.10	22.77	20.04	9.03	11.00	0.55
19	18	1.09	22.98	22.04	9.17	12.86	0.58
21	20	1.08	23.13	24.04	9.27	14.78	0.61
23	22	1.08	23.23	26.04	9.34	16.70	0.64
25	24	1.07	23.29	28.04	9.39	18.65	0.67
27	26	1.07	23.34	30.04	9.42	20.62	0.69
29	28	1.07	23.37	32.04	9.44	22.60	0.71
31	30	1.07	23.39	34.04	9.45	24.58	0.72
33	32	1.07	23.41	36.04	9.46	26.57	0.74
35	34	1.07	23.42	38.04	9.47	28.57	0.75
37	36	1.07	23.43	40.04	9.48	30.56	0.76
39	38	1.07	23.43	42.04	9.48	32.56	0.77
41	40	1.07	23.43	44.04	9.48	34.56	0.78

Standard Step Method; Stepped Spillway Design Example
q = 25 cfs/ft θ = 26.6° step height *h* = 2.0 ft

Step Number N	Height H (ft)	Nh/yc	friction factor f	Station s (ft)	Δs (ft)	d_w (ft)	U_{avg} (ft/s)	U_{avg}^2/2g (ft)	S_f	Avg. S_f	S_o	E	h_f	E	ΔE
1	0	0.00	0.25	0.0	0.0	2.69	9.29	1.34	0.03		0.50	4.03			
2	2	0.74	0.25	4.5	4.0	2.65	9.43	1.38	0.03	0.03	0.50	6.03	0.13	4.16	-0.13
3	4	1.49	0.25	8.9	4.0	1.54	16.25	4.10	0.17	0.10	0.50	7.64	0.40	6.04	-0.01
4	6	2.23	0.25	13.4	4.0	1.33	18.75	5.46	0.26	0.21	0.50	8.79	0.85	7.64	0.00
5	8	2.97	0.25	17.9	4.0	1.23	20.30	6.40	0.32	0.29	0.50	9.63	1.16	8.79	0.00
6	10	3.72	0.25	22.4	4.0	1.17	21.32	7.06	0.38	0.35	0.50	10.23	1.40	9.63	0.00
7	12	4.46	0.25	26.8	4.0	1.14	22.00	7.51	0.41	0.39	0.50	10.65	1.58	10.23	0.00
8	14	5.20	0.25	31.3	4.0	1.11	22.46	7.83	0.44	0.43	0.50	10.94	1.71	10.65	0.00
9	16	5.95	0.25	35.8	4.0	1.10	22.77	8.05	0.46	0.45	0.50	11.15	1.80	10.94	0.00
10	18	6.69	0.25	40.2	4.0	1.09	22.98	8.20	0.47	0.46	0.50	11.29	1.86	11.15	0.00
11	20	7.43	0.25	44.7	4.0	1.08	23.13	8.31	0.48	0.48	0.50	11.39	1.90	11.29	0.00
12	22	8.18	0.25	49.2	4.0	1.08	23.23	8.38	0.49	0.48	0.50	11.45	1.93	11.39	0.00
13	24	8.92	0.25	53.7	4.0	1.07	23.29	8.43	0.49	0.49	0.50	11.50	1.95	11.45	0.00
14	26	9.66	0.25	58.1	4.0	1.07	23.34	8.46	0.49	0.49	0.50	11.53	1.97	11.50	0.00
15	28	10.41	0.25	62.6	4.0	1.07	23.37	8.48	0.50	0.49	0.50	11.55	1.98	11.53	0.00
16	30	11.15	0.25	67.1	4.0	1.07	23.39	8.50	0.50	0.50	0.50	11.57	1.98	11.55	0.00
17	32	11.89	0.25	71.6	4.0	1.07	23.41	8.51	0.50	0.50	0.50	11.58	1.99	11.57	0.00
18	34	12.63	0.25	76.0	4.0	1.07	23.42	8.52	0.50	0.50	0.50	11.58	1.99	11.58	0.00
19	36	13.38	0.25	80.5	4.0	1.07	23.43	8.52	0.50	0.50	0.50	11.59	1.99	11.58	0.00
20	38	14.12	0.25	85.0	4.0	1.07	23.43	8.52	0.50	0.50	0.50	11.59	2.00	11.59	0.00
21	40	14.86	0.25	89.4	4.0	1.07	23.43	8.53	0.50	0.50	0.50	11.59	2.00	11.59	0.00

Bulking Coefficent; Stepped Spillway Design Example

Step Number N	Height H (ft)	Nh/yc	d_w (ft)	Bulking Coefficient ε	y_{90} (ft)
1	0	0.00	2.69		
2	2	0.74	2.65		
3	4	1.49	1.54		
4	6	2.23	1.33		
5	8	2.97	1.23		
6	10	3.72	1.17	1.75	2.05
7	12	4.46	1.14	1.75	1.99
8	14	5.20	1.11	1.75	1.95
9	16	5.95	1.10	1.75	1.92
10	18	6.69	1.09	1.75	1.90
11	20	7.43	1.08	1.75	1.89
12	22	8.18	1.08	1.75	1.88
13	24	8.92	1.07	1.75	1.88
14	26	9.66	1.07	1.75	1.87
15	28	10.41	1.07	1.75	1.87
16	30	11.15	1.07	1.75	1.87
17	32	11.89	1.07	1.75	1.87
18	34	12.63	1.07	1.75	1.87
19	36	13.38	1.07	1.75	1.87
20	38	14.12	1.07	1.75	1.87
21	40	14.86	1.07	1.75	1.87

Energy Dissipation; Stepped Spillway Design Example

Step Number N	Height H (ft)	d_w (ft)	U_{avg} (ft/s)	Eo (ft)	E1 (ft)	Eo-E1 (ft)	Eo-E1 / Eo
1	0	2.69	9.29	4.04	4.04	0.00	0.00
2	2	2.65	9.43	6.04	3.75	2.29	0.38
3	4	1.54	16.25	8.04	5.48	2.56	0.32
4	6	1.33	18.75	10.04	6.65	3.38	0.34
5	8	1.23	20.30	12.04	7.50	4.53	0.38
6	10	1.17	21.32	14.04	8.11	5.93	0.42
7	12	1.14	22.00	16.04	8.53	7.51	0.47
8	14	1.11	22.46	18.04	8.83	9.21	0.51
9	16	1.10	22.77	20.04	9.03	11.00	0.55
10	18	1.09	22.98	22.04	9.17	12.86	0.58
11	20	1.08	23.13	24.04	9.27	14.76	0.61
12	22	1.08	23.23	26.04	9.34	16.70	0.64
13	24	1.07	23.29	28.04	9.39	18.65	0.67
14	26	1.07	23.34	30.04	9.42	20.62	0.69
15	28	1.07	23.37	32.04	9.44	22.60	0.71
16	30	1.07	23.39	34.04	9.45	24.58	0.72
17	32	1.07	23.41	36.04	9.46	26.57	0.74
18	34	1.07	23.42	38.04	9.47	28.57	0.75
19	36	1.07	23.43	40.04	9.48	30.56	0.76
20	38	1.07	23.43	42.04	9.48	32.56	0.77
21	40	1.07	23.43	44.04	9.48	34.56	0.78

Standard Step Method; Smooth Spillway Example

q = 25 cfs/ft θ = 26.6° smooth spillway

Height H (ft)	Nh/yc	friction factor f	Station s (ft)	Δs (ft)	d_w (ft)	U_{avg} (ft/s)	U_{avg}^2/2g (ft)	S_f	Avg. S_f	S_o	E	h_f	E	ΔE
0	0.00	0.071	0.0	0.0	2.69	9.29	1.34	0.01		0.50	4.03			
2	0.74	0.071	4.5	4.0	2.71	9.24	1.32	0.01	0.01	0.50	6.03	0.04	4.07	-0.04
4	1.49	0.071	8.9	4.0	1.48	16.88	4.43	0.05	0.03	0.50	7.91	0.12	6.03	0.00
6	2.23	0.071	13.4	4.0	1.23	20.28	6.38	0.09	0.07	0.50	9.62	0.29	7.91	0.00
8	2.97	0.071	17.9	4.0	1.10	22.80	8.07	0.13	0.11	0.50	11.17	0.45	9.62	0.00
10	3.72	0.071	22.4	4.0	1.01	24.82	9.57	0.17	0.15	0.50	12.57	0.60	11.17	0.00
12	4.46	0.071	26.8	4.0	0.94	26.47	10.88	0.20	0.19	0.50	13.83	0.75	12.57	0.00
14	5.20	0.071	31.3	4.0	0.90	27.85	12.04	0.24	0.22	0.50	14.94	0.89	13.83	0.00
16	5.95	0.071	35.8	4.0	0.86	29.01	13.06	0.27	0.25	0.50	15.93	1.01	14.94	0.00
18	6.69	0.071	40.2	4.0	0.83	29.98	13.96	0.30	0.28	0.50	16.79	1.13	15.93	0.00
20	7.43	0.071	44.7	4.0	0.81	30.81	14.74	0.32	0.31	0.50	17.55	1.24	16.79	0.00
22	8.18	0.071	49.2	4.0	0.79	31.52	15.42	0.35	0.33	0.50	18.22	1.33	17.55	0.00
24	8.92	0.071	53.7	4.0	0.78	32.12	16.02	0.37	0.36	0.50	18.80	1.42	18.22	0.00
26	9.66	0.071	58.1	4.0	0.77	32.63	16.53	0.38	0.37	0.50	19.30	1.50	18.80	0.00
28	10.41	0.071	62.6	4.0	0.76	33.07	16.98	0.40	0.39	0.50	19.74	1.56	19.30	0.00
30	11.15	0.071	67.1	4.0	0.75	33.44	17.37	0.41	0.41	0.50	20.11	1.62	19.74	0.00
32	11.89	0.071	71.6	4.0	0.74	33.76	17.70	0.42	0.42	0.50	20.44	1.67	20.11	0.00
34	12.63	0.071	76.0	4.0	0.73	34.04	17.99	0.43	0.43	0.50	20.72	1.72	20.44	0.00
36	13.38	0.071	80.5	4.0	0.73	34.27	18.24	0.44	0.44	0.50	20.97	1.76	20.72	0.00
38	14.12	0.071	85.0	4.0	0.73	34.47	18.45	0.45	0.45	0.50	21.17	1.79	20.97	0.00
40	14.86	0.071	89.4	4.0	0.72	34.64	18.63	0.46	0.45	0.50	21.35	1.82	21.17	0.00

Bulking Coefficent; Smooth Spillway Example

Height H (ft)	Nh/yc	d_w (ft)	Bulking Coefficient ε	y_{90} (ft)
0	0.00	2.69		
2	0.74	0.07		
4	1.49	0.07		
6	2.23	0.07		
8	2.97	0.07		
10	3.72	0.07	1.75	0.12
12	4.46	0.07	1.75	0.12
14	5.20	0.07	1.75	0.12
16	5.95	0.07	1.75	0.12
18	6.69	0.07	1.75	0.12
20	7.43	0.07	1.75	0.12
22	8.18	0.07	1.75	0.12
24	8.92	0.07	1.75	0.12
26	9.66	0.07	1.75	0.12
28	10.41	0.07	1.75	0.12
30	11.15	0.07	1.75	0.12
32	11.89	0.07	1.75	0.12
34	12.63	0.07	1.75	0.12
36	13.38	0.07	1.75	0.12
38	14.12	0.07	1.75	0.12
40	14.86	0.07	1.75	0.12

Energy Dissipation; Smooth Spillway Example

Height H (ft)	d_w (ft)	U_{avg} (ft/s)	Eo (ft)	E1 (ft)	Eo-E1 (ft)	Eo-E1 / Eo
0	2.69	9.29	4.04	4.04	0.00	0.00
2	2.71	9.24	6.04	3.74	2.29	0.38
4	1.48	16.88	8.04	5.75	2.29	0.28
6	1.23	20.28	10.04	7.49	2.55	0.25
8	1.10	22.80	12.04	9.06	2.98	0.25
10	1.01	24.82	14.04	10.47	3.57	0.25
12	0.94	26.47	16.04	11.73	4.31	0.27
14	0.90	27.85	18.04	12.85	5.19	0.29
16	0.86	29.01	20.04	13.83	6.20	0.31
18	0.83	29.98	22.04	14.70	7.33	0.33
20	0.81	30.81	24.04	15.47	8.57	0.36
22	0.79	31.52	26.04	16.13	9.90	0.38
24	0.78	32.12	28.04	16.71	11.32	0.40
26	0.77	32.63	30.04	17.22	12.82	0.43
28	0.76	33.07	32.04	17.66	14.38	0.45
30	0.75	33.44	34.04	18.04	16.00	0.47
32	0.74	33.76	36.04	18.36	17.67	0.49
34	0.73	34.04	38.04	18.65	19.39	0.51
36	0.73	34.27	40.04	18.89	21.15	0.53
38	0.73	34.47	42.04	19.10	22.94	0.55
40	0.72	34.64	44.04	19.28	24.76	0.56